PAPER

Plasma-based conversion of CO_2: current status and future challenges

Annemie Bogaerts,[*] Tomas Kozak, Koen van Laer and Ramses Snoeckx

This paper discusses our recent results on plasma-based CO_2 conversion, obtained by a combination of experiments and modeling, for dielectric barrier discharge (DBD), microwave plasma and a packed bed DBD reactor. The results illustrate that plasma technology is quite promising for CO_2 conversion, but more research is needed to better understand the underlying mechanisms and to further improve the capabilities.

1 Introduction

The conversion of greenhouse gases (mainly CO_2 and CH_4) into value-added chemicals and liquid fuels is considered as one of the great challenges for the 21st Century.[1] A lot of research has been carried out to develop energy-efficient technologies.[2–4] One of these technologies gaining increasing interest is plasma technology.

Plasma is a partially ionized gas, consisting of a large number of neutral species (different types of molecules, radicals and excited species), as well as electrons and various types of ions. These species can all interact with each other, making plasma a highly reactive chemical cocktail and of interest for many applications.[5,6]

The great potential of plasma technology for CO_2 conversion is due to the presence of energetic electrons. Indeed, plasma is created by applying electric power to a gas, causing the gas to breakdown, *i.e.*, the formation of electrons and positive ions (in addition to other reactive species). As the electrons are much lighter than the other plasma species, they gain the most energy from the electric field, and they do not lose their energy so efficiently by collisions with the other plasma species, explaining their higher energy. These energetic electrons can activate the (inert) gas by electron impact ionization, excitation and dissociation, and the reactive species (*i.e.*, ions, excited species and radicals, respectively) created in this way, will easily undergo other reactions, yielding the formation of new molecules. Thus, the gas itself (*e.g.*, CO_2) does not have to be heated as a whole, but can remain near room temperature. In this way, even strongly

Research Group PLASMANT, University of Antwerp, Department of Chemistry, Universiteitsplein 1, Antwerp, Belgium. E-mail: annemie.bogaerts@uantwerpen.be; Fax: +32-3-265-23-43; Tel: +32-3-265-23-77

ART ■ C5FD00053J

endothermic reactions, like CO_2 splitting and dry reforming of methane (DRM), can occur with reasonable energy consumption under mild reaction conditions. However, as the plasma is created by applying electrical power, the energy efficiency of this process is still an important issue.

The most common types of plasma used for CO_2 conversion are dielectric barrier discharges (DBDs),[7–31] microwave (MW) plasma[32–37] and gliding arc (GA) discharges.[38–45] The highest energy efficiency was reported for a MW plasma, *i.e.*, up to 90%,[32] but this was under very specific conditions, *i.e.*, supersonic gas flow and reduced pressure (~100–200 Torr), and a pressure increase to atmospheric pressure, which would be desirable for industrial applications, yields a dramatic drop in energy efficiency. Indeed, at normal flow conditions and atmospheric pressure, an energy efficiency up to 40% was reported.[6] A GA plasma also exhibits a rather high energy efficiency, even at atmospheric pressure, *i.e.*, around 43% for a conversion of 18% in the case of CO_2 splitting,[45] and even around 60% for a conversion of 8–16%, for DRM.[38] The energy efficiency of a DBD is more limited, *i.e.*, in the order of 2–10%,[8–17] but as demonstrated already for other applications,[46] it should be possible to improve this energy efficiency by inserting a (dielectric) packing into the reactor, *i.e.*, a so-called packed bed DBD reactor. Moreover, it also operates at atmospheric pressure, and has a very simple design, which is beneficial for upscaling, as has been demonstrated already for the large scale production of ozone,[47] and therefore it also has high potential for industrial applications. Finally, when combined with catalytic packing, it should enable the selective production of targeted compounds.[18–23]

Within our research group PLASMANT, we investigate both pure CO_2 conversion[15,48–50] and DRM,[16,17] by means of experiments and computer modeling. We have also investigated the effect of adding H_2 or CH_4, as a means to better separate the product gases,[24] the effect of adding He or Ar,[31] or N_2[51] which is mostly present in industrial gas flows. Our research up to now was focused on DBD and MW plasma. By means of computer simulations, validated by experiments, we try to elucidate the underlying reaction chemistry, and to investigate how the process can be optimized in terms of conversion and energy efficiency. In this paper, we give an overview of some characteristic, recent results obtained within our group to illustrate the state-of-the-art of plasma-based CO_2 conversion, and we will also try to identify the most important challenges for the future.

2   Experimental setup

The experiments were all carried out in a DBD reactor, of which a schematic drawing is presented in Fig. 1. It consists of a central grounded electrode with variable diameter (between 8 and 13 mm), surrounded by a coaxial dielectric tube, with inner and outer diameter of 17 and 22 mm, respectively. The dielectric tube is covered by a stainless steel mesh, which serves as the outer electrode and is powered by a high voltage power source. The length of this outer electrode is 9 cm, and this defines the length of the plasma zone.

The DBD reactor is coupled to a gas chromatograph to analyse the gas flowing out of the reactor, and to calculate the CO_2 conversion, the yields and selectivities of the formed products, and the energy efficiency, as calculated from the conversion, the power input in the plasma and the gas flow rate (see *e.g.*, ref. 15 for more details).
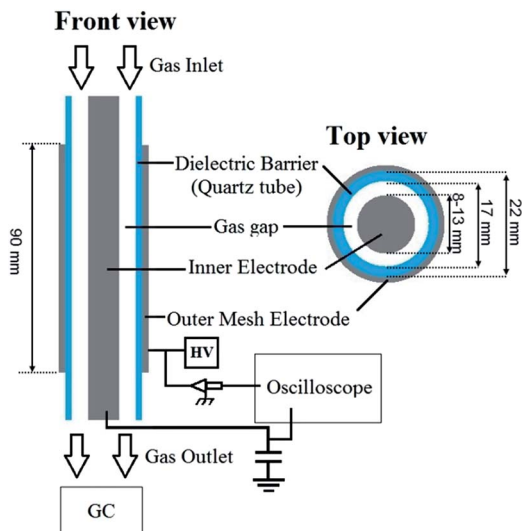
Fig. 1   Schematic diagram of the experimental setup, in front view and top view.

We performed experiments in a normal (*i.e.*, empty) DBD reactor, as well as in a DBD reactor filled with dielectric packing, *i.e.*, a packed bed DBD reactor. For this purpose, we used the smallest rod diameter, yielding a discharge gap (*i.e.*, distance between the central electrode and dielectric tube) of approximately 4.5 mm, and a discharge volume of about 15 cm^3. We introduced ZrO_2 beads (SiLi-Beads), with five different bead size ranges, *i.e.*, 0.90–1.00, 1.00–1.18, 1.25–1.40, 1.60–1.80 and 2.00–2.24 mm diameter.

3   Computational model

We used a zero-dimensional (0D) chemical reaction kinetics model to describe the underlying plasma chemistry of CO_2 conversion. It consists of solving balanced equations for the species densities, based on production and loss rates, as determined by the chemical reactions (see *e.g.* ref. 16 and 48 for details).

One balanced equation is solved for each species included in the model, *i.e.*, different types of molecules, radicals, ions, excited species, as well as electrons (see below). These balanced equations yield the time-evolution of the species densities, averaged over the plasma reactor volume. Indeed, because it is a 0D model, it only accounts for time-variations, while spatial variations, due to transport in the plasma, are not considered. However, based on the gas flow rate, we can translate the time-variation into a spatial variation, *i.e.*, as a function of distance travelled through the plasma reactor. Besides the species densities, the average electron energy is also calculated, based on an energy balanced equation, again with the energy source and loss terms as defined by the chemical reactions.

We developed a 0D chemical kinetics model for different gas mixtures relevant for CO_2 conversion, *i.e.*, pure CO_2,[15,48–50] CO_2/CH_4 [16,17] and CO_2/N_2,[51] but here we only show results for pure CO_2. Table 1 gives an overview of the species included in the pure CO_2 model.

Table 1   Overview of the species included in the CO_2 model

Molecules	Charged species	Radicals	Excited species
CO_2, CO	CO_2^+, CO_4^+, CO^+, $C_2O_2^+$, $C_2O_3^+$, $C_2O_4^+$, C_2^+, C^+, CO_3^-, CO_4^-	C_2O, C, C_2	CO_2(Va, Vb, Vc, Vd), CO_2(V1–V21), CO_2(E1, E2), CO(V1–V10), CO(E1–E4)
O_2, O_3,	O^+, O_2^+, O_4^+, O^-, O_2^-, O_3^-, O_4^- Electrons	O	O_2(V1–V4), O_2(E1–E2)

The vibrational levels of CO_2 can play an important role in CO_2 conversion, depending on the type of plasma to be studied. Indeed, while they are of minor importance in a DBD,[48] they are crucial for CO_2 splitting in MW plasma.[49,50] This will be illustrated in Section 4.2 below. For this reason, we have developed an extensive chemical kinetics model, taking into account the CO_2, CO and O_2 vibrational levels.[49,50] Hence, the symbols "V" and "E" between brackets for CO_2, CO and O_2 represent the vibrationally and electronically excited levels of these species respectively. Details about these notations can be found in.[49,50]

These species will all chemically react with each other. Hence, a large number of chemical reactions are incorporated in these models, including electron impact reactions, electron–ion recombinations, ion–ion, ion–neutral and neutral–neutral reactions. All details about these chemical reaction sets, as well as the corresponding rate coefficients, can be found in ref. 15, 48–50.

4   Results and discussion

We present here the results obtained from our experiments and computer simulations, first for CO_2 splitting in a DBD reactor, followed by a comparison of a DBD reactor and MW plasma, and finally, we will show how the CO_2 conversion and energy efficiency can be improved in a packed bed DBD reactor.

4.1 CO_2 splitting in a DBD reactor

Fig. 2 illustrates CO_2 conversion and the corresponding energy efficiency as a function of the specific energy input (SEI), measured in a DBD reactor. The SEI is the ratio of plasma power over gas flow rate. Therefore, different combinations of power and gas flow rate can give rise to the same SEI. The SEI is typically considered as the major determining factor for conversion and energy efficiency.

It is clear that the CO_2 conversion rises with SEI, which is logical as more energy is put into the system, either by applying more power for the same amount of gas, or by applying a lower gas flow rate (which corresponds to a longer residence time) at the same power. However, above a certain SEI, the measured conversion seems to saturate, and we did not obtain higher conversion values than 35% in our experiments. On the other hand, the energy efficiency drops upon increasing SEI, which is also logical, given the formula in Section 2 above. Indeed, it is obvious from this formula that when the conversion does not rise to the same extent as the SEI, the energy efficiency will drop.

The highest energy efficiency obtained in this case is 8%, but this corresponds to a very low conversion of only a few %. On the other hand, the highest conversion of 35% corresponds to a very low energy efficiency of only 2%. Thus,
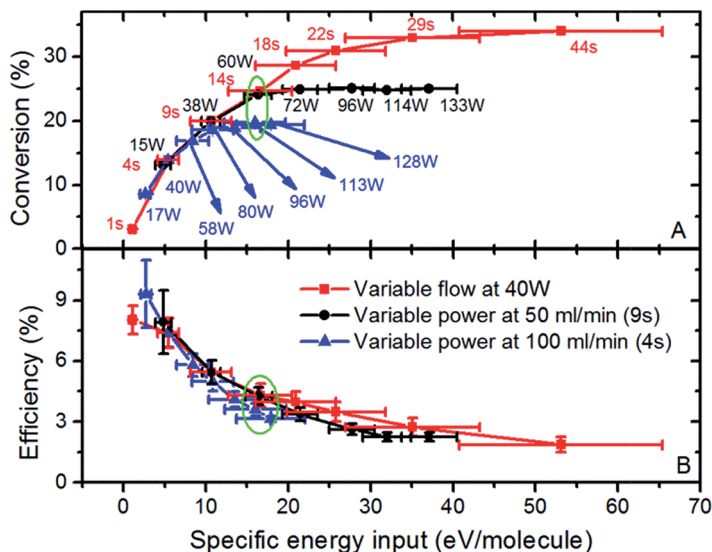
Fig. 2 Measured CO_2 conversion (A) and energy efficiency (B) in a DBD reactor, as a function of the specific energy input (SEI), using alumina dielectrics. The corresponding values of plasma power, result in certain SEI values at fixed gas flow rates of 50 and 100 ml min^{-1} (black and blue curves), as well as the corresponding values of the residence time, resulting in certain SEI values at a fixed plasma power of 40 W (red curve), are also shown in (A). The calculation of the error bars is based on the uncertainties of the power, the flow rate and the GC measurements. For the sake of clarity, the error bars are only presented for the energy efficiency. Adopted from ref. 15 with kind permission of Wiley-VCH Verlag.

there is clearly a trade-off between conversion and energy efficiency as a function of SEI.

The values obtained for conversion and energy efficiency are comparable to the data reported in the literature for similar conditions (e.g., ref. 7 and 8). We can conclude that the obtained CO_2 conversion is reasonable in a DBD reactor, but the energy efficiency is clearly too low for industrial implementation. Indeed, Spencer et al. estimated that if all the electrical energy for CO_2 splitting originated from fossil fuels, an energy efficiency of 52% would be needed to ensure that more CO_2 can be split in the plasma than the amount of CO_2 created by fossil fuel combustion in the electricity production needed for sustaining the plasma.[52] When using renewable electricity, this criterion might be somewhat less severe, but still, the energy efficiency is an important issue.

In addition to the experiments, we have also developed a detailed model for CO_2 conversion in DBD plasma, to investigate in detail the role of the various processes contributing to CO_2 splitting.[48] The calculations predict that electron impact dissociation of ground-state CO_2 is the dominant process for CO_2 conversion in a DBD, and the role of the CO_2 vibrational levels is limited in this case[48] (see more details in Section 4.2 below).

Subsequently, the model was extended to calculate the CO_2 conversion in real time.[15] The obtained CO_2 conversion and energy efficiency were in very good agreement with measured data.[15] Therefore, the model can be used to elucidate the underlying reaction paths of CO_2 conversion.

A simplified reaction scheme of CO_2 splitting, as obtained from the model, is illustrated in Fig. 3. It is clear that the actual CO_2 splitting is quite straightforward. The most important reactions are electron impact dissociation into CO and O (reaction r1), electron impact ionization into CO_2^+ (r2), which recombines with electrons or O_2^- ions into CO and O and/or O_2 (r3, r4), and electron dissociative attachment into CO and O^- (r5). The created CO molecules are relatively stable, but at a long enough residence time, they can recombine with O^- ions or O atoms, to form CO_2 again (r6, r7). This explains, among others, why CO_2 conversion tends to saturate at high SEI values (corresponding to low gas flow rates or long residence times). At shorter residence times, the O atoms will, however, almost immediately recombine into O_2 or O_3. Moreover, there are several other reactions possible between O, O_2 and O_3, sometimes also involving O^- and O_2^- ions. The details of these reactions are not indicated in Fig. 3, but can be found in ref. 15. These reactions will affect the balance between the formation of O_2 and O_3 as stable products. Our model indeed predicts that the selectivity towards CO formation is always close to 50%, but the selectivity towards O_2 formation varies between 45 and 50%, depending on O_3 production.

4.2 Comparison of CO_2 splitting in DBD and MW plasma

The fact that the energy efficiency for CO_2 splitting is quite limited in DBD plasma, as mentioned above, is because the reduced electric field is quite high (typically above 200 Td or 200×10^{-21} V m^2), yielding an average electron energy of 2–3 eV,[48] which is somewhat too high for efficient population of the CO_2 vibrational levels.[49] To illustrate this, Fig. 4 depicts the fraction of the electron energy transferred to different channels of excitation, ionization and dissociation
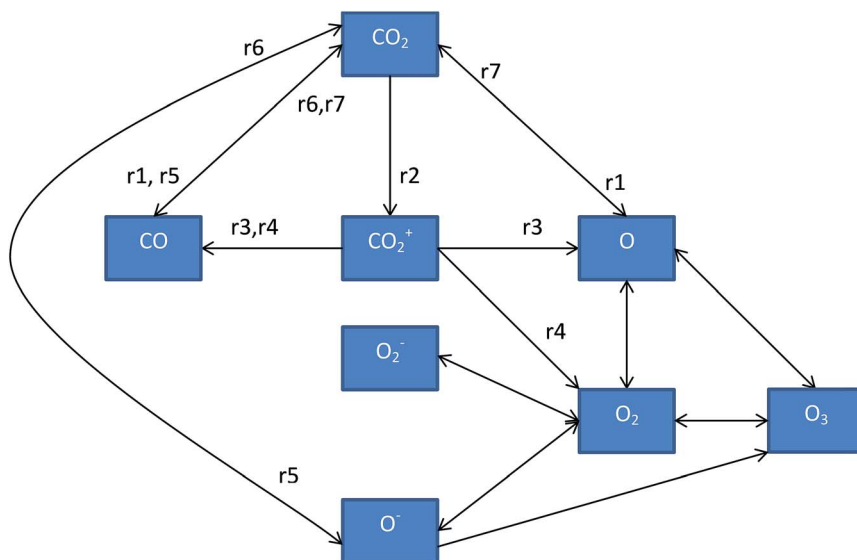
Fig. 3 Chemical reaction scheme, illustrating the chemistry of CO_2 splitting and further reactions between O, O_2 and O_3, as predicted by the model. The labels of the arrows are explained in the text.
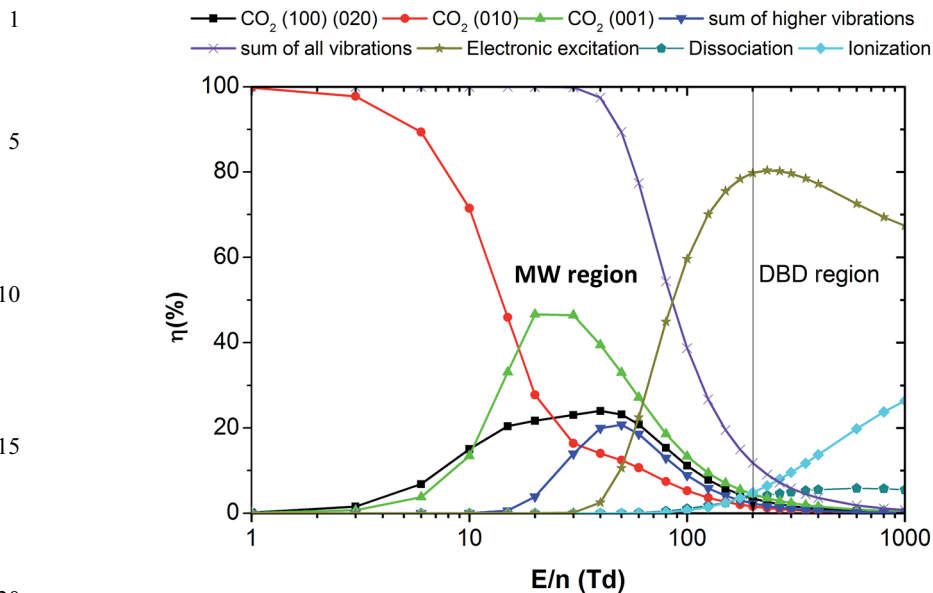
Fig. 4 The fraction of electron energy transferred to different channels of excitation as well as ionization and dissociation of CO_2, as a function of the reduced electric field (E/n), as calculated from the corresponding cross sections of the electron impact reactions. The E/n region characteristic for MW plasma and DBD plasma are indicated.

of CO_2, as a function of the reduced electric field (E/n), as calculated from the cross sections of the corresponding electron impact reactions. It is clear that in the region above 200 Td, indicated as "DBD region", 70–80% of the electron energy goes into electronic excitation, while the remaining 20–30% is used for ionization (increasing with rising E/n) and about 5% goes into dissociation. Note that this electron impact dissociation is also induced by electronic excitation, and thus requires a lot of energy.[48] The fraction of the electron energy going into vibrational excitation is 12% at $E/n = 200$ Td, but drops quickly upon increasing E/n. Thus, vibrational excitation is of minor importance in the "DBD region".

In MW plasma, the reduced electric field is typically around 50 Td, which is most appropriate for vibrational excitation of CO_2; see Fig. 4. The green curve is especially important, as this represents the first vibrational level of the asymmetric stretching mode, which is known to provide the most important channel for dissociation.[6,49] Thus, we can deduce already from Fig. 4 that MW plasma will give rise to a high population of CO_2 vibrational levels, which contribute to energy-efficient CO_2 splitting.

Fig. 5 shows a comparison of the CO_2 conversion and energy efficiency in a MW plasma and DBD reactor as a function of SEI, as predicted by our model taking into account the CO_2 vibrational levels.[49] Note that the results of the MW plasma are obtained for a reduced pressure of 2660 Pa (20 Torr), as used in the experiments of ref. 33 and 34 while the DBD results are for atmospheric pressure. Therefore, to compare both discharges, we need to show them at the same SEI in eV per molec, because this is the most fundamental parameter for comparison. Furthermore, the DBD results are obtained at a gas temperature of 300 K, while
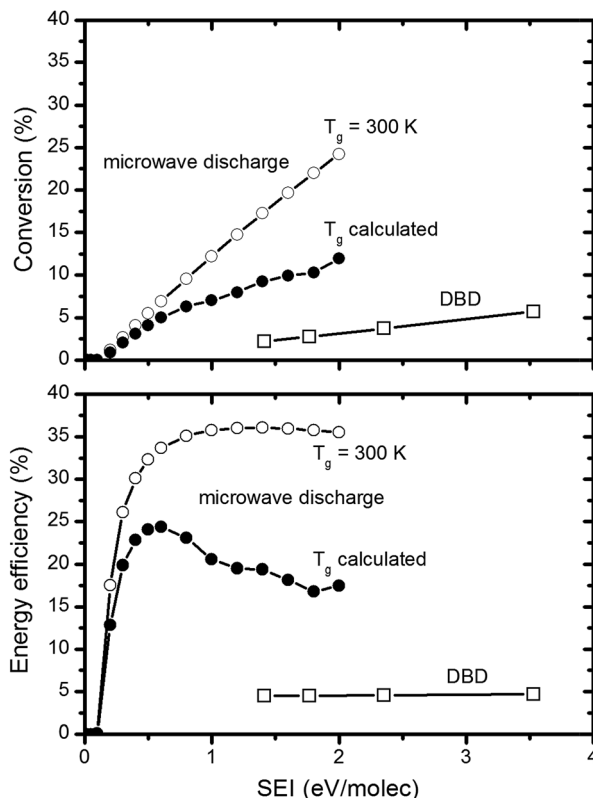
Fig. 5 Calculated CO_2 conversion (top) and energy efficiency (bottom) in a moderate pressure MW discharge and atmospheric pressure DBD reactor, as a function of SEI. The pressure in the MW plasma is 2660 Pa (20 Torr). Calculations are performed for two different gas temperatures, i.e., 300 K, like assumed in the DBD reactor, and a more realistic self-consistently calculated gas temperature as a function of time, reaching values up to 1000 K.

the MW results are shown both for a fixed gas temperature of 300 K (to allow a more direct comparison with the DBD results, as the rate coefficients of most chemical reactions are a function of gas temperature), as well as for a more realistic gas temperature, self-consistently calculated in the model as a function of time (or distance in the reactor).[50] In this case, values up to 1000 K are reached; see temperature profile in ref. 50.

It is clear that both the CO_2 conversion and energy efficiency are calculated to be much higher in the MW plasma than in the DBD reactor. The conversion rises as a function of SEI in both cases, which is logical (see also previous section). However, in the DBD reactor, the conversion reaches only about 5%, at an SEI of 3.5 eV per molecule, while in the MW plasma with a realistic (calculated) gas temperature, the CO_2 conversion is already 12% at an SEI of 2 eV per molecule. Note that the calculated conversion in the MW plasma at a fixed gas temperature of 300 K is much higher (and thus overestimated), compared to the result at the higher (more realistic) gas temperature. The reason is that the higher gas temperature gives rise to more vibrational-translational (VT) relaxation collisions

ART ■ C5FD00053J

of the CO_2 vibrational levels, which is the most important loss mechanism for the vibrational population.[49,50] This explains the lower conversion in the case with a higher gas temperature. Nevertheless, the CO_2 conversion is still significantly higher than in the DBD reactor operating at 300 K.

The latter is certainly also true for the energy efficiency, which is calculated to be around 5% in the DBD reactor (more or less independent from the SEI, as the conversion rises proportionally with the SEI), and it reaches values above 35% (when assuming a constant gas temperature of 300 K; thus overestimated) and around 25% (in the case of the self-consistently calculated gas temperature). In the latter case, the energy efficiency reaches its maximum at an SEI around 0.6 eV per molecule, which is in good agreement with the theoretical and experimental results presented in ref. 6, although in that case, energy efficiencies up to 80–90% were reported. Below, we will discuss the major effects that limit the maximum energy efficiency in our case.

As mentioned above, the reason for the higher CO_2 conversion and energy efficiency in MW plasma is attributed to the higher population of the CO_2 vibrational levels. This is indeed apparent from Fig. 6, where the calculated vibrational distribution function of the CO_2 asymmetric mode levels (*i.e.*, the mode which is most important for CO_2 splitting; *cf.* above) is plotted, for both the DBD and MW plasma, for an SEI of 0.6 eV per molecule. In the DBD reactor, the population of the vibrational levels drops over several orders of magnitude compared to the ground state density, even for the lowest levels. The corresponding vibrational temperature is calculated to be 961 K. In the MW plasma, the vibrational distribution drops much more smoothly, yielding a vibrational temperature of 4115 K. Although the population of the highest vibrational levels is much lower than the ground state density, they still play an important role in the CO_2 splitting process, which explains the higher CO_2 conversion and energy efficiency. Indeed, while in the DBD reactor, electron impact excitation–dissociation from the CO_2 ground state is mainly responsible for CO_2 splitting (*cf.*
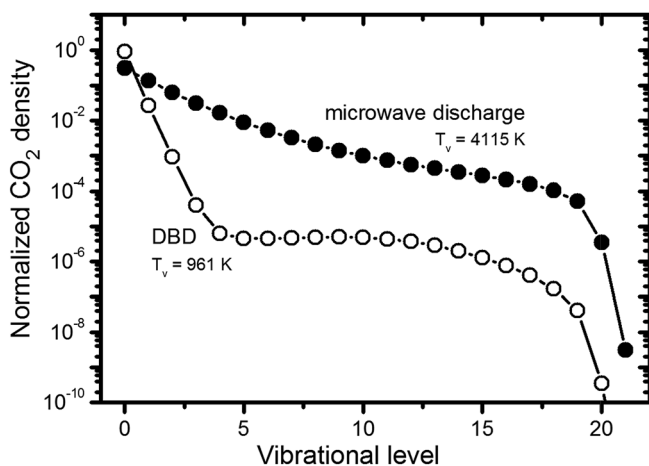
Fig. 6 Normalized vibrational distribution function of the asymmetric mode levels of CO_2 in a moderate pressure MW discharge and atmospheric pressure DBD plasma, at an SEI of 0.6 eV per molecule, both taken at the time of maximum vibrational temperature.

previous section), in MW plasma, the CO_2 splitting predominantly proceeds by electron impact vibrational excitation of the lowest vibrational levels, followed by vibrational–vibrational (VV) collisions, gradually populating the higher vibrational levels, which then lead to dissociation of the CO_2 molecule. This stepwise vibrational excitation process, or so-called "ladder-climbing" process, is schematically illustrated in Fig. 7, and is indeed responsible for the much higher energy efficiency in MW plasma.

Our model also allows us to identify the discharge conditions that favour the highest energy efficiency for CO_2 conversion. The highest value reached in our calculations, in the case of the realistic gas temperature, was around 32%. This value was obtained at an SEI in the range of 0.4–1.0 eV per molecule and a reduced electric field in the range of 50–100 Td.[50] Moreover, our calculations predict that a shorter residence time favours a higher energy efficiency, because in that case the time for VT relaxation, which depopulates the vibrational levels, is longer than the residence time of the gas within the plasma. This corresponds well with the fact that the highest energy efficiencies were reported at supersonic flow conditions.[32,35]

The best energy efficiencies obtained experimentally in a MW plasma at moderate pressure were 80% in subsonic flow, and up to 90% in supersonic flow conditions.[6,32] These results were obtained in 1983, and to our knowledge, nobody has been able to reproduce them since. Recently however, Goede et al. were able to reach energy efficiencies as high as 55% with a MW plasma at moderate pressure and again under supersonic flow conditions,[35] which is still higher than the values obtained by our model. Thus, to better understand the limitations in the energy
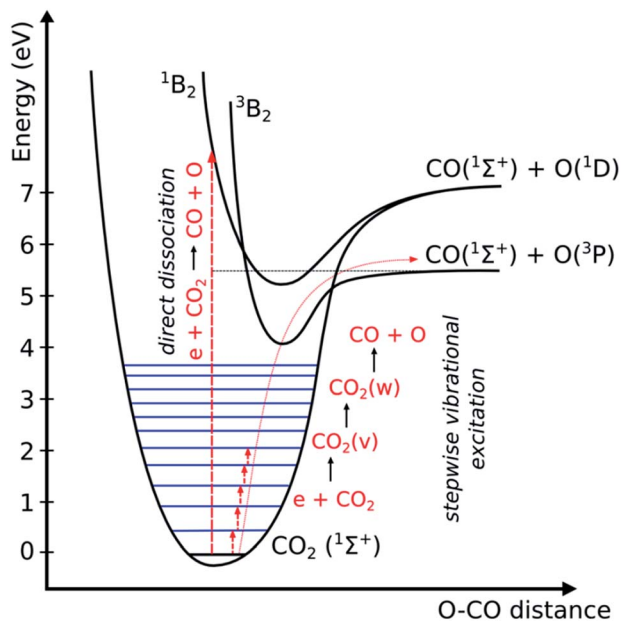
Fig. 7 Schematic diagram of some CO_2 electronic and vibrational levels, illustrating that much more energy is needed for direct electronic excitation–dissociation than for stepwise vibrational excitation, i.e., the so-called ladder climbing process.

efficiency, we have analysed how the vibrational energy of CO_2 is consumed by individual reactions. Our model predicts that up to 60% of the energy available in the CO_2 vibrational levels can be used for CO_2 dissociation, at least at high enough electron density (order of 10^{20} m^{-3} at a pressure of 100 Torr). The remaining fraction of the energy is largely lost by VT relaxation, which gives rise to the gas heating. *Vice versa*, because a higher gas temperature gives rise to higher VT relaxation rates, it is desirable to keep the gas temperature as low as possible, to minimize VT relaxation losses in the vibrational population. This is also one of the reasons why the energy efficiency drops upon increasing gas pressure, because of the increasing V-T relaxation processes. One way to reduce this effect is by using a fast gas flow, as mentioned above.

4.3 CO₂ splitting in a packed bed DBD reactor

Finally, we have also investigated whether we can improve the energy efficiency in DBD plasma, by adding a dielectric packing in the reactor. More specifically, we have inserted ZrO_2 beads, with five different bead size ranges, *i.e.*, 0.90–1.00, 1.00–1.18, 1.25–1.40, 1.60–1.80 and 2.00–2.24 mm diameter, in a DBD reactor with a gap size of 4.5 mm.
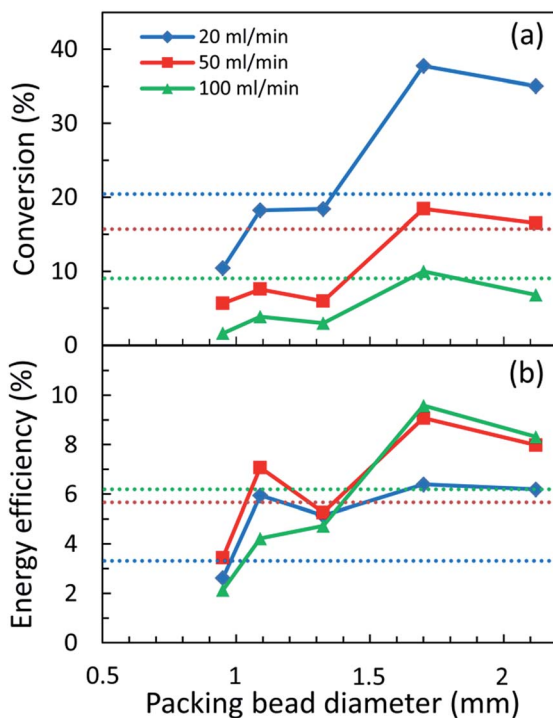
Fig. 8 Measured CO_2 conversion (a) and corresponding energy efficiency (b), as a function of packing bead diameter for ZrO_2, at a power of 60 W and three different gas flow rates. The corresponding results without packing are indicated with dashed horizontal lines.

ART ■ C5FD00053J

Fig. 8 shows the measured CO_2 conversion (a) and corresponding energy efficiency (b), as a function of bead diameter, for three different gas flow rates, *i.e.* 20, 50 and 100 ml min^{-1} at an applied power of 60 W. The results are also compared with experiments without packing (dashed horizontal lines), which serve as a benchmark to define the improvement in conversion and energy efficiency.

It is clear that a packed bed reactor can result in a better conversion and energy efficiency than without packing, but only for bead diameters above 1.4 mm. Indeed, the results for lower bead sizes are even worse than without packing. This can be explained because the residence time in the reactor filled with smaller beads is probably too low to benefit from the enhancement effect due to the presence of the packing material. The best results, in terms of both conversion and energy efficiency, are obtained for a flow rate of 20 ml min^{-1} and a bead diameter of 1.6–1.8 mm. In this case, the conversion reaches 38%, which is almost a factor 2 higher than without packing, while the energy efficiency is 6.4%, which is also nearly a factor 2 higher than without packing. In particular, the fact that both conversion and energy efficiency are improved simultaneously is quite promising. The combination of maximum conversion and energy efficiency obtained here, is comparable to or slightly better than the results reported in the literature for a packed bed DBD reactor with various types of dielectric materials (silica gel, quartz, α-Al$_2$O$_3$, γ-Al$_2$O$_3$, CaTiO$_3$ and BaTiO$_3$) under similar conditions.[8,25]

To explain why the packed bed reactor yields a better conversion and energy efficiency, we have developed a 2D fluid model within a COMSOL Multiphysics software, for a simplified axisymmetric geometry of a packed bed reactor, consisting of only two beads with a diameter of 2.25 mm. This simplified geometry in 2D is needed to keep the simulation time reasonable. Indeed, to resolve the plasma behaviour near the contact points of the beads, a very narrow mesh size is needed (*i.e.*, typically around 50 μm in the bulk, but up to 0.1 μm near the contact points). Thus, the simulation domain contains in the order of 100.000 mesh points, leading to calculation times of a few weeks for a few periods of the applied voltage, even for this simple geometry. Therefore, this model is, in the first instance, developed for a helium plasma instead of a CO_2 plasma, because this yields a more simple plasma chemistry, and it is sufficient to explain the behaviour of the packed bed effect.

Fig. 9 illustrates the calculated electric displacement field distribution within the beads and in the plasma and the resulting electron temperature profile in the plasma in this simplified geometry. It is clear that the electric displacement field is much higher near the contact points. This is attributed to polarization of the dielectric material as a result of the applied potential. At the contact points there will thus be local charges of opposite sign close together, which leads to a higher electric displacement field, as well as a locally enhanced electric field in the plasma. The latter gives rise to an enhanced electron temperature for the same applied power. Indeed, the electron temperature is up to 8 eV near the contact points, while it is only 2–3 eV in an empty DBD reactor (or far away from the contact points; see Fig. 9). This means that the applied electric power is used more efficiently for heating the electrons, which can then transfer their energy to CO_2 splitting, by electron impact ionization and excitation–dissociation, and this explains the higher CO_2 conversion and energy efficiency, as shown in Fig. 8.
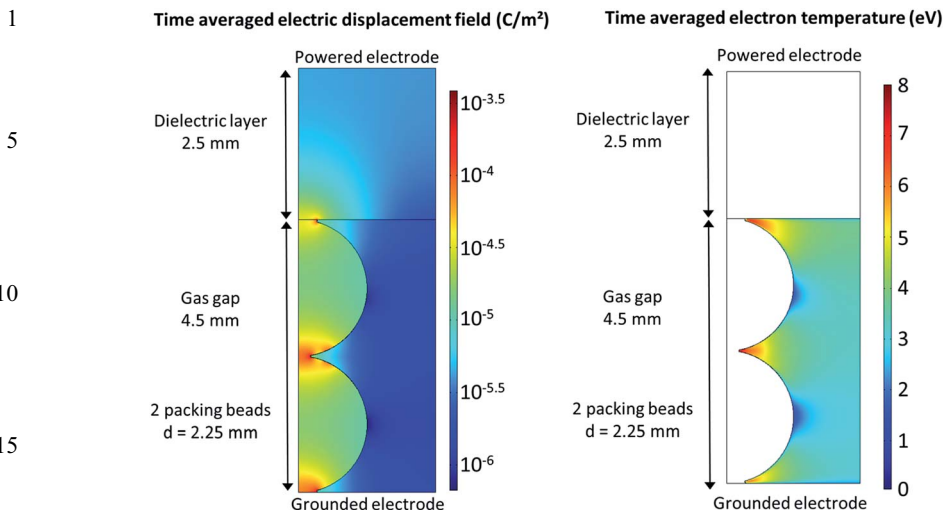
Fig. 9 Calculated time averaged electric displacement field and electron temperature over one period of the applied potential.

5 Conclusion and outlook for future work

We have presented our recent results on CO_2 conversion, obtained by means of combined experimental and computer modeling efforts, for a DBD reactor and MW plasma. DBD plasma provides a reasonable conversion, in the order of 30%. However, the corresponding energy efficiency is only in the order of 10%, and this is probably too low for industrial implementation. Indeed, when all the electrical energy to sustain the plasma originates from fossil fuels, it was estimated that an energy efficiency of 52% would be needed for CO_2 conversion, to compensate for the CO_2 production by the fossil fuel combustion. On the other hand, DBD plasma is very flexible, as it can easily be switched on and off. Therefore, it has great potential to be combined with renewable energy sources (wind turbines or solar panels), *i.e.*, for the storage of peak renewable energy into chemicals or fuels.

Furthermore, there is still room for improvement in the conversion and energy efficiency of a DBD plasma, by inserting dielectric beads, *i.e.*, in a packed bed DBD reactor, as demonstrated in this paper for ZrO_2. The reason for this higher conversion and energy efficiency is the enhanced electric field near the contact points of the beads, yielding a higher electron temperature, which facilitates electron impact dissociation of CO_2, as could be explained by our model. Moreover, when inserting catalytic packing in a DBD reactor, the selective production of specific products can be targeted. This was already demonstrated many times in the literature for air pollution control (*e.g.*, ref. 46 and 53–55), but it has also great potential for CO_2 conversion.[18–23] Nevertheless, we believe that a lot of research will still be needed to find out which catalyst materials are most promising for the selective production of specific compounds.

When comparing DBD and MW plasma, it is clear that MW plasma exhibits a much better CO_2 conversion and energy efficiency. This is attributed to the important role of the CO_2 vibrational levels. Indeed, our model calculations have

elucidated that the CO_2 conversion proceeds by direct electron impact excitation–dissociation in DBD plasma, whereas in MW plasma, the dominant process is electron impact excitation to the lowest vibrational levels, followed by vibrational–vibrational collisions, gradually populating the higher vibrational levels, which give rise to dissociation. As this stepwise vibrational excitation process, or so-called ladder climbing process, requires significantly less energy than direct electron impact excitation–dissociation from the CO_2 ground state, this explains the much better energy efficiency in the MW plasma compared to the DBD reactor.

However, this good energy efficiency is obtained at a moderate pressure (order of 3000 Pa), and this was also the case for the experimental data published in the literature (*e.g.*, ref. 32 and 35). This is not so practical for high-throughput processing of exhaust gases. Increasing the pressure leads, however, to a clear reduction in energy efficiency,[6,36,37] although at atmospheric pressure, a CO_2 conversion of 45% with an energy efficiency of 20% were recently reported,[37] which is still better than the results obtained with DBD plasma.

We also illustrated that computer modelling can contribute to a better insight in the underlying plasma chemistry of CO_2 conversion, and this will be useful for further improving the performance of plasma technology for this application.

To conclude, we believe that plasma technology is very promising for CO_2 conversion into value-added chemicals and new fuels, but still a lot of research will be needed to further improve the capabilities.

Acknowledgements

References

1 *Climate Change 2007: The Physical Science Basis*, Contribution of Working Group I to the Fourth Assesment Report of the Intergovernmental Panel on Climate Change, S. Solomon, D. Qin, M. Manning, M. Marquis, K. Averyt, M. M. B. Tignor, H. L. Miller and Z. Chen, Cambridge University Press, New York, 2007.
2 G. Centi, E. A. Quadrelli and S. Perathoner, *Energy Environ. Sci.*, 2013, **6**, 1711.
3 M. Aresta, A. Dibenedetto and A. Angelini, *Chem. Rev.*, 2014, **114**, 1709.
4 P. Styring, E. A. Quadrelli and K. Armstrong, *Carbon Dioxide Utilization: Closing the Carbon Cycle*, Elsevier, Amsterdam, 2015.
5 A. Bogaerts, E. Neyts, R. Gijbels and J. J. A. M. van der Mullen, *Spectrochim. Acta, Part B*, 2002, **57**, 609.
6 A. Fridman, *Plasma Chemistry*, Cambridge University Press, Cambridge, 2008.
7 S. Paulussen, B. Verheyde, X. Tu, C. De Bie, T. Martens, D. Petrovic, A. Bogaerts and B. Sels, *Plasma Sources Sci. Technol.*, 2010, **19**, 034015.

ART ■ C5FD00053J

8 Q. Yu, M. Kong, T. Liu, J. Fei and X. Zheng, *Plasma Chem. Plasma Process.*, 2012, **32**, 153.

9 Q. Wang, B.-H. Yan, Y. Jin and Y. Cheng, *Plasma Chem. Plasma Process.*, 2009, **29**, 217.

10 V. Goujard, J.-M. Tatibouët and C. Batiot-Dupeyrat, *Appl. Catal., A*, 2009, **353**, 228.

11 X. Zhang and M. S. Cha, *J. Phys. D: Appl. Phys.*, 2013, **46**, 415205.

12 X. Tu and J. C. Whitehead, *Appl. Catal., B*, 2012, **125**, 439.

13 Y. Zhang, Y. Li, Y. Wang, C. Liu and B. Eliasson, *Fuel Process. Technol.*, 2003, **83**, 101.

14 A. Ozkan, T. Dufour, G. Arnoult, P. De Keyzer, A. Bogaerts and F. Reniers, *J. CO2 Util.*, 2015, **9**, 74.

15 R. Aerts, W. Somers and A. Bogaerts, *ChemSusChem*, 2015, **8**, 702.

16 R. Snoeckx, R. Aerts, X. Tu and A. Bogaerts, *J. Phys. Chem. C*, 2013, **117**, 4957.

17 R. Snoeckx, Y. X. Zeng, X. Tu and A. Bogaerts, *RSC Adv.*, 2015, **5**, 29799.

18 A.-J. Zhang, A.-M. Zhu, J. Guo, Y. Xu and C. Shi, *Chem. Eng. J.*, 2010, **156**, 601.

19 A. Gómez-Ramírez, V. J. Rico, J. Cotrino, A. R. González-Elipe and R. M. Lambert, *ACS Catal.*, 2014, **4**, 402.

20 M. Scapinello, L. M. Martini and P. Tosi, *Plasma Processes Polym.*, 2014, **11**, 624.

21 Q. Wang, Y. Cheng and Y. Jin, *Catal. Today*, 2009, **148**, 275.

22 Q. Wang, B.-H. Yan, Y. Jin and Y. Cheng, *Energy Fuels*, 2009, **23**, 4196.

23 B. Eliasson, U. Kogelschatz, B. Xue and L.-M. Zhou, *Ind. Eng. Chem. Res.*, 1998, **37**, 3350.

24 R. Aerts, R. Snoeckx and A. Bogaerts, *Plasma Processes Polym.*, 2014, **11**, 985.

25 D. Mei, X. Zhu, Y. He, J. D. Yan and X. Tu, *Plasma Sources Sci. Technol.*, 2015, **24**, 015011.

26 J. Wang, G. Xia, A. Huang, S. L. Suib, Y. Hayashi and H. Matsumoto, *J. Catal.*, 1999, **185**, 152.

27 R. Li, Q. Tang, S. Yin and T. Sato, *J. Phys. D: Appl. Phys.*, 2007, **40**, 5187.

28 S. Wang, Y. Zhang, X. Liu and X. Wang, *Plasma Chem. Plasma Process.*, 2012, **32**, 979.

29 C. De Bie, T. Martens, J. van Dijk, S. Paulussen, B. Verheyde and A. Bogaerts, *Plasma Sources Sci. Technol.*, 2011, **20**, 024008.

30 N. R. Pinhao, A. Janeco and J. B. Branco, *Plasma Chem. Plasma Process.*, 2011, **31**, 427.

31 M. Ramakers, I. Michielsen, R. Aerts, V. Meynen and A. Bogaerts, *Plasma Processes Polym.*, 2015, **12**, DOI: 10.1002/ppap.201400213.

32 R. I. Asisov, V. K. Givotov, E. G. Krasheninnikov, B. V. Potapkin, V. D. Rusanov and A. Fridman, *Soviet Physics - Doklady*, 1983, **271**, 94.

33 N. Britun, T. Godfroid and R. Snyders, *Plasma Sources Sci. Technol.*, 2012, **21**, 035007.

34 T. Silva, N. Britun, T. Godfroid and R. Snyders, *Plasma Sources Sci. Technol.*, 2014, **23**, 025009.

35 A. P. H. Goede, W. A. Bongers, M. F. Graswinckel, M. C. M. van de Sanden, M. Leins, J. Kopecki, A. Schulz and M. Walker, *EPJ Web Conf.*, 2013.

36 A. Vesel, M. Mozetic, A. Drenik and M. Balat-Pichelin, *Chem. Phys.*, 2011, **382**, 127.

37 L. F. Spencer and A. D. Gallimore, *Plasma Sources Sci. Technol.*, 2013, **22**, 015019.

38 X. Tu and J. C. Whitehead, *Int. J. Hydrogen Energy*, 2014, **39**, 9658.

39 A. Indarto, D. R. Yang, J.-W. Choi, H. Lee and H. K. Song, *J. Hazard. Mater.*, 2007, **146**, 309.

40 A. Indarto, J. Choi, H. Lee and H. K. Song, *Environ. Eng. Sci.*, 2006, **23**, 1033.

41 Z. Bo, J. Yan, X. Li, Y. Chi and K. Cen, *Int. J. Hydrogen Energy*, 2008, **33**, 5545.

42 Y.-C. Yang, B.-J. Lee and Y.-N. Chun, *Energy*, 2009, **34**, 172.

43 N. Rueangjitt, T. Sreethawong, S. Chavadej and H. Sekiguchi, *Chem. Eng. J.*, 2009, **155**, 874.

44 C. S. Kalra, Y. I. Cho, A. Gutsol, A. Fridman and T. S. Rufael, *Rev. Sci. Instrum.*, 2005, **76**, 025110.

45 T. Nunnally, K. Gutsol, A. Rabinovich, A. Fridman, A. Gutsol and A. Kemoun, *J. Phys. D: Appl. Phys.*, 2011, **44**, 274009.

46 H. L. Chen, H. M. Lee, S. H. Chen and M. B. Chang, *Ind. Eng. Chem. Res.*, 2008, **47**, 2122.

47 U. Kogelschatz, *Plasma Chem. Plasma Process.*, 2003, **23**, 1.

48 R. Aerts, T. Martens and A. Bogaerts, *J. Phys. Chem. C*, 2012, **116**, 23257.

49 T. Kozák and A. Bogaerts, *Plasma Sources Sci. Technol.*, 2014, **23**, 045004.

50 T. Kozák and A. Bogaerts, *Plasma Sources Sci. Technol.*, 2015, **24**, 015024.

51 S. Heijkers, R. Snoeckx, T. Kozák, T. Silva, T. Godfroid, N. Britun, R. Snyders and A. Bogaerts, *J. Phys. Chem. C*, (in press).

52 L. F. Spencer and A. D. Gallimore, *Plasma Chem. Plasma Process.*, 2011, **31**, 79.

53 H. L. Chen, H. M. Lee, S. H. Chen, M. B. Chang, S. J. Yu and S. N. Li, *Environ. Sci. Technol.*, 2009, **43**, 2216.

54 J. van Durme, J. Dewulf, C. Leys and H. van Langenhove, *Appl. Catal., B*, 2008, **78**, 324.

55 H.-H. Kim and A. Ogata, *Eur. Phys. J.: Appl. Phys.*, 2011, **55**, 13806.

ART ■ C5FD00053J

PAPER

A framework for the analysis of the security of supply of utilising carbon dioxide as a chemical feedstock

Eric S. Fraga* and Melvin Ng

Recent developments in catalysts have enhanced the potential for the utilisation of carbon dioxide as a chemical feedstock. Using the appropriate energy efficient catalyst enables a range of chemical pathways leading to desirable products. In doing so, CO_2 provides an economically and environmentally beneficial source of C_1 feedstock, while improving the issues relating to security of supply that are associated with fossil-based feedstocks. However, the dependence on catalysts brings other supply chains into consideration, supply chains that may also have security of supply issues. The choice of chemical pathways for specific products will therefore entail an assessment not only of economic factors but also the security of supply issues for the catalysts. This is a multi-criteria decision making problem. In this paper, we present a modified 4A framework based on the framework suggested by the Asian Pacific Energy Research centre for macro-economic applications. The 4A methodology is named after the criteria used to compare alternatives: availability, acceptability, applicability and affordability. We have adapted this framework for the consideration of alternative chemical reaction processes using a micro-economic outlook. Data from a number of sources were collected and used to quantify each of the 4A criteria. A graphical representation of the assessments is used to support the decision maker in comparing alternatives. The framework not only allows for the comparison of processes but also highlights current limitations in the CCU processes. The framework presented can be used by a variety of stakeholders, including regulators, investors, and process industries, with the aim of identifying promising routes within a broader multi-criteria decision making process.

1   Introduction

Carbon dioxide (CO_2) is a non-toxic and abundant C_1 (1 carbon atom) feedstock. The release of CO_2 has contributed to global warming and the greenhouse effect making emissions an increasing concern for society and policy makers. In recent years carbon capture and sequestration (CCS) has been mooted as the solution to

Centre for Process Systems Engineering, Department of Chemical Engineering, University College London (UCL), UK. E-mail: e.fraga@ucl.ac.uk

ART ■ C5FD00038F

controlling emissions but has raised the question of what to do with the increasing large amounts of CO_2. A potential solution is to use CO_2 as a chemical feedstock and a raw product in the production of chemicals. This is known as carbon capture and utilisation (CCU).

There are several benefits that arise from the utilisation of carbon dioxide as a chemical feedstock.[1] Firstly, like CCS, CCU is able to mitigate emissions of carbon dioxide through capture. CCU, unlike CCS, may allow for a closed loop recycling system. Secondly, an economic benefit may arise from the generation of economically valuable products. Finally, it may help address an individual country's security of supply for energy.

As C_1 feedstock is currently predominantly sourced from oil derived hydrocarbons, the security of supply for oil may be a concern. Most nations depend on foreign oil imports, often from areas of geo-political instability. As a result, market volatility and uncertainty disrupts national sustainability and forward planning. Through a carbon economy, reliance on volatile sources of oil could be mitigated or even eliminated through the use of secure domestic carbon sources.

Currently, there are a few chemical pathways that utilise CO_2 on a commercial scale: the production of urea, salicylic acid and sodium carbonate. However, CO_2 utilisation has a key limitation. CO_2 is a kinetically and thermodynamically stable molecule. This results in a high activation energy and a large quantity of energy may be required to react carbon dioxide. Unfortunately, energy generation currently emits more CO_2 than would be consumed in generating valuable products, leading to an overall net increase in emissions. Although these emissions could be reduced or eliminated through the use of renewable energy generation, any energy requirements could also be ameliorated through the development of suitable catalysts, as can the potentially high activation energy. This has led to an increasing level of research and development in the field of catalysis. This research is leading to new potential products that can be derived from CO_2 as a feedstock.

However, the use of catalysts brings up the issue of security of supply yet again. Many catalysts are made from rare materials and these materials may also be sourced from geo-politically unstable regions. Recycling of many of the catalysts may be difficult.[2] This paper presents a methodology for the assessment of alternative CO_2 utilisation routes, incorporating a number of factors that may characterise the security of supply. The methodology provides an attractive graphical visualisation of the characteristics of an individual route which enables the comparison of alternatives. This may help decision makers identify those routes which best achieve the potential benefits of CCU with improved security of supply.

2   Carbon dioxide as a feedstock

The pathways currently utilising CO_2 on an industrial scale are few. Examples include the Solvay process to produce sodium carbonate,[3] the production of urea *via* the Bosch–Meiser process,[4] and the production of salicylic acid through the Kolbe–Schmitt process.[5] These only account for a fraction of the number of pathways theoretically possible using CO_2 as a C_1 feedstock. Alternative pathways are being considered and a selection of these are summarised in Table 1, grouped according to the compounds used to react with CO_2.

Table 1   Summary of CO_2 pathways

Group	Substrate	Product
Oxygen containing compounds	Epoxides	Cyclic carbonate
		Alternating polycarbonates
		Aromatic polycarbonates
	Alcohols	Acyclic carbonates
Nitrogen containing compounds	Ammonia, amines	Urea
		Carbamic acid esters
		Polyurethanes
Carbon–carbon unsaturated compounds	Aromatic compounds	Carboxylic acids
	Alkynes	Carboxylic acid esters
	Alkenes	Lactones
Other	Hydrogen	Formic acid
		Methanol

Many of the routes in Table 1 are currently commercially viable. Table 2 illustrates the level of production for some of these processes. The most mature CCU process is the production of urea. The rates for the other CCU routes are orders of magnitude smaller. The level of production of each of these products correlates well with the level of development in terms of technology.[6] A summary of the utilisation levels is presented in Table 3 with polymers separated out into individual products.

Given the level of technological development, current market saturation and potential demand, we can shortlist promising CCU product targets for immediate consideration:

(1) Methanol.

(2) Urea.

(3) Formic acid.

(4) Polymers, mainly polyalkylene carbonates.

(5) Cyclic carbonates.

The promise in technologies for the production of these targets derives predominantly from catalyst development. However, in order to determine commercial viability, the security of supply for each overall process must be considered. The next section describes a methodology for assessing the security of

Table 2   Current levels of production of products, showing levels for both CCU and traditional (non CO_2) routes

Chemical	CO_2 utilising production (kT)	Global production (kT)	CO_2 (%)
Cyclic carbonates[7]	80	200	40
Formic acid[8]	0	300	0
Methanol[9]	4	100 000	≈ 0
Polypropylene carbonate[10]	76	≈ 0	0
Polycarbonate[11]	605	3700	16
Salicylic acid[6]	90	90	100
Urea[12]	157 000	157 000	100

Table 3   Current state of carbon capture & utilisation technologies. A double ✓ indicates significant levels of activity and a single ✓ an area that is showing increasing levels of acitivity[6]

Technology	Research	Demonstration	Feasibility	Mature market
Chemical production				
Acyclic carbonates	✓✓			
Alternating polycarbonates	✓✓	✓		
Aromatic polycarbonates	✓✓	✓		
Carboxylic acids	✓✓			
Carboxylic acid esters	✓✓			
Cyclic carbonates	✓✓			
Lactones	✓✓			
Polyurethanes	✓✓	✓		
Sodium carbonate				✓✓
Urea				✓✓
CO_2 to fuels				
Methanol		✓✓	✓	
Formic acid	✓✓	✓		

supply, and presents this in the context of other factors that decision makers will wish to consider.

3   Methodology

The target products described above illustrate the potential for effective CO_2 utilisation. However, beyond purely economic and technical issues, other aspects may affect the adoption of any particular route to a product. One such aspect is the *security of supply*. This term is most often used in the context of energy and is defined as follows:

"the ability of an economy to guarantee the availability of energy resource supply in a sustainable and timely manner with the energy price being at a level that will not adversely affect the economic performance of the economy."[13]

In the context of energy, security of supply is dependent on 5 main factors: availability of fuels domestically and externally, the ability to acquire supply to meet demand, level of an economy's diversification, accessibility to fuel resources through sufficient infrastructure, and geo-political challenges in sourcing energy. From these factors, the Asian Pacific Energy Research Centre (APERC) proposed the categorisation of these factors into *availability*, *accessibility*, *acceptability* and *applicability*, collectively called *the 4 As of Energy Security*.[13]

We adapt this 4As approach to the security of supply to the specific case of CO_2 utilisation. The framework proposed by APERC was intended for a macro-economic analysis of the energy system. Each A value was quantified on the basis of macro-energy system characteristics.[13] In the context of CO_2 utilisation, it makes sense to also consider smaller scale analyses, *e.g.* at the process route level, while still including macro-economic aspects. The key is the suitable re-definition of the 4A categories for their application to CO_2 utilisation. In what follows, we will be defining the parameters that quantify each A with a value between 0 (bad) to 10 (good).

3.1 Availability

The availability of the supply side of the product will be defined by the catalyst. The catalyst is often the limiting factor in the production rate. Further, few of the catalysts used for the products noted above are replaceable because many are tailored for the specific reaction. The availability of the catalyst will be estimated using a combination of parameters:

Crustal abundance. Crustal abundance is a measure of the scarcity of a metal on a macro scale with the abundance measured in parts per million.[14] For example, the abundance of ruthenium is 0.00057 ppm, which indicates a high risk catalyst, whereas aluminium, with an abundance of 84 149 ppm, would be low risk. Each metal within each of the catalysts is given a score based on its abundance, as quantified in Table 4.

Production concentration. Production concentration is an indicator of the distribution of regions in which the metal is produced, and data are provided by the British Geological Survey.[15] A commodity with a limited distribution of production is at a higher risk than one produced in many places around the world. For instance, 91% of iridium is produced in South Africa, and the top 3 countries producing iridium control 98% of the global production. In contrast, the cumulative production of the top 3 copper producers accounts for less than half of the global production. A score is allocated to the geographic concentration of metals production concentration as shown in Table 5.

Reserves concentration. Reserves concentration is similar to the production concentration but relates to the distribution of the reserves. A score is allocated to the metals reserve concentration as shown in Table 6.

Political corruption and stability. Political corruption has become an increasing concern as black-market dealings and market inconsistencies reduce the transparency of what should be a free market. Societal pressure is also increasingly becoming a factor. Whilst corruption has an effect on stability, both factors are included separately. This is because political instability will describe the current situation, whilst political corruption could lead to increased instability due to pressures on the system. The measures for corruption and stability are based on data from the World Bank.[16] These data provide an index rating of political corruption and stability in [1,100], where 1 is the most corrupt/unstable and 100 the least. We have mapped the index rating to scores for our framework as shown in Table 7. This factor contributes 4 values to the overall availability measure: a value of stability and of corruption separately for each of two countries; the top producer and the country that has the most reserves.

Table 4   Crustal abundance scoring

Abundance (ppm)	Score
≥100	4 (low risk)
50–100	3 (medium/low risk)
1–50	2 (medium/high risk)
<1	1 (high risk)

Table 5 Production concentration scoring

Concentration (%)	Score
0–25	4 points
25–50	3 points
50–75	2 points
75–100	1 point

Table 6 Reserves concentration scoring

Concentration (%)	Score
0–25	4 points
25–50	3 points
50–75	2 points
75–100	1 point

The maximum score for availability based on the above is 28 (4×7). A perfect score of 28 means that a metal has high levels of availability where both the production and reserves are not highly concentrated in single regions, and that the main producers and owners of the reserves present low levels of corruption and high levels of stability. A scaled value in the desired range was achieved by dividing the sum of all of the above by 2.8.

In calculating the availability of the catalyst material, we have firstly assumed that there is an equal weighting between each of the parameters in terms of importance. For example, that the extent of corruption in the country where the reserves are held, is as important as the abundance. Secondly, in measuring the abundance of a mineral, the abundance measure does not take into account the spatial distribution within a region. For example, in one region there may be an abundance of zinc although it may be spread uniformly over the whole region. This means that the crustal abundance may not necessarily be a realistic measure of the ability to extract the material through mining. Finally, this index is based on results at one point in time and does not include future projections and historical context. These assumptions can, of course, be addressed subsequently and the scorings adapted, if desired.

3.2 Affordability

The second A is economic, based on the revenue generated per unit of catalyst:

$$\text{Catalyst to revenue ratio} = \frac{\text{catalyst price}}{\text{product price} \times \text{product amount}} \quad (1)$$

This assumes an equal turnover frequency for all catalysts which is not typically the case. For instance, cheaper catalysts may have a shorter life than a more expensive or robust catalyst. However, the measure should be appropriate as an

Table 7 Political corruption & stability scoring

Measure	Score
75–100	4 points
50–75	3 points
25–50	2 points
1–25	1 point

indication of affordability. Other measures of affordability can be used, of course. In any case, the mapping of ratio to score is shown in Table 8.

It is worth noting that the process cost is not considered, only the cost of any catalyst required. This is based on the assumption that the general plant cost is comparatively less volatile and hence affects security of supply negligibly. It is also assumed that other raw materials will have lower costs than the catalyst, which is generally the case.

3.3 Applicability

Applicability has been defined according to the technological readiness level[17] (TRL) of the process. The TRL rating is a systematic approach that assesses the level of maturity for a given technology, allowing for consistency in comparison. The TRL method classifies a technology into one of 9 levels, from level 1 indicating that the basic principles are understood, through to level 9 indicating that commercial operations exist. The TRL is incorporated by scaling by 10/9.

3.4 Acceptability

The final A value is dependent on two main parameters: a life cycle assessment (LCA) in terms of CO_2 emissions (Table 9) and a measure of the lifetime of storage of CO_2 in the product (Table 10). The use of these factors is motivated by one of the key motivations for CCU: the need to reduce the impact of CO_2 emissions on the global climate. The life storage measure for carbon dioxide in a product is included to mitigate the lack of comparable LCA data in some cases. For example, methanol may only have temporary storage due to its use as a combustible fuel,

Table 8 Affordability score system

Catalyst to revenue ratio	Score
0–0.001	10 points
0.001–0.0025	9 points
0.0025–0.005	8 points
0.005–0.01	7 points
0.01–0.025	6 points
0.025–0.05	5 points
0.05–0.1	4 points
0.1–1	3 points
1–10	2 points
10–20	1 points
20+	0 points

ART ■ C5FD00038F

Table 9 LCA score system based on the ratio of amount of CO_2 emissions to the amount of CO_2 utilised in the process

Ratio	Score
0–0.5	10 points
0.5–1	9 points
1–1.5	8 points
1.5–2	7 points
2–2.5	6 points
2.5–3	5 points
3–3.5	4 points
3.5–4	3 points
4.5–5	2 points
5+	1 point

whereas polyalkylene presents a long term store for the CO_2. The scores from the two factors are combined with equal weighting after scaling to yield a score in the range [1,10].

3.5   Visualising the 4As

The 4As framework described above generates a quantitative assessment of the individual factors. Displaying this multi-dimensional information can be done in a variety of ways. We have chosen to use star charts, otherwise known as radar charts and spider charts, to present this multi-dimensional information. This is a simple graphical representation that facilitates the comparison of different alternatives and is illustrated in Fig. 1.

Each of the 4 measures is itself an indicator of the security of supply for a given process, but it is the overall combination of these factors that needs to be compared when looking at alternative catalysts and products. A perfect rhombus is an illustration of a technology that would be considered to have a secure supply.

3.6   Assumptions

There have been 5 key assumptions made in this framework:

(1) The catalyst is the limiting factor for the success of the process. Given that overcoming the thermodynamic constraints of carbon dioxide based reactions is the key, this assumption is reasonable.

(2) A second assumption is that the availability and the affordability are dependent solely on the catalyst. We assume that the general plant cost and material sourcing is comparatively less volatile given available knowledge of developing chemical process. For example, in processing polyalkylene

Table 10 CO_2 life storage in the final product

Storage life	Score
No storage	1 point
Temporary storage	2 points
Permanent storage	3 points

ART ■ C5FD00038F
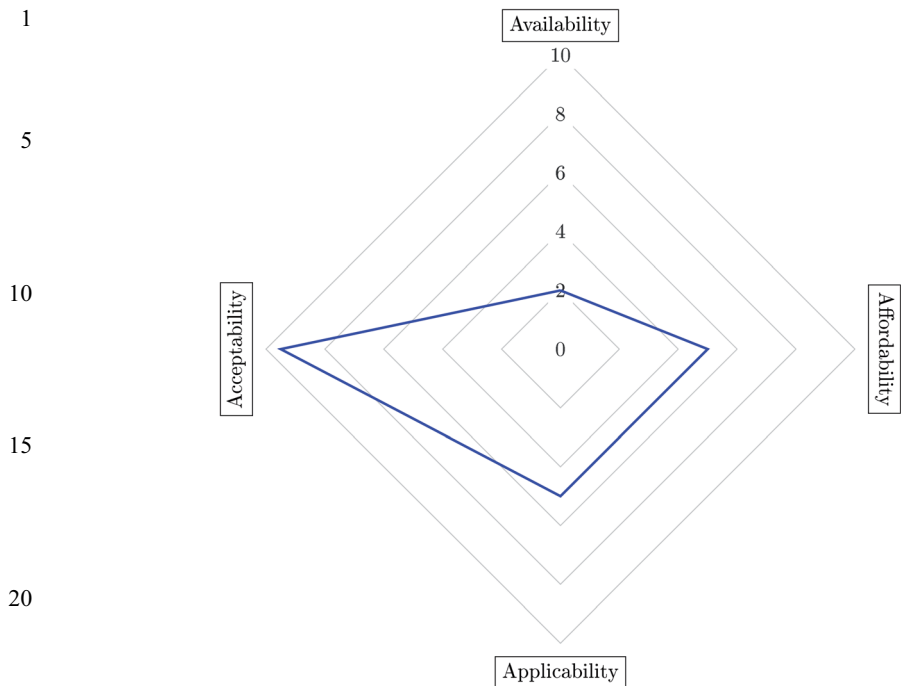
Fig. 1 Example radar chart for visualising the 4A measure showing a case with high acceptability (score of 9.5), low availability (2), average applicability (5) and affordability (5).

carbonates, the majority of the processing units will be similar if not the same for a process without CCU and one with CCU. However, the catalytic reactor and the capture cost are the key differences in the processes.

(3) The turnover frequency (TOF) is assumed to be the same for different catalysts. This is not true in general but we believe is sufficient for an initial comparison. A more accurate approach would involve a full economic analysis, including product revenue and catalyst costs. These data are often proprietary and therefore difficult to obtain generally.

(4) Equal weighting is given to sub-items within each category, *e.g.* corruption *versus* stability within the availability category. For specific cases, it may be useful to have non-equal weightings. This would be straightforward to implement should it be desirable.

(5) The results presented below are based on current estimates for each of the categories with no attempt at projecting into the future. For instance, the political situation in relevant countries may change, new sources of raw materials may be discovered, or improved mining operations could change the affordability of a specific catalyst. Furthermore, historical context could be useful in estimating the values of some of the sub-items, especially in terms of the impact of stability or corruption on availability. However, updating individual inputs to the framework is straightforward.

It is also worth noting that the framework need not be limited to 4 categories. In fact, it is highly likely that further economic considerations for the particular

product, *e.g.* process cost and market demands, would be included to define a 5As framework. We have not included such elements as the data required are often sensitive and company specific. The overall methodology, however, does not preclude such an extension.

4   Carbon utilisation targets and processes

The information required for the assessment of each target, on the basis of the methodology described above, is given in this section. The various processes, including both chemistry and actual processing, are described, and any catalysts required are specified.

4.1   Urea

Urea accounts for approximately 50% of global nitrogen fertiliser production. Urea has the highest concentration of nitrogen of all solid nitrogenous fertilisers which are widely used in agriculture.[18] Ammonia, a key reactant for the production of urea, and urea plants are often combined as one plant.[19]

The basic synthesis of urea has been established since 1922, using a process known as the Bosch–Meiser process.[4] This process consists of two main equilibrium reactions. The first is carbamate formation in a fast exothermic reaction which is then followed by urea conversion, a slow endothermic decomposition of the ammonium carbamate into urea and water.

$$2NH_3 + CO_2 \rightleftharpoons NH_2COONH_4$$

$$2NH_2COONH_4 \rightleftharpoons H_2O + NH_2CONH_2$$
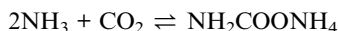
The synthesis of urea is a non-catalytic process and therefore does not require any catalyst material.

Interestingly, historically the production of ammonia has often exceeded the amount required stoichiometrically when compared with the amount of CO_2 readily available for the production of urea. Combined ammonia and urea plants would sell the surplus ammonia because the cost of CO_2 to meet the deficiency was not economically justified. However, with the potential increase in CCS, there would be an opportunity to boost urea production economically in these plants. This is known as the KM-CDR process, which is used to enhance the yield in urea production.[19] This aligns well with the desire to increase CCU.

4.2   Polyalkylene carbonate

Polyalkylene carbonates are polymers that have a range of uses from biodegradable polymers in medical use to high temperature tolerance polymers. Polypropylene carbonate, a polyalkylene derivative, is amongst the most promising polymer products. The synthesis of polyalkylene carbonates is through the reaction between epoxides and CO_2. The process conditions determine the generated product. Conditions can vary from 30–40 °C for polymers obtained from polypropylene oxide and up to temperatures of 110–120 °C for polymers from cyclohexene epoxide. Pressure also has an impact on the reactions.[20] Current methods

utilise biomass feedstocks. If CO_2 were used to generate these polymers, competition with food production would be reduced (which highlights that security of supply is also an issue for food and water, but out of scope for this paper).

Various catalysts have been researched for the co-polymerisation process. Inoue *et al.*[21] discovered that the combination of $ZnEt_2$ and water allowed viable catalyst performance for the co-polymerisation of carbon dioxide and propylene oxide. Further validation on the performance of a zinc catalyst was made when Kawachi *et al.*[22] demonstrated high catalytic activity for polymerization of epoxides and CO_2. Previous varieties include aryl, alkyl, diimines, Schiff bases and zinc compounds. More recently, researchers have focused on 3 main catalysts: chromium, cobalt and zinc. For example, Noh *et al.*[23] discuss the reaction between carbon dioxide and propylene oxide in the presence of Co(salen). The cobalt catalyst showed a superior turnover number at 22 000 g per gcat (ref. 23) whilst zinc only yields a turnover value of 1441 g per gcat. The catalyst proved to be highly active in the reaction for CO_2 and propylene oxide co-polymerization although commercial viability of the process has yet to be demonstrated.

4.3 Formic acid

Formic acid, HCOOH, has a wide range of uses including silage, additives to pharmaceutical intermediates, and as a fundamental feedstock in the chemicals industry to produce aldehydes, ketones and carboxylic acids.[24] More recently there has been strong interest in utilising formic acid within fuel cells due to its strong electrochemical oxidation ability for Pt–Ru electrodes. Formic acid is traditionally produced through the reaction of methanol and carbon monoxide which produces an intermediate, methyl formate:

$$CH_3OH + CO \rightarrow HCOOCH_3$$
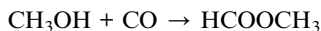
Hydrolysis then produces formic acid and methanol:

$$HCOOCH_3 + H_2O \rightarrow HCOOH + CH_3OH$$
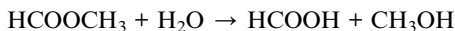
However, the hydrogenation of CO_2 is also possible using both transition and non-transition metal compounds as catalysts, with a resulting benefit in the reduction of the cost of raw materials:

$$CO_2 + H_2 \rightarrow HCOOH \tag{2}$$

Farlow[25] investigated the reaction in the presence of a nickel catalyst under high pressure, 20–40 MPa, and high temperature, 353–423 K. This eventually progressed to favourable conditions (298 K) through catalyst complexes of Ru or Pd combined with halides and hydrides.[26] Simultaneously, there has been research in homogeneous catalysts, such as supercritical CO_2, water and ionic liquids. This can achieve comparable reaction rates to transition complexes in the supercritical phase. However, the heterogeneous catalysts proved more attractive as the separation of the formic acid from the catalyst is easier. An activated carbon

supporting ruthenium through impregnation is preferred as it does not use the hazardous and expensive reagents used in other approaches.[8] Using ruthenium as the active component results in high activity and selectivity.

4.4 Methanol

Methanol is widely used as a fuel for transport and as a chemical feedstock.[27] There are over 90 process plants worldwide producing 75 million tons of methanol annually.[9] Methanol has traditionally been produced through fossil fuels *via* syngas chemistry. Therefore, elements of energy security of supply come into play in global methanol production from C_1 feedstocks. However, recently new pathways and catalysts have been developed.

Olah[27] devised an approach to produce methanol through what is known as "metgas". Metgas is composed of CO and H_2 at a 1 : 2 ratio through a single step by reacting CO_2, $3CH_4$ and steam. This is known as *bireforming*. The temperature is high, 1073–1273 K, whilst pressure is held between 0.5–4 MPa in the presence of a nickel based catalyst:

$$3CH_4 + CO_2 + 2H_2O \rightarrow 4CO + 8H_2 \rightarrow 4CH_3OH \tag{3}$$
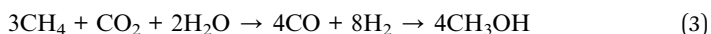
The hydrogenation of CO_2 has become an increasingly promising solution given an appropriate catalyst. The conversion has favourable thermodynamics although the high activation energy barrier remains a challenge.[28] Heterogeneous catalysts have therefore been widely investigated. Copper has proven to be the most favourable catalyst. With the use of copper catalysts, such as Cu/ZnO, CuO/ZnO and CuO–ZnO/ZrO_2, the hydrogenation proceeds at lower temperatures and under higher pressures.

4.5 Cyclic carbonates

Cyclic carbonates are commonly used as degreasing agents, polar aprotic solvents and electrolytes for lithium ion batteries.[7,29] Cyclic carbonates can also be converted into dimethyl carbonate which is used as a quality oxygenating additive for both petrol and aviation fuel. The main chemical pathway for cyclic carbonates is the reaction between epoxides and carbon dioxide.

The development of the catalysts and the mechanisms for this reaction has been well documented over several permutations of catalysts, including organic bases,[30] zeolites, metal oxides,[31] alkali metal halides[32] and metal complexes.[7] Whilst the synthesis has been applied to industry with a variety of such catalysts, the recovery and stability of the catalyst itself has yet to be improved. More recently, research has focused on using ionic liquids as the catalyst due to advantageous negligible vapour pressures.[33] The use of ionic liquids as a clean catalytic form has proven to improve reaction rate and reaction selectivity. However, the use of ionic liquids exhibits low catalyst stability and activity and requires a co-catalyst. Whilst Dai *et al.*[34] suggested that the performance was substantiated through the use of Lewis acidic compounds as co-catalysts, it still held industrial limitations due to challenges in separation. Recent research has begun to tackle this by immobilising the ionic liquid onto solid supports.

A further form of catalyst proposed for this reaction has been through using metal complexes such as Co, Cr, Ni, Al, Zn and Re mounted onto supports. North

ART ■ C5FD00038F

& Young[7] have proposed a catalyst based on bimetallic aluminium(acen) complexes. This allows the reaction to take place at room temperature and at atmospheric pressure.

5   Assessing carbon utilisation targets

The 4As methodology has been applied to the processes described above. Table 11 summarises the results which are also presented using radar charts in Table 12 for easy comparison. Data from a number of sources,[6,14–16,18,27] along with those cited in the discussion above and below, were used to determine these scores. For all the categories, except for acceptability, the scores cover almost the full range of values possible, indicating that the scoring system for these categories is able to discriminate between alternatives. The acceptability scores cover only half of the range. This is mostly due to the energy requirements of each process. Currently, energy sources are typically not carbon neutral, and so there is a significant impact on emissions in each case. What these scores show, besides the possibility of comparing the alternatives, is that there is scope for improvement, in this category in particular.

The results can be used to identify which processes show the most promise, in comparison with the others, in the context of security of supply. For each individual case, the different factors can help focus the attention on any aspects that could be addressed by stakeholders to reduce supply risks. The benefit of the 4As model for a process is that the nature of future and current challenges can be efficiently identified.

Some discussion about each target process follows.

5.1   Urea

Overall, urea is the most promising target with maximum values for three of the criteria. First of all, the applicability is high because the process has been used for a long time and is well established. With respect to availability and affordability, the process requires no catalyst. It is useful to compare this process for the production of urea with an alternative that is based on the use of ruthenium as a catalyst.[35]

In either case, the acceptability score ranked second overall. This is due to unfavourable CO_2 emissions by these processes.

Table 11   Summary of scores for each process/catalyst combination. The maximum score in each category is 10

Product	Catalyst	Avail.	Afford.	Applic.	Accept.	Average
Cyclic carbonates	Al	5	9	2	4	5
Formic acid	Ir	5	1	3	2	3
Formic acid	Ru	5	2	3	2	3
Methanol	Cu	7	8	6	4	6
Polyalkylene carbonates	Co	3	5	9	4	5
Polyalkylene carbonates	Zn	7	9	9	4	7
Urea	Ru	5	2	10	5	5
Urea	None	10	10	10	5	9

Table 12 Star charts for the 8 CCU process alternatives
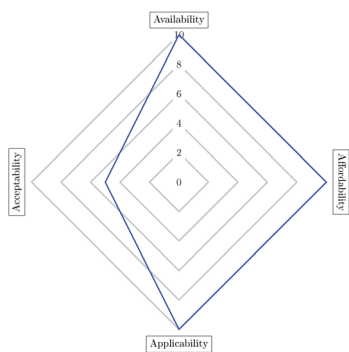
Urea with no catalyst
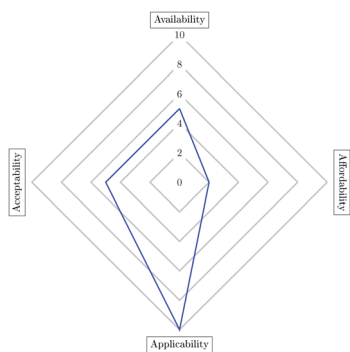
Urea with ruthenium
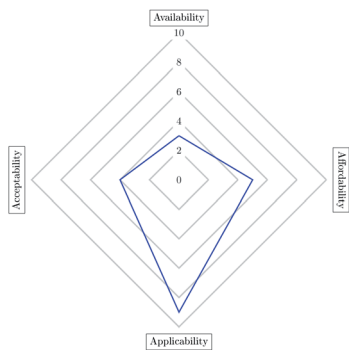
Carbonate with cobalt
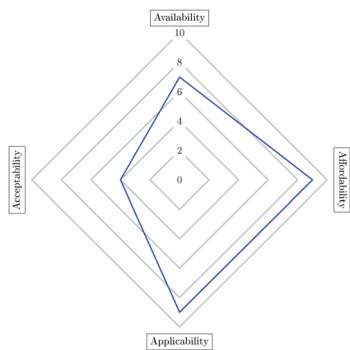
Carbonate with zinc
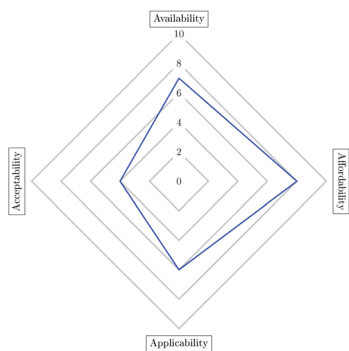
Methanol with copper

Cyclic carbonates

ART ■ C5FD00038F

Availability
10
8
6
4
2
0

Acceptability

Affordability

Applicability
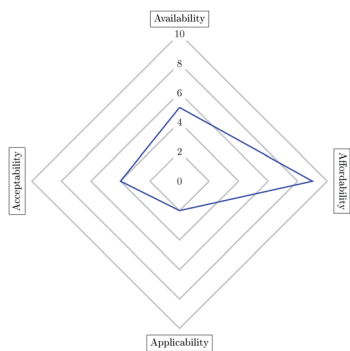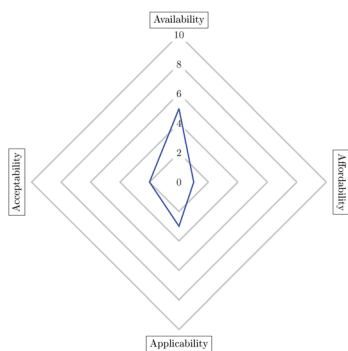
Formic acid with iridium

Availability
10
8
6
4
2
0

Acceptability

Affordability

Applicability
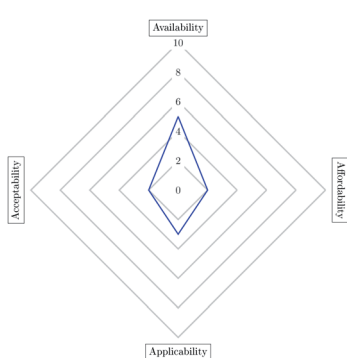
Formic acid with ruthenium

5.2 Polyalkylene carbonate

Two different catalysts, cobalt and zinc, have been considered for the production of polyalkylene carbonates. The radar charts for the two options (second row of Table 12) show significant differences, particularly in availability and affordability. Zinc is more easily available and also more affordable when compared with cobalt (see Table 13). In both cases, the relatively low score for acceptability was mostly due to CO_2 emissions.

For availability, a zinc catalyst is preferred for both economic and geo-political factors. Cobalt is 3 times less abundant than zinc and the production levels of zinc are 84 times that of cobalt. The ability to source the catalyst is also a consideration: 81% of cobalt production is concentrated in 3 producing countries, whilst only 49% of zinc production is in its top 3 producing countries. The risk to supply is lower for zinc, *i.e.* were there to be instability in one of the top producing regions, a large amount will be available from other sources. The political considerations of production and of reserve distribution led to the low score for cobalt: the top producing country for cobalt (Democratic Republic of the Congo) is ranked high in global corruption levels whereas, for zinc, the top producing country (P. R. China) has a better ranking for both corruption and political stability.

The high score for applicability is based on the fact that existing technologies can be used for the production of these polymers. Also, current production is

Table 13   Price of catalyst relative to the price of aluminium

Material	Relative cost
Al	1
Zn	1.14
Cu	4
Co	18
Ru	1529
Ir	11 418

ART ■ C5FD00038F

based on food based feedstocks such as corn. Replacing these with CO_2 will help address food security and therefore increase the applicability of this CCU alternative.

5.3 Methanol

Methanol rates reasonably well in availability and affordability, with applicability average. Acceptability is low, again mostly due to emissions of CO_2 due to energy requirements for the process. There are no particular concerns beyond this and so methanol can be considered a good choice as a target, especially if CO_2 neutral energy sources are available.

5.4 Cyclic carbonates

The key factor in the production of cyclic carbonates is the low applicability score. This is primarily due to the low TRL value of 2. Although there has been significant research into catalysts for the production of cyclic carbonates, no commercial implementations exist.[7] The existing processes for cyclic carbonates, not based on CO_2 utilisation, perform well enough that the incentive to develop CO_2 based processes is not there currently. As pressure, financial and regulatory, on utilising CO_2 increases, there will be increasing incentives to take existing lab-scale processes into pilot and eventually plant scale. This will increase the applicability score and, depending on the energy requirements, may also lead to an increase in the acceptability score.

The availability score of 5 is the same as for urea with ruthenium. Although aluminium has a much higher abundance, the overall score is the same due to the political and corruption assessments of the countries with greatest production and reserves. The overall security of supply is deemed to be similar, although this is a function of the weighting of the different criteria that form the basis for the availability score.

5.5 Formic acid

The progress of formic acid production through CO_2 utilisation is the least mature of all the processes presented, leading to low applicability scores. Furthermore, both of the catalysts considered are costly, having a significant impact on the affordability scores. However, because of the potential applications, *e.g.* the use of formic acid in fuel cells, there is an incentive to develop and to improve these processes; see, for instance, the press release from Market Wired.[36]

6 Conclusion

This paper presents a framework for the analysis of the security of supply for carbon dioxide utilising processes. Development in CCU has concentrated on catalysis to ameliorate the energy requirements for reactions involving CO_2. At these early stages of CCU development, gaining insight into any potential limitations that arise from security of supply issues is of value to various stakeholders, including industry, governments and potential end-users of the products.

The 4As approach, proposed by the Asian Pacific Energy Research Centre for energy security, has been adapted to CCU, combining micro- and macro-

ART ■ C5FD00038F

economic criteria with process considerations. The framework enables us to compare and contrast alternative products and processes through the analysis of the impact of catalyst choice. It also highlights those aspects which could benefit from further development. The cases considered show that urea production is currently the most secure, while formic acid is at the other end of the scale. The reasons for the differences amongst the various target products range from geopolitical, through to the stage of development of the individual processes.

A number of assumptions have been made. These are all subject to change as the framework is fundamentally extensible. Of primary concern to industrial users of the framework would be the addition of process and market economics beyond the impact of the catalysts. However, economics will necessarily trade-off with security of supply and eventual decisions will be based on the stakeholders' own perceptions of relative importance.

References

1 C. Creutz and E. Fujita, *Carbon Management: Implications for R&D in the Chemical Sciences and Technology: A workshop Report to the Chemical Sciences Roundtable*, 2001.

2 T. E. Graedel, J. Allwood, J.-P. Birat, M. Buchert, C. Hagelueken, B. K. Reck, S. F. Sibley and G. Sonnemann, *J. Ind. Ecol.*, 2011, **15**, 355–366.

3 T. Paul, Process for producing sodium carbonate, *US Pat.*, US25256763A, 1965.

4 N. MacDowell, N. Florin, A. Buchard, J. Hallett, A. Galindo, G. Jackson, C. S. Adjiman, C. K. Williams, N. Shah and P. Fennell, *Energy Environ. Sci.*, 2010, **3**, 1645–1669.

5 A. Lindsey and H. Jeskey, *Chem. Rev.*, 1957, **57**, 583–620.

6 P. Zakkour, Implications of the reuse of captured CO_2 for European climate action policies, 2013, http://setis.ec.europa.eu/setis-deliverables/setis-workshops-hearings/workshop-co2-re-use-technologies.

7 M. North and C. Young, *Catal. Sci. Technol.*, 2011, **1**, 93–99.

8 G. Peng, S. J. Sibener, G. C. Schatz and M. Mavrikakis, *Surf. Sci.*, 2012, **606**, 1050–1055.

9 Methanol Institute, http://www.methanol.org/Methanol-Basics/The-Methanol-Industry.aspx, retrieved 22 October 2014.

10 S. Moolji, Global Polymer Business – Trends & Market Dynamics, Presented at IOCL Petrochem Conclave, http://www.petrochemconclave.com/presentation/2013/Mr.SMoolji.pdf, 2013, retrieved 15 April 2015.

11 Asahi Kasei Chemicals Corporation, Phosgene-free polycarbonate process, http://www.asahi-kasei.co.jp/chemicals/en/license/page01.html, retrieved 15 April 2015.

12 Ernst & Young, http://iffcocan.com/iffco/IFFCO-CF_FinalΩReport-w-App-20130904.pdf, retrieved 22 October 2014.

13 Asia Pacific Energy Research Centre,http://aperc.ieej.or.jp/file/2010/9/26/APERC_2007_A_Quest_for_Energy_Security.pdf, retrieved 24 October 2014.

14 R. L. Rudnick and S. Gao, in *The Crust*, ed. K. Turekian and H. Holland, Elsevier, 2013, vol. 3, ch. 1.

15 T. J. Brown, A. S. Walters, N. E. Idoine, R. A. Shaw, C. E. Wrighton and T. Bide, *World Mineral Production 2006–2010*, British Geological Survey, Keyworth, Nottingham, 2012.

16 World Bank, http://info.worldbank.org/governance/wgi/index.aspx#home, retrieved 24 October 2014.

17 J. C. Mankins, Technology Readiness Levels, A White Paper, Advanced Concepts Office, Office of Space Access and Technology, NASA technical report, 1995.

18 Ceresana, http://www.ceresana.com/en/market-studies/agriculture/urea/, retrieved 22 October 2014.

19 M. Iijima, Mitsubishi Heavy Industries, http://www.gpcafertilizers.com/pdf/2011/12.pdf, retrieved 23 October 2014.

20 V. Macho, M. Králik, M. Olšovský, J. Jorniaková and D. Mravec, *Pet. Coal*, 2008, **50**, 30–38.

21 S. Inoue, H. Koinuma and T. Tsuruta, *J. Polym. Sci., Part B: Polym. Lett.*, 1969, **7**, 287.

22 H. Kawachi, S. Minami, J. N. Armor, A. Rokicki, B. K. Stein and Mitsui Petrochemical Industries Ltd., Pulverized reaction product of zinc oxide and dicarboxylic acid, *US Pat.*, 4,981,948, 1989.

23 E. K. Noh, S. J. Na, S. Sujith, S.-W. Kim and B. Y. Lee, *J. Am. Chem. Soc.*, 2007, **129**, 8082–8083.

24 C. Hao, S. Wang, M. Li, L. Kang and X. Ma, *Catal. Today*, 2011, **160**, 184–190.

25 M. W. Farlow and H. Adkins, *J. Am. Chem. Soc.*, 1935, **57**, 2222–2223.

26 A. Behr, P. Ebbinghaus and F. Naendrup, *Chem. Eng. Technol.*, 2004, **27**, 495–501.

27 G. A. Olah, *Angew. Chem., Int. Ed.*, 2005, **44**, 2636–2639.

28 R. Raudaskoski, E. Turpeinen, R. Lenkkeri, E. Pongracz and R. L. Keiski, *Catal. Today*, 2009, **144**, 318–323.

29 J. A. Castro-Osma, M. North and X. Wu, *Chem.–Eur. J.*, 2014, **20**, 15005–15008.

30 C. R. Gomes, D. M. Ferreira, C. J. Leopoldo Constantino and E. R. Perez Gonzalez, *Tetrahedron Lett.*, 2008, **49**, 6879–6881.

31 T. Yano, H. Matsui, T. Koike, H. Ishiguro, H. Fujihara, M. Yoshihara and T. Maeshima, *Chem. Commun.*, 1997, 1129–1130.

32 H. Zhu, L. B. Chen and Y. Y. Jiang, *Polym. Adv. Technol.*, 1996, **7**, 701–703.

33 L. A. Blanchard, D. Hancu, E. J. Beckman and J. F. Brennecke, *Nature*, 1999, **399**, 28–29.

34 W.-L. Dai, B. Jin, S.-L. Luo, X.-B. Luo, X.-M. Tu and C.-T. Au, *Catal. Sci. Technol.*, 2014, **4**, 556–562.

35 R. Voorhoeve, L. Trimble and D. Freed, *Science*, 1978, **200**, 759–761.

36 Market Wired, Mantra Signs Technology Development Cooperation Agreement for the Production of Green Chemicals in Korea Using Proprietary Carbon Capture and Recycling (CCR) Technology, 2010, http://www.marketwired.com/printer_friendly?id=1305650, retrieved 15 April 2015.

ART ■ C5FD00038F

A MALDI-TOF MS analysis study of the binding of 4-(*N*,*N*-dimethylamino)pyridine to amine-bis(phenolate) chromium(III) chloride complexes: mechanistic insight into differences in catalytic activity for CO_2/epoxide copolymerization

Christopher M. Kozak,* April M. Woods, Christina S. Bottaro, Katalin Devaine-Pressing and Kaijie Ni

Tetradentate amine-bis(phenolato)chromium(III) chloride complexes, [LCrCl], are capable of catalyzing the copolymerization of cyclohexene oxide with carbon dioxide to give poly(cyclohexane) carbonate. When combined with 4-(*N*,*N*-dimethylamino)pyridine (DMAP) these catalyst systems yield low molecular weight polymers with moderately narrow polydispersities. The coordination chemistry of DMAP with five amine-bis(phenolato)chromium(III) chloride complexes was studied by matrix assisted laser desorption/ionization time-of-flight mass spectrometry (MALDI-TOF MS). The amine-bis(phenolato) ligands were varied in the nature of their neutral pendant donor-group and include oxygen-containing tetrahydrofurfuryl and methoxyethyl moieties, or nitrogen-containing *N*,*N*-dimethylaminoethyl or 2-pyridyl moieties. The relative abundance of mono and bis(DMAP) adducts, as well as DMAP-free ions is compared under various DMAP : Cr complex ratios. The [LCr]$^+$ cations show the ability to bind two DMAP molecules to form six-coordinate complex ions in all cases, except when the pendant group is *N*,*N*-dimethylaminoethyl (compound **3**). Even in the presence of a 4 : 1 ratio of DMAP to Cr, no ions corresponding to [L^{3}Cr(DMAP)$_2$]$^+$ were observed for the complex containing the tertiary sp^3-hybridized amino donor in the pendant arm. The difference in DMAP-binding ability of these compounds results in differences in catalytic activity for alternating copolymerization of CO_2 and cyclohexene oxide. Kinetic investigations by infrared spectroscopy of compounds **2** and **3** show that polycarbonate formation by **3** is twice as fast as that of compound **2** and that no initiation time is observed.

Department of Chemistry, Memorial University of Newfoundland, St. John's, Newfoundland, A1B 3X7, Canada.
E-mail: ckozak@mun.ca; Tel: +1-709-864-8082

ART ■ C5FD00046G

Introduction

The copolymerization of carbon dioxide with epoxides to yield polycarbonates has become one of the most extensively studied process that generates potentially valuable materials from CO_2.[1-6] Carbon dioxide is an appealing C1 feedstock because it is widely available, inexpensive, and nontoxic.[7] The variety of metal complexes shown to perform this reaction is impressive and complexes containing metals such as Mg,[8] Al,[9-13] Zn,[14-22] Cr,[23-38] Co[6,39-58] and Fe[59] have been examined for use in the copolymerization of carbon dioxide (CO_2) and epoxides, particularly cyclohexene oxide (CHO) and propylene oxide (PO).

Homogeneous catalysts for epoxide/CO_2 copolymerization have involved various ligand classes including, for example, porphyrin Cr[24,60,61] and Al[13] compounds. Darensbourg and Holtcamp introduced the use of Zn phenoxides for epoxide/CO_2 copolymerization,[62-64] whereas Coates and co-workers explored the use of β-diketiminate (BDI) ligand systems with Zn at lower pressures and temperatures than had previously been reported.[14] Tetravalent group 4 (Ti and Zr) and 14 (Ge and Sn) metals supported by planar trianionic bis(phenolato) ligands reported by Nozaki and co-workers have shown activity towards epoxide and CO_2 copolymerization.[65] By far the most widely studied ligands for epoxide/CO_2 copolymerization have been the salen[3-5] and, more recently, the salan ligands, which have been primarily used with Cr (Fig. 1)[23,25-30,33,36,38,66] and Co.[39,44,45,52,53,67] These catalysts typically require nucleophilic co-catalysts such as chlorides, bromides or azides paired with bulky cations such as PPN (PPN = bis(-triphenylphosphoranylidene)ammonium) or tetrabutylammonium, or neutral bases such as N-methylimidazole (N-MeIm) or dimethylaminopyridine (DMAP).

Whereas compounds of the salen and salan ligands represent the most investigated homogeneous systems for CO_2/epoxide copolymerization, we are interested in the use of the related tetradentate amine-bis(phenolato) ligand class.[68-71] This ligand offers possibilities for the development of potentially highly active catalysts because of the modifiable nature of the donor sites, their steric and electronic properties, and their geometry, which differs from that exhibited by the salen and salan-based systems. Mechanistic information is, of course, beneficial for the design of highly efficient catalyst systems for CO_2/epoxide copolymerization[17,29,66,72-75] and mass spectrometry has been particularly useful in this regard. Electrospray ionization (ESI) mass spectrometry and collision-induced dissociation (CID) have been employed to study the interactions of DMAP co-catalyst with salen- and salan chromium chloride complexes and how these interactions influence catalyst activity.[66] ESI-MS has also been used to confirm intermediates in CO_2/PO copolymerization by single-site cobalt salen
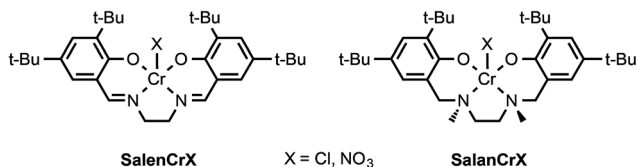
Fig. 1 Salen and salan chromium(III) complexes used in CO_2/epoxide copolymerization.

ART ■ C5FD00046G

catalysts.[54] Matrix assisted laser desorption/ionization time-of-flight (MALDI-TOF) MS has been used by Duchateau and co-workers to investigate zinc catalyzed copolymerization of cyclohexene oxide and CO_2.[76,77]

Darensbourg and co-workers have conducted elegant kinetics studies on epoxide/CO_2 copolymerization catalyzed by binary salenCrX (where X = Cl^- or N_3^-) with Lewis basic (neutral or ionic) co-catalysts, wherein initiation was proposed to occur *via* a bimetallic process and propagation *via* a monometallic enchainment of epoxides.[25,26,78,79] These reports suggest that the binding of the co-catalyst to the metal centre labilizes the *trans*-orientated growing polymer chain. A released "free" alkoxide or carboxylate-terminated polymer fragment promotes insertion of CO_2 into the metal–alkoxide bond. These salen-based complexes also exhibit long induction periods that are not observed in related salan-based systems employing DMAP as the added Lewis base. In this report, we use MALDI-TOF MS to examine the DMAP binding affinity for five amine-bis(phenolato)chromium chloride complexes (Fig. 2). The observed resistance to dimer and bis(DMAP) adduct formation in complex **3** is believed to corroborate with the absence of an induction period, and a faster rate of polycarbonate formation catalyzed by this complex *vs.* the other derivatives. These studies provide a comparative assessment of the mechanistic behaviour of amine-bis(phenolate)chromium-based catalysts for CO_2/epoxide copolymerization against the benchmark of salen and salan chromium(III) systems.

Experimental

Unless otherwise stated, all manipulations were performed under an atmosphere of dry, oxygen-free nitrogen by means of standard Schlenk techniques or using an MBraun Labmaster DP glove box. Anhydrous dichloromethane was obtained by purification using an MBraun Manual Solvent Purification System. Reagents were purchased either from Aldrich or Alfa Aesar and used without further purification. Complexes **1–5** were prepared *via* previously reported methods.[68,80]
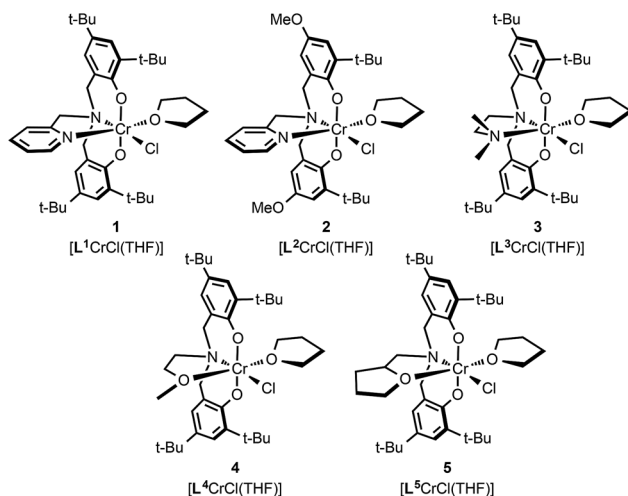
Fig. 2 Chromium(III) complexes used in this study.

MALDI-TOF MS was performed using an Applied Biosystems 4800 MALDI TOF/ TOF Analyzer equipped with a reflectron, delayed ion extraction and high performance nitrogen laser (200 Hz operating at 355 nm). Samples were prepared in the glove box and sealed under nitrogen in a Ziploc© bag for transport to the instrument. Anthracene was used as the matrix. The matrix, complex and DMAP were dissolved in dichloromethane at a concentration of approximately 1 mg per 0.1 mL. The complex and DMAP were mixed together in ratios of 1 : 0.5, 1 : 1, 1 : 2 and 1 : 4, and once combined with the matrix, 0.5 μL of this mixture was spotted onto a MALDI plate and left to dry under nitrogen in a glove box. Images of the mass spectra were prepared using mMass™ software (http://www.mmass.org).

Infrared spectra of the reaction progress were obtained using a Mettler-Toledo ReactIR™ 15 spectrometer equipped with silver halide fibre conduit attached to a SiComp Sentinel™ high-pressure window fitted to a 100 mL stainless steel Parr autoclave reactor.

A representative preparation of samples for analysis by MALDI-TOF MS is provided. 0.2094 g of complex **1** (3.3225×10^{-4} mol) and 0.0397 g of DMAP (3.249×10^{-4} mol) were placed in a sample vial and just enough dichloromethane was added to dissolve the solids. This solution was filtered through a glass fibre plug into another sample vial and the vial was capped, sealed with Parafilm and stored at $-35\ ^{\circ}$C in the glove box freezer until required.

A stock solution of 8.7 mg of anthracene in 800 μL of dichloromethane was prepared. Samples of complex **1** with their required DMAP loading were dried under vacuum. A measured quantity of each sample was dissolved in 200 μL of CH_2Cl_2 and 80 μL of this solution was transferred to another vial along with 80 μL of the stock anthracene solution. These solutions were spotted onto a MALDI plate and the spectra were obtained.

For MALDI-TOF MS analysis on samples exposed to air, all prepared samples, once analyzed under the air-free preparation described above, were removed from the glove box and exposed to air. The solvents were allowed to evaporate and after two or three days the samples were redissolved in CH_2Cl_2 and analyzed once again.

Results and discussion

The binding of DMAP to five chromium complexes (Fig. 2) was investigated by preparing dichloromethane solutions of each complex with varying ratios of DMAP. The resulting solutions were evaporated until dry and then re-dissolved with the matrix (anthracene). These solutions of analyte and matrix were spotted onto the MALDI plate in air and under air-free conditions. The MALDI-TOF mass spectra of complexes **1**, **2**, **4** and **5** in the absence of DMAP exhibited numerous ions, including ions resulting from dimers and their fragments. The exception was complex **3**, which gave a relatively clean spectrum showing two main ions corresponding to $[\mathbf{L^3}CrCl]^{+\cdot}$ and $[\mathbf{L^3}Cr]^+$. Ions containing the weakly coordinating THF present in **1–5** are, as anticipated, consistently absent from the mass spectra of these complexes. The MALDI-TOF MS of mixtures of complexes **1– 5** and varying amounts of DMAP showed the presence of complicated mixtures of ions. The ions observed or predicted for complex **2** in the presence of DMAP are given in Fig. 3. The labels **F1–F12** also apply to ions arising from complexes **1** and **3–5**, except of course for the nature of the amine-bis(phenolato) ligand present ($\mathbf{L^1}$
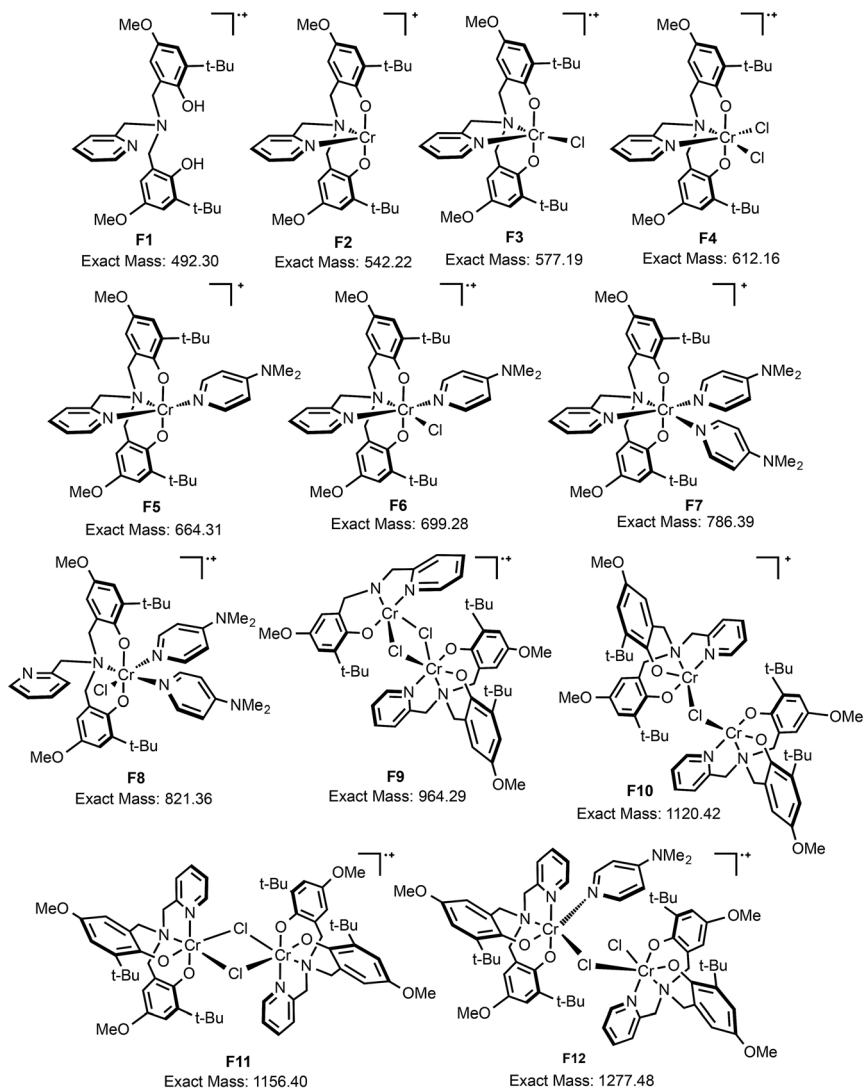
Fig. 3 Anticipated and observed fragments for complex **2**. Fragments of complexes **1** and **3–5** are represented by the analogous structures shown for **F1–F12**.

to L^5, present in complexes **1–5**, respectively). The MALDI-TOF mass spectra for **2**/DMAP and **3**/DMAP mixtures in different molar ratios are shown in Fig. 4. When the molar ratio of **2** to DMAP is 1 : 0.5, a complicated mass spectrum results and many ions could not be readily identified. It is clear, however, that dichromium-containing ions are present along with DMAP-containing fragments, including $[L^2CrCl(DMAP)]^{+\bullet}$, **F6**. Furthermore, a significant abundance of ions attributed to an unmetallated ligand, H_2L^2 (**F1**), are observed. With an increase in the DMAP to Cr ratio of 1 : 1, the mass spectrum simplifies considerably and readily identifiable ions are observed. Under these conditions, the base peak occurs at m/z 577.1, corresponding to $[L^2CrCl]^{+\bullet}$ (**F3**), with the next most abundant peak at m/z 699.2,
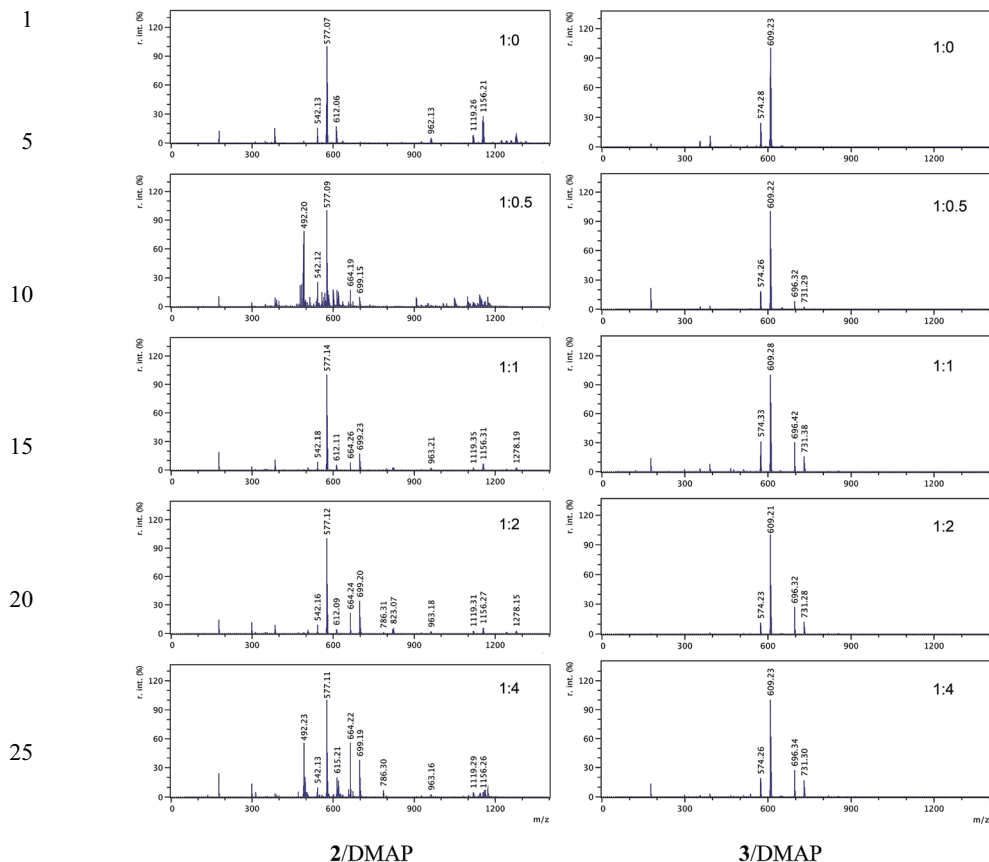
Fig. 4 MALDI-TOF mass spectra of the mixtures resulting from combinations of complex **2** (left) and complex **3** (right) with different molar ratios of DMAP as shown: 1 : 0, 1 : 0.5, 1 : 1, 1 : 2 and 1 : 4.

representing $[\mathbf{L^2CrCl(DMAP)}]^{+\bullet}$. Ions at higher m/z corresponding to dichromium-containing fragments **F9**, **F10**, **F11** and **F12** were also observed. Increasing the loading of DMAP further (**2** : DMAP of 1 : 2 and 1 : 4) resulted in the formation of $[\mathbf{2} - \text{THF} - \text{Cl} + 2\text{DMAP}]^+$ ions, **F7**. The **3**/DMAP system demonstrates much less complex mass spectra. The addition of 0.5 equiv. of DMAP per Cr centre causes the appearance of $[\mathbf{L^3Cr(DMAP)}]^+$ (**F5**) and $[\mathbf{L^3CrCl(DMAP)}]^{+\bullet}$ (**F6**), and increasing the DMAP to Cr ratio (2 and 4 equiv. DMAP to Cr) has little influence on the number of ions observed and there was no evidence of $[\mathbf{L^3Cr(DMAP)_2}]^+$ (**F7**) or dichromium-containing ions. The other significant species observed in the **3**/DMAP system is **F4** (m/z 574.3), which results from chloride loss to give $[\mathbf{L^3Cr}]^+$. It is interesting that even with 4 equiv. of DMAP the base peaks for both **2** and **3** correspond to the DMAP-free ion, **F3**, with a m/z of 577.1 for **2** and 609.2 for **3**, which suggests that this ion exhibits a surprisingly high stability even to loss of chloride. Six-coordinate species of **3** appear to be unfavourable, as shown by the much higher abundance of the four- and five-coordinate ions, **F2**, **F4** and **F5**.

A comparison of the relative abundance of the various fragment ions in compounds **1–5** with different amounts of DMAP added is shown in Fig. 5. For all five complexes, the abundance of the DMAP-coordinated cation, $[\text{LCr(DMAP)}]^+$ **F5**, increases expectedly when increasing amounts of DMAP are added. Changing the pendant donor group, however, appears to influence the coordination chemistry of DMAP with these complexes, as well as the stability of the complexes themselves in the gas phase. The nitrogen donor pendant arms, *i.e.* pyridyl in **1** and **2** (abbreviated as BuBuPyr and BuMethPyr in Fig. 5), and dimethylaminoethyl in **3** (abbreviated as BuBuNMe$_2$ in Fig. 5) generate very stable molecular ions **F3**, which comprise the base peaks in their respective mass spectra. Oxygen donor pendant arms, *i.e.* methoxyethyl in **4** (abbreviated as BuBuMe in Fig. 5) and, in particular, tetrahydrofurfuryl in **5** (abbreviated as BuBuTHF in Fig. 5) show a lower stability
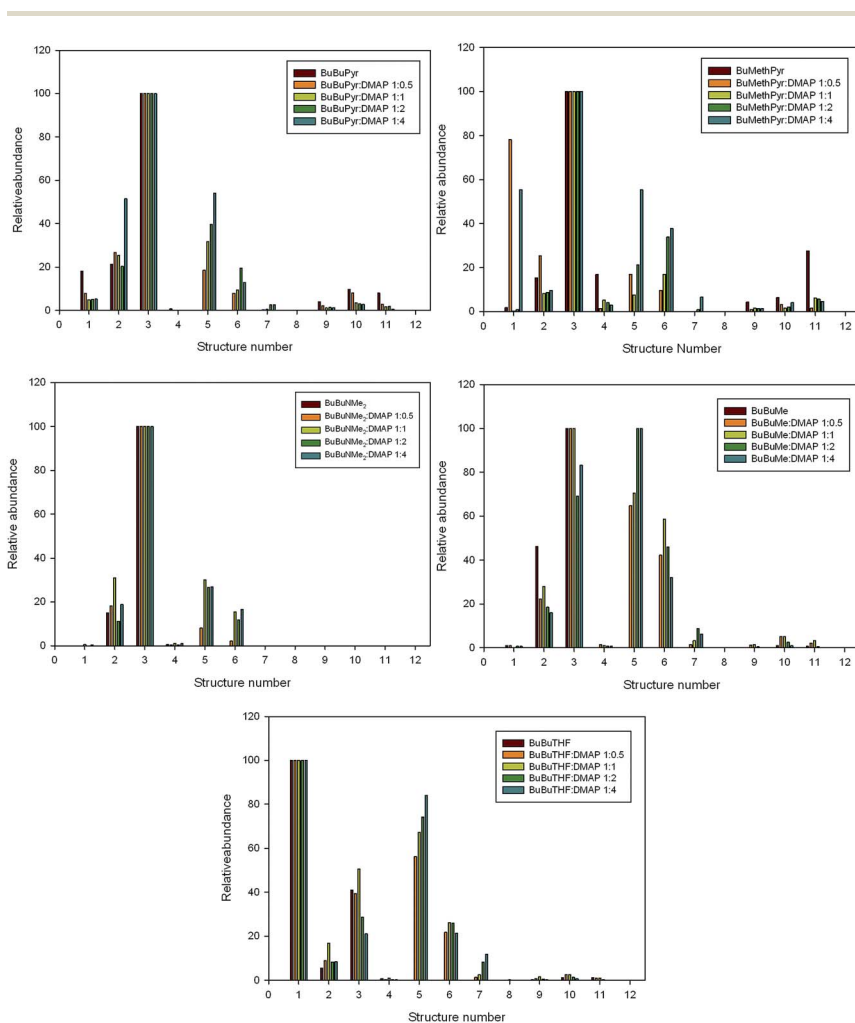
Fig. 5 Comparison of the relative abundance of fragment ions in compounds **1–5** with varying amounts of DMAP, as indicated. Relative abundance is given in % and structure numbers 1–12 correspond to the fragments/ions shown in Fig. 3.

ART ■ C5FD00046G

of the molecular ions as judged by the lower relative abundance. As the amount of DMAP is increased compared to **4**, the DMAP adduct accompanied by chloride loss ([**L⁴**Cr(DMAP)]⁺, **F5**) becomes more abundant as well as the DMAP coordinated radical cation, [**L⁴**CrCl(DMAP)]⁺˙ **F6**. Complex **5** stands out as being most readily fragmented under MALDI conditions. The base peak was consistently identified as the unmetallated ligand, $H_2\mathbf{L}^5$ at m/z 537.4 (the isotopic pattern of this ion is actually a combination of the radical cation of $[H_2\mathbf{L}^5]^{+\bullet}$ as well as $[H\mathbf{L}^5]^{+\bullet}$ and $[\mathbf{L}^5]^{+\bullet}$ resulting from losses of H˙ and/or single electrons during laser desorption). This suggests that $\mathbf{L}^5$ is (relatively) poor at stabilizing Cr(III) complexes. Our previous reports of the CO_2/cyclohexene oxide copolymerization catalyzed by **5** with a DMAP co-catalyst showed moderate activities (conversions of 64%, average TONs of 300, $M_n \sim 6000$ g mol⁻¹, $Đ = 1.5$–1.7).[70] By comparison, we observed that the catalyst system comprised of **1**/DMAP under these conditions provided conversions of 80% (TON of 400, $M_n \sim 10\,000$ g mol⁻¹, $Đ = 1.1$ to 1.7).[68]

The difference in ion stability observed between compound **3** and the other four complexes can perhaps be attributed to the steric hindrance created by the dimethylaminoethyl group found in $\mathbf{L}^3$/complex **3**. Furthermore, the presence of two sp³-hybridized amino donors in **3** reduces the Lewis acidity of the metal centre. Therefore, sterically the Cr centre is more encumbered preventing the formation of chloride-bridged dimers, as previously[68] crystallographically authenticated for $[\mathbf{L}^1\text{Cr}]_2(\mu\text{-Cl})_2$ and as postulated based on the presence of m/z 1260.6 (corresponding to **F11**) in the MALDI-TOF mass spectrum of **1**. Electronically, the more electron-rich Cr centre in **3** compared to **1**, for example, results in a lower affinity for the neutral DMAP than the anionic chloride ligand. A similar trend has been observed in comparing the affinity of salenCrX and salanCrX complexes (Fig. 1) for DMAP.[66] These trends in binding affinity for DMAP are believed to influence the CO_2/epoxide copolymerization activity of the binary catalyst systems of salenCrCl and salanCrCl with DMAP. Rieger and co-workers reported the selectivity for copolymerization of CO_2 with propylene oxide (PO) catalyzed by salenCrCl and DMAP improved considerably with a salenCrCl : DMAP ratio of 1 : 0.5.[27] Therefore, the formation of species containing one DMAP rather than two is likely preferred for initiation of copolymerization.[66]

The mechanism of copolymerization of CO_2 and cyclohexene oxide by binary catalyst systems of salenCrX and N-heterocyclic bases such as DMAP has been investigated in detail by Darensbourg.[29] The proposed mechanism involves the formation of carbamate intermediates resulting from the reaction of DMAP with CO_2 to generate a zwitterion, which was identified by ν_{CO_2} bands at 2097 and 2017 cm⁻¹. Furthermore, Darensbourg reports a correlation between the disappearance of "free DMAP" as observed by *in situ* FTIR with the initiation time observed for the formation of polycarbonate. Lu and co-workers studied the initiator role of DMAP in CO_2/propylene oxide copolymerization by ESI-MS and observed species corresponding to [–OCH(CH₃)CH₂–DMAP⁺ + H⁺] and, with time, the growth of peaks corresponding to the addition of units of PO + CO_2, that is, m/z [181.1 + $n(102)$]. This was interpreted as evidence that the formation of carbamate zwitterions is not required for initiation of copolymerization. We have conducted detailed end group analysis of poly(cyclohexane)-carbonate[68,70] and poly(propylene)carbonate[69] formed by catalyst systems composed of **1**, **2** and **5** with DMAP. Use of complex **1** or **2** with 0.5 or 1 molar equiv. of DMAP in 500 molar equiv. of neat CHO shows only –Cl and –OH end groups with no initiation by

DMAP observed. When a mixture of co-catalysts is used, the end group properties become more complicated. The polymer obtained using a $1:1:1$ mixture of complex **2**, DMAP and PPNCl (bis(triphenylphosphine)iminium chloride) under the same conditions results in MALDI-TOF mass spectra where –Cl, –DMAP and –OH end groups are observed (Fig. 6). It is likely that the presence of the additional equiv. of nucleophile competes with the binding of DMAP to the chromium centre, hence generating more "free DMAP", which can undergo an intermolecular nucleophilic attack at a chromium-bound epoxide. We also previously reported the MALDI-TOF MS characterization of a polymer obtained using the tetrahydrofurfuryl-functionalized complex **5** and DMAP.[70] Interestingly, the **5**/DMAP catalyst system *also* showed complicated mass spectra with –Cl, DMAP and –OH end groups despite using equimolar amounts of **5** and DMAP and the apparent stronger bonding affinity of DMAP to the Cr centre in **5** (*i.e.* the appearance of $[\mathbf{L^5Cr(DMAP)_2}]^+$ ions for $1:1$ rations of $\mathbf{5}:\mathrm{DMAP}$). However,

$[122\ (C_7H_{10}N_2) + 142n\ (\text{repeating unit}) + 82\ (C_6H_{10}) + 17\ (OH)]$
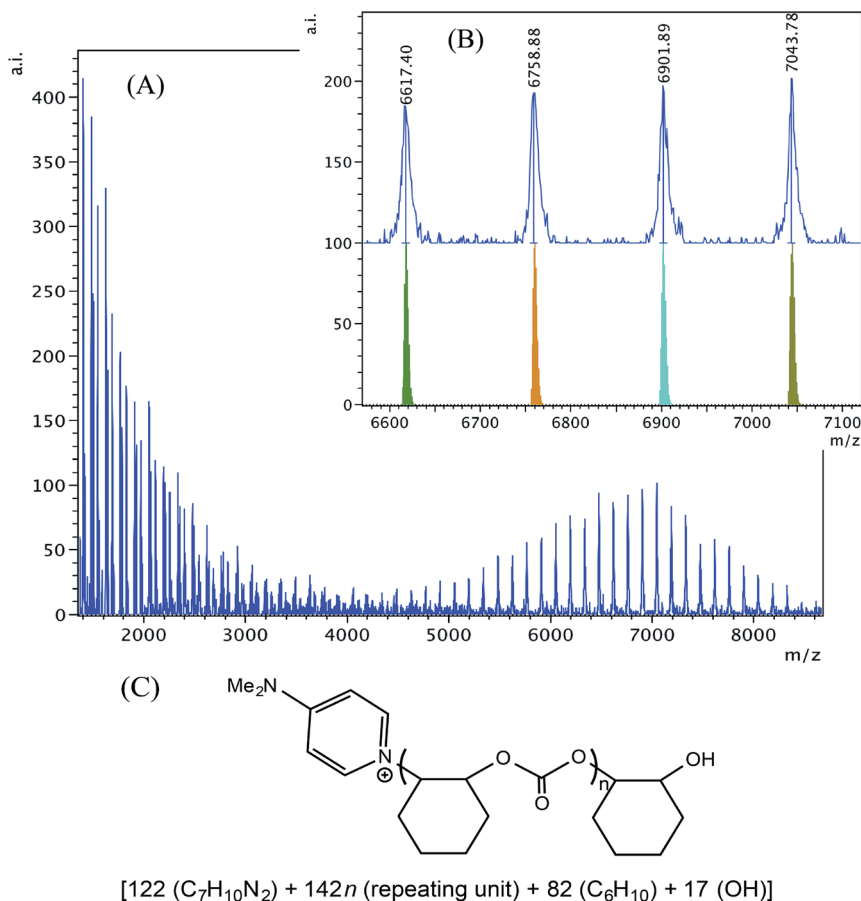
Fig. 6 (A) MALDI-TOF mass spectrum of polycarbonate produced by equimolar **2**/DMAP/PPNCl at 60 °C and 40 bar CO_2. (B) Higher mass region (m/z 6600–7100, $n = 45$–48) of the spectrum with calculated masses of fragments shown beneath the observed spectrum. (C) Proposed structure of the high mass range polymer.

whereas the base peak for compounds **1–4** correspond to $[\text{LCrCl}]^{+\bullet}$ (**F3**) the base peak for **5** is the unmetallated ligand, $[\text{H}_2\text{L}^5]^{+\bullet}$ (**F1**), regardless of the DMAP concentration. This suggests the L^5 ligand coordinates more weakly to the metal than L^1–L^4, and this results in the poorly controlled polymerization previously observed.

It has been observed that the salenCrX/DMAP system differs considerably from the salanCrX/DMAP system in that it exhibits a lengthy induction period of up to 2 h for the copolymerization of CO_2/PO. The salanCrX/DMAP system, on the other hand, shows propagation of the polymer after a period of 10 min.[66] Also, the salanCrX system displays higher TOFs, selectivity for polymer over cyclic carbonate formation, and gives higher polymer molecular weights with narrow dispersities. The differences in activity were attributed to the differing affinity for DMAP binding to the salan- and salen chromium compounds. Furthermore, as DMAP loading is increased, a decrease in polymer molecular weight is observed for both the salanCrX and salenCrX catalyst systems.[25,27,66,79] The relationship between induction period, reaction rate and DMAP-binding affinity for amine-bis(phenolate)chromium chloride complexes was investigated in order to assess whether a similar trend is observed to that of the salan and salen-based systems. The copolymerization of CHO with CO_2 by complexes **2** and **3** using $1:1$ DMAP : Cr in 500 molar equiv. of neat epoxide was conducted at 60 °C and 40 bar CO_2. The reaction rates were monitored by infrared spectroscopy following the carbonate region (absorbance at 1750 cm^{-1}) over time (Fig. 7). The time profile for the first hour shows virtually no induction period for **3**/DMAP, and only a short one (approx. 10 min.) for **2**/DMAP. The polymerization rate of **3**/DMAP was also observed to be much faster than that of complex **2** (Fig. 8). These results are in agreement with the MALDI-TOF MS analysis above, namely the propensity of **2** to form stable, six-coordinate adducts and dimers results in a lower activity towards
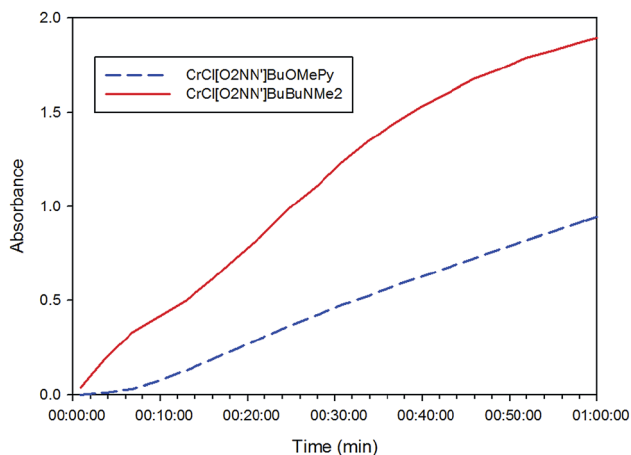
Fig. 7   Time profiles (for the first h) of the absorbance at 1750 cm^{-1} (corresponding to polycarbonate) using **2** (dashed blue line) and **3** (solid red line) as the catalyst. Reaction conditions: [Cr] : [CHO] : [DMAP] $= 1 : 500 : 1$, 24 h total experiment time, 60 °C, 40 bar CO_2.
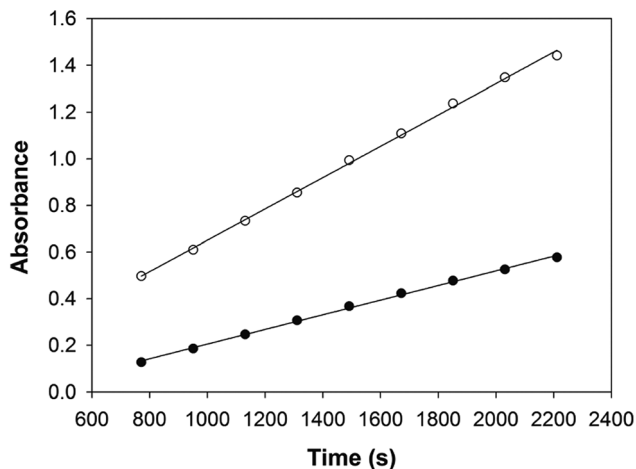
Fig. 8 Representative plots of absorbance *vs.* time for the linear portion of polycarbonate formation for the data presented in Fig. 7. Straight lines represent best fits of the data for compound **2** (●), $y = 3.15 \times 10^{-4}x$ to 1.10×10^{-1}, $R^2 = 9.99 \times 10^{-1}$; and compound **3** (○) $y = 6.72 \times 10^{-4}x$ to 2.09×10^{-2}, $R^2 = 9.99 \times 10^{-1}$.

epoxide/CO_2 copolymerization than complex **3**, which shows no evidence of dimer formation and a relatively low abundance of six-coordinate $[\mathbf{L^3}CrCl(DMAP)]^{+\bullet}$.

Comparisons of the possible mechanisms of action of salenCrX and salanCrX complexes have identified the nature of the binding of the tetradentate ligand as being influential in catalyst activity.[29,35,37,66,81] The crystallographically authenticated salenCrX and salenCrXL complexes (where X is a monodentate anionic ligand, *e.g.* Cl^- or $N_3{}^-$, and L is a neutral monodentate ligand, *e.g.* DMAP or O=PCy_3) show the salen ligand exhibits a planar orientation. SalanCrXL complexes, however, with the presence of sp^3-hybridized tertiary amino donors give distorted octahedral structures where the tetradentate salan ligand occupies *cis*-α or *cis*-β orientations, where the two monodentate ligands are found in *cis*-positions rather than the *trans* coordination mode often found in salenCrXL complexes. The amine-bis(phenolate) complexes **1–5** exhibit bonding orientations related to the salan systems. Based on the above comparisons and on the observed end-groups in the polycarbonates obtained under equimolar ratios of DMAP/PPNCl to the Cr compounds, and comparisons of the influence of the ligand on the ability for stable six-coordinate ions to be observed by MALDI-TOF MS, a mechanism can be proposed for CO_2/epoxide copolymerization by **1–5** with DMAP as the co-catalyst. The initiation steps available for the complex **3**/DMAP catalyst system are shown in Scheme 1. The relative abundance of **F3** and **F5** compared to **F6** suggests that the first equilibrium lies to the right, leading to a very short induction period. Also, whereas dimer formation is observed in the MALDI-TOF mass spectrum of **1**, **2**, **4** and **5**, no evidence of dimeric **3** was observed. Dimer formation, therefore, may be a reason for the presence of the induction period observed for **2** but not for complex **3**. As previously proposed by Lu and co-workers, progress along either path A or B may be inhibited by excess DMAP, leading to the formation of $[\mathbf{L}Cr(DMAP)_2]^+$ in the case of path A, or increase the reversibility of the first equilibrium step in path B by hindering DMAP dissociation. Competitive binding

ART ■ C5FD00046G
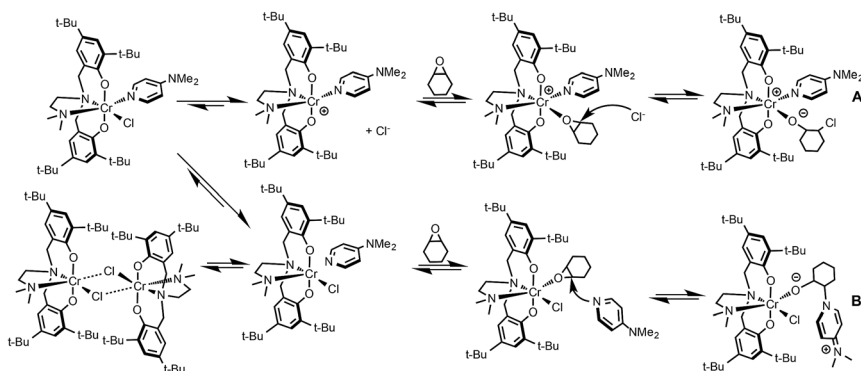
Scheme 1 Two initiation paths *via* an intermolecular nucleophilic attack available for **3**/DMAP. Path A leads to initiation by Cl; path B leads to initiation by DMAP.

of epoxide allows activation of the first monomer fragment, which undergoes nucleophilic attack by either Cl⁻ or DMAP. For conditions where DMAP end groups are absent (as for 1 : 0.5 or 1 : 1 combinations of complex **1** or **2** with DMAP as discussed above), path A is preferred resulting from the high affinity of DMAP bonding to the metal centre. For complex **3**, which is more electron rich at the Cr centre, DMAP dissociation at lower concentrations of that base is more prevalent, hence "free DMAP" is available to induce ring opening of the epoxide, generating –DMAP terminated polycarbonate (path B). DFT studies have been reported on the mechanism of epoxide/CO_2 copolymerization by metal salen complexes.[82] Rieger and co-workers proposed that the growing polymer chains undergo dissociation from the metal centre during polymerization, with chain-transfer resulting from high co-catalyst loading leading to low molecular weight polymers.[73] Baik and Nguyen studied the role of DMAP in salenCr-catalyzed PO/CO_2 copolymerization.[72] Their findings support the role of the salenCrCl complex as a Lewis acid that activates the epoxide ring, promoting its opening by an external nucleophile, such as DMAP. No evidence for a bimetallic pathway or simultaneous activation of both the epoxide and CO_2 was obtained. Unlike Rieger's proposal, attempts at creating an unsaturated Cr(III) centre through chloride loss or alkoxide dissociation resulted in significant energy penalties. Baik and Nguyen concluded that such steps were not possible in this case, therefore a ring-opening step similar to that shown in Scheme 1B is favoured. If the same case holds for compounds **1–5**, the presence of an epoxide ring opening by chloride (leading to the observed –Cl end groups using MALDI-TOF MS) implies this step must happen by an intramolecular mechanism akin to a migratory insertion between cisoid ligands on the metal centre. Computational studies to investigate this possibility are currently underway.

Conclusions

The MALDI-TOF mass spectra of amine-bis(phenolato)chromium(III) chloride complexes in the presence of DMAP in various amounts demonstrated that the ability of DMAP to bind to the chromium centre was influenced by the nature of the pendant neutral donor group on the tetradentate ligand. Where the donor was

an ether (methoxyethyl or tetrahydrofurfuryl) or pyridyl group (complexes **1**, **2**, **4** and **5**), binding of two DMAP molecules was observed. These complexes also demonstrated a propensity to form dimeric species, likely *via* chloride-bridges that we have previously structurally authenticated. For dimethylaminoethyl-functionalized ligands, no evidence for the binding of two DMAP molecules was observed, even at four equiv. of DMAP per Cr. Furthermore, no dimeric species were observed in their mass spectra. This difference in coordination chemistry was found to influence the catalytic activity of these compounds towards the copolymerization of CO_2 with cyclohexene oxide. In the presence of **1** equiv. of DMAP, the activity of the diamino-bis(phenolato)chromium chloride complex **3** was found to be faster than that of complex **2**. End group analysis of the polymers by MALDI-TOF MS suggests that the DMAP-containing end groups occur when the concentration of unbound DMAP is high, suggesting an inter-molecular nucleophilic attack. Chloride-containing end-groups were most commonly observed at molar equiv. levels of DMAP loading, suggesting that DMAP is not competitive with chloride in terms of epoxide ring-opening, and that binding to the metal centre is more favourable. Interestingly, increasing the chloride concentration leads to DMAP-containing polycarbonate, which may be explained by the formation of dichloride chromium species and release of free DMAP into the reaction.

Acknowledgements

Notes and references

1 D. J. Darensbourg, *Chem. Rev.*, 2007, **107**, 2388–2410.

2 G. W. Coates and D. R. Moore, *Angew. Chem., Int. Ed.*, 2004, **43**, 6618–6639.

3 M. R. Kember, A. Buchard and C. K. Williams, *Chem. Commun.*, 2011, **47**, 141–163.

4 D. J. Darensbourg, *Inorg. Chem.*, 2010, **49**, 10765–10780.

5 S. Klaus, M. W. Lehenmeier, C. E. Anderson and B. Rieger, *Coord. Chem. Rev.*, 2011, **255**, 1460–1479.

6 X.-B. Lu and D. J. Darensbourg, *Chem. Soc. Rev.*, 2012, **41**, 1462–1484.

7 M. Aresta, *Carbon Dioxide as Chemical Feedstock*, Wiley-VCH, Weinheim, 2010.

8 M. R. Kember and C. K. Williams, *J. Am. Chem. Soc.*, 2012, **134**, 15676–15679.

9 D. J. Darensbourg and D. R. Billodeaux, *Inorg. Chem.*, 2005, **44**, 1433–1442.

10 T. Aida and S. Inoue, *Acc. Chem. Res.*, 1996, **29**, 39–48.

11 T. Aida, M. Ishikawa and S. Inoue, *Macromolecules*, 1986, **19**, 8–13.

12 T. Aida and S. Inoue, *J. Am. Chem. Soc.*, 1983, **105**, 1304–1309.

13 F. Kojima, T. Aida and S. Inoue, *J. Am. Chem. Soc.*, 1986, **108**, 391–395.

14 M. Cheng, E. B. Lobkovsky and G. W. Coates, *J. Am. Chem. Soc.*, 1998, **120**, 11018–11019.

ART ■ C5FD00046G

15 M. Super, E. Berluche, C. Costello and E. Beckman, *Macromolecules*, 1997, **30**, 368–372.

16 T. Sarbu and E. J. Beckman, *Macromolecules*, 1999, **32**, 6904–6912.

17 M. Cheng, D. R. Moore, J. J. Reczek, B. M. Chamberlain, E. B. Lobkovsky and G. W. Coates, *J. Am. Chem. Soc.*, 2001, **123**, 8738–8749.

18 D. R. Moore, M. Cheng, E. B. Lobkovsky and G. W. Coates, *Angew. Chem., Int. Ed.*, 2002, **41**, 2599–2602.

19 B. Y. Lee, H. Y. Kwon, S. Y. Lee, S. J. Na, S. I. Han, H. S. Yun, H. Lee and Y. W. Park, *J. Am. Chem. Soc.*, 2005, **127**, 3031–3037.

20 M. Kroger, C. Folli, O. Walter and M. Doring, *Adv. Synth. Catal.*, 2005, **347**, 1325–1328.

21 M. R. Kember, P. D. Knight, P. T. R. Reung and C. K. Williams, *Angew. Chem., Int. Ed.*, 2009, **48**, 931–933.

22 Y. L. Xiao, Z. Wang and K. L. Ding, *Chem.–Eur. J.*, 2005, **11**, 3668–3678.

23 R. L. Paddock and S. T. Nguyen, *J. Am. Chem. Soc.*, 2001, **123**, 11498–11499.

24 S. Mang, A. I. Cooper, M. E. Colclough, N. Chauhan and A. B. Holmes, *Macromolecules*, 2000, **33**, 303–308.

25 D. J. Darensbourg and J. C. Yarbrough, *J. Am. Chem. Soc.*, 2002, **124**, 6335–6342.

26 D. J. Darensbourg, J. C. Yarbrough, C. Ortiz and C. C. Fang, *J. Am. Chem. Soc.*, 2003, **125**, 7586–7591.

27 R. Eberhardt, M. Allmendinger and B. Rieger, *Macromol. Rapid Commun.*, 2003, **24**, 194–196.

28 D. J. Darensbourg, R. M. Mackiewicz, J. L. Rodgers, C. C. Fang, D. R. Billodeaux and J. H. Reibenspies, *Inorg. Chem.*, 2004, **43**, 6024–6034.

29 D. J. Darensbourg and R. M. Mackiewicz, *J. Am. Chem. Soc.*, 2005, **127**, 14026–14038.

30 D. J. Darensbourg, R. M. Mackiewicz and D. R. Billodeaux, *Organometallics*, 2005, **24**, 144–148.

31 B. Li, R. Zhang and X. B. Lu, *Macromolecules*, 2007, **40**, 2303–2307.

32 X. Q. Xu, C. M. Wang, H. R. Li, Y. Wang, W. L. Sun and Z. Q. Shen, *Polymer*, 2007, **48**, 3921–3924.

33 B. Li, G. P. Wu, W. M. Ren, Y. M. Wang, D. Y. Rao and X. B. Lu, *J. Polym. Sci., Part A: Polym. Chem.*, 2008, **46**, 6102–6113.

34 D. J. Darensbourg and S. B. Fitch, *Inorg. Chem.*, 2009, **48**, 8668–8677.

35 D. J. Darensbourg, M. Ulusoy, O. Karroonnirum, R. R. Poland, J. H. Reibenspies and B. Çetinkaya, *Macromolecules*, 2009, **42**, 6992–6998.

36 K. Nakano, M. Nakamura and K. Nozaki, *Macromolecules*, 2009, **42**, 6972–6980.

37 D. J. Darensbourg, R. R. Poland and A. L. Strickland, *J. Polym. Sci., Part A: Polym. Chem.*, 2012, **50**, 127–133.

38 L. P. Guo, C. M. Wang, W. J. Zhao, H. R. Li, W. L. Sun and Z. Q. Shen, *Dalton Trans.*, 2009, 5406–5410.

39 C. T. Cohen, T. Chu and G. W. Coates, *J. Am. Chem. Soc.*, 2005, **127**, 10869–10878.

40 C. T. Cohen and G. W. Coates, *J. Polym. Sci., Part A: Polym. Chem.*, 2006, **44**, 5182–5191.

41 M. R. Kember, F. Jutz, A. Buchard, A. J. P. White and C. K. Williams, *Chem. Sci.*, 2012, **3**, 1245–1255.

42 M. R. Kember, A. J. P. White and C. K. Williams, *Macromolecules*, 2010, **43**, 2291–2298.

ART ■ C5FD00046G

43 B. Liu, Y. Gao, X. Zhao, W. Yan and X. Wang, *J. Polym. Sci., Part A: Polym. Chem.*, 2010, **48**, 359–365.

44 B. Liu, X. Zhao, H. Guo, Y. Gao, M. Yang and X. Wang, *Polymer*, 2009, **50**, 5071–5075.

45 X. B. Lu and Y. Wang, *Angew. Chem., Int. Ed.*, 2004, **43**, 3574–3577.

46 K. Nakano, S. Hashimoto, M. Nakamura, T. Kamada and K. Nozaki, *Angew. Chem., Int. Ed.*, 2011, **50**, 4868–4871.

47 K. Nakano, S. Hashimoto and K. Nozaki, *Chem. Sci.*, 2010, **1**, 369–373.

48 K. Nakano, T. Kamada and K. Nozaki, *Angew. Chem., Int. Ed.*, 2006, **45**, 7274–7277.

49 Y. S. Niu, H. C. Li, X. S. Chen, W. X. Zhang, X. Zhuang and X. B. Jing, *Macromol. Chem. Phys.*, 2009, **210**, 1224–1229.

50 Y. S. Niu, W. X. Zhang, X. Pang, X. S. Chen, X. L. Zhuang and X. B. Jing, *J. Polym. Sci., Part A: Polym. Chem.*, 2007, **45**, 5050–5056.

51 E. K. Noh, S. J. Na, S. Sujith, S.-W. Kim and B. Y. Lee, *J. Am. Chem. Soc.*, 2007, **129**, 8082–8083.

52 R. L. Paddock and S. T. Nguyen, *Macromolecules*, 2005, **38**, 6251–6253.

53 Z. Q. Qin, C. M. Thomas, S. Lee and G. W. Coates, *J. Am. Chem. Soc.*, 2003, **42**, 5484–5487.

54 W.-M. Ren, Z.-W. Liu, Y.-Q. Wen, R. Zhang and X.-B. Lu, *J. Am. Chem. Soc.*, 2009, **131**, 11509–11518.

55 W. M. Ren, X. Zhang, Y. Liu, J. F. Li, H. Wang and X. B. Lu, *Macromolecules*, 2010, **43**, 1396–1402.

56 J. E. Seong, S. J. Na, A. Cyriac, B.-W. Kim and B. Y. Lee, *Macromolecules*, 2010, **43**, 903–908.

57 L. Shi, X. B. Lu, R. Zhang, X. J. Peng, C. Q. Zhang, J. F. Li and X. M. Peng, *Macromolecules*, 2006, **39**, 5679–5685.

58 S. Sujith, J. K. Min, J. E. Seong, S. J. Na and B. Y. Lee, *Angew. Chem., Int. Ed.*, 2008, **47**, 7306–7309.

59 A. Buchard, M. R. Kember, K. G. Sandeman and C. K. Williams, *Chem. Commun.*, 2011, **47**, 212–214.

60 W. J. Kruper and D. V. Dellar, *J. Org. Chem.*, 1995, **60**, 725–727.

61 L. M. Stamp, S. A. Mang, A. B. Holmes, K. A. Knights, Y. R. de Miguel and I. F. McConvey, *Chem. Commun.*, 2001, 2502–2503.

62 D. J. Darensbourg and M. W. Holtcamp, *Macromolecules*, 1995, **28**, 7577–7579.

63 D. J. Darensbourg, M. W. Holtcamp, G. E. Struck, M. S. Zimmer, S. A. Niezgoda, P. Rainey, J. B. Robertson, J. D. Draper and J. H. Reibenspies, *J. Am. Chem. Soc.*, 1999, **121**, 107–116.

64 D. J. Darensbourg, J. R. Wildeson, J. C. Yarbrough and J. H. Reibenspies, *J. Am. Chem. Soc.*, 2000, **122**, 12487–12496.

65 K. Nakano, K. Kobayashi and K. Nozaki, *J. Am. Chem. Soc.*, 2011, **133**, 10720–10723.

66 D. Y. Rao, B. Li, R. Zhang, H. Wang and X. B. Lu, *Inorg. Chem.*, 2009, **48**, 2830–2836.

67 X. B. Lu, L. Shi, Y. M. Wang, R. Zhang, Y. J. Zhang, X. J. Peng, Z. C. Zhang and B. Li, *J. Am. Chem. Soc.*, 2006, **128**, 1664–1674.

68 R. K. Dean, L. N. Dawe and C. M. Kozak, *Inorg. Chem.*, 2012, **51**, 9095–9103.

69 R. K. Dean, K. Devaine-Pressing, L. N. Dawe and C. M. Kozak, *Dalton Trans.*, 2013, **42**, 9233–9244.

70 H. Chen, L. N. Dawe and C. M. Kozak, *Catal. Sci. Technol.*, 2014, **4**, 1547–1555.

71 L. N. Saunders, N. Ikpo, C. F. Petten, U. K. Das, L. N. Dawe, C. M. Kozak and F. M. Kerton, *Catal. Commun.*, 2012, **18**, 165–167.

72 D. Adhikari, S. T. Nguyen and M.-H. Baik, *Chem. Commun.*, 2014, **50**, 2676–2678.

73 G. A. Luinstra, G. R. Haas, F. Molnar, V. Bernhart, R. Eberhardt and B. Rieger, *Chem.–Eur. J.*, 2005, **11**, 6298–6314.

74 M. H. Chisholm and Z. P. Zhou, *J. Am. Chem. Soc.*, 2004, **126**, 11030–11039.

75 Y. L. Xiao, Z. Wang and K. L. Ding, *Macromolecules*, 2006, **39**, 128–137.

76 W. J. van Meerendonk, R. Duchateau, C. E. Koning and G. J. M. Gruter, *Macromolecules*, 2005, **38**, 7306–7313.

77 R. Duchateau, W. J. van Meerendonk, L. Yajjou, B. B. P. Staal, C. E. Koning and G.-J. M. Gruter, *Macromolecules*, 2006, **39**, 7900–7908.

78 D. J. Darensbourg and A. D. Yeung, *Polym. Chem.*, 2015, **6**, 1103–1117.

79 D. J. Darensbourg and A. L. Phelps, *Inorg. Chem.*, 2005, **44**, 4622–4629.

80 R. K. Dean, S. L. Granville, L. N. Dawe, A. Decken, K. M. Hattenhauer and C. M. Kozak, *Dalton Trans.*, 2010, **39**, 548–559.

81 D. J. Darensbourg, R. M. Mackiewicz, A. L. Phelps and D. R. Billodeaux, *Acc. Chem. Res.*, 2004, **37**, 836–844.

82 D. J. Darensbourg and A. D. Yeung, *Polym. Chem.*, 2014, **5**, 3949–3962.

PAPER

Investigating public perceptions of carbon dioxide utilisation (CDU) technology: a mixed methods study†

C. R. Jones,*[ac] D. Kaklamanou,[b] W. M. Stuttard,[a] R. L. Radford[a] and J. Burley[a]

Carbon dioxide utilisation (CDU) technologies hold promise for helping to limit atmospheric releases of CO_2 while generating saleable products. However, while there is growing investment in the research and development required to bring CDU to the market, to date there has been very little systematic research into public perceptions of the technology. The current research reports upon the findings of a series of six qualitative focus groups (and an associated questionnaire) held with members of the UK public in order to discuss the perceived benefits and risks of CDU technology. The findings reveal that public awareness of CDU is currently very low and that there is a desire to learn more about the technology. While our participants did, on average, appear to develop an overall positive attitude towards CDU, this attitude was tentative and was associated with a number of caveats. The implications for the findings in terms of the development of communication and broader strategies of public engagements are outlined.

Introduction

Anthropogenic emissions of carbon dioxide (CO_2) are a primary cause of current global warming and climate change.[1] Carbon dioxide utilisation (CDU) technologies have the potential to help mitigate the release of CO_2 to the atmosphere by making use of some of the emissions from carbon intensive processes like fossil-fuel power generation. By utilising the CO_2 as a carbon source for the manufacture of saleable chemical products (*e.g.* polymers) and fuels, or through direct use in other industries (*e.g.* enhanced oil recovery); CDU also holds promise for

[a]Department of Psychology, University of Sheffield, Western Bank, Sheffield, UK. E-mail: c.r.jones@sheffield.ac.uk; Tel: +44 (0)114 222 6592

[b]Department of Psychology, Sociology and Politics, Sheffield Hallam University, Collegiate Crescent, Sheffield, UK

[c]UK Centre for Carbon Dioxide Utilisation (CDUUK), University of Sheffield, Western Bank, Sheffield, UK

† The informational video used within the current research is available at http://www.co2chem.co.uk/research-clusters/public-perception.

ART ■ C5FD00063G

generating economic revenue. This revenue could help to offset some of the costs associated with CDU/CCS processes and present a viable alternative to fossil-fuel based feedstocks in the manufacture of these products.[2,3] As such, there is growing interest into the research, development and deployment (RD&D) of CDU technology – exemplified by this Faraday discussion.

Social acceptability of CDU

A key consideration in the RD&D of CDU should be the systematic assessment of the *social acceptability* of the technology. Social acceptability (*i.e.* the extent to which a phenomenon, like CDU, is endorsed or rejected by key social actors, *e.g.* politicians, financiers, the general public, *etc.*) is now recognised as being necessary for the successful implementation of new technologies.[4]

As key groups of actors are known to affect the social acceptability of emerging technologies at a number of levels (*e.g.* household, community, national), understanding and responding to the opinions of the general public (*i.e.* examining *public acceptability*) should be a priority consideration for CDU proponents.[5] However, with the exception of a preliminary pilot study conducted by the current authors, to date there has been no systematic research in this field.[6]

Assessing public perceptions of CDU

Public engagement is a diverse term covering any attempt to contact members of the public in order to inform decision making.[5] Research shows that more deliberative, participatory forms of engagement – which involve affected publics earlier (*i.e.* upstream) and in a sustained and transparent way – will tend to yield better outcomes for those behind the engagement activity (*e.g.* increased public trust and decreased objection to decisions, *etc.*).[7,8]

While there is an emerging precedent for upstream engagement, there are evident challenges and risks to realising this in any meaningful sense with emerging technologies, like CDU. Not only will a lack of awareness of the technology likely prove to be a barrier to people's willingness to engage, but once engaged there are risks that the opinions registered towards the technology could be misleading if appropriate forms of attitude assessment are not employed. Reference to literature on the formative assessment of public opinion to CCS, for example, indicated the potential for registering pseudo-opinions (or pseudo-attitudes) if traditional questionnaire-based survey methods were used.[9,10] Pseudo-opinions are, in essence, uniformed judgements that people provide on issues which they have given little or no thought and are problematic as they tend to be weak, unstable and not very predictive of later thought and behaviour.[9,11]

The prospect of registering pseudo-opinions is increased when using traditional questionnaire-based surveys because they provide limited contextual information on the issues being discussed and are often self-completed, thereby offering little opportunity to clarify misunderstanding. In the context of understanding public perceptions of other emerging technologies (*e.g.* CCS, hydrogen), the spectre of recording pseudo-opinions has been addressed through the use of non-traditional survey methods (*i.e.* information choice questionnaires [ICQs]) and qualitative research techniques (*e.g.* focus groups, interviews).[9,10,12,13]

ART ■ C5FD00063G

Focus groups (FGs), for instance, provide a good forum for exploring controversial, unfamiliar and/or complex issues, by offering a setting within which information can be presented to and discussed by participants, and where responses and understanding can be probed.[14] If facilitated carefully, FGs provide a useful context for establishing: (a) 'why' people feel the way they do about issues and; (b) how such issues become represented and shared.[15]

Comparative case study: public perceptions of CCS

The importance of seeking to understand and appropriately assess the opinion of *the public* towards emerging carbon mitigation technologies is exemplified in work into the public perception of CCS. As a sister technology of CDU, such research provides an appropriate analogue for communicating the value of conducting similar work into CDU. For instance, public opinion research conducted over the last decade or so in a number of countries (*e.g.* USA,[10] UK,[12] Europe,[16] and Japan[17]) has proven invaluable in elucidating the roots of subjective concerns about CCS at a national, regional and local level; leading to guidance on how best to tailor education, communication and development practices to more appropriately address public concerns.[18-20]

Together, these studies have illustrated the multifaceted nature of lay (and expert) opinion of CCS, revealing that public attitudes are not simply a sum of anticipated technical risks but are also influenced by myriad social and economic considerations (*e.g.* mistrust in the proponents of the technology).[18,21]

The current research

We argue that forging a better understanding of emerging public opinion towards CDU is timely and should be seen as an integral accompaniment to the ongoing RD&D of the technology. In view of the current dearth of research into the public opinion of CDU technology, our team is conducting a series of studies with the dual objectives of (1) learning more about public perceptions of the perceived benefits, risks, utility and relevance of CDU; and (2) identifying appropriate means of communicating with the lay public about the science and technology behind CDU (*i.e.* the 'What a Waste!' programme).

We feel that appropriate engagement and communication efforts *should* be predicated on developing a systematic understanding of public attitudes towards the technology. As such, the current research builds upon that reported in a recently published communication article[6] by detailing the results and implications of six qualitative FGs and an associated survey-based activity designed with these objectives in mind.‡

In addition to providing insight into people's opinions of CDU, these FGs also provided a forum to 'market test' a pilot informational video about CDU being developed by the CO2Chem Network (www.co2chem.org).

---

‡ The two FGs mentioned as part of the communication article do also feature within the present article. However, the current article presents new systematic analysis of these FGs alongside 4 new FGs, details of which have not previously been published.

To our knowledge this study is the first to formally investigate and assess public perception of CDU. While a relatively small qualitative study, this research should be considered as part of a preliminary but growing body of research in this novel and important field.

Methods

Participants

Six focus groups (FGs), each comprising 6–8 participants (44 participants total: 14 female, 30 male; 15–54 years) were convened. All participants were offered a monetary incentive for participating.§ Further details of the participants comprising each FG can be found in Table 1. FGs 1–4 took place at the University of Sheffield in June or December 2013. Participants were recruited *via* a university volunteers list. FG4 also included members of the general public recruited from the part-time workplace of one of the authors. FGs 5 and 6 were convened in December 2013 and comprised year 11 pupils from a local high school. Staff at the school selected students based upon their interest and ability in science and/or their presence on outreach schemes previously run by the University of Sheffield. All participants were aged 15–16 years; both groups comprised a mix of genders.

Materials

Focus group information sheet. Provided details of the research team and sponsor; an outline of what to expect from the research activity; and a very brief introduction to CDU. Participants were told that CDU can make use of the CO_2 emitted from carbon intensive processes like fossil fuel power generation. They were informed that the CO_2 could be used in things like plastic manufacture, meaning that CDU could help to limit atmospheric CO_2 emissions and provide a use for an otherwise 'waste' greenhouse gas.

Pre-discussion questionnaire. Recorded participants' age, gender and occupation; their awareness of CDU and CCS ("*Have you heard of Carbon Capture & Storage/Carbon Dioxide Utilisation?*" Yes/No/Don't Know); their self-reported level of knowledge about CDU and CCS ("*How much do you think you know about …?*" Not a lot/A little/A fair amount/A lot); their attitudes to CDU and CCS ("*Overall, what is your attitude to…?*" 5-point Likert scale: very positive *to* very negative, plus a 'Don't Know' option) and their attitude certainty for both technologies ("*How certain or uncertain are you of your attitude to…?*" 5-point Likert scale: very certain *to* very uncertain, plus a 'Don't know' option).

Pre-discussion presentation. Contextualised the FG discussion by presenting participants with some background information on CDU *via* PowerPoint. This presentation expanded on the information sheet by verbally introducing the research team and outlining the central aims for the focus group (*i.e.* to gather

§ Monetary incentives varied by group. All participants age 18+ received a personal monetary incentive. Members of FGs 1 and 2 each received £20 on account of the fact they also took part in a secondary research task following the FG. Members of FGs 3 and 4 each received £5. The high school students did not receive individual payment but the school received a lump-sum of £80 as reimbursement for the students' time.

Table 1 Focus group descriptive characteristics

Grp	Date	Participant profile	No.	Age (years)	Gender	Aware of CDU	Mean CDU knowledge[a]	Aware of CCS	Mean CCS knowledge[a]
1	June 2013	University students & non-academic university staff	8	Mean = 25.6 SD = 7.6 Range = 20–43	3 Female 5 Male	1 Yes 5 No 2 DK	1.00 (0)	3 Yes 3 No 2 DK	1.38 (0.52)
2	June 2013	University students & non-academic university staff	8	Mean = 26.6 SD = 11.6 Range = 19–54	3 Female 5 Male	0 Yes 8 No 0 DK	1.00 (0)	5 Yes 3 No 0 DK	1.88 (0.99)
3	Dec 2013	University students & non-university support workers	7	Mean = 32.4 SD = 13.4 Range = 20–53	4 Female 3 Male	1 Yes 6 No 0 DK	1.14 (0.38)	2 Yes 5 No 0 DK	1.29 (0.49)
4	Dec 2013	University students & academic/non-academic university staff	6	Mean = 26.5 SD = 13.4 Range = 19–53	1 Female 5 Male	1 Yes 4 No 0 DK	1.00 (0)	3 Yes 3 No 0 DK	1.33 (0.52)
5	Dec 2013	High school students (year 11, England)	7	Mean = 15.4 SD = 0.5 Range = 15–16	1 Female 6 Male	2 Yes 5 No 0 DK	1.14 (0.38)	5 Yes 2 No 0 DK	1.57 (0.53)
6	Dec 2013	High school students (year 11, England)	8	Mean = 15.4 SD = 0.5 Range = 15–16	2 Female 6 Male	0 Yes 6 No 2 DK	1.13 (0.35)	5 Yes 2 No 1 DK	1.88 (0.99)
		Totals:	44	Mean = 23.5 SD = 10.8 Range = 15–54	14 Female 30 Male	5 Yes 34 No 4 DK	1.07 (0.26)	23 Yes 18 No 3 DK	1.57 (0.73)

[a] "How much do you think you know about CDU/CCS?" (1 = not a lot; 2 = a little; 3 = a fair amount; 4 = a lot).

public opinions on CDU and to aid the creation of a video for the CO2Chem Network).

Participants were briefly talked through a diagram of the CCS process associated with a coal-fired power station. The CCS concept was used as a counterpoint for introducing two often cited benefits of CDU: (a) the value of CDU in offsetting some of the costs associated with CCS by creating saleable chemical

ART ■ C5FD00063G

products; and (b) the value of CDU in reducing the current reliance on fossil-fuel derived carbon as a feedstock for these products.

Participants were then shown Fig. 1 and informed of some of the products that CO_2 could be converted to *via* CDU. It was noted that many of the depicted conversion processes would require energy and that this would necessarily have to come from renewable sources to mitigate the release of additional CO_2 during the manufacture of the products. The presentation ended with a slide outlining a protocol for the remainder of the session. This told participants they would first watch and then comment on a video about CDU before being asked to talk more generally about their opinions of CDU.

Informational video about CDU. A short (75 seconds) informational video combining a mix of cartoon animation and cutaways to real life industrial CDU operations. This video was being developed for the CO2Chem Network in order to communicate fundamental details of CDU technology to an interested, lay audience.¶ People watching the video were first introduced to the CO2Chem Network and its purpose in furthering the research and development of CDU. The video then spoke of the relationship between CO_2 emissions and climate change. CCS was mentioned as a way of achieving reductions in CO_2 emissions and the process of separating and storing the CO_2 in geological reservoirs was illustrated. Making use of captured CO_2 to create chemical products *via* CDU was then introduced and framed as a means of offsetting some of the costs associated with CCS. CDU was also registered as a way to reduce reliance on fossil fuels as a feedstock for producing these chemical products. The video ended by noting that CDU would need energy to produce the chemical products and confirmed that this would necessarily need to come from renewable sources to avoid the release
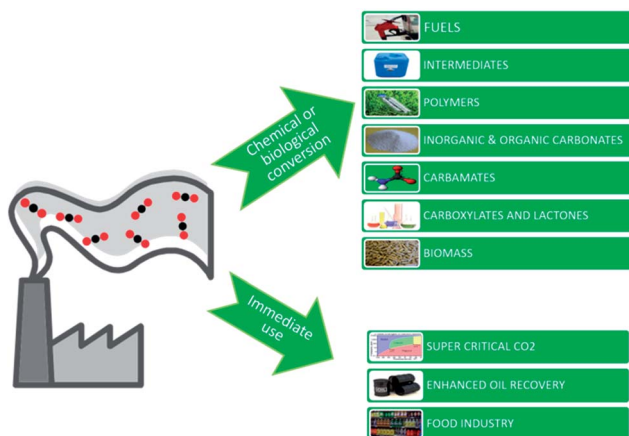
Fig. 1 Some products that CO_2 can be converted to *via* carbon dioxide utilisation (CDU) processes. Source: CO2Chem Network, available at http://www.co2chem.co.uk.

¶ There was a problem with the video in FG6, which meant that it did not run smoothly. This issue was taken into consideration when analysing responses towards the video in this group.

ART ■ C5FD00063G

of more CO_2 emissions (note: the video is available to view at: www.co2chem.co.uk/research-clusters/public-perception).

Post-discussion questionnaire. Asked for participants' opinion about 26 risks and benefits of CDU technology ("*To what extent would you agree or disagree with each of the following statements relating to CDU?*" 5-point scale: strongly disagree *to* strongly agree) (see Appendix 1 for a full list of statements); their self-claimed knowledge, attitude and attitude certainty towards CDU (assessed as outlined in pre-discussion questionnaire); their environmental worldview (revised New Ecological Paradigm [NEP] scale);[22] and their 'green' identity (4-item scale).[23]

FGs 1 and 2 completed the questionnaire online 1–2 weeks after the FGs. This was necessary as the questionnaire was partially developed on the basis of their responses within the FGs. The remaining FGs (3–6) completed a paper-pencil version of the questionnaire immediately following the focus group discussion.‖

Procedure

All groups were audio-recorded for later transcription and analysis. Upon arrival participants were provided with refreshments and asked to: (a) read the *infor-mation sheet*; (b) provide their written consent for their participation; and (c) complete the *pre-discussion questionnaire*.

The FG then began with participants being invited to first provide their names and occupation in order to acquaint themselves with one another. The *pre-discussion presentation* and *informational video* were then provided and partici-pants were invited to provide feedback on the video – focusing upon both issues of style and content (*e.g.*, how engaging, informative and understandable it was). Discussion about the video lasted approximately 20 minutes, at which point participants re-viewed the video and were invited to provide any final comments. Participants were then asked to discuss their general opinions about CDU and to comment on: (a) any perceived risks and benefits of the technology; (b) the utility of CDU in tackling climate change and; (c) comparative preferences for CDU *vs.* other carbon mitigation options. This discussion lasted approximately 20 minutes and took a semi-structured format.

Having completed the FG discussion, participants spent the last part of the session completing the *post-discussion questionnaire*. They were finally invited to ask any final questions or make any final comments before being debriefed, thanked, paid and dismissed.

Data transcription and analysis

The FG audio-recordings were fully transcribed and analysed using an exploratory thematic analysis approach.[25] All transcripts were first-coded by one of the authors (WS) who was not present during the FGs. Two additional members of the research team (CJ and DK) then independently second-coded one FG transcript using the coding manual created by WS. All coders then convened to discuss and confirm the emergent themes from the FG and to check the reliability of the initial coding scheme created by WS. Any missed coding or disagreement was

‖ Additional questions were included in the post-discussion questionnaire; however, due to small differences in how these questions were asked in FGs 1–2 *versus* FGs 3–6, these data are not reported on further.

discussed, before relevant adaptations were made to the coding manual. CJ and DK then independently analysed a further three FGs before convening a second meeting. Within this meeting any disagreements or missed coding were again discussed, before any final, relevant changes were made to the coding manual. WS then used the revised coding manual to recode (where relevant) all the FG transcripts.

Results

Focus group findings

The thematic analysis of the FG data is presented and discussed in accordance with participants' evaluation of: (1) the style and content of the informational video; and (2) the perceived risks and benefits of CDU. In order to aid interpretation of the comments relating to the video, the analysis is structured according to the issues of source, message and audience.[25]

Informational video

Source factors. Participants noted that it was unclear who the source of the video was. This led to questions about who was behind the video (and CDU more generally) and what their motivation was. The lack of clear authorship, in combination with the perceived "simplistic" nature of the video, negatively affected perceptions of its scientific credibility:

…it definitely wasn't a scientific backed-up video. It could've been an advert for anything. (FG4)

Participants suggested that this issue could be resolved if the video were to include interviews with visible, neutral, expert sources. It was suggested that this would put a face to the technology, which should help to engender more trust in the message content and more generally CDU.

Message factors. Opinions were shaped by the perceived intent of the video (*i.e.* whether it was designed to entertain or inform) and the groups discussed what level of entertainment might be needed in order to keep peoples interest. Participants agreed that more visually and emotionally engaging video content was needed and they criticised the video for being quite rushed, lacking a consistent visual style and for being quite dull.

Participants questioned whether the information in the video contained sufficient detail and clarity of expression to effectively describe the technology, its purpose and how it differs from CCS.

It [the video] doesn't necessarily very well convey the difference between CCS and CDU. I think you need to make clear that CCS proposes to store it [CO_2]; you are proposing to do something else. On reflection I don't think that comes over particularly well or easily. (FG1)

Some participants suggested that the central message behind the video was not apparent and that the explanation provided in the video needed to follow a more logical, narrative structure in order to appropriately engage with the audience.

…actually seeing what the problem is and explaining the problem, and what is the solution that you are looking for, that is the main focus of the research, and that was not very deeply touched upon. (FG4)

ART ■ C5FD00063G

Comments were also made about some of the technical language (or jargon) used within the video. The following exchange highlights how a number of scientific terms used within the video promoted confusion and misunderstanding among some of our participants, also leading them to question the viability of the video for a general, lay audience.

P1: *…no-one cares about carbonates, I'm probably one of the only people in the university who cares about them, no one knows what they are.*

P2: *I don't know what synth oil is?*

P3: *It's synthetic oil.*

P2: *If [the video] is for a general audience then …*

P4: *What does feed-stock mean? When I hear that I think of animals. (Laughter) I don't have a background in chemistry.* (FG2)

The video was also perceived to be lacking a balanced critique of CDU. Participants suggested that the potential risks of CDU were not fully addressed and therefore the video came across as one-sided and as an effort to persuade people to like the technology. This imbalance negatively affected the perceived credibility of the message and led to suspicion as to why CDU was being presented in such a positive light.

P1: *Like you said, there is no debate [about the risks] so you think well 'what are you not saying'.*

P2: *It is just like one sided, they are trying to sell you something.* (FG3)

Audience factors. Participants commented that it was unclear as to who the intended audience was for the video and agreed that establishing this was a high priority for understanding the purpose of the video and determining the appropriateness of the style and message content.

I don't understand the point of the video, or whether it was trying to tell me to take action or to improve something or to go on the website, I don't know what the point was. (FG1)

Participants tended to agree that the video provided a reasonable basic introduction to CDU but that it was lacking in depth analysis and detail if it were to be used for any other purpose than a basic introduction to the concept. This led to a tension among our participants, who desired more detail (to fully engage in the focus group) but recognised that such detail would increase the length and complexity of the video and thus negatively affect audience interest outside of the experimental context.

Having more facts or figures might make your video altogether a bit boring because it really wouldn't make sense to the wider audience who are not involved in the research. A little bit of it [more detail] would definitely help, giving more examples, actually seeing what the problem is and explaining the problem, and what is the solution that you are looking for, that is the main focus of the research, and that was not very deeply touched upon. (FG4)

Participants' age appeared to shape evaluations of the adequacy of the video. While our adult participants tended to feel that the video was too simplistic and lacked seriousness (bearing in mind the seriousness of the issue it was trying to resolve), our high school groups tended to be less critical on these grounds. It was suggested that developing multiple, tailored videos intended for different age groups would be very useful in the future.

I think it [the video style/content] depends on the audience, because you were trying to appeal to everyone by having facts and stuff in as well as the cartoons and the music

and stuff, so they should split it up ideally, one for a younger audience and one for older audience. (FG5)

Perceived risks and benefits of CDU

Three principal areas were discussed by participants, relating to the *conceptual issues, technical issues* and *societal issues* associated with CDU. Conceptual issues related to the general underlying principles of the CDU concept and its position relative to other carbon mitigating options (*i.e. should we do this*); technical issues focused on the technological and market feasibility of CDU (*i.e. can we do this*); and societal issues related to the implications that might result from an investment in the technology (*i.e. what are the consequences*).

Conceptual issues. Participants saw CDU to be a technology that would not provide a long term solution to CO_2 emissions but would simply stall an inevitable release of CO_2 into the atmosphere.

…I like it [CDU] because it is doing something, but it shouldn't be seen as a long term fix, because you are not really going anywhere you are just hiding it [CO_2] right? (FG2)

Some examples of CDU were particularly susceptible to this criticism (*e.g.* synthetic fuels) and tended to be negatively evaluated by participants. In contrast, CDU options that implied a longer-term storage of CO_2 option (*e.g.* plastics, concrete) tended to be more positively evaluated.

I think also a lot of what you think about this technology will also depend on its application, […] if you are getting carbon dioxide from a coal fired power plant and turning that carbon dioxide into polymers that go into plastic, you have created kind of a legitimate carbon sink where it is fixed and it is not going into the atmosphere […]. But if you are turning it into, somehow managing to turn it into a fossil fuel, that you can use to run on a car, train, whatever, then all the effort that you are going to put into turning that CO_2 into some sort of fuel it is still going to end up as carbon dioxide in the atmosphere. (FG1)

While 'delaying the inevitable release of CO_2' was considered problematic, participants did note the pragmatic value of CDU as a 'stop-gap' technology option (*i.e.* something which could 'buy us time' as we transition to a low-carbon economy) and as something symbolic of efforts being made to combat climate change.

I just feel that it [CDU] is a step in the right direction, providing that […] if you can do this and it works then brilliant. (FG3)

There was also a sense that investing in current CDU technologies could also expedite the development of other CDU options that would not suffer as much from the prospect of re-releasing captured carbon (*e.g.* using CO_2 from the air).

I think if there was potential in the future of just not using CO_2 from power plants and just using CO_2 from the atmosphere then I might feel like the power plant one might be a step on the way and maybe that would swing it [their opinion]. (FG1)

CDU was conceptually criticized for presenting an 'end of pipe' solution to the problem of CO_2 emissions; a solution that did not address the root cause of the problem (*i.e.* the activities that were producing CO_2 in the first place). In short, CDU was seen as treating the symptoms of the problem as opposed to the cause.

…they [CDU technologies] are trying to fix something but they are not going to the root of the problem, that there is more cars, more population more pollution, more

everything so they are trying to fix that but not the actual problem that humans are creating more and more pollution. (FG2)

Participants outlined an array of alternative supply and demand side options that they felt would more appropriately address the CO_2 problem at source (*e.g.* promotion of more sustainable living practices, direct investment in renewables). These points are noteworthy bearing in mind some participants believed CDU to be a barrier to necessary lifestyle changes and questioned why renewable energy was being used in the conversion of CO_2, rather than being used to more directly power the economy (see below).

Technical issues. High investment costs and cheaper alternatives (*e.g.* unmitigated emission) were thought to be an economic obstacle to CDU (particularly in a climate of austerity). Participants questioned as to whether CDU would ever become cost-effective without some kind of market intervention.

…there is also a question of cost-effectiveness. Kind of sticking a chimney up and spewing out CO_2 I imagine is going to be a whole lot cheaper than the capital investment needed to build either a carbon capture and storage facility or kind of a CDU facility. So there would have to be some sort of pricing mechanism in place. (FG1)

The value of CDU was calculated in more than just economic terms. Many participants suggested that they would endorse the economic cost of investment in CDU if there were significant environmental benefits in doing so. However, there was uncertainty about how readily demonstration CDU operations could be scaled-up and what magnitude of environmental benefit would be realised by CDU.

It [CDU] might be significant but we don't know how significant it might be. General logic says that it should be, because CO_2 emissions would increase, we will have more cars, more people, carbon dioxide and utilizing them would help. But I don't know what impact or how much of an impact it could make for the future generations. (FG4)

This uncertainty was related to the fact that participants felt ill-informed about the relative technical and economic feasibility of CDU *vs.* alternatives. Indeed, while participants appeared to have a generally favourable attitude to CDU, this opinion was evidently conditional upon CDU performing well against these other options.

The question is what alternatives are there, because I'm all for 'we'll spend a little bit more if it has benefits' [CDU]. But if we spend a little bit more on this and there is actually something out there that will work better I'd probably rather spend my money on that. (FG3)

Debate of the likely impact of CDU was also tied to perceptions about the timeframes for bringing the technology to market. There was tension between the seemingly long period of time needed to develop CDU into an economically competitive technology option and the urgency of addressing climate change. However, it was recognised that financial investment in CDU would be necessary for it to become economically competitive. Parallels were drawn with the photo-voltaic industry, where investment in solar had eventually made it competitive with more traditional energy sources.

P1: *Well that [economic cost] is an argument that they had against early solar but as oil production starts to come lower and lower, prices do go up and eventually the argument could be that if they develop the technology to do this [CDU] then it will become cost effective as the cost of this [CDU] decreases and the cost of petroleum goes up.*

P2: *By the time that happens it will be probably too late.*

P1: *I don't know; solar got there, solar is cost-efficient now, competitive with oil.* (FG2)

Participants were sceptical about whether CDU would result in a net reduction in CO_2 emissions across the whole lifecycle. The sense was that emissions associated with the energy needed to convert CO_2 into commodity chemicals would undermine any savings resulting from utilisation. Participants drew upon other purportedly 'green' initiatives (*e.g.* early solar) which turned out to emit more CO_2 than they would save to back up this concern.

…we have had too many cons, I think especially some of the early solar panels and things like that when they were so inefficient that […] once you had it in its box it was saving carbon dioxide, but to produce the sucker and especially if you went back to the mines to mine the silicon […] you were causing so much more damage than anything that you were saving. (FG1)

This issue was deemed particularly important when considering CDU for fuel synthesis. For some participants it seemed counter intuitive (and thermodynamically infeasible) to burn a fossil fuel only to then capture the CO_2 produced and expend significant amounts of energy to convert it into another 'fossil fuel'.

Participants' recognition that CDU processes were energy intensive also highlighted the importance to them of using renewables to power the processes. The prospect of using large amounts of renewable energy in CDU, however, led participants to consider whether or not there would be more benefits from just using the renewable energy more directly.

…I like the fact that you show that you use renewable energy to do it. So it is not as if we are going to produce 20 tons of CO_2 to get the energy to use up 1 ton of CO_2. That to me was a crucial message. (FG1)

…if you are using renewable energy to convert carbon dioxide into something else, couldn't you use the renewable energy sources to make energy [electricity]. (FG2)

Societal issues. There was concern that as an 'end of pipe' solution CDU might be used as an excuse for people to continue their environmentally-damaging lifestyles. Participants therefore tended to believe that CDU should only be considered alongside demand-side CO_2 reduction strategies.

…people might sort of think like 'great we can you know keep going and use loads of cars and doing this that and the other because we've got all this green stuff now'. It's not quite as it might seem. (FG3)

It was also feared that CDU would propagate a 'business as usual' approach to the use of fossil fuels in powering the economy and it was felt that the technology might create societal complacency towards tackling climate change.

…sometimes these things [CDU] can get used to justify more and more coal power stations, 'ah we can capture, you know, a bit of the CO_2 from them and make a plastic cup' […] if it was like that then it wouldn't be worth it. (FG3)

The belief that CDU might produce ostensibly 'unsustainable products' was also of concern to some participants. Plastics and chemicals, even produced from captured CO_2, were deemed to run counter to a drive to reduce anthropogenic environmental impact. This led some to devalue the products of CDU.

…most of the things that are mentioned [in the video] do look like they have a bit of, they don't look exactly environmentally friendly, things like chemicals, you know people don't look at chemicals and think that is good for the environment. Plastic, cars, fuels are not things that people associate with environmentally friendliness. (FG2)

Finally, there was a sense that there might be unknown chemical risks and localised environmental impacts from CDU processes (*e.g.* acidification of soil or chemical explosions). However, in the absence of a full outline of the CDU process, participants felt that they could not comment on these 'capture' risks with certainty. Instead, when considering the risks of CDU, the discussions principally focused on the issue of CO_2 sequestration (*e.g.* CO_2 leakage) as opposed to specific concerns with utilisation *per se*.

There must be dangers involved in like the manipulation of carbon dioxide I would think, I must be done in a safe, or some sort of factory, I'm not sure of the process so … (FG2)

Overall evaluation of CDU. Overall, participants appeared to be generally favourable towards CDU. They knew that there were drawbacks but could see value in the idea of trying to recycle CO_2. There was also recognition that with new industry would come new jobs, and it was acknowledged that CDU could produce useful products. However, this positivity was caveated by participants' realisation that they still knew very little about CDU, leaving some requiring more convincing of its value.

The idea of recycling CO_2 sounds like a good idea in theory but I don't know enough about this process at all, to say whether the process is a good idea. (FG4)

I'm more favourable to capture than to utilisation […] I believe that the CDU, it is a bit bizarre, it is trying to, well you know it is making plastic that… I'm not convinced by CDU basically. (FG4)

Also, participants only appeared willing to entertain the prospect of investing in CDU alongside investment in other mitigation options.

P1: *I think that it [CDU] is good because they are looking at another [option to mitigate climate change], it is just one of the things that they are looking at…*

P2: *Yes, it is good to consider them all.* (FG3)

Quantitative survey findings

Statistical analysis of some of the key questions in the pre- and post-discussion questionnaires was conducted. This analysis focused on identifying participants' attitudes to CDU and the factors underlying these attitudes. The analysis also indicated the presence of any initial pseudo-opinions.

Pre-discussion questionnaire

Pseudo-opinions. Of 44 participants, 5 stated that they had heard of CDU before beginning the FG. The remaining 39 participants stated that they had 'not heard' of CDU ($n = 34$) or that they 'didn't know' ($n = 5$). Congruently, self-reported knowledge of CDU was low, with just 2 participants holding 'a little' knowledge of the technology. Factoring out those who had heard of the technology and/or stated holding 'a little' knowledge of CDU ($n = 6$), we investigated the stated pre-discussion attitudes of the participants. While the majority of these participants stated that they held a neutral attitude ($n = 9$) or that they 'didn't know' what their attitude was towards CDU ($n = 18$); 11 participants registered holding either a fairly ($n = 8$) or very positive ($n = 3$) attitude. We feel that this can be taken as reasonable evidence of these participants (25% of our sample) having registered pseudo-opinions before beginning the study and, as such, as a justification for using FGs within the current research activities.

Post-discussion questionnaire

CDU belief statements. Responses to the 26 belief items were assessed by comparing the mean score for each statement with the scale midpoint (*i.e.* 'neutral') using one-sample *t*-tests. Items where there was a significant deviation from the midpoint were indicative of emerging agreement on the positive or negative attributes of CDU among our participants. Six items showed a significant positive deviation (*t* values $\geq$ 3.85, *p* values < 0.001) from the midpoint, with six showing a significant negative deviation (*t* values $\geq$ 3.60, *p* values $\leq$ 0.001). Details of these items can be found in Table 2. The remaining items were statistically comparable to the midpoint using a Bonferonni-corrected alpha level of 0.002 (*t* values $\leq$ 3.15, *p* values $\geq$ 0.003).

The six *positive* items related to three key issues: (1) the value of CDU as an example of efforts being made to combat climate change; (2) the positive delaying potential for CDU in helping to address climate change; and (3) the potential for CDU to create useful products and employment opportunities. The retained *negative* items also related to three key issues: (1) the potential for CDU to undermine necessary behaviour and/or lifestyle change; (2) the limited impact of CDU on CO_2 emissions; and (3) a concern that investment in CDU might affect other, more preferred, options for addressing climate change.

Table 2 CDU belief statements showing significant positive or negative deviation from the scale midpoint[a]

	N	Mean	SD
Positive deviation from scale midpoint			
CDU is a step in the right direction for combating climate change	41	3.78	0.85
CDU will help to delay the negative effects of having too much CO_2 in the atmosphere	41	3.59	0.97
CDU will create new employment opportunities	41	4.05	0.77
CDU will produce useful products	43	3.93	0.77
CDU indicates a commitment to tackling climate change	42	3.69	0.90
CDU will 'buy us time' as we aim to tackle climate change	42	3.52	0.86
Negative deviation from scale midpoint			
CDU will promote a 'business as usual' approach to current wasteful lifestyle practices	39	2.56	0.85
CDU will have a limited impact on CO_2 emissions	37	2.35	0.95
CDU should only be considered alongside other technologies for tackling climate change	41	1.81	0.90
CDU will draw funding from other technologies better suited to tackling climate change	33	2.21	0.82
CDU will undermine efforts to promote behaviour change among the general public	40	2.43	1.01
CDU will only delay the inevitable release of CO_2 at high economic cost	38	2.42	0.91

[a] Notes: negatively worded items were reverse coded such that higher scores for all statements reflected a more pro-CDU opinion. All means discount missing data and respondents who answered 'Don't Know' when responding to the item. Significance *vs.* scale midpoint (3.00) using one-sample *t*-tests, calculated using Bonferroni-corrected alpha value of $p = 0.002$. Statement 1 ("CDU will help to slow the negative effects of climate change") was removed from the analysis due to the misspelling of the word *slow* in the surveys distributed to FGs 3–6. A full list of the 26 belief statements can be found in Appendix 1.

ART ◼ C5FD00063G

Post-discussion knowledge, attitudes and attitude certainty. Forty-three participants completed the post-discussion questions relating to their CDU knowledge, attitude and attitude certainty. Self-claimed knowledge of CDU improved markedly from pre-discussion levels, with 41 participants stating that they now knew either 'a little' ($n = 24$) or 'a fair amount' ($n = 17$) about the technology after the FG. On the basis of these findings, we can be fairly certain that our participants had developed a basic understanding of CDU.

Overall, post-discussion attitudes towards CDU were fairly positive, with the mean attitude (mean = 3.35, SD = 0.84) differing significantly from the scale midpoint, $t(42) = 2.72$, $p = 0.010$. Overall, post-discussion attitude certainty (mean = 3.47, SD = 0.80) was also found to differ from the scale midpoint in an affirmative direction, $t(42) = 3.83$, $p < 0.001$. This is indicative that participants were on average 'fairly certain' of their opinions about CDU post-discussion.

Post-discussion attitudes, green identity and ecological worldview. With the emerging ambivalence in the perceived 'green credentials' of CDU within our sample (*e.g.* CDU was seen as a delaying solution for climate change but a threat to lifestyle change), we investigated how participants' green identity and ecological worldview related to their post-discussion attitudes towards CDU. Two of the 44 participants were omitted from these analyses as they did not provide useable response data.

Spearman's *rho* correlations (two-tailed, pairwise deletion) confirmed the expected significant positive relationship between participants' green identity (mean = 3.92, SD = 0.61) and NEP (mean = 3.61, SD = 0.48) scores, $r(42) = 0.31$, $p < 0.045$; and indicated that there was a significant negative relationship between ecological worldview and attitudes (mean = 3.36, SD = 0.85), $r(42) = -0.31$, $p = 0.048$. Participants with a stronger pro-ecological worldview tended to hold less favourable attitudes towards CDU. The correlation between green identity and attitude was not statistically significant, $r(42) = -0.07$, $p = 0.665$.

Discussion

This study combined focus group (FG) and survey methods to (a) establish more about public perceptions of CDU; and (b) help identify appropriate means of communicating with the lay public about CDU. While there are limitations to the current research design; we believe we have fulfilled both aims and that our findings offer pioneering insight into the emerging nature of public opinion towards CDU. The remainder of this article will seek to summarize the main findings from the study in relation to public engagement and communication efforts before outlining some of the limitations and key future directions for research in this field.

Main research findings

The findings indicate that by the end of the research process our participants had, on average, formed a tentative positive attitude towards CDU. This attitude appeared to stem principally from the 'delaying potential' offered by CDU in combating climate change, its symbolic status as an attempt to address climate change and its potential to generate useful products and employment opportunities. This positivity was, however, firmly caveated by participants' recognition

that they knew little about CDU (related to perceived inadequacies in the informational video) and by several conceptual, technical and societal tensions.

Lack of awareness. Before participating, only 5 of 44 participants stated that they had heard of CDU and even then self-claimed knowledge among those 5 participants was low. Despite claiming to have no awareness or little knowledge of CDU, 11 participants (25%) claimed to hold (very) positive attitudes towards the technology. While it should not be assumed that these participants were being deceitful, these data confirm the potential for registering 'pseudo-opinions'[9,11] in the current context and thus arguably justify our choice of a focus group method for our research.

The lack of awareness and knowledge of CDU negatively affected participants' ability and willingness to comment on the perceived risks, benefits and applications of the technology. While evidently posing problems for maintaining fluid FG discussion, we feel that this confirms the opportunity facing CDU proponents at the present time. Specifically, not only is there growing evidence of the benefits of upstream public engagement (if done correctly) in helping to foster the success of emerging technology[5,8] but it is recognised that the optimum time to shape opinion towards new phenomena is when awareness is low and attitudes have yet to form.[18] CDU evidently fulfils these criteria and confirms that now is the time to begin a dialogue with the public about CDU.

Importantly, our results also point to the importance of considering the purpose and adequacy of any planned communication in order to lessen the potential for misunderstanding or misrepresentation of the technology. Indeed, one of the key findings from the FGs related to how our participants evaluated the adequacy of the informational video used as an aide to discussion. While many felt that this video could reasonably act to spark public interest in CDU, they questioned the sufficiency of the information in providing the depth of coverage required to debate the technology in full. In short, the perceived quality of the video was tied to beliefs about its intended purpose (and the intended audience). Some participants were also seen to question *why* they were being asked to discuss CDU at all, which is to say they were unclear as to the purpose of the engagement activity (*e.g.* what implications there would be for their comments). While we did attempt to clarify the purpose of the research activity, we feel that both these comments underline the same issue: the importance of communicating the purpose of engagement activities and careful selection of communication tools. This conclusion is not novel – the importance of identifying and communicating the goals of planned engagement is well-established[26,27] – but we feel that the point is illustrated well in the present context, in that a brief informational video was deemed incongruent with the apparent substantive goals of the FG and hence was more negatively evaluated by participants.[28]

There were a number of other stylistic and content concerns that affected participants' evaluations of the adequacy of the video. Issues of message clarity (*e.g.* words used, structure of narrative) were important and it appeared that trust in the video was undermined by its 'facelessness' and the lack of discussion of risk. These factors led participants to speculate over who would stand to benefit from the technology, what risks had gone unmentioned and whether the video had positive persuasive intent. To the extent that trust is used as a heuristic in guiding decision-making has been found to be important in shaping perceptions of similar technologies (*e.g.* CCS[21]). If the intent of future communications is to

provide impartial information so as to allow people to make an informed judgement about CDU technology, then including a fuller description of the anticipated risks and more clearly identifying the source (and beneficiaries) would appear prudent.

Conceptual, technical and social tensions. There was a desire for more information among our participants and it is possible that many of the registered *technical concerns* (*e.g.* issues of technical and economic feasibility; lifecycle CO_2 emissions and energy critique, *etc.*), might have been addressed by the presence of more detail on these matters. Arguably, future correspondence should build upon our findings in order to formally address these concerns and counter the emerging gaps and misperceptions in lay understanding of the technology. Importantly though, while more information is perhaps needed, one should not assume that the simple provision of this information alone will guarantee acceptance of CDU. Not only are there known limitations to interventions centred solely on presumed knowledge deficit[29] but there is evidence within our study that attitudes were shaped by more than a simple lack of technical understanding. Rather, attitudes were also governed by more subjective considerations of the *conceptual* (*e.g.* end of pipe critique) and *societal* (*e.g.* encouraging wasteful lifestyles) implications of investing in CDU.

Further research into how these *conceptual* and *societal* concerns might shape perceptions of CDU is a key avenue for future research. Not only will they likely shape public opinion of CDU in their own right but they may also impact upon how any provided technical information is interpreted and used.[30] A particular focus of future research might be placed upon the apparent conflict forming over the pro-environmental credentials of CDU. For instance, while we found that participants with a stronger environmental worldview tended to be less favourable to CDU; it cannot be inferred that more pro-ecological individuals will automatically reject CDU outright. Rather, whilst they might see CDU as making a direct (*e.g.* locking away CO_2) or indirect (*e.g.* raising the profile of CO_2 reduction attempts) contribution to tackling climate change, it is possible that such individuals might show a reluctant acceptance of the technology – akin to that shown in the responses to the recent reframing of nuclear power as a low-carbon energy option.[31,32]

Agnosticism on CDU attributes. While a large number of interesting issues were raised and discussed within the FGs, relatively few were clearly evaluated as positive or negative. Rather, participants remained largely agnostic about many perceived attributes of the technology. These findings are remarkably similar to those from a study by Flynn and colleagues[13] into public perceptions of hydrogen energy technologies (HET) and help to confirm the challenges faced by engaging in upstream discussions about a new technology. We feel that as more information on the relative costs and benefits of CDU becomes available, systematic investigation of how this information affects public agnosticism on some of the identified issues will be important. Thus it should help to clarify whether the tentative positivity seen towards CDU in our study will likely become strengthened and less caveated, or undermined and more negative over time.

Limitations & future directions

While the current research has succeeded in providing some initial insight into public perceptions of CDU technology; when seeking to transfer our research findings to other groups or contexts, one should carefully consider the limitations relating to this study.

Transferability of findings. The present research was conducted on a convenience sample of participants recruited principally *via* a university mailing list. While few of the university participants were engineers and/or pure scientists; the self-selected, well-educated nature of our participants presents limitations to the direct transferability of our research findings. This argues in favour of repeating the research – perhaps with more purposive sampling – on participants from more diverse backgrounds. This should help to identify the extent to which the opinions of our participants are socially shared.

Future research could continue to have a qualitative focus although confirming our findings *via* quantitative methods would also be useful. One option would be to conduct a nationally representative survey of public opinion; however, such activity would need to recognise the issues presented by the low levels of public awareness (*e.g.* the prospect of registering pseudo-opinions). Distributing an Information-Choice Questionnaire (ICQ)[9] could present one solution to this problem and formative efforts to pilot a CDU ICQ have already been made by the current authors.[6]

Framing of materials. The perceived imbalance in the description of CDU present within the informational video (*i.e.* the absence of considerations of risk) indicates that the technology was *positively* framed in this research. While this did not prevent participants engaging in considering potential drawbacks of CDU, it does have implications for the strength of the conclusions that can be drawn. Specifically, studies show that the manner in which information is presented or framed, can exert an impact upon people's decisions and preferences.[33] Thus, one could hypothesise that the positive tone of the video may have yielded more favourable opinions of the technology than would have arisen in a context where the potential drawbacks of CDU were more explicitly considered (or were the focus of the video). While the deliberative nature of the FG context (*i.e.* where both the benefits and risks of CDU were debated) should have lessened the impact of this positive framing in the current context; we contend that a systematic investigation of the impact of purposive framing on comparative preferences for CDU (or different CDU options) presents an important, empirical question for future research.

Conclusions

With a growing recognition of the impact that public opinion can have in shaping the social acceptance (and likely success) of emerging technologies,[4] investing time and appropriate resources for developing public engagement and communication strategies is essential.[5] In the context of CCS, an awareness of the value of public engagement has not only promoted invaluable social scientific research into the factors underlying public perceptions of the technology but has given rise to best practice guidelines designed to inform more effective engagement and education programmes.[18,19]

ART ■ C5FD00063G

Consistent with this precedent, the current study has provided formative insight into the beliefs that are likely to underlie emerging public opinion of CDU; helping to shed light on the current low level of awareness of the technology and how this might feed technical misunderstanding and shape perceptions about conceptual fit and societal implications. While we found that participants generally valued the idea of recycling CO_2, this general-level support masked differences in the favourability of different CDU options and was strongly qualified. We feel that now is the time to work with the findings and limitations of the current study to engage in a fuller programme of research in order to investigate how this qualified support of CDU holds up to further scrutiny and which CDU options are most preferred.

Appendices

Appendix 1

The full list of the 26 CDU risk and benefit statements presented to participants in the post-discussion questionnaire ("*To what extent would you agree or disagree with each of the following statements relating to CDU?*" 5-point scale: strongly disagree *to* strongly agree). CDU is/will/should/has: (1) a step in the right direction for combating climate change; (2) help to delay the negative effects of having too much CO_2 in the atmosphere; (3) create new employment opportunities; (4) be good for the environment; (5) be good for the UK economy; (6) a cost-effective way of tackling climate change; (7) promote a 'business as usual' approach to current wasteful lifestyle practices; (8) have a limited impact on CO_2 emissions; (9) only be considered alongside other technologies for tackling climate change; (10) the wrong solution for tackling climate change; (11) produce useful products; (12) be accepted by the general public; (13) indicates a commitment to tackling climate change; (14) be negatively evaluated by the general public; (15) draw funding from other technologies better suited to tackling climate change; (16) undermine efforts to promote behaviour change among the general public; (17) promote an unwelcome continuing use of fossil fuels; (18) only delay the inevitable release of CO_2 at high economic cost; (19) alleviate the storage risks associated with Carbon Capture and Storage (CCS); (20) only delay the inevitable release of CO_2 at high energy cost; (21) a 'green' technology; (22) many unknown risks; (23) more risks than benefits; (24) 'buy us time' as we aim to tackle climate change; (25) not become a commercial reality in my lifetime; (26) help to slow the negative effects of climate change.

Acknowledgements

Notes and references

1 IPCC, Climate Change 2014: Synthesis Report, Contribution of Working Groups I, II and III to the Fifth Assessment Report of the Intergovernmental Panel on Climate Change, 2014, IPCC, Geneva, Switzerland.

ART ■ C5FD00063G

2 P. Styring, D. Jansen, H. de Coninck, H. Reith and K. Armstrong, *Carbon Capture and Utilisation in the Green Economy*, UK, 2011, Centre for Low Carbon Futures.

3 *Carbon Dioxide Utilisation: Closing the Carbon Cycle*, ed. P. Styring, E. A. Quadrelli and K. Armstrong, Elsevier, 2014.

4 R. Wüstenhagen, M. Wolsink, and M. J. Bürer. *Energy Policy*, **35**, 2683.

5 Energy Research Partnership (ERP), Engaging the Public in the Transformation of the Energy System, 2014, available at: http://erpuk.org/wp-content/uploads/2014/12/ERP-Public-Engagement-Report-May-2014.pdf.

6 C. R. Jones, R. L. Radford, K. Armstrong and P. Styring, *J. CO$_2$ Util.*, 2014, **7**, 51.

7 *Renewable Energy and the Public: from NIMBY to Participation*, ed. P. Devine-Wright, Routledge, 2014.

8 J. Wilsdon and R. Willis, *See-through science: Why public engagement needs to move upstream*, Demos, 2004.

9 M. de Best-Waldhober, D. Daamen and A. Faaij, *Int. J. Greenhouse Gas Control*, 2009, **3**, 322.

10 E. L. Malone, J. J. Dooley and J. A. Bradbury, *Int. J. Greenhouse Gas Control*, 2010, **4**, 419.

11 G. F. Bishop, A. J. Tuchfarber and R. W. Oldendick, *Publ. Opin. Q.*, 1986, **50**, 240.

12 S. Shackley, C. McLachlan and C. Gough, *Clim. Pol.*, 2004, **4**, 377.

13 R. Flynn, P. Bellaby and M. Ricci, The limits of 'upstream' public engagement: citizens' panels and deliberation over hydrogen energy technologies, in *Renewable Energy and the Public: from NIMBY to Participation*, ed. P. Devine-Wright, Routledge, 2014.

14 V. Price and P. Neijens, *Int. J. Publ. Opin. Res.*, 1997, **9**, 336.

15 L. Litosseliti, *Using Focus Groups in Research*, A&C Black, 2003.

16 P. Upham and T. Roberts, *Int. J. Greenhouse Gas Control*, 2011, **5**, 1359.

17 K. Tokushige, K. Akimoto and T. Tomoda, *Int. J. Greenhouse Gas Control*, 2007, **1**, 101.

18 P. Ashworth, N. Boughen, M. Mayhew and F. Millar, *Int. J. Greenhouse Gas Control*, 2010, **4**, 426.

19 P. Ashworth, J. Bradbury, S. Wade, C. Y. Feenstra, S. Greenberg, G. Hund and T. Mikunda, *Int. J. Greenhouse Gas Control*, 2012, **9**, 402.

20 W. Bruine de Bruin, L. A. Mayer and M. G. Morgan, *J. Risk Res.*, 2015, 1, ahead-of-print.

21 B. W. Terwel, E. Ter Mors and D. D. Daamen, *Int. J. Greenhouse Gas Control*, 2012, **9**, 41.

22 R. E. Dunlap, K. D. Van Liere, A. G. Mertig and R. E. Jones, *J. Soc. Issues*, 2000, **56**, 425.

23 L. Whitmarsh and S. O'Neill, *J. Environ. Psychol.*, 2010, **30**, 305.

24 V. Braun and V. Clarke, *Qual. Res. Psychol.*, 2006, **3**, 77.

25 C. I. Hovland, I. L. Janis and H. H. Kelley, *Communication and Persuasion: Psychological Studies of Opinion Change*, Yale University Press, 1953.

26 M. C. Powell and M. Colin, *Sci. Comm.*, 2008, **30**, 126.

27 R. Wooden, *Social Research: An International Quarterly*, 2006, vol. 73, p. 1057.

28 A. Stirling, *Sci. Tech. Hum. Val.*, 2008, **33**, 262.

29 P. Sturgis and N. Allum, *Publ. Understand. Sci.*, 2004, **13**, 55.

30 J. C. Stephens, J. Bielicki and G. M. Rand, *Energy Procedia*, 2006, **1**, 4655.

ART ■ C5FD00063G

31 K. Bickerstaff, I. Lorenzoni, N. F. Pidgeon, W. Poortinga and P. Simmons, *Publ. Understand. Sci.*, 2008, **17**, 145.

32 A. Corner, D. Venables, A. Spence, W. Poortinga, C. Demski and N. Pidgeon, *Energy Policy*, 2011, **39**, 4823.

33 D. Chong and J. N. Druckman, *Annu. Rev. Polit. Sci.*, 2007, **10**, 103.

PAPER

Environmental potential of carbon dioxide utilization in the polyurethane supply chain†

Niklas von der Assen, André Sternberg, Arne Kätelhön and André Bardow

Potential environmental benefits have been identified for the utilization of carbon dioxide (CO_2) as a feedstock for polyurethanes (PUR). CO_2 can be utilized in the PUR supply chain in a wide variety of ways ranging from direct CO_2 utilization for polyols as a PUR precursor, to indirect CO_2 utilization for basic chemicals in the PUR supply chain. In this paper, we present a systematic exploration and environmental evaluation of all direct and indirect CO_2 utilization options for flexible and rigid PUR foams. The analysis is based on an LCA-based PUR supply chain optimization model using linear programming to identify PUR production with minimal environmental impacts. The direct utilization of CO_2 for polyols allows for large specific impact reductions of up to 4 kg CO_2 eq. and 2 kg oil eq. per kg CO_2 utilized, but the amounts of CO_2 that can be utilized are limited to 0.30 kg CO_2 per kg PUR. The amount of CO_2 utilized can be increased to up to 1.7 kg CO_2 per kg PUR by indirect CO_2 utilization in the PUR supply chain. Indirect CO_2 utilization requires hydrogen (H_2). The environmental impacts of H_2 production strongly affect the impact of indirect CO_2 utilization in PUR. For current H_2 production, environmentally optimal PUR production utilizes much less CO_2 than theoretically possible. Thus, utilizing as much CO_2 in the PUR supply chain as possible is not always environmentally optimal. Clean H_2 production is required to exploit the full CO_2 utilization potential for environmental impact reduction in PUR production.

1. Introduction

The use of fossil fuels inherently leads to carbon dioxide (CO_2) emissions. Aiming to reduce both CO_2 emissions and fossil fuel use, CO_2 can be captured and utilized as a feedstock for fuels, materials and chemicals.[1–3] In particular, CO_2 has recently been successfully utilized in the production of polyurethanes (PUR),

resulting in both lower CO_2 emissions and lower use of fossil fuels than conventional PUR.[4–6]

PUR production is particularly well suited for incorporation of CO_2 as PUR allows for both direct and indirect CO_2 utilization as follows: polyurethanes consist of polyols and isocyanates. In polyol synthesis, the CO_2 molecule can be directly inserted 'as such' in (poly)carbonate units, *i.e.*, without energy-intensive full cleavage of the C=O bonds.[5,6] In addition to the direct CO_2 utilization in polycarbonate units of the polyols, CO_2 can also be utilized indirectly in upstream processes of the polyol supply chain. For example, CO_2 can be converted to methanol[7] and subsequently to formaldehyde, which constitutes a potential monomer for polyols.[8]

As well as direct and indirect CO_2 utilization for polyols, CO_2 can also be used in the production of isocyanates. While the direct utilization of CO_2 for isocyanates still remains a dream in industry today,[9] conventional isocyanate production requires the feedstock carbon monoxide (CO),[10] which can be obtained by reduction of CO_2.[11]

Thus, a wide variety of options exist for the direct and indirect utilization of CO_2 in the supply chain of PUR. However, a systematic exploration and environmental evaluation of all direct and indirect CO_2 utilization options for PUR is missing. Therefore, the first goal of this article is to identify the total CO_2 utilization potential in the entire PUR supply chain. In other words, we identify the maximum amount of mass CO_2 utilized per mass PUR.

Intuitively, utilizing as much CO_2 as possible might seem environmentally most favorable. However, the energy requirements for both CO_2 capture and utilization (CCU) can lead to additional CO_2 emissions, fossil fuel use and other environmental impacts.[12] Thus, it is not always environmentally most reasonable to utilize as much CO_2 as possible. Instead, only those CO_2-based processes should be employed that allow for reductions of environmental impacts. The environmental impacts of a process can be determined by life cycle assessment (LCA). LCA is a methodology to quantify the environmental impacts of products and processes along the entire life cycle from cradle to grave. Applications of the LCA to CCU process are still very limited as recently reviewed.[13] For the application of LCA to CO_2 utilization, specific guidelines have recently been developed.[12,14] Based on these guidelines, the second goal of this article is to analyze which CO_2-based processes in the PUR supply chain allow for the largest reduction of CO_2 emissions and fossil fuel use. From this analysis, we determine the minimum CO_2 emissions and minimum fossil fuel use for the PUR supply chain.

Indirect CO_2 utilization processes usually require cleavage of C=O bonds, often *via* hydrogenation.[15–18] Whether CO_2 hydrogenation is environmentally favorable compared to a fossil-based benchmark depends strongly on the provision of hydrogen (H_2).[19,20] Conventional production of H_2 *via* steam methane reforming is typically energy- and emission-intensive.[21] The impacts of H_2 production can be significantly reduced by the combination of water electrolysis with renewable electricity sources.[19] Therefore, the third goal of this article is to analyze the minimum environmental impacts of CO_2 utilization in the PUR supply chain as a function of the environmental impacts of H_2 production. Based on this analysis, we determine threshold values for the environmental impacts of H_2 production that are tipping points for utilization of major amounts of CO_2 for PUR production.

The article is structured as follows. In Section 2, we review specific guidelines for the application of LCA for CO_2 utilization in polymers and state the goal and scope for the present LCA study of CO_2-based PUR. In Section 3, we present the considered PUR supply chain including conventional and CO_2-based processes. Furthermore, we introduce the optimization model using linear programming for the analysis of maximum amounts of CO_2 utilization and minimal environmental impacts. In Section 4, we present our findings, *i.e.*, the maximum amounts of utilized CO_2 per kg PUR, the CO_2-based processes with the largest environmental benefits, and the minimum environmental impacts of the PUR supply chain for H_2 production alternatives. Finally, in Section 5, conclusions are drawn for the utilization of CO_2 in the PUR supply chain.

2.   LCA for CO_2 utilization in PUR production

Both capture and utilization of CO_2 typically require energy whose provision is often based on fossil fuels and thus causes indirect CO_2 emissions. For example, post-combustion CO_2 capture from flue gases of power plants demands the equivalent of about 20–25% of the total electricity output of the power plant.[22,23] Utilization, or more precisely, conversion of the inert CO_2 molecule usually requires direct energy input or high-energetic co-reactants such as epoxides or hydrogen (H_2).[24] Thus, the intuitively expected environmental impacts of CO_2 capture and utilization are not given by default and a detailed environmental assessment is required. Life cycle assessment (LCA) is frequently acknowledged as suitable methodology for the environmental assessment of CCU.[1,2,25–27] Recently developed guidelines[12,14] for the application of LCA to CCU have already been applied to CO_2-based polyol synthesis.[28] Relevant aspects of these guidelines are reviewed and specified for the present context of CO_2 utilization in PUR production in the following.

2.1   Functional unit and comparability

The basis for any LCA is the definition of the so-called functional unit. The functional unit is a quantitative measure for the function of the system under study.[29,30] In the case of polymer production, the functional unit could be defined as "1 kg of polymer produced". However, since polymers have very different properties and a broad range of applications, this mass-based definition may fall short of a fair comparison of different polymers.[14]

In this work, we consider the theoretical production of polyurethanes from alternative fossil- and CO_2-based monomers. In reality, the product properties of the polyurethanes will differ for alternative monomers. An integrated approach to identify environmentally optimal polyols with specified properties has recently been proposed by our group.[8] However, accurate models for prediction of PUR properties are missing. As a first step, we therefore define the functional unit of this work as "production of 1 kg of polyurethane foam" regardless of its chemical structure and resulting properties. Nevertheless, chemical limitations for the incorporation of CO_2 are taken into account (*cf.* Section 3.1). Still, our study neglects many practical constraints on PUR production to explore the full design space and to provide inspiration to chemists facing the practical challenges involved. The obtained LCA results thus serve as lower bound estimates for the

environmental impacts of PUR production and can guide chemists towards more sustainable PUR synthesis.

2.2 Co-product allocation

Polyurethanes are typically produced together with many co-products along the PUR supply chain. For example, most technologies for the production of propylene oxide generate co-products such as *tert*-butyl alcohol or styrol.[28] In the context of CO_2-based PUR, the 'production' of CO_2 *via* CO_2 capture from point-sources is also coupled to production of the point-sources' primary product: for example, power plants with CO_2 capture provide electricity as a primary product.[12] To account for co-products, three methods exist in LCA: *system expansion*, *allocation* and *avoided burden*.[31,32]

In *system expansion*, the scope of the study is extended to include the co-products as functions. In other words, the functional unit is defined as a basket of products: the original product, here PUR, and all co-products. As system expansion can lead to very large baskets of products, interpretation and communication can be difficult. Therefore, it is often desirable to compute product-specific impacts for PUR.

Product-specific impacts can be obtained by methods of *allocation* and *avoided burden*. For *allocation*, environmental impacts are allocated to the individual products based on criteria such as mass content, energy content or price share. However, the choice of an allocation criterion is ambiguous.[33] For *avoided burden*, the co-products are assigned with an environmental credited since co-production avoids an alternative production of the co-product and the related environmental burdens. Thus, avoided burden implies a comparison to an alternative production. Avoided burden is therefore useful for a comparison with today's production technologies.

In this work, we are interested in the reduction of impacts compared to today's situation rather than in the exact value of absolute environmental impacts. For such a comparison, a change-oriented viewpoint is recommended[34] and thus, we employ the avoided burden method to obtain environmental impact reductions compared to the conventional PUR production today. Precisely, avoided burdens are credited for the production of excess hydrogen (H_2) and heat. For some of the feedstocks, we use data from LCA databases where allocation has already been applied.[35,36]

2.3 Environmental impact categories

LCA intends to cover a broad range of environmental impacts to avoid problem shifting between impact categories. The most prominent impact category 'global warming' (also named 'climate change' or carbon footprint) aggregates CO_2 and other greenhouse gas emissions according to their global warming potential in CO_2-equivalents.[37] The impact category 'fossil fuel depletion' quantifies the use of the limited fossil resources based on their energy content in kg oil equivalents.[38] CO_2 Capture and Utilization (CCU) aims at reducing CO_2 emissions and establishing an alternative carbon source, thus also reducing the use of fossil fuels. However, from Carbon Capture and Storage (CCS), a tradeoff is known between CO_2 emission reduction and fossil fuel use.[39–41] Therefore, CCU processes should be evaluated at least regarding impacts on global warming and fossil fuel use.[14] Of

course, it is desirable to perform a more complete LCA study with a broad range of environmental impacts.[42,43]

In this work, we assess the environmental potential of CO_2 utilization in PUR production with respect to CO_2 emissions and fossil fuel use.

2.4 CO_2 sources and CO_2 capture

CO_2 capture from diluted CO_2 sources requires energy for the separation of CO_2 from other gases. Moreover, CO_2 capture requires operating materials such as capture solvents, and process technologies such as absorption and desorption columns. All of these efforts for CO_2 capture are typically associated with fossil fuel use and thus CO_2 emissions. Therefore, the CO_2 emission reduction of CO_2 capture is lower than 1 kg CO_2 eq. per kg $CO_{2,feed}$. Here, CO_2 eq. refers to CO_2 emissions and other greenhouse gas emissions, and $CO_{2,feed}$ refers to the captured and subsequently utilized CO_2.

In this work, we consider a coal-fired power plant as a standard CO_2 source. For the considered coal-fired power plant, CO_2 capture can reduce CO_2 emissions by 0.84 kg CO_2 eq. and increases fossil fuel use by 0.05 kg oil eq. per kg $CO_{2,feed}$ compared to a power plant without CO_2 capture.[44] As the worst-case scenario, we also consider CO_2 capture from ambient air with CO_2 emission reductions of 0.51 kg CO_2 eq. and fossil fuel use of 0.18 kg oil eq. per kg $CO_{2,feed}$.[44] As the best-case scenario, we consider a hypothetical, ideal CO_2 source with CO_2 emission reductions of 1 kg CO_2 eq. per kg CO_2 captured and no increase in fossil fuel use. The best-case scenario corresponds to a CO_2 source which can be readily used in the CO_2 conversion but is vented to the atmosphere today.

2.5 Temporary carbon storage in PUR

Polyurethanes have a lifetime of several decades. Incorporating CO_2 into PUR can thus be considered as temporary carbon storage during the PUR lifetime. Temporary carbon storage generally has a positive effect on climate mitigation.[45,46] The absolute effect of temporary carbon storage is, however, argued to be small for the following reasons.[12]

If conventional and CO_2-based PUR syntheses yield PURs with identical properties, then use, lifetime and end-of-life (EOL) treatment of both PURs will also be identical. Differences only occur during PUR syntheses and thus, it is sufficient to limit an LCA-based comparison of conventional and CO_2-based PUR syntheses to a so-called cradle-to-gate scope. In this case, a climate benefit can only be achieved if CO_2-based PUR synthesis causes fewer emissions than conventional synthesis. A climate benefit from temporary carbon storage cannot be expected for CO_2-based PUR synthesis compared to conventional PUR synthesis.

If, however, CO_2 utilization for PUR synthesis alters PUR properties, changes in use, lifetime and EOL treatment can occur. An increased PUR lifetime and a reduction of EOL CO_2 emissions constitute relevant changes for assessing the effect of temporary carbon storage in LCA: a longer lifetime can shift EOL CO_2

emissions into the future. As a rule of thumb, this shift of CO_2 emissions can reduce the global warming impact of EOL emissions by about 1% for each year of lifetime extension.‡ Total EOL CO_2 emissions account for about one third of the total CO_2 eq. emissions in the life cycle of conventional PUR without credits for thermal energy recovery.[35] Thus, even for a 10 year longer lifetime, the temporary carbon storage effect reduces overall PUR global warming impact by only 3%. However, this simple analysis does not consider the general environmental benefit of longer product use.[47]

For PUR, a tradeoff is expected regarding the effect of CO_2 incorporation on EOL emissions: on the one hand, CO_2 utilization in PUR typically lowers the C content in PUR and thus lowers EOL CO_2 emissions. On the other hand, the lower C content also reduces the heating value leading to reduced thermal energy recovery in EOL. The reduced thermal energy recovery usually has to be compensated by fossil-based heating leading to additional CO_2 emissions.

For the above mentioned reasons, the climate mitigation effect of temporary carbon storage of CO_2 utilization for PUR is expected to be small. Nevertheless, we suggest quantifying the exact climate mitigation effect of temporary carbon storage on a case-by-case basis.

Due to difficulties in predicting the PUR lifetime from the chemical structure and due to the expectedly small climate effect of a PUR lifetime extension, temporary carbon storage is not considered in this work.

3.   The PUR supply chain optimization model

3.1   Overview of the PUR supply chain

The considered PUR supply chain is illustrated in Fig. 1. In the main article, we focus on the production of flexible PUR foams. Results for rigid PUR foams are presented in the ESI.† In the following, the considered production steps are briefly described.

   3.1.1   Flexible PUR foam production. Flexible PUR foams are produced from the feedstocks polyol and toluol-2,4-diisocyanat (TDI).[36] We assume water as an indirect foam blowing agent that reacts with TDI to CO_2 as the actual blowing agent. This CO_2 is directly released to the atmosphere. We consider a fixed mass ratio of TDI and polyol of $m_{TDI}/m_{polyol} = 0.4$.[36]

   3.1.2   Rigid PUR foam production. Rigid PUR foams are produced from the feedstocks polyol and methylene diphenyl diisocyanate (MDI).[36] We assume pentane as the foam blowing agent although CO_2 can be used as an alternative or co-blowing agent.[48] We consider a fixed mass ratio of MDI and polyol of $m_{MDI}/m_{polyol} = 1.6$.[36]

   3.1.3   Polyol production. Polyols are synthesized from a starter (here assumed as glycerol) and from the alternative monomer building blocks polyether, polycarbonate and poly oxymethylene. Conventional polyether polyols are made mainly from propylene oxide (PO).[10] For production of PO, environmental impacts are considered according to the technology mix.[28] PO can be partly substituted by CO_2 which co-polymerizes with PO to polycarbonate units.[5] Furthermore, poly

---

‡ The rule of thumb of 1% global warming impact reductions is only valid for considering the absorbed radiation over a fixed time horizon of 100 years.[12] In this context, it should be mentioned that the choice of an adequate time horizon plays a key role for the assessment of temporary carbon storage.[57]

ART ■ C5FD00067J
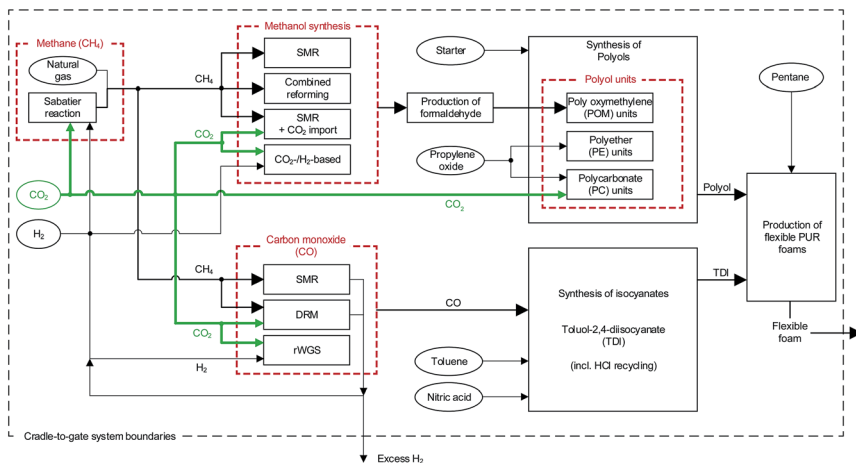
Fig. 1 The PUR supply chain for flexible foams. For simplicity, only material flows are shown; heat and electricity are also considered in the supply chain optimization model. (Green) very thick arrows indicate CO_2 feedstock flows. Large arrowheads indicate feedstock flows with carbon that potentially stems from carbon dioxide. Smaller arrow heads indicate feedstock flows from non-CO_2 sources. The (red) dashed boxes indicate choices between (i) methane sources, (ii) methanol synthesis, (iii) CO sources, and (iv) polyol units. Color online.

oxymethylene (POM) diols have been tested for polyurethane production.[49] POM is polymerized from formaldehyde, which is exclusively produced from methanol.[50]

3.1.4 Methanol production. Conventionally, methanol is synthesized from syngas produced by steam methane reforming (SMR).[51] Since syngas from SMR usually does not have the optimal composition for methanol synthesis, CO_2 can be added (SMR + CO_2 import) to obtain the desired syngas composition. A fossil-based alternative for methanol production is the combined reforming using SMR and partial oxidation of methane.[52] This process requires O_2 as an input. An exclusively CO_2-based alternative for methanol production is the direct reforming of CO_2 and H_2 to methanol.[7]

3.1.5 Methylene diphenyl diisocyanate (MDI) production. MDI is produced from phosgene and methylenedianiline (MDA). MDA is produced by the reaction of formaldehyde and aniline. Aniline results from the hydrogenation of nitrobenzene. Nitrobenzene is produced by the nitration of benzene with nitric acid. Phosgene is produced by the reaction of carbon monoxide (CO) and chlorine gas. A by-product of the MDI production is hydrochloric acid (HCl). HCl is separated by HCl electrolysis to provide chlorine as feedstock for the phosgenation. HCl electrolysis also provides H_2 which is assumed to be used internally in MDI production.[10]

For our analysis, the production of MDI described above is modelled as a single process based on stoichiometric inputs (formaldehyde, benzene, nitric acid, H_2 and CO) and outputs (MDI). Furthermore, the electricity demand for HCl electrolysis is included.

3.1.6 Toluol-2,4-diisocyanate (TDI) production. TDI is produced from phosgene and diaminotoluene (TDA). TDA results from the hydrogenation of dinitrotoluene (DNT). DNT is produced by the nitration of toluene with nitric acid.[10] Phosgene production and HCl recycling *via* electrolysis are equivalent to the processes in MDI production (see Section 3.1.5).

For our analysis, the production of TDI described above is modelled as a single process based on stoichiometric inputs (toluene, nitric acid and CO) and outputs (TDI and waste). Furthermore, electricity demand for HCl electrolysis is included.

3.1.7 CO and hydrogen (H_2) supply. CO and hydrogen (H_2) are feedstocks for MDI and TDI production. If H_2 from internal HCl electrolysis is used (assumed here, see Sections 3.1.5 and 3.1.6), MDI production requires another 2 mol H_2 per mol CO, whereas TDI does not require additional H_2.[10] We consider the following processes for CO and H_2 supply for MDI and TDI production.

Conventionally, both CO and H_2 are supplied by SMR.[53] Part of the methane can be substituted by CO_2 through the dry reforming of methane (DRM).[11] However, for the same amount of CO, DRM produces less hydrogen compared to SMR. The complete substitution of methane is enabled by the reverse water gas shift (rWGS) reaction. For rWGS, hydrogen and CO_2 are required as feedstocks. The rWGS reaction produces only CO (and water as a by-product).[54]

3.1.8 Methane supply. Conventionally, the feedstock methane (CH_4) is supplied by natural gas. Methane can also be produced from H_2 and CO_2 through the Sabatier reaction.[55]

An overview of the employed LCA datasets for all processes is given in the ESI.†

3.2 Optimization model

To rigorously study the environmental potential of utilizing CO_2 in the PUR supply chain, a superstructure-based optimization model is used. The superstructure comprises all processes of the PUR supply chain (*cf.* Section 3.1). The optimization model is used to identify the maximum CO_2 utilization potential (Section 3.2.1) and the minimal environmental impacts (Section 3.2.2) for the PUR supply chain.

3.2.1 Maximum CO_2 amount in the PUR supply chain. As the first step, optimization is carried out maximizing the total amount of CO_2 utilized ($m_{CO_2,feed}$) to identify the maximum CO_2 utilization potential in the entire PUR supply chain. The amount of PUR produced is set to $m_{PUR} = 1$ kg (functional unit, *cf.* Section 2.2). While the total CO_2 feed ($m_{CO_2,feed}$) is to be maximized for 1 kg PUR, mass and energy balances must be fulfilled across the entire PUR supply chain. This optimization problem can be formulated as a so-called linear program (LP):

$$\max_{x} \quad m_{CO_2,feed} = d^T x \, ,$$
$$\text{s.t. } m_{PUR} = 1 \text{ kg (functional unit)}, \tag{1}$$
$$A\,x = 0 \text{ (mass and energy balances in supply chain)}.$$

The so-called scaling vector x describes which processes are employed and to what extent. The vector d describes how much CO_2 is directly utilized in each process. Thus, the overall amount of CO_2 utilized is obtained by $m_{CO_2,feed} = d^T x$, to be maximized here. The matrix A contains all inputs and outputs of the individual

processes in the PUR supply chain. Matrix A and vector d are given explicitly in the ESI.†

3.2.2 Minimal environmental impact for PUR supply chain: effect of CO_2 utilized.

To identify minimal environmental impacts for the PUR supply chain, optimization is carried out minimizing the total environmental impacts of all processes required for PUR production. In this paper, we consider the environmental impact categories 'global warming' and 'fossil fuel use' (*cf.* Section 2.3). The amount of PUR produced is again set to $m_{PUR} = 1$ kg, and mass and energy balances must be fulfilled across the PUR supply chain. The corresponding optimization problem can be formulated as follows:

$$\max_{x} \quad z = Bx,$$
$$\text{s.t. } m_{PUR} = 1 \text{ kg (functional unit)}, \quad (2)$$
$$Ax = 0 \text{ (mass and energy balances in supply chain)}.$$

The matrix B contains the direct environmental impacts of the individual processes in the PUR supply chain. The cradle-to-gate environmental impacts z for production of 1 kg PUR are obtained by $z = Bx$. Matrix B is given in the ESI.†

For the environmental impacts of CO_2 supply, the three cases presented in Section 2.4 are analyzed: CO_2 capture from a coal-fired power plant (standard case), CO_2 capture from ambient air (worst case) and an ideal CO_2 source (best case).

Effect of CO_2 utilized. To determine the effect of the amount of CO_2 utilized, the minimization of environmental impacts is repeated for fixed amounts of CO_2 utilized. For this purpose, the amount of CO_2 utilized is varied between zero and $m_{CO_2,feed,max}$. For this analysis, we consider three cases of hydrogen production: (i) conventional steam methane reforming (SMR), (ii) water electrolysis, and (iii) ideal hydrogen production with no environmental impacts at all. The corresponding environmental impacts are given in Table 1.

Effect of H_2 production alternatives. To analyze the effect of hydrogen production alternatives more rigorously, the environmental impact of hydrogen supply is also varied continuously. For this purpose, the optimization is repeated for the full range of environmental impacts of the considered hydrogen production alternatives, *i.e.*, for global warming impacts from zero to 10 kg CO_2 eq. per kg H_2, and for fossil depletion impacts from zero to 5 kg oil eq. per kg H_2.

Table 1 Considered environmental impacts for hydrogen production alternatives

	Global warming impact (kg CO_2 eq. per kg H_2)	Fossil depletion impact (kg oil eq. per kg H_2)
Steam methane reforming	10	5
Water electrolysis[a]	5	2.5
Ideal H_2 production	0	0

[a] The environmental impacts for H_2 from water electrolysis depend largely on the electricity source for electrolysis. For production of 1 kg H_2, the electricity demand of electrolysis is about 50 kW h.[54] With this electricity demand, the presented environmental impacts of water electrolysis correspond to environmental impacts of electricity generation of 100 kg CO_2 eq. and 50 kg oil eq. per MWh (similar to the grid mix characteristics of Sweden).[35]

4. Results

In this section, we present the maximum CO_2 utilization potential and minimal environmental impacts for PUR production. In the first scenario, we consider only direct utilization of CO_2 for polycarbonate (PC) units in polyol production and indirect CO_2 utilization in the isocyanate supply chain. The utilization of poly oxymethylene (POM) units as polyol building blocks is not permitted, regardless of whether POM is produced from fossil or CO_2-based feedstocks. This first scenario ('without POM') includes technically feasible CO_2 utilization options. The utilization of POM for polyols and PUR is a promising approach; however, utilization of POM in polyols is still in the research phase.[49] As a second scenario, and for future outlook, we consider all CO_2 utilization options in the PUR supply chain including fossil- and CO_2-based POM units for polyols (scenario 'with POM').

4.1 Maximum CO_2 utilization amount in the PUR supply chain

The maximum CO_2 utilization potential refers to the maximum amount of CO_2 utilized in the entire PUR supply chain. The amount of CO_2 utilized can be greater than 1 kg CO_2 for production of 1 kg PUR since it is simply the total amount of CO_2 utilized in the PUR supply chain; it does not refer to the amount of CO_2 incorporated or the CO_2 content in the final PUR. The maximum CO_2 amount in the PUR supply chain is presented in Fig. 2 for both flexible and rigid PUR foams.

The maximum potential for direct CO_2 utilization in PC units in polyols is about twice as large in flexible PUR foam compared to rigid PUR foam: in flexible foam, up to 0.30 kg CO_2 per kg PUR can be utilized directly in polyols, while 0.16 kg CO_2 per kg PUR can be utilized for rigid foam. The larger potential for flexible foam is due to the typically higher mass content of polyols in flexible foams compared to rigid foams (*cf.* Section 3.1.1 and 3.1.2).
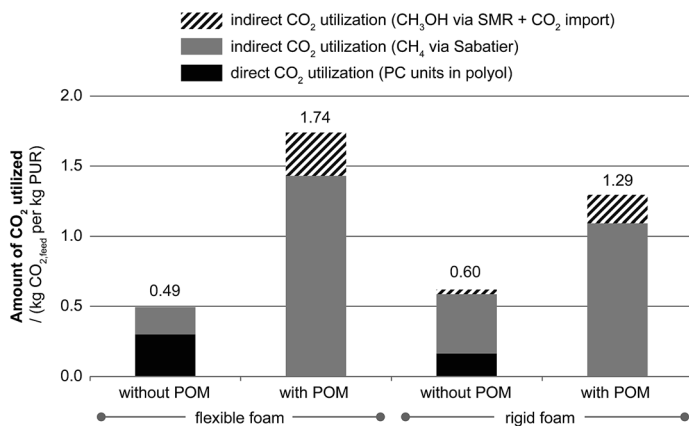
Fig. 2 CO_2 utilization potential in the PUR supply chain as the amount of CO_2 utilized per kg PUR. Scenario 'without POM' does not permit utilization of poly oxymethylene (POM) units as polyol building blocks; all other CO_2 utilization options in the PUR supply chain are possible. Scenario 'with POM' allows all CO_2 utilization options in the PUR supply chain including fossil- and CO_2-based POM units for polyols.

ART ■ C5FD00067J

If POM units are not allowed for polyol production, the maximum CO_2 utilization potential can still be increased by indirect CO_2 utilization in the isocyanate supply chain: the indirect CO_2 utilization potential is 0.20 kg CO_2 and 0.46 kg CO_2 per kg PUR for flexible and rigid foams, respectively. For flexible foams, the indirectly utilized CO_2 is completely converted to methane via the Sabatier reaction; methane is then converted via steam methane reforming (SMR) to CO and H_2 for isocyanate production. For rigid foams, 93% of the indirectly utilized CO_2 is converted to methane, of which 69% is converted via SMR to CO and H_2 and 31% is converted via SMR (with CO_2 import) to methanol for subsequent form-aldehyde and MDI production. Methanol production via SMR (with CO_2 import) utilizes the remaining 7% of the indirectly utilized CO_2.

The global maximum CO_2 utilization potential can be achieved if POM units are allowed in polyol synthesis. For flexible foams, up to 1.74 kg CO_2 can be utilized, exclusively through indirect CO_2 utilization. 82% of the indirectly utilized CO_2 are converted via the Sabatier reaction to methane, of which 14% are converted via SMR to CO and H_2 and 86% are converted via SMR (with CO_2 import) to methanol for subsequent formaldehyde and POM production. Meth-anol production via SMR (with CO_2 import) utilizes the remaining 18% of the indirectly utilized CO_2. For rigid foams, up to 1.29 kg CO_2 can be utilized, again exclusively through indirect CO_2 utilization. 84% of the indirectly utilized CO_2 is converted via the Sabatier reaction to methane, of which 27% is converted via SMR to CO and H_2 and 73% is converted via SMR (with CO_2 import) to methanol. Methanol production via SMR (with CO_2 import) also utilizes the remaining 16% of the indirectly utilized CO_2. The produced methanol is converted to formalde-hyde for subsequent POM (84%) and MDI production (16%).

In the following part of this paper, we focus on CO_2 utilization for flexible PUR foams. The corresponding results for rigid PUR foams are presented in the ESI.†

4.2 Minimal environmental impact for PUR supply chain: effect of CO_2 utilization amount

In the previous section, maximum CO_2 utilization amounts have been identified. Since it might not be environmentally favorable to utilize as much CO_2 as possible, we now identify the minimal environmental impacts for PUR produc-tion for variable amounts of CO_2 utilized as described in Section 3.2.2.

Fig. 3 shows minimal global warming impacts for flexible PUR foams with and without POM units. For foams without POM units, increasing the amount of CO_2 utilized generally leads to a reduction of CO_2 emissions compared to conventional foams from fossil-based polyether (PE) polyols and TDI. In particular, the direct utilization of CO_2 in polycarbonate (PC) units of polyols allows for a reduction of 3.7–4.1 kg CO_2 eq. per kg CO_2 utilized. The CO_2 reductions stem from CO_2 capture (0–0.84 kg CO_2 eq. per kg CO_2 utilized, $cf.$ Section 2.4) and from substitution of emission-intensive epoxides (3.1 kg CO_2 eq. perkg CO_2 utilized); $cf.$ von der Assen $et~al.$, 2014.[14] The potential to further reduce CO_2 emissions through indirect CO_2 utilization depends on the emissions from hydrogen production. Nevertheless, for all hydrogen production alternatives, the CO_2 reduction potential for indirect CO_2 utilization is very small in flexible PUR foams without POM units.

If POM units can be incorporated into polyols for flexible PUR foams, the potential to reduce CO_2 emissions is much larger for two reasons: first, even

ART ■ C5FD00067J
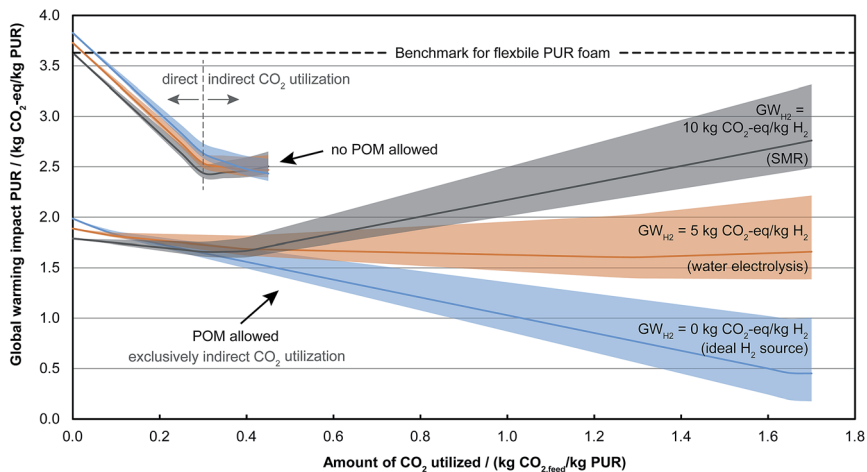
Fig. 3 Minimum global warming impact for flexible PUR foams for variable amounts of CO_2 utilized. The transparent areas indicate the range for alternative CO_2 sources: lower bounds correspond to an ideal source, upper bounds correspond to CO_2 capture from ambient air, and the solid lines correspond to CO_2 capture from a coal-fired power plant.

fossil-based production of POM units causes much lower CO_2 emissions than production of conventional PE units (*cf.* Fig. 3 for $m_{CO_2,feed} = 0$). Second, the CO_2 utilization potential is much higher for polyols with POM units (*cf.* Section 4.1). More CO_2 utilization reduces CO_2 emissions at the CO_2 source by CO_2 capture. However, for indirect CO_2 utilization, POM units require provision of hydrogen as a feedstock for methanol synthesis. Whether indirect CO_2 utilization for PUR with POM actually reduces CO_2 emissions therefore depends largely on the emissions from hydrogen production: for ideal hydrogen production with no CO_2 emissions, the computed minimal CO_2 emissions for PUR production strictly decrease with increasing amounts of CO_2 utilized. For hydrogen from water electrolysis, the computed minimal CO_2 emissions are almost constant for variable amounts of CO_2 utilized. For today's conventional hydrogen production *via* SMR, the computed minimal CO_2 emissions decrease up to a CO_2 utilization amount of 0.35 kg CO_2. Further increasing the CO_2 utilization amount increases CO_2 emissions of PUR production. Thus, increasing the amount of CO_2 utilized then leads to additional CO_2 emissions.

Fig. 3 also shows that utilization of 1 kg CO_2 does not lead to a reduction of 1 kg CO_2 emissions.[3,56] In some cases, utilization of CO_2 even increases CO_2 emissions. For this reason, the overall minimum CO_2 emissions do not necessarily occur for the maximum amount of CO_2 utilized. In most cases, CO_2 utilization reduces CO_2 emissions. Here, some processes reduce more CO_2 emissions per CO_2 utilized than others. For example, the direct utilization of CO_2 for PC units in polyols allows for the largest CO_2 reduction per amount of CO_2 utilized. However, since CO_2 is not a restricted resource, CO_2 should be utilized not only in processes with the largest CO_2 reductions but instead in such amounts that the overall minimum of CO_2 emissions is reached. The overall minimum for flexible PUR foams with POM units depends largely on the hydrogen production alternative.

In addition to global warming impacts, we identified the minimal fossil fuel use in flexible PUR foam for variable CO_2 utilization amounts. The qualitative behavior is very similar for global warming impacts and fossil fuel use, *c.f.* Fig. 3 and 4. Thus, we focus on global warming impacts in the following. The corresponding results for fossil fuel use are given in the ESI.†

4.3 Minimal environmental impact for the PUR supply chain: effect of H_2 production alternatives

In the previous section, three distinct cases for hydrogen production have been analyzed in the context of minimal environmental impacts for CO_2 utilization in PUR production. Environmentally favorable hydrogen production has been identified as an important factor to increase the amount of CO_2 utilized for environmentally favorable PUR production. In contrast to the three discrete cases, this section investigates the effects of the environmental impacts of hydrogen production in more detail. In the main article, impacts on global warming are shown; the fossil fuel use is presented in the ESI.†

Fig. 5 shows that the global warming impact of flexible PUR foam can be reduced from 1.68 to 0.43 kg CO_2 eq. per kg PUR (for CO_2 captured from a coal-fired power plant, solid line) if the global warming impact of H_2 production decreases from 10 to 0 kg CO_2 eq. per kg H_2. For this decrease in global warming impact of H_2 production, the amount of CO_2 utilized increases from 0.42 to 1.68 kg CO_2 per kg PUR (right *y*-axis in Fig. 5). In particular, the amount of CO_2 utilized increases sharply if the global warming impact of H_2 production drops below 5.6 kg CO_2 eq. per kg H_2, and even further for a drop below 4.1 kg CO_2 eq. per kg H_2. The first increase in CO_2 utilization is mainly due to a switch in methanol production from SMR + CO_2 import to entirely CO_2-based methanol production. Before the first increase (above 5.6 kg CO_2 eq. per kg H_2), no hydrogen is utilized
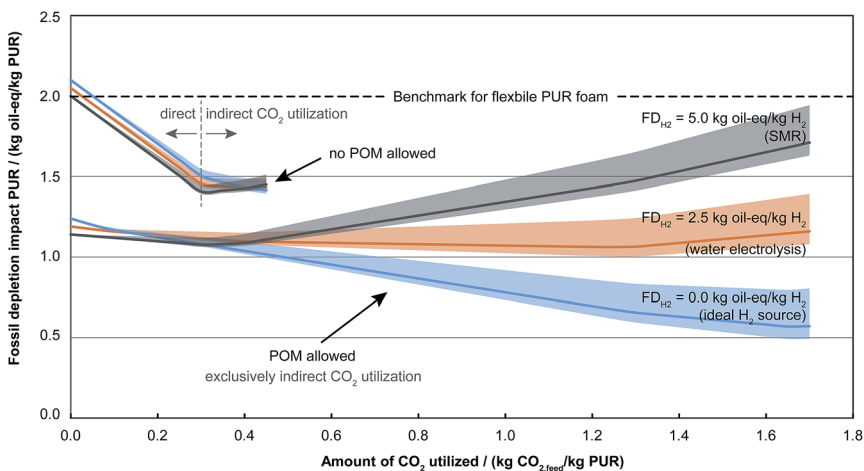
Fig. 4 Minimum fossil depletion for flexible PUR foams for variable amounts of CO_2 utilized. The transparent areas indicate the range for alternative CO_2 sources: lower bounds correspond to an ideal source, upper bounds correspond to CO_2 capture from ambient air, and the solid lines correspond to CO_2 capture from a coal-fired power plant.
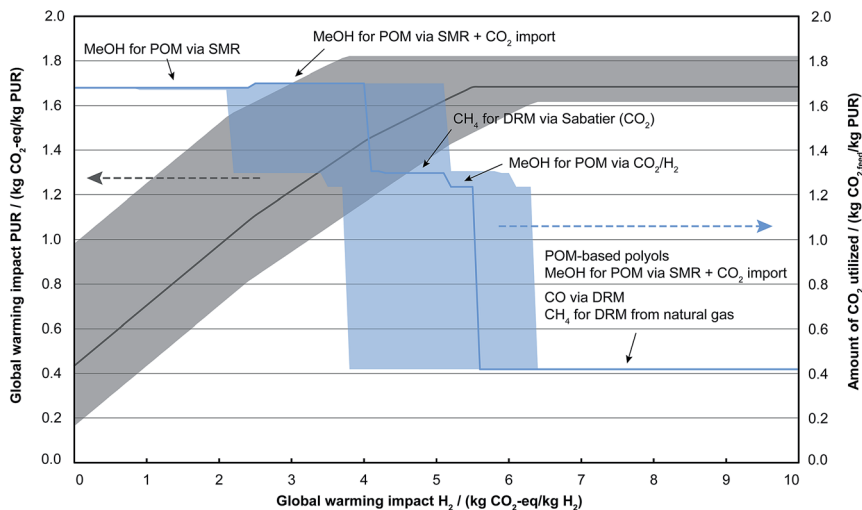
Fig. 5 Minimum global warming impacts for flexible PUR foam for a variable global warming impact of hydrogen production. The solid lines refer to CO_2 captured from a coal-fired power plant. The lower bound of the global warming impact of PUR and the upper bound of the CO_2 utilization amount refer to an ideal CO_2 source (best case). The upper bound of the global warming impact of PUR and the lower bound of the CO_2 utilization amount refer to CO_2 capture from ambient air (worst case).

for PUR production and thus, the global warming impact of PUR is independent from the global warming impact of H_2 production. The second increase is mainly due to a switch from methane from natural gas, to methane from CO_2 *via* the Sabatier reaction.

The analysis in this section highlights that hydrogen production with low environmental impacts is important for the indirect utilization of CO_2 in the PUR supply chain.

5.   Conclusions

Many options exist for the utilization of CO_2 in the polyurethane (PUR) supply chain. In this paper, we present a systematic exploration and environmental evaluation of all direct and indirect CO_2 utilization options for PUR production. Our analysis shows that direct CO_2 utilization for polycarbonate units in polyols is limited in the amount of CO_2 utilized; however, direct CO_2 utilization allows for large reductions of up to 4 kg CO_2 eq. per kg CO_2 utilized. The CO_2 utilization amount can be increased by indirect CO_2 utilization for reduction to carbon monoxide in isocyanate production. However, the environmental potential of indirect CO_2 utilization in the isocyanate supply chain is rather small. Both the CO_2 utilization amount and the reduction of environmental impacts can be largely increased through indirect CO_2 utilization if poly oxymethylene (POM) units can be incorporated into polyols. In this case, large environmental impact reductions are already possible for fossil-based POM production. Additional environmental benefits from CO_2-based POM production depend largely on the required hydrogen (H_2) source. Current H_2 production *via* steam methane

reforming (SMR) does not allow for additional reductions of environmental impacts. Even worse, for H_2 from SMR, increasing the amount of CO_2 utilized can even lead to additional CO_2 emissions. Thus, utilizing as much CO_2 in the PUR supply chain as possible is not always environmentally optimal. Instead, minimal environmental impacts are achieved for CO_2 utilization amounts below the maximum possible utilization amount. To still exploit the full CO_2 utilization potential for environmental impact reduction in PUR production with POM units, environmentally friendly H_2 production with CO_2 emissions below 4 kg CO_2 eq. per kg H_2 is required. The present study has neglected many practical challenges for researchers to be able to explore the full theoretical design space for environmentally optimal polyurethane production. Our work aims at inspiring future research on sustainable CO_2 utilization for polyurethanes.

Acknowledgements

References

1 E. A. Quadrelli, G. Centi, J.-L. Duplan and S. Perathoner, *ChemSusChem*, 2011, **4**, 1194–1215.

2 M. Peters, B. Köhler, W. Kuckshinrichs, W. Leitner, P. Markewitz and T. E. Müller, *ChemSusChem*, 2011, **4**, 1216–1240.

3 M. Aresta, A. Dibenedetto and A. Angelini, *Chem. Rev.*, 2014, **114**, 1709–1742.

4 D. J. Darensbourg and S. J. Wilson, *Green Chem.*, 2012, **14**, 2665–2671.

5 J. Langanke, A. Wolf, J. Hofmann, K. Böhm, M. A. Subhani, T. E. Müller, W. Leitner and C. Gürtler, *Green Chem.*, 2014, **16**, 1865–1870.

6 A. M. Chapman, C. Keyworth, M. R. Kember, A. J. J. Lennox and C. K. Williams, *ACS Catal.*, 2015, **5**, 1581–1588.

7 L. K. Rihko-Struckmann, A. Peschel, R. Hanke-Rauschenbach and K. Sundmacher, *Ind. Eng. Chem. Res.*, 2010, **49**, 11073–11078.

8 N. von der Assen, M. Lampe, L. Müller and A. Bardow, in *12th International Symposium on Process Systems Engineering and 25th European Symposium on Computer Aided Process Engineering*, ed. K. V. Gernaey, J. K. Huusom and R. Gani, Elsevier, 2015, vol. 37, pp. 1235–1240.

9 T. E. Waldman and W. D. McGhee, *J. Chem. Soc., Chem. Commun.*, 1994, 957–958.

10 PlasticsEurope, Eco-profiles, 2014, http://www.plasticseurope.org/plasticssustainability/eco-profiles.aspx, http://www.plasticseurope.org/plasticssustainability/eco-profiles.aspx, accessed 17 Dec 2014.

11 E. Schwab, A. Milanov, S. A. Schunk, A. Behrens and N. Schödel, *Chem. Ing. Tech.*, 2015, **87**, 347–353.

12 N. von der Assen, J. Jung and A. Bardow, *Energy Environ. Sci.*, 2013, **6**, 2721–2734.

13 R. M. Cuéllar-Franca and A. Azapagic, *J. CO2 Util.*, 2015, **9**, 82–102.

14 N. von der Assen, P. Voll, M. Peters and A. Bardow, *Chem. Soc. Rev.*, 2014, **43**, 7982–7994.

15 P. G. Jessop, T. Ikariya and R. Noyori, *Chem. Rev.*, 1995, **95**, 259–272.

16 W. Wang, S. Wang, X. Ma and J. Gong, *Chem. Soc. Rev.*, 2011, **40**, 3703–3727.

17 S. Wesselbaum, U. Hintermair and W. Leitner, *Angew. Chem., Int. Ed.*, 2012, **51**, 8585–8588.

18 S. Wesselbaum, T. vom Stein, J. Klankermayer and W. Leitner, *Angew. Chem., Int. Ed.*, 2012, **51**, 7499–7502.

19 G. Reiter and J. Lindorfer, *Int. J. Life Cycle Assess.*, 2015, **20**, 477–489.

20 C. van der Giesen, R. Kleijn and G. J. Kramer, *Environ. Sci. Technol.*, 2014, **48**, 7111–7121.

21 E. Cetinkaya, I. Dincer and G. Naterer, *Int. J. Hydrogen Energy*, 2012, **37**, 2071–2080.

22 International Energy Agency, *Cost and Performance of Carbon Dioxide Capture From Power Generation*, 2011, https://www.iea.org/publications/freepublications/publication/costperf_ccs_powergen.pdf, accessed 20 April 2015.

23 D. Y. Leung, G. Caramanna and M. M. Maroto-Valer, *Renewable Sustainable Energy Rev.*, 2014, **39**, 426–443.

24 T. Sakakura, J.-C. Choi and H. Yasuda, *Chem. Rev.*, 2007, **107**, 2365–2387.

25 M. Aresta and A. Dibenedetto, *Dalton Trans.*, 2007, **28**, 2975–2992.

26 G. Centi and S. Perathoner, *Greenhouse Gases: Sci. Technol.*, 2011, **1**, 21–35.

27 P. Markewitz, W. Kuckshinrichs, W. Leitner, J. Linssen, P. Zapp, R. Bongartz, A. Schreiber and T. E. Müller, *Energy Environ. Sci.*, 2012, **5**, 7281–7305.

28 N. von der Assen and A. Bardow, *Green Chem.*, 2014, **16**, 3272–3280.

29 ISO 14040:2009, *Environmental management – Life cycle assessment – Principles and framework*, European Committee for Standardisation, Brussels, 2009.

30 ISO 14044:2006, *Environmental management – Life cycle assessment – Requirements and guidelines*, European Committee for Standardisation, Brussels, 2006.

31 *Life Cycle Assessment Handbook: A Guide for Environmentally Sustainable Products*, ed. M. A. Curran, WILEY-VCH, Weinheim, 2012.

32 R. Heijungs and R. Frischknecht, *Int. J. Life Cycle Assess.*, 1998, **3**, 321–332.

33 J. Jung, N. von der Assen and A. Bardow, *Int. J. Life Cycle Assess.*, 2014, **19**, 661–676.

34 N. Pelletier, F. Ardente, M. Brandão, C. De Camillis and D. Pennington, *Int. J. Life Cycle Assess.*, 2015, **20**, 74–86.

35 PE International, *GaBi LCA Software and LCA Databases*, 2012, http://www.gabi-software.com/databases/gabi-databases, accessed nov 13, 2014.

36 Swiss Centre for Life Cycle Inventories, *Ecoinvent Data V2.2*, 2010, http://www.ecoinvent.org/, accessed Nov 13, 2014.

37 P. Forster, V. Ramaswamy, P. Artaxo, T. Berntsen, R. Betts, D. Fahey, J. Haywood, J. Lean, D. Lowe, G. Myhre, J. Nganga, R. Prinn, G. Raga, M. Schulz and R. V. Dorland, Climate Change, in *The Physical Science Basis. Contribution of Working Group I to the Fourth Assessment Report of the Intergovernmental Panel on Climate Change*, ed. S. Solomon, D. Qin, M. Manning, Z. Chen, M. Marquis, K. Averyt, M. Tignor and H. Miller, Cambridge University Press, Cambridge, United Kingdom and New York, 2007, ch. 2, pp. 129–234.

ART ■ C5FD00067J

38 M. Goedkoop, R. Heijungs, M. Huijbregts, A. D. Schryver, J. Struijs and R. V. Zelm, *ReCiPe 2008, A life cycle impact assessment method which comprises harmonised category indicators at the midpoint and the endpoint level*, 1st edn, (version 1.08) Report I: Characterisation, 2013, http://www.lcia-recipe.net, accessed 17 Dec 2014.

39 R. Sathre, M. Chester, J. Cain and E. Masanet, *Energy*, 2012, **37**, 540–548.

40 J. Marx, A. Schreiber, P. Zapp, M. Haines, J.-F. Hake and J. Gale, *Energy Procedia*, 2011, **4**, 2448–2456.

41 A. Schreiber, P. Zapp and J. Marx, *J. Ind. Ecol.*, 2012, **16**, S155–S168.

42 M. Z. Hauschild, M. Goedkoop, J. Guinée, R. Heijungs, M. Huijbregts, O. Jolliet, M. Margni, A. De Schryver, S. Humbert, A. Laurent, S. Sala and R. Pant, *Int. J. Life Cycle Assess.*, 2013, **18**, 683–697.

43 ICCA, International Council of Chemical Associations, *How to Know If and When it's Time to Commission a Life Cycle Assessment*, 2013.

44 N. von der Assen, L. Müller, A. Steingrube, P. Voll and A. Bardow, 2015, submitted.

45 S. V. Jørgensen, M. Z. Hauschild and P. H. Nielsen, *Int. J. Life Cycle Assess.*, 2015, **20**, 451–462.

46 M. Brandão, A. Levasseur, M. Kirschbaum, B. Weidema, A. Cowie, S. Jørgensen, M. Hauschild, D. Pennington and K. Chomkhamsri, *Int. J. Life Cycle Assess.*, 2012, **18**, 230–240.

47 M. Mequignon, L. Adolphe, F. Thellier and H. A. Haddou, *Build. Environ.*, 2013, **59**, 654–661.

48 U.S. Environmental Protection Agency, Transitioning to low-GWP foam blowing agents, 2011,http://www.epa.gov/ozone/downloads/EPA_HFC_ConstFoam.pdf, accessed 6 May 2015.

49 Bayer MaterialScience, From Dream Production to Dream Polymers. Presentation at the 4th BMBF Status Conference on CO2 Utilization, 8. April 2014, Königswinter, Germany, http://www.chemieundco2.de/_media/01_DreamPolymers_status_080414.pdf, 2014, accessed 6 May 2015.

50 G. Reuss, W. Disteldorf, A. O. Gamer and A. Hilt, in *Ullmann's Encyclopedia of Industrial Chemistry*, Wiley-VCH, Weinheim, 2012, vol. 15, ch. Formaldehyde, pp. 735–768.

51 S. G. Jadhav, P. D. Vaidya, B. M. Bhanage and J. B. Joshi, *Chem. Eng. Res. Des.*, 2014, **92**, 2557–2567.

52 N. Dave and G. A. Foulds, *Ind. Eng. Chem. Res.*, 1995, **34**, 1037–1043.

53 L. Chen, Y. Lu, Q. Hong, J. Lin and F. Dautzenberg, *Appl. Catal., A*, 2005, **292**, 295–304.

54 A. Sternberg and A. Bardow, *Energy Environ. Sci.*, 2015, **8**, 389–400.

55 E. V. Kondratenko, G. Mul, J. Baltrusaitis, G. O. Larrazabal and J. Perez-Ramirez, *Energy Environ. Sci.*, 2013, **6**, 3112–3135.

56 M. Aresta and M. Galatola, *J. Cleaner Prod.*, 1999, **7**, 181–193.

57 S. V. Jørgensen and M. Z. Hauschild, *Int. J. Life Cycle Assess.*, 2013, **18**, 747–754.

ART ■ C5FD00067J

PAPER

Hydrothermal conversion of carbon dioxide into formic acid with the aid of zerovalent iron: the potential of a two-step approach

K. Michiels,*[ab] B. Peeraer,[a] W. van Dun,[a] J. Spooren[a] and V. Meynen[b]

Our research focuses on the hydrothermal conversion of carbon dioxide into formic acid with the aid of zerovalent iron. Conventionally, a one-step approach is applied wherein both (i) the production of hydrogen gas, through the oxidation of zerovalent iron in an aqueous medium and (ii) the conversion of carbon dioxide with this hydrogen gas into formic acid, are performed under the same reaction conditions at a temperature of approximately 300 °C. Until now, the yields of formic acid mentioned in the literature are, in the absence of a catalytic substance, low (13.5%). Recently, we developed a hydrothermal hydrogen gas production method based on the oxidation of zerovalent iron and performed under mild conditions (temperature of 160 °C). This synthesis method produces hydrogen gas with a high purity (>99 mol%) and a significant yield (approximately 80 mol%). These experimental results suggested that the optimal hydrothermal reaction conditions for the production of hydrogen gas and the conversion of carbon dioxide, are strongly different in case of applying zerovalent iron as the reducing agent. Therefore, this paper studies the potential of a two-step approach to enhance the carbon conversion yields. The first step is the production of hydrogen gas via the developed method at 160 °C. The second step is the conversion of carbon dioxide at higher temperatures (250–350 °C). This study reveals that the solubility of hydrogen gas into the aqueous solution is a key parameter in order to achieve a high amount of carbon conversion. Therefore, a high temperature, the degree of filling and the initial hydrogen gas amount are necessary to successfully perform the carbon dioxide conversion step with high carbon conversion yields. Applying these insights have led to the experimental observation that via a two-step approach the conversion of potassium hydrogen carbonate into potassium formate can be successfully performed with higher carbon conversion yields, up to 77.9 wt%, and a selectivity of at least 81% when applying a reaction temperature of 280 °C for 24 hours,

[a]Waste Recycling Technologies, Sustainable Materials Management, Flemish Institute for Technological Research, VITO N.V., Boeretang 200, 2400 Mol, Belgium. E-mail: koen.michiels@vito.be; Tel: +32 14335664
[b]Laboratory of Adsorption and Catalysis, Department of Chemistry, University of Antwerp, UAntwerp, Universiteitsplein 1, 2610 Wilrijk, Belgium

ART ■ C5FD00104H

a degree of filling with water of 50 vol% and an initial amount of hydrogen gas of 100 mmol.

Introduction

Natural hydrothermal systems occur at different places on our planet.[1] Bevan M. French[2,3] was the first scientist to recognise these natural hydrothermal systems as plausible sites for abiotic synthesis of organic compounds such as methane, CH_4.[4] Abiotic synthesis can be defined as the formation of compounds through purely chemical processes, without the participation of biological organisms.[5] Following the work by French, scientists have been focusing on lithospheric hydrothermal environments as potential sites for abiotic synthesis of organic molecules.[4] This interest arose due to the proposition that the origin of life on Earth occurred in submarine hydrothermal systems where abiotic synthesis may have supplied the prebiotic organic compounds from which life emerged. That is, as CH_4 and other organic compounds in hydrothermal fluids may be able to provide sources of metabolic energy and fixed carbon for biological communities at the sea floor and in the overlying water column.[4-6] Generally, the abiotic formation of hydrocarbons and other organic compounds (carboxylic acids, amino acids, …) in natural hydrothermal systems takes place *via* the conversion of carbon dioxide CO_2, or other inorganic carbon sources such as carbon monoxide CO and hydrogen carbonate HCO_3^-, with the aid of hydrogen H_2.[5] Such conversions occur *via* mechanisms which may include Fischer–Tropsch type reactions.[5,7] These reactions can be defined as surface-catalysed reduction and polymerisation reactions of oxidised single carbon compounds.[5,7] High H_2 concentrations can result from fluid–rock interactions, represented by reaction (1), which is a general reaction.[5]

$$2(FeO)_{rock} + H_2O \rightarrow (Fe_2O_3)_{rock} + H_2 \qquad (1)$$

Herein, water reacts with iron(II)-containing minerals $(FeO)_{rock}$, such as olivine, pyroxene and pyrrhotite, whereby Fe(II) oxidises to Fe(III), which precipitates as magnetite Fe_3O_4 or in general Fe(III)-containing minerals $(Fe_2O_3)_{rock}$, and H_2O reduces to H_2.[5]

In 2003, Yamasaki[8] proposed how information obtained from the study of fundamental Earth principles can inspire the development of new technologies in order to establish a sustainable society. One of the proposals described the possibility to reduce CO_2 to organic compounds under hydrothermal conditions in the presence of H_2 that could be produced *via* redox reactions between zer-ovalent iron or/and iron(II)-containing compounds and water.[8] Since then scientific research papers on the technological possibilities of the conversion of carbon dioxide under hydrothermal conditions are being published on a regular basis.[9]

The earliest reports on laboratory scale hydrothermal experiments data back to 1845.[1] Hydrothermal synthesis has evolved from being used in geological studies to materials chemistry, where it enabled controlled synthesis of materials with practical applications, such as zeolites, transition metal oxides and even nitrides or sulphides.[10] The definition of laboratory scale hydrothermal reactions is, according to Rabenau,[11] '*reactions which take place in a sealed reaction container,*

ART ■ C5FD00104H

such as an autoclave, if water is used as a solvent and the temperature is raised above
100 °C'. These conditions generate an autogenous pressure (i.e. self-developing
and not externally applied pressure).[10] This pressure increases with tempera-
ture, but also depends on other factors, such as the percentage fill of the
vessel.[10,12,13] Furthermore, the properties of water change by applying hydro-
thermal conditions. For example, density, dielectric constant, dynamic viscosity,
heat capacity and ionic product are significantly different in comparison with
standard ambient temperature and pressure conditions.[14] One can state that a
completely 'new solvent' is found at high temperature and elevated pressure,[10]
which may be beneficial for the involved reaction system, as the following
examples prove.

• A low dielectric constant influences the solubility of different products. For
example, the solubility of hydrophobic organic compounds increases. The solu-
bility of certain salts, on the other hand, such as Na_2SO_4, decreases.[14]

• A low viscosity has a positive impact on the mobility of dissolved ions and
molecules.[10] Therefore, in combination with a high diffusion rate, interphase
mass transfer resistances are substantially reduced or even eliminated and effi-
cient heat transfer is guaranteed.[15,16] These factors will make reactions fast,
especially in heterogeneous catalytic reaction systems.[16]

• The ionic product of water is relatively high at certain conditions. These high
levels of H^+ and OH^- ions may accelerate many acid- or base-catalysed reactions.[14]

Therefore, the properties of water under hydrothermal conditions may play a
defining role in the conversion of a very stable molecule such as CO_2. Based on the
used H_2 source, hydrothermal CO_2 conversion methods can be divided in two
main categories: metal based methods and non-metal based methods. Metal
based methods make use of water as a H_2 source, via redox reactions between a
zerovalent metal M and water, as generally described in reaction (2).

$$xM + yH_2O \rightarrow M_xO_y + yH_2 \tag{2}$$
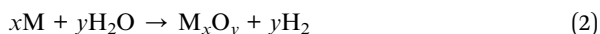
Largely available and cheap metals with a low redox potential are therefore
preferred. Zerovalent iron,[17–27] zinc,[25,28–34] aluminium,[25,30,35–37] manganese[38] and
magnesium[25] have been already studied as potential reductants. Instead, non-
metal based methods make use of different H_2 sources, as the following exam-
ples prove. Sulphur containing compounds such as hydrogen sulphide H_2S,
which may be in situ released (desulphurisation) via the hydrothermal cracking of
certain types of polymer waste such as ethylene propylene diene monomer EPDM,
can reduce water in H_2.[39] Furthermore, the conversion of alcohols such as iso-
propanol C_3H_7OH and glycerine $C_3H_8O_3$ into acetone C_3H_6O and lactic acid
$C_3H_6O_3$, respectively, can occur together with the hydrogenation of CO_2 and its
derivatives (transfer hydrogenation).[40,41] H_2 can also be generated by the in situ
decomposition of hydrazine N_2H_4.[42] However, since the work presented in this
paper is related to metal based methods, non-metal based methods will not be
discussed further.

So far, metal based methods are reported as one-step processes: where the
production of H_2 and the conversion of CO_2 take place under the same reaction
conditions in the same reactor. However, it is unclear if this one-step approach is
(always) synergic. Experimental observations indicate that a one-step method may
be beneficial. On the one hand, the oxidised metal phases, including possible

intermediates, may enhance the conversion of CO_2, *e.g.* by a catalytic activation.[33,34,38] However, often the addition of catalytic substances, such as metallic nickel or metallic copper, is necessary in order to obtain efficient kinetics.[31,32,37] We mention 'catalytic substances' because in most cases significant, non-catalytic amounts of the additives are required to enhance the kinetics: *e.g.* the mole ratio M : Ni or M : Cu is frequently at least 1 : 1. On the other hand, the consumption of produced H_2, due to the conversion of CO_2, may shift the equilibria to the product side of the total H_2 production reaction and the conversion reactions of CO_2, depending on the involved kinetics of the reactions that take place (*cf.* Le Chatelier's principle).[33,38] Concretely, in most cases it is unknown whether the production of H_2 and the conversion of CO_2 take place simultaneously, or take place simultaneously for a certain time period, or take place as subsequent reactions.

Metal based methods experimentally show the possibility to convert CO_2 into a range of products. Depending on the applied method and reaction parameters, different products such as formic acid HCOOH, methanol CH_3OH or methane CH_4 have been obtained with high selectivity coinciding in many cases with a high conversion yield. The total CO_2 conversion reactions are shown in reactions (3), (4) and (5). For example, a highly selective (98%) conversion with a high percentage yield (76%) into sodium formate, the sodium salt of HCOOH, was observed under the following conditions: 8 mmol Mn, mole ratio Mn : $NaHCO_3$ = 8 : 1, degree of filling 55 vol%, a reaction temperature of 325 °C, a reaction time of 1 hour and in the absence of a catalytic substance.[38]

$$CO_2 + H_2 \rightarrow HCOOH \tag{3}$$

$$CO_2 + 3H_2 \rightarrow CH_3OH + H_2O \tag{4}$$

$$CO_2 + 4H_2 \rightarrow CH_4 + 2H_2O \tag{5}$$

However, without the addition of a catalytic substance, the conversion yields of formate are strongly different when comparing different metals, as shown in Table 1.[21,25,33,38] Upon applying Fe, the percentage yield of formate is found to be significantly low compared to the other metals. However, no (possible) explanation can be found in the literature. In our opinion, the oxidation degrees of the applied metals and, more specifically, the corresponding amounts of produced H_2 may explain the observed differences. The hydrogen yield, which is sometimes estimated based on the formate yield, the amount of H_2 in the gas phase after reaction, and the maximal producible amount of H_2, seemed to be significantly lower in the case of Fe compared to the corresponding amounts obtained with other metals. As a matter of fact, Fe is the most noble metal of the four mentioned metals. Hence, in the case of Fe, we suggest that the low formation of H_2 led to a low percentage yield of formate.

In the case of Fe, the addition of a potential catalytic substance, such as Ni or Cu, leads to an increase of the percentage yields of formate, as shown in Table 2.[26] However, the extent of the increases is dissimilar. In the case of applying Ni, the highest reported percentage yield of formate is 20.7% while under similar conditions with Cu, the obtained percentage yield of formate is 48%. The highest percentage yield of formate, 76.7%, is in the case of adding Cu. The

Table 1 Highest reported percentage yields of formate, with corresponding selectivities and hydrogen yield, as a function of different metals in the case of applying NaHCO$_3$ as the CO$_2$ source and in the absence of an added catalytic substance[21,25,33,38]

Metal (74 μm)	Metal amount (mmol)	Mole ratio metal : NaHCO$_3$	Temperature (°C)	Degree of filling (vol%)	Reaction time (hours)	Percentage yield of formate (%)	Selectivity to formate (%)	(Indication of) H$_2$ yield (%)
Fe	6	6 : 1	325	35	2	13.5	98	25[a]
Zn	10	10 : 1	325	35	1.5	78.0	±100	±100
Al	6	6 : 1	300	35	2	62.8	±100	99.4
Mn	8	8 : 1	325	55	1	76.0	98	77.5[b]

[a] After a hydrothermal treatment of 1 mmol NaHCO$_3$ in the presence of 6 mmol Fe at 300 °C for 2 hours (degree of filling, 35 vol%), a percentage yield of formate of 10.5% was observed. The amount of H$_2$, which was present in the gas phase after reaction, was recovered and quantified as 48 mL (20 °C, 1 atm). Based on the formate yield (0.105 mmol H$_2$), the amount of H$_2$ in the gas phase after reaction (2 mmol) and the maximal producible amount of H$_2$ (8 mmol), we estimate the hydrogen yield on 25% (dissolved amount of H$_2$ at 20 °C not included). [b] After a hydrothermal treatment of 1 mmol NaHCO$_3$ in the presence of 8 mmol Mn at 300 °C for 2 hours (degree of filling of 35 vol%), a percentage yield of formate of 43% was observed. The amount of H$_2$ which was present in the gas phase after reaction was recovered and quantified as 140 mL (20 °C, 1 atm). Based on the formate yield (0.43 mmol H$_2$), the amount of H$_2$ in the gas phase after reaction (5.8 mmol) and the maximal producible amount of H$_2$ (8 mmol), we estimate the hydrogen yield on 77.5% (dissolved amount of H$_2$ at 20 °C not included).

ART ■ C5FD00104H

Table 2 Highest reported percentage yields of formate in the case of applying Fe, $NaHCO_3$ as the CO_2 source, and the addition of a catalytic substance[26]

Fe amount (mmol)	Mole ratio Fe : $NaHCO_3$	Mole ratio Fe : additive	Temperature (°C)	Degree of filling (vol%)	Reaction time (hours)	Percentage yield of formate (%)
12	6 : 1	1 : 1 (Ni)	300	35	2	20.7
12	6 : 1	1 : 1 (Cu)	300	35	2	48.0
13.2	6 : 1	1 : 1 (Cu)	300	35	2	63.6
108	6 : 1	1 : 1 (Cu)	300	55	2	76.7

corresponding conditions in order to achieve this yield, such as the high amount of Fe and the degree of filling, are remarkable compared to the other described experiments. Unfortunately, and to the best of our knowledge, these results obtained *via* the addition of potential catalytic substances, are only mentioned in a review paper[26] since the herein referred article was never published. Hence, no discussion is available on the influence of the addition of Ni or Cu, or the influence of reaction parameters such as the applied degree of filling. In our opinion, Ni and especially Cu may enhance the formation of H_2, and may even change the mechanism of the conversion of CO_2, which could lead to a higher formate yield.

Recently, we have shown that the hydrothermal production of H_2, from (zerovalent) Fe and water, is optimal when under milder conditions of temperature in comparison to the conditions applied in a conventional one-step CO_2 conversion method (generally approximately 300 °C).[43] In the presence of a specific amount of carbonate ions CO_3^{2-} (0.0375 M), a highly pure (purity > 99 mol%) and significant amount (yield of approximately 80 mol%) of H_2 was experimentally obtained after a reaction time of 16 hours, and at a reaction temperature of 160 °C. It was proven that in the studied reaction system the presence of a specific amount of carbonate ions (0.0375 M) was crucial since the formation of H_2 is carbonate assisted. More specifically, the oxidation of Fe into Fe_3O_4 is suggested to take place *via* the formation of iron(II) carbonate $FeCO_3$ as an intermediate. The catalytic effect of carbonate ions decreases significantly, and eventually fades out, as higher temperatures or/and other amounts of carbonate ions are applied. At lower temperatures (>100 °C and <160 °C), the kinetics of the occurring reactions is slow. Hence, our experimental research suggests that the optimal reaction conditions for the two occurring reactions, *i.e.* production of H_2 and conversion of CO_2, are strongly different in the case of the hydrothermal conversion of CO_2 in the presence of Fe. This hypothesis of an imbalance of reaction conditions could explain why an efficient one-step hydrothermal conversion of CO_2 in the case of Fe, and in the absence of a catalyst, is difficult at elevated temperatures such as 300 °C. Hence, the goal of this paper is to study the potential of a two-step approach for the hydrothermal conversion of CO_2 into HCOOH with Fe: the first step is the production of H_2 *via* the developed method at 160 °C, the second step is the conversion of CO_2 at a higher temperature (250–350 °C). More specifically, the influence of different reaction parameters on the second step will be discussed, with a specific focus on the degree of filling and the (initial) amount

ART ■ C5FD00104H

of H_2. In conclusion, with the herein described work, we aim at elucidating the chemical feasibility of a two-step approach for the hydrothermal conversion of CO_2 into HCOOH with Fe.

Materials and methods

Materials

Metallic iron powder (min. 99.5 wt%) with an average grain size of 10 μm and magnetite powder (min. 97 wt%) with a grain size smaller than 44 μm were both obtained from Merck Millipore. Potassium hydroxide, KOH (min. 85 wt%), potassium hydrogen carbonate, $KHCO_3$ (min. 99.5 wt%), and anhydrous potassium carbonate, K_2CO_3 (min. 99.9 wt%), were purchased from Alfa Aesar, UCB and JT Baker respectively. All hydrothermal experiments made use of degassed Milli-Q water. The applied high purity gases, namely carbon dioxide (99.5 vol%), nitrogen (99.998 vol%) and hydrogen (99.999 vol%), were supplied by Air Products.

Experimental

The hydrothermal experiments were performed in closed 100 mL stainless steel (1.4435) stirred premex reactor ag autoclaves. For safety reasons, the maximal reaction temperature and the maximal degree of filling of the autoclaves were 280 °C and 50 vol%, respectively. A digital control unit and a logging unit allowed for the temperature, pressure and stirring speed to be adjusted and logged online. The heating time, defined as the time to increase the temperature to the set point, is dependent on the desired reaction temperature. Inherent to the settings of the applied heating system (PID controlled), a short-time temperature overshoot of maximum 5 °C was observed. However, in all cases the set point was reached in less than 30 minutes. Based on the applied H_2 source, two variants of hydrothermal CO_2 conversion reactions were performed and studied in this work of which the procedures are described hereafter.

CO_2 conversion reactions which apply hydrogen gas produced *via* a hydrothermal method. The optimisation of the production of H_2 by a mild hydrothermal method is described elsewhere.[43] In brief, this synthesis procedure of 15 bar absolute H_2 (15 bar, 20 °C, 70 mL volume intake: approximately 42 mmol H_2) is described here. Firstly, 40 mmol Fe was loaded into an autoclave. Secondly, 40 mL of a 1 M KOH solution was added. Subsequently, the autoclave was flushed with N_2 to create an oxygen free atmosphere. Thereafter, the autoclave was filled with 6 bar absolute of CO_2 (6 bar, 20 °C, 60 mL volume intake: approximately 15 mmol CO_2). Finally, the temperature was raised to 160 °C and stirring was applied at 250 rpm. The reaction was carried out for 16 hours, which includes the heating time and excludes the time to cool down to 35 °C. During cooling down, stirring was still performed at 250 rpm to prevent aggregation of the solid phase.

Subsequently, CO_2 conversion reactions were carried out in the same autoclave. Concretely, when the autoclave was cooled down after the production of H_2, the temperature was increased to 280 °C. This temperature was held constant for 24 hours. Stirring was still continuously performed at 250 rpm. Note that some of the experiments are performed under different conditions. In such cases, the differences in conditions are explicitly mentioned.

CO₂ conversion reactions which apply commercial hydrogen gas. When applying commercially produced and pressurised H_2, the following general method was applied. Firstly, 9 mmol $KHCO_3$ was loaded in an autoclave, serving as the CO_2 source. Secondly, a specific amount of degassed Milli-Q water (30, 40 or 50 mL) was added. Subsequently, after stirring manually to dissolve $KHCO_3$ in a homogeneous way and measuring pH, the autoclave was flushed with N_2 to create an oxygen free atmosphere. Finally, before increasing the temperature to 280 °C, and stirring at 250 rpm, the autoclave was filled at approximately 25 °C with a specific amount of H_2 (42, 84 or 100 mmol) with the aid of a pressure regulator. In general, each reaction was performed for 24 hours, which includes the heating time and excludes the time to cool down to room temperature (<35 °C). Note that some of the experiments were performed under different conditions. In such cases, the differences in conditions are explicitly mentioned.

Analysis. At the end of each hydrothermal CO_2 conversion reaction, the autoclave was cooled down to room temperature (<35 °C) with continuous stirring at 250 rpm. At room temperature, the gas phase constituents were identified and quantified by coupling the autoclave to a Bruker 450-GC system. The TCD channel (helium as reference) was calibrated for H_2, CO_2, N_2, CH_4 and CO with the aid of calibration gas mixtures (defined in mol%) delivered by Air Products. The FID channel was used to check if other hydrocarbons than CH_4 were present in the gas phase.

If applicable, after opening the autoclave, the solid phase and liquid phase were rapidly separated over a Whatman mixed cellulose ester membrane filter ME25 (0.45 μm pore size). The liquid phase was collected in a closed polyethylene bottle and stored in a refrigerator at approximately 2 °C.

Different measurements were performed on the liquid phase. Firstly, the pH was measured using a METTLER TOLEDO SevenMulti system, which was calibrated on a daily basis. Subsequently, the amount of non-purgeable organic carbon NPOC was measured to have an estimation of the converted amount of carbon (dioxide). In our opinion, NPOC measurements provide valid estimations since the formation of purgeable organic carbon compounds, such as benzene and derivatives and halogenated hydrocarbons, is expected to be low to non-existent. Measurements were performed using a Analytik Jena AG multi N/C 3100 system. The applied procedure is as follows. Firstly, acidified diluted liquid samples were purged for 10 minutes with oxygen. In this way, inorganic carbon, for example derived from hydrogen carbonate, is removed through the formation of CO_2. Next, the liquid sample is catalytically combusted at 850 °C. Finally, the corresponding generated CO_2 is measured *via* infrared detection. Based on a calibration curve, the amount of carbon can be determined. This procedure was successfully validated for a prepared formic acid solution of 1000 mg C per L: a recovery percentage of approximately 100 wt% was obtained. Throughout the paper, the amount of carbon conversion is mentioned. This amount is defined as the weight percentage of the absolute amount of NPOC (mg) to the absolute initial amount of carbon before reaction (mg). Furthermore, the selectivity of the conversion of CO_2 was checked by analysing the liquid samples with proton NMR spectroscopy (Bruker Avance II 400 MHz, measuring method with water suppression). The liquid samples were diluted with D_2O, TMS was used as reference. In addition, in case of high carbon conversion amounts, HPLC

measurements were performed on the pure, non-acidified liquid samples in order to quantify the amount of potassium formate/formic acid. These measurements were performed with an Agilent 1200 series system equipped with an Agilent 1260 Refraction Index Detector, which operated at 55 °C. An ion-exchange ligand-exchange column, namely Agilent Hi-Plex H (7.7 × 300 mm, 8 μm particle size), was applied at 60 °C. The mobile phase, a 10 mM sulphuric acid solution, was used in an isocratic way (1 mL min^{-1}). The quantification was performed based on a calibration curve. Based on the concentration of potassium formate/formic acid (mg L^{-1}) and the amount of NPOC (mg L^{-1}), the selectivity to potassium formate/formic acid was calculated, and expressed as a percentage (%).

Results and discussion

The possibilities of a two-step approach: exploratory experiments

As described above, H_2 is optimally produced *via* the developed iron-based hydrothermal method at 160 °C in the presence of a small amount of CO_2, which completely dissolves in a 1 M KOH solution and is mainly present as CO_3^{2-} ions (approximately 15 mmol). In order to verify if any conversion of CO_2 has already taken place during the developed production method of H_2, the gas and liquid phases obtained at the end of the H_2 production method were analysed. GC analyses showed that the gas phase did not contain any detectable amounts of hydrocarbons. However, proton NMR spectroscopic analyses on the corresponding liquid phase proved the presence of a complex mixture of organic compounds. Especially between 0.5 and 2.5 ppm [δ_H (400 MHz; D_2O; Me_4Si)] different peaks were observed, which may indicate the presence of aliphatic compounds. Furthermore, the presence of formate was confirmed [δ_H (400 MHz; D_2O; Me_4Si), 8.47, 1H, s]. Therefore, reactions between CO_2 and the produced H_2 appear to have taken place under the applied reaction conditions of the developed H_2 production method although unselective. Nevertheless, the amount of the formed organic compounds was small since NPOC analyses suggested a carbon conversion amount of approximately 0.7 wt%.

The mild reaction conditions of this process compared to one-step metal based CO_2 conversion methods reported in the literature (Table 1), and could be the reason for this low carbon conversion amount. Therefore, an experiment was performed in which, after performing the hydrothermal H_2 production at 160 °C for 16 hours (step 1), the temperature of the autoclave was increased to 280 °C for 24 hours (step 2). GC analyses demonstrated that the gas phase did contain traces of CO and CH_4 (much below 1 mol%). Furthermore, the presence of a complex mixture of organic compounds was confirmed *via* proton NMR spectroscopic analyses on the corresponding liquid phase. In the proton NMR spectrum, the proton peak of formate [δ_H (400 MHz; D_2O; Me_4Si), 8.47, 1H, s] had the highest intensity by far and thus formate seemed to be the main product. NPOC analyses suggested a carbon conversion amount of approximately 9.7 wt%. Hence, hydrothermal reactions between H_2 and CO_2 appear to take place better at 280 °C, as expected. However, the observed carbon conversion was still low. Therefore, in order to enhance the conversion of CO_2 *via* the proposed two-step method, significant modifications are necessary. Concretely, a systematic study of all reaction parameters of the second step should be performed in order to improve the hydrothermal conversion of CO_2 with H_2.

In the study of the influence of different reaction parameters on this second step, we chose to switch from mainly CO_3^{2-} ions, *in situ* produced through the dissolution of 15 mmol CO_2 gas in 40 mL of a 1 M KOH solution, to mainly HCO_3^- ions as CO_2 source, in order to be able to compare to the experimental results obtained with similar one-step hydrothermal methods described in literature. A hydrogen carbonate salt, such as $NaHCO_3$, is often dissolved in water and used as a CO_2 source (natural pH approximately 8.6) in the literature.[21] In the above described experiments, on the other hand, the CO_2 source is mainly CO_3^{2-} ions (pH approximately 11), obtained by dissolving CO_2 in a 1 M KOH solution. In order to obtain mainly HCO_3^- ions, the addition of extra CO_2 is necessary after the first step of hydrothermal H_2 production. However, performing an exactly quantified addition of CO_2 without losing the produced amount of hydrogen gas is complicated, as we experimentally encountered. Therefore, we conducted our study on the influence of different reaction parameters on the hydrothermal CO_2 conversion reaction in a separate autoclave with commercial $KHCO_3$ and commercial H_2. We chose to use 9 mmol of $KHCO_3$ for each reaction throughout this study. This amount is a midpoint setting, based on the two extrema mentioned in literature considering the conversion of CO_2 *via* one-step iron based hydrothermal methods: the minimum amount of applied $NaHCO_3$ is 1 mmol,[21] the corresponding maximum amount is 18 mmol.[26]

The possibilities of a two-step approach: parameter study of the CO_2 conversion reaction

In literature, parameter studies describe the impact of different reaction parameters, such as the amount of Fe, mole ratio $Fe : NaHCO_3$, reaction temperature, reaction time and alkalinity, on the hydrothermal conversion of CO_2 in the presence of Fe as the reductant, and in the absence of a catalyst.[21] However, no study investigated the effect or the optimisation of (i) the degree of filling and (ii) the (initial) amount of H_2. Hence, we designed a series of experiments in order to understand the role of these parameters (Table 3). The minimal amounts of both parameters, namely 30 vol% and 42 mmol H_2, were selected based on the obtained parameters *via* the developed H_2 production method.

Table 3 Design of a series of experiments, with a constant amount of 9 mmol $KHCO_3$, to investigate the role of the degree of filling with water and the presence of a significant amount of H_2

Experiment	Degree of filling with water (vol%)	Initial amount of H_2 (mmol) (corresponding absolute pressure in bar at 25 °C)	Mole ratio $H_2 : KHCO_3$
1	30	42 (15)	4.67
2	30	84 (30)	9.33
3	30	100 (36)	11.11
4	40	42 (17)	4.67
5	40	84 (35)	9.33
6	40	100 (42)	11.11
7	50	42 (21)	4.67
8	50	84 (42)	9.33
9	50	100 (51)	11.11

ART ■ C5FD00104H

Table 4   Amount of carbon conversion and selectivity to formate/formic acid in case of conducting Experiment 5 for 2, 4 and 24 hours at 280 °C

Time in hours	Amount of carbon conversion (wt%)	Selectivity to formate/formic acid (%)
2	14.7	97
4	22.6	±100
24	46.2	±100

The maximal amounts of both parameters, namely 50 vol% and 100 mmol H_2, were chosen based on the safety sheets of the autoclaves. In particular, both the filling degree and the introduction of H_2 will augment the pressure during reaction, which is limited to 200 bar for the used autoclaves.

Furthermore, to be able to perform this series of experiments, other reaction parameters such as reaction temperature, reaction time and the presence/absence of magnetite had to be defined. Based on literature, the temperature has to be approximately 300 °C up to 325 °C.[21] However, the experiments were conducted at 280 °C, which is the maximal operating temperature of the applied autoclaves in this study. Since this reaction temperature is lower, a longer reaction time was expected than those reported in literature from 1 up to 2 hours.[21] Hence, we chose to empirically determine the required time to convert a sufficient amount of CO_2. Therefore, we chose to conduct Experiment 5, the midpoint of the experimental design with a filling degree of 40 vol% and an initial hydrogen content of 84 mmol, for 2, 4 and 24 hours at a reaction temperature of 280 °C. The obtained amounts of carbon conversion are shown in Table 4.

GC analyses showed that the gas phases did not contain any detectable amounts of hydrocarbons after a reaction time of 2 and 4 hours. After a reaction time of 24 hours, traces of CO and CH_4 (much below 1 mol%) were detected in the gas phase. However, in all cases, the selectivity to potassium formate/formic acid was approximately 100%. The highest amount of carbon conversion, namely 46.2
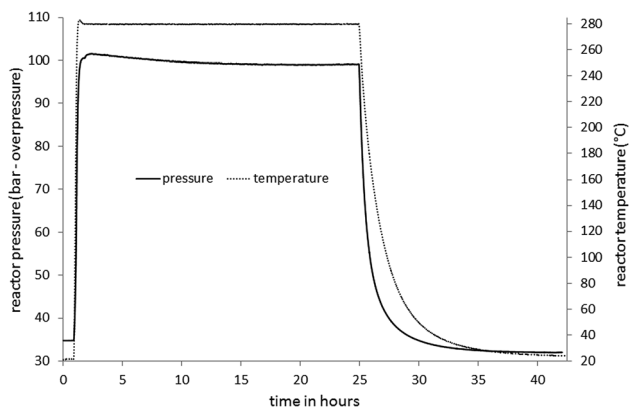
Fig. 1   Evolution of the reactor pressure and temperature as a function of time when conducting Experiment 5 for 24 hours at 280 °C.

wt%, was found after 24 hours, showing that the kinetics of the occurring reaction(s) is slow.

The evolution of the reactor pressure as a function of time of the corresponding experiment is shown in Fig. 1. When the set reaction temperature of 280 °C is reached and kept constant, the reactor pressure decreases as a function of time. However, the rate of decrease is variable within this time range of a constant temperature: in the beginning the rate is significantly higher compared with at the end. We suggest that this decrease of reactor pressure is coupled to the consumption of dissolved H_2 due to the conversion of CO_2. Because of the consumption of dissolved H_2, the concentration of H_2 in the liquid phase decreases. On the one hand, this will drive more H_2 in the gas phase to dissolve according to Le Chatelier's principle. On the other hand, the decrease in H_2 present in the gas phase will weaken the H_2 solubility due to the loss in pressure and eventually lead to a decrease in concentration of H_2 in the liquid phase. This might mean that, after a certain time, the conversion of CO_2 becomes diffusion/reagent limited. Considering Experiment 5, a reaction time of 15 up to 16 hours could be the turning point of these changes in kinetics because the reactor pressure did not significantly decrease any more from that moment (end point of reaction). Based on the graph of the evolution of the reactor pressure as a function of time (Fig. 1), and the amounts of carbon conversion obtained after different reaction times (Table 4), in combination with the possibility that a different degree of filling with water or/and a different initial amount of H_2 might have an impact on kinetics, we defined 24 hours as the reaction time for the series of experiments.

The last parameter which had to be defined before being able to perform the series of experiments, concerns the influence of a significant amount of Fe_3O_4
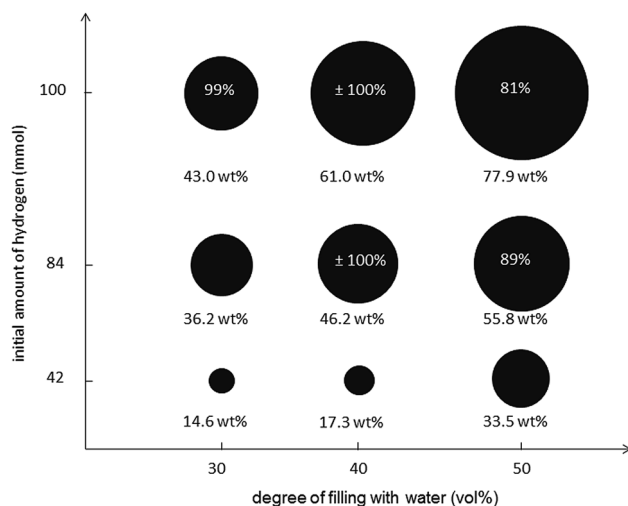
Fig. 2 Amounts of carbon conversion as a function of the applied filling degree and initial amount of H_2. When obtaining an amount of carbon conversion comparable to or higher than the amount of carbon conversion obtained *via* Experiment 5, the midpoint (46.2 wt%), the corresponding selectivity to potassium formate/formic acid was determined. These selectivities can be found in the spheres.

ART ■ C5FD00104H

being present in the reaction solution. Since Fe is oxidised into Fe_3O_4 during the hydrogen production step, Fe_3O_4 will be available in a significant amount, as a solid present in the solution after this step: approximately 11 mmol Fe_3O_4 is obtained *via* the developed hydrogen production process. Hence, we chose to investigate whether the presence of 9 mmol Fe_3O_4 (mole ratio $KHCO_3$: Fe_3O_4 = 1 : 1) would influence the conversion of CO_2 when performing Experiment 5 for 24 hours at 280 °C.

We observed an identical evolution of the reactor pressure as a function of time and an identical amount of carbon conversion (46.2 wt%) in comparison with a similar experiment in which Fe_3O_4 is not present (Fig. 1 and Table 4). The selectivity to potassium formate/formic acid was approximately 100%, and in the gas phase, no detectable amounts of hydrocarbons were found. Hence, in this case, we did not observe any indication that Fe_3O_4, available in a significant amount, influences the kinetics nor the occurring reactions of the carbon dioxide conversion. Hence, in order to make handling easier and to prevent possible effects of Fe_3O_4 under other conditions, we chose to perform the series of experiments in absence of Fe_3O_4.

In summary, the selected constant reaction parameters were defined as follows: a reaction temperature of 280 °C, a reaction time of 24 hours and the absence of magnetite. Hence, the series of experiments to understand the role of the degree of filling with water and the presence of a significant initial amount of H_2 on the carbon dioxide conversion step (Table 3) could be performed. In the different gas phases, none to very low (much below 1 mol%) amounts of reduced CO_2 species (CO and CH_4) were detected. The amounts of carbon conversion obtained in the different experiments are graphically shown in Fig. 2. When an amount of carbon conversion was obtained comparable to or higher than the amount of carbon conversion obtained *via* Experiment 5, the midpoint of the design (46.2 wt%), the corresponding selectivity to potassium formate/formic acid was determined. These selectivities can also be found in Fig. 2. The observed

Table 5 Data obtained from the graphs of the evolution of the reactor pressure as a function of time for the different experiments

Experiment	Operating pressure range in bar (overpressure)	(Estimated) amount of converted $H_2{}^a$ (mmol)	Endpoint of reaction[b] (hours)
1	65–70	5.2	7–8
2	90–95	7.0	14–15
3	100–105	7.7	>24
4	65–70	4.4	14–15
5	100–105	7.6	15–16
6	110–115	9.6	>24
7	75–80	6.5	22–23
8	110–115	7.9	22–23
9	125–130	10.8	23–24

[a] Value is equal to the difference of the present H_2 pressures before and after reaction at 25 °C. Since the applied pressure values are not highly accurate, these calculated values have to be considered as estimations rather than absolute values. [b] Estimated reaction time, represented as a range in hours, at which the reactor pressure did not significantly decrease any more.

ART ■ C5FD00104H
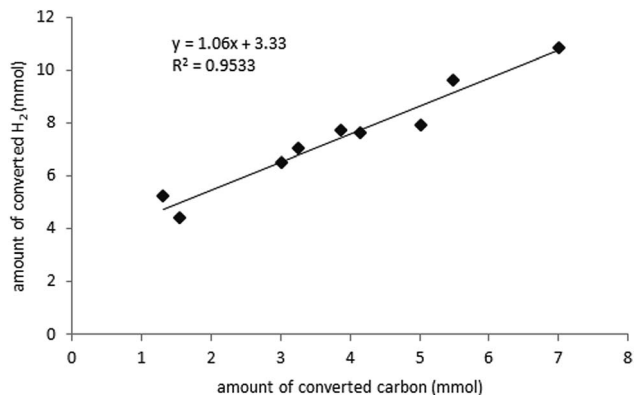
Fig. 3 Estimated, non-absolute amounts of converted H_2 plotted *versus* the amounts of converted carbon. A relative strong correlation ($R^2 = 0.9533$) can be observed.

results prove the importance of the filling degree and the initial amount of H_2: increasing the degree of filling with water and/or increasing the initial amount of H_2 results in a significant increase of the amount of carbon conversion within the selected reaction conditions.

Hence, the highest amount of carbon conversion, namely 77.9 wt%, was obtained with a degree of filling with water of 50 vol% and an initial amount of H_2 of 100 mmol. We believe that these observations can be explained by the solubility of H_2 in water at hydrothermal conditions: increasing the degree of filling with water and/or increasing the initial amount of H_2 leads to a higher absolute amount of dissolved H_2 to execute the conversion of CO_2, here mainly present as dissolved HCO_3^- ions. This postulation is enhanced by the data obtained from the graphs of the evolution of the reactor pressure as a function of time for the different experiments (Table 5). Firstly, the (estimated, non-absolute) amounts of converted H_2 are directly proportional with the amounts of carbon conversion, as
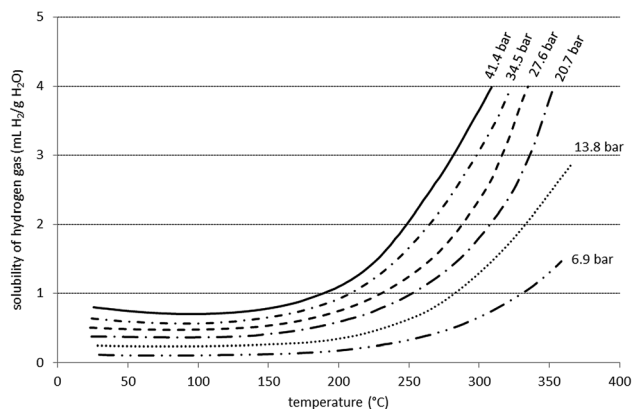
Fig. 4 Relationship between the solubility of hydrogen gas and the applied temperature and partial pressure of hydrogen gas (after Pray[44]).

shown in Fig. 3. Secondly, the estimated end point of the reaction seems to shift to longer times as the (estimated, non-absolute) amount of converted H_2 increases up to values greater than 7.5 mmol, which is the case when the reaction conditions (high degree of fill and/or H_2 pressure) allow for more H_2 to dissolve. These two observations further suggest that the conversion of CO_2 might become diffusion/reagent limited after a certain reaction time due to the consumption of H_2 and the consequent lower solubility of H_2 in solution.

However, it should be mentioned that the selectivity to potassium formate/formic acid seemed to decrease as the filling degree increased to 50 vol%. As mentioned above, the corresponding gas phases contained none to very low amounts of reduced CO_2 species such as CO and CH_4. Hence, we suggest, in the case of higher degrees of filling, the occurrence of side reactions of CO_2 conversion or the further reduction of formate in the liquid phase, leading to the formation of other carbon containing products. In the case of the highest amount of carbon conversion (77.9 wt%), which was obtained with a degree of filling of 50 vol%, the selectivity to potassium formate/formic acid was 81%.

The possibilities of a two-step approach: evaluation and discussion

The experimental results above suggest that the solubility of H_2 in water is a key parameter. Since, as expected, the reduction of CO_2, mainly present as dissolved hydrogen carbonate ions, with H_2 seems to be taking place in the water phase and not in the gas phase. The absolute amount of H_2 that dissolves into an aqueous solution is dependent on the operating temperature, the initial hydrogen pressure and the operating pressure (of the system), as well as the volume of the aqueous solution which is correlated with the degree of filling. The relationship between the solubility of H_2 and the applied temperature and partial pressure of H_2 is shown in Fig. 4.[44] The solubility of H_2 in an aqueous solution decreases as a function of temperature up to a certain temperature (mostly between 100–150 °C).[44] Above this temperature, the solubility of H_2 increases rapidly as a function of temperature.[44] Besides, pressure has an influence on the solubility of a gas in an aqueous solution: a pressure increase leads to a higher solubility (Henry's Law). As described above, the autogenous pressure depends on factors such as temperature and the percentage fill of the vessel with water.[12,13] However, a percentage fill lower or equal to 50 vol% has an especially large influence on the reactor pressure above the supercritical point of water.[11] At 280 °C and a degree of filling lower than 80 vol%, a subcritical regime is present and the autogenous

Table 6 Overview of the observed and suggested influences of reaction temperature, degree of filling with water and initial H_2 pressure

	Temperature increase	Increase of the degree of filling with water[a]	Initial H_2 pressure increase
Absolute amount of dissolved H_2	↑	↑	↑
Total pressure	↑	↑	↑
Chemical kinetics	↑	↑	↑

[a] In the case of a constant initial hydrogen amount and a reaction temperature of 280 °C.

pressure is in accordance with the vapour–pressure curve, namely approximately 65 bar.[11]

Therefore, the differences in operating pressure are due to a variation of the initial amount of H_2. However, the degree of filling with water influences the (absolute) dissolved amount of H_2. In the case of a constant initial hydrogen pressure, a higher degree of filling with water leads to a higher absolute dissolved amount of H_2 (only a volume effect occurs, concentration of dissolved H_2 is in this case independent of the degree of filling). In the case of a constant initial hydrogen amount, a higher degree of filling with water requires a higher initial hydrogen pressure, which leads to a higher dissolved amount of H_2 due to (i) an increase of the absolute dissolving of H_2 (volume effect) and (ii) an increase of the concentration of dissolved H_2 due to the higher initial hydrogen pressure (concentration of H_2 is in this case dependent on the degree of filling). We conducted our experiments with a constant initial hydrogen amount.

In the case of the performed experiments, the highest amount of carbon conversion, namely 77.9 wt%, was observed at the conditions at which the solubility of H_2 is the highest, namely a degree of filling with water of 50 vol% and an initial amount of H_2 of 100 mmol at a temperature of 280 °C. We expect an even higher amount of carbon conversion can be obtained by further optimising these three parameters. Unfortunately, due to restrictions of the operating conditions of our autoclaves, we are not able to experimentally prove this expectation. We already applied a relatively high initial pressure of H_2 (100 mmol H_2: 51 bar absolute at 25 °C, taking in a volume of 50 mL) and degree of filling with water (50 vol%) in our best case. Therefore, we expect that the most room for improvement can be achieved by varying the temperature. Increasing the temperature will have a significant effect on the solubility of hydrogen.[44] A temperature of 300 °C already leads to a significant difference in the solubility of hydrogen compared with a temperature of 280 °C.[44] Nevertheless, the selectivity to potassium formate might decrease due to a possible lower stability of this product at higher temperatures or the occurrence of side reactions of carbon dioxide conversion. An overview of the observed and suggested influences of the three parameters on the amount of carbon conversion can be found below in Table 6.

Conclusions

This study investigated the potential benefits or drawbacks of applying a one-step approach for the hydrothermal conversion of carbon dioxide to formate/formic acid with the aid of *in situ* produced hydrogen gas, obtained through the oxidation of zerovalent iron in an aqueous medium. However, we have shown that the optimal reaction conditions for the two occurring reactions, *i.e.* production of hydrogen gas and conversion of carbon dioxide, are strongly different due to thermodynamic and kinetic limitations, respectively. The imbalance of reaction conditions could explain why an efficient one-step hydrothermal conversion of carbon dioxide in the case of zerovalent iron, and in the absence of a catalyst, is difficult at elevated temperatures around 300 °C. Hence, the experimental study further focused on a two-step approach for the hydrothermal system: the first step is the production of hydrogen gas *via* a recently developed hydrothermal method which operates at 160 °C, and the second step is the conversion of carbon dioxide, present as dissolved potassium hydrogen carbonate, at higher temperatures (250–

350 °C). More specifically, the influence of the process parameters, on this second step were investigated and discussed, with a specific focus on the degree of filling and the (initial) amount of hydrogen.

This study revealed that a high solubility of hydrogen gas into the aqueous solution during reaction is a key parameter in order to achieve a good carbon conversion. Thus, the presence of a higher amount of hydrogen gas in solution, where the conversion reaction between hydrogen gas and potassium hydrogen carbonate into potassium formate takes place, shifts the thermodynamic equilibrium to the product side. As a result, a high temperature, degree of filling with water and initial hydrogen pressure are necessary to successfully perform the second step of the approach. Applying these insights have led to the experimental observation that *via* a two-step approach, separating hydrogen production conditions from carbon dioxide conversion conditions, the conversion of potassium hydrogen carbonate into potassium formate can be successfully performed with high carbon conversion yields, up to 77.9 wt%, and a selectivity of at least 81%. This result was obtained by applying a reaction temperature of 280 °C, a degree of filling with water of 50 vol% and an initial amount of hydrogen of 100 mmol for 24 hours. However, it should be mentioned that the selectivity to potassium formate/formic acid seemed to decrease as the filling degree increased to 50 vol%. We suggest, in case of higher degrees of filling, the occurrence of side reactions of carbon dioxide conversion or the further reduction of formate in the liquid phase, leading to the formation of other carbon containing products. In our opinion, an even higher amount of carbon conversion can be obtained by further optimising the reaction conditions of the second step reaction, in particular the reaction temperature. Unfortunately, we were not able to perform these experiments due to restrictions of the operating conditions of the autoclave systems we used. We expect the most room for improvement would be by increasing the reaction temperature: a rise to 300 °C could lead to both a higher hydrogen gas solubility and enhanced carbon dioxide conversion reaction kinetics. Nevertheless, the selectivity to potassium formate might decrease due to a possible lower stability of this product at higher temperatures or the occurrence of side reactions of carbon dioxide conversion. Finally, this study did not take into account the addition of moieties with catalytic activity to further improve the kinetics and selectivity of the second reaction step.

Acknowledgements

Notes and references

1 K. Byrappa and M. Yoshimura, in *Handbook of Hydrothermal Technology*, ed. W. Andrew, Elsevier, Oxford, 2nd edn, 2013.

2 B. M. French, (1) Synthesis and Stability of Siderite, $FeCO_3$, (2) Progressive Contact Metamorphosis of the Biwabik Iron Formation on the Mesabi

Range, Ph.D. thesis, The Johns Hopkins University, Baltimore, Minnesota, 1964.

3 B. M. French, Stability Relations of Siderite, FeCO3, Determined in Controlled fO2 Atmospheres, Document X-644-70-102, Goddard Space Flight Center, Planetology Branch, NASA, Greenbelt, MD, 1970.

4 N. G. Holm and E. Andersson, *Astrobiology*, 2005, **5**, 444–460.

5 T. M. McCollom and J. S. Seewald, *Chem. Rev.*, 2007, **107**, 382–401.

6 M. Yoshimura and K. Byrappa, *J. Mater. Sci.*, 2008, **43**, 2085–2103.

7 T. M. McCollom, *Rev. Mineral. Geochem.*, 2013, **75**, 467–494.

8 N. Yamasaki, *J. Ceram. Soc. Jpn.*, 2003, **111**, 709–715.

9 G. Demazeau, *Res. Chem. Intermed.*, 2011, **37**, 107–123.

10 R. I. Walton, *Chem. Soc. Rev.*, 2002, **31**, 230–238.

11 Rabenau, *Angew. Chem., Int. Ed. Engl.*, 1985, **24**, 1026–1040.

12 G. C. Kennedy, *Econ. Geol.*, 1950, **45**, 623–629.

13 R. A. Laudise, *Chem. Eng. News*, 1987, **65**, 30–43.

14 S. S. Toor, L. Rosendahl and A. Rudolf, *Energy*, 2011, **36**, 2328–2342.

15 A. A. Peterson, F. Vogel, R. P. Lachance, M. Fröling, M. J. Antal Jr and J. W. Tester, *Energy Environ. Sci.*, 2008, **1**, 32–65.

16 Y. Long and Z. Fang, *Biofuels, Bioprod. Biorefin.*, 2012, **6**, 686–702.

17 Y. Yashiro, H. Takahashi, N. Yamasaki and T. Kori, *Proceedings of the Seventh International Symposium on Hydrothermal Reactions*, Changchun, 2003.

18 H. Takahashi, L. H. Liu, Y. Yashiro, K. Ioku, G. Bignall, N. Yamasaki and T. Kori, *J. Mater. Sci.*, 2006, **41**, 1585–1589.

19 H. Takahashi, T. Kori, T. Onoki, K. Tohji and N. Yamasaki, *J. Mater. Sci.*, 2008, **43**, 2487–2491.

20 G. Tian, H. Yuan, Y. Mu, C. He and S. Feng, *Org. Lett.*, 2007, **9**, 2019–2021.

21 B. Wu, Y. Gao, F. Jin, J. Cao, Y. Du and Y. Zhang, *Catal. Today*, 2009, **148**, 405–410.

22 G. Tian, C. He, Y. Chen, H. Yuan, Z. Liu, Z. Shi and S. Feng, *ChemSusChem*, 2010, **3**, 323–324.

23 C. He, G. Tian, Z. Liu and S. Feng, *Org. Lett.*, 2010, **12**, 649–651.

24 H. Zhong, F. Jin, B. Wu, H. Chen and G. Yao, *AIP Conf. Proc.*, 2010, **1251**, 213–216, 2nd International Symposium on Aqua Science, Water Resource and Low Carbon Energy, Sanya Hainan, 2009.

25 F. Jin, Y. Gao, Y. Jin, Y. Zhang, J. Cao, Z. Wei and R. L. Smith Jr, *Energy Environ. Sci.*, 2011, **4**, 881–884.

26 F. Jin, X. Zeng, Z. Jing and H. Enomoto, *Ind. Eng. Chem. Res.*, 2012, **51**, 9921–9937.

27 Z. Liu, G. Tian, S. Zhu, C. He, H. Yue and S. Feng, *ACS Sustainable Chem. Eng.*, 2013, **1**, 313–315.

28 P. Yan, F. Jin, J. Cao, B. Wu and G. Zhang, *AIP Conf. Proc.*, 2010, **1251**, 242–245, 2nd International Symposium on Aqua Science, Water Resource and Low Carbon Energy, Sanya Hainan, 2009.

29 M. Hu, F. Jin, C. Ma and H. Chen, *AIP Conf. Proc.*, 2010, **1251**, 238–241, 2nd International Symposium on Aqua Science, Water Resource and Low Carbon Energy, Sanya Hainan, 2009.

30 M. Cheng, B. Wu, F. Jin, X. Duan and Y. Wang, *AIP Conf. Proc.*, 2010, **1251**, 234–237, 2nd International Symposium on Aqua Science, Water Resource and Low Carbon Energy, Sanya Hainan, 2009.

ART ■ C5FD00104H

31 J. Liu, X. Zeng, M. Cheng, J. Yun, Q. Li, Z. Jing and F. Jin, *Bioresour. Technol.*, 2012, **114**, 658–662.

32 Z. Huo, M. Hu, X. Zeng, J. Yun and F. Jin, *Catal. Today*, 2012, **194**, 25–29.

33 F. Jin, X. Zeng, J. Liu, Y. Jin, L. Wang, H. Zhong, G. Yao and Z. Huo, *Sci. Rep.*, 2014, **4**, 4503.

34 X. Zeng, M. Hatakeyama, K. Ogata, J. Liu, Y. Wang, Q. Gao, K. Fujii, M. Fujihira, F. Jin and S. Nakamura, *Phys. Chem. Chem. Phys.*, 2014, **16**, 19836–19840.

35 H. Yao, X. Zeng, M. Cheng, J. Yun, Z. Jing and F. Jin, *Bioresearch*, 2012, **7**(1), 972–983.

36 X. Zeng, F. Jin, H. Yao and M. Cheng, *Adv. Mater. Res.*, 2012, **347–353**, 3677–3680.

37 L. Lyu, F. Jin, H. Zhong, H. Chen and G. Yao, *RSC Adv.*, 2015, **5**, 31450–31453.

38 L. Lyu, X. Zeng, J. Yun, F. Wei and F. Jin, *Environ. Sci. Technol.*, 2014, **48**, 6003–6009.

39 X. Zeng, F. Jin, Z. Huo, T. Mogi, A. Kishita and H. Enomoto, *Energy Fuels*, 2011, **25**, 2749–2752.

40 Z. Shen, Y. Zhang and F. Jin, *Green Chem.*, 2011, **13**, 820–823.

41 Z. Shen, Y. Zhang and F. Jin, *RSC Adv.*, 2012, **2**, 797–801.

42 F. Chen, G. Yao, Z. Huo and F. Jin, *RSC Adv.*, 2015, **5**, 11257–11260.

43 K. Michiels, J. Spooren and V. Meynen, *Fuel*, submitted.

44 H. A. Pray, C. E. Schweickert and B. H. Minnich, *Ind. Eng. Chem.*, 1952, **44**, 1146–1151.

ART ■ C5FD00104H

PAPER

CO$_2$ capture systems based on saccharides and organic superbases†

G. V. S. M. Carrera,* N. Jordão, L. C. Branco* and M. Nunes da Ponte

In this report, novel systems, based on highly abundant saccharides, D-mannose, D-glucose, β-cyclodextrin, alginic acid and mannitol, in combination with an organic superbase, tetramethylguanidine (TMG) or 1,8-diazabicyclo[5.4.0]undec-7-ene (DBU), are studied for carbon dioxide capture. With D-mannose and D-glucose, several ratios of equivalents of alcohol groups of saccharide : superbase were tested: 1, 0.625, 0.5 and 0.25. High wt% values of CO$_2$ uptake were obtained with TMG-based systems. However, TMG itself can react directly with CO$_2$, and, in the presence of D-mannose, competition between carbonate and carbamate based products was established. In order to circumvent this competition and obtain exclusively the carbonate-based product, DBU was used instead as an organic superbase. In the D-mannose series the highest result was obtained with a D-mannose : DBU ratio eq. = 0.625 (13.9% CO$_2$ uptake, 3.3/5 alcohol groups converted into carbonates). A more effective stirring system, designed to overcome the high viscosity of the products, allowed the use of a D-glucose : DBU = 1 : 1 ratio with 11.5 wt% of CO$_2$ uptake and 2.47/5 alcohol groups converted into carbonates. Additionally a DSC thermal study was performed in order to study the stability/reversibility of the CO$_2$ loaded systems.

Introduction

Carbon dioxide capture and utilization is a fundamental concept to develop in the current environmental and energetic context.[1] The benchmark scrubbing systems for CO$_2$ capture that have been available in the market for more than 60 years are aqueous solutions of alkanolamines, which have a drawback of the requirement of dilution of the capture agent in water (in order to avoid corrosion and mitigate excessive release of heat during reaction), leading to poor performances in CO$_2$ capture (7 wt% of CO$_2$ uptake in 30% aqueous solution of ethanolamine) and high energy demand for CO$_2$ stripping, due to the high heat capacity of water. Additionally, the solvent is lost during operations.[2,3] A competitive system should fulfil the criteria of high capacity to store this gas and sustainability from an energetic,

LAQV, REQUIMTE, Departamento de Química, Faculdade de Ciências e Tecnologia, Universidade Nova de Lisboa, 2829-516 Caparica, Portugal. E-mail: goncalo.carrera@fct.unl.pt; l.branco@fct.unl.pt

ART ■ C5FD00044K

economic and environmental point of view. The possibility to avoid water as a reaction solvent made task specific ionic liquids (TSILs) interesting alternatives for CO_2 capture.[4–6] Ten years ago, Jessop and collaborators[7] developed the concept of a reversible ionic liquid, using a mono-alcohol, an organic superbase and CO_2. These reagents led to an ionic liquid, formed by an alkylcarbonate and the protonated superbase cation. The reaction could be reverted by bubbling an inert gas, like nitrogen or argon. The initial goal of this pioneering work was to develop solvents where polarity could be tuned by the introduction or displacement of an acid gas such as CO_2. Following it, other studies with modification of several parameters such as the nucleophile (amines,[8,9] amino-esters,[10] amino-alcohols,[11] amino-acids[12] and mono-saccharides[13]), type of organic superbase,[9] element of reversibility[14] and number of functionalities in the same molecules able to react with CO_2 [9,13] have been reported. In parallel, several applications based on the same principle of reversibility, such as media to promote reactions and extractions,[15] dissolution of biomolecules,[16] quenching of fluorescence,[17] reversible manipulation of colour[14] and CO_2 capture have also been described. Regarding this last aspect, it is important to highlight that Heldebrant et al.[2] could achieve a maximum of 19 wt% of CO_2 uptake using a system of hexanol : diazabicyclo[5.4.0] undec-7-ene (DBU), an excellent performance compared with the conventional scrubbing system. The authors also state that alkyl carbonates are less stable than bicarbonates or carbamates, due to hydrogen bond interaction decrease. Naturally-occurring molecules with multiple alcohol groups could therefore become suitable platforms to reversibly capture CO_2. In agreement with these conjectures, Zhang et al. have recently reported a dramatic enhancement of the solubility of cellulose in DMSO after admission of CO_2 to cellulose : superbase systems.[16] The authors suggested that the reason for this behavior is related to the conversion of the alcohol groups of cellulose into carbonates. On the other hand, the order of alcohol reactivity is primary > secondary > tertiary, which may decrease the effectiveness of carbon capture by saccharides in comparison with primary alcohols. Herein, we present a study of saccharides and derived sugar structures containing multiple alcohol groups: D-glucose, D-mannose, alginic acid, mannitol and β-cyclodextrin, in combination with one of two organic superbases, diazabicyclo[5.4.0]undec-7-ene (DBU) or tetramethylguanidine (TMG). Considering reactivity constraints due to diffusion of CO_2 from the gas to liquid phase associated to stirring efficiency[2,13] different ratios of saccharide to superbase, from equivalent amounts to large excesses of superbase–alcohol equivalents in saccharide/mol of superbase from 1 to 0.25 were tested in the present work. Additionally, magnetic coupled stirring was tested as alternative method to a conventional magnetic bar coupled system. Contrarily to our previous report,[13] no solvents were used.

Experimental

Materials

All chemicals were used as purchased, with the exception of 1,8-diazabicyclo [5.4.0]undec-7-ene (DBU), with a purity of at least 99%, provided by Fluka and 1,1,3,3-tetramethylguanidine (TMG), supplied by Sigma-Aldrich (99%), where water was removed using molecular sieves. The remaining chemicals used were D-

(+)-mannose (99%), D-(+)-glucose (99%), D-mannitol (99%), alginic acid, β-cyclo-dextrin from Alfa Aesar and carbon dioxide (Air Liquid, 99.998 mol%).

Methods

5

The prepared compounds were characterized by ^{1}H and ^{13}C-NMR, HMBC (heteronuclear multiple bond correlation) and HSQC (heteronuclear single quantum coherence) and in specific cases by TOCSY (total correlated spectroscopy) on a Bruker AMX400 spectrometer. Chemical shifts are reported downfield in parts per
10 million from a tetramethylsilane reference, using d_6-DMSO as the deuterated solvent. IR spectra were recorded on a Perkin-Elmer FTIR Spectrometer, Spectrum 1000. The samples were prepared in a KBr matrix. DSC analysis was carried out by using a TA Instruments Q-series TM Q2000 DSC with a refrigerated cooling system. The sample was continuously purged with 50 mL min^{-1} nitrogen gas and
15 2–20 mg of salt was crimped into an aluminum standard sample pan with a lid. The samples were submitted to an isothermal step (40 °C, 1 minute), cooled to −90 °C (20 °C min^{-1}, isothermal step 1 minute at −90 °C) and then heated to 150 °C (20 °C min^{-1}, isothermal step 1 minute at 150 °C). Followed by another cycle of cooling (−90 °C, 20 °C min^{-1}) and heat (150 °C, 20 °C min^{-1}). The glass transition
20 temperature, the melting point and the decomposition temperature were determined on the heating process of the first cycle.

Synthetic procedures

25
The syntheses were performed in a cylindrical high pressure steel reactor (11 mL) with sapphire windows at both ends (Fig. 2), allowing a full view of the contents of the cell. In each experiment, 2.5 g of superbase (DBU or TMG) was used, alone or in combination with the proper number of equivalents (alcohol or carboxylic acid groups) of each saccharide. In the case of D-mannose and D-glucose, the ratios (in
30 equivalents) of saccharide : DBU were 1, 0.625, 0.5 and 0.25, whereas for β-cyclodextrin, alginic acid and mannitol, they were 0.5, 1 and 0.5 respectively. Stirring of the saccharide + superbase mixtures was done with a small magnetic bar, coupled to a common laboratory plate, for at least 20 min until complete dissolution of the saccharide in the (liquid) base. CO_2 was then introduced into
35 the cell, at room temperature, normally until a pressure of 5 MPa was reached (exceptions were 2 MPa for TMG alone, and 4 MPa for TMG in combination with D-mannose). The pressure dropped continuously until reaching a stable minimum, usually in less than 3 hours. In some situations it was necessary to refill the cell with CO_2 in order to complete the reaction. Decompression of the reactor was
40 then carried out slowly, in order to avoid the release of any fine powder. The reactor was weighed prior to CO_2 supply and after decompression, in order to measure the carbon dioxide uptake. The products were stored in a freezer at temperatures below 0 °C for their analysis.

   Visual observations of the reactions as they proceeded indicated that a solid
45 progressively formed and separated from the liquid mixture. In the cases of higher concentrations of saccharide in the superbase (1 : 1 ratio), the solid could even block the magnetic bar and stop stirring. In order to check whether in these cases the kinetics of the reaction were significantly decreased; one experiment
50 was carried out using different apparatus, with a more effective stirring system. A 250 mL reactor with a magnetically coupled stirring system, built by Thar, was

used. This stirring system is often used in high-pressure reactions, and consists of a powerful external electromagnet that rotates, and couples its movement with permanent magnets attached to the top of a rod, located inside the reactor, with a stirring helix at the bottom. The nominal torque exerted by this configuration is at least 5 times higher than what we could obtain with the magnetic bar in the reactor of Fig. 2.

Although several disadvantages would not allow the systematic use of that experimental apparatus for our purposes, continuous stirring throughout the whole time of reaction was obtained for a (1 : 1) DBU + glucose mixture, consisting of 20.36 g of DBU combined with an equivalent amount of D-glucose. The mixture was stirred 35 min prior to the reaction with CO_2.

Results and discussion

Saccharides or derived sugar structures with different numbers of OH groups were studied (Fig. 1). In the cases of D-glucose and D-mannose (five OH groups per molecule), two highly abundant natural compounds, several numbers of equivalents of OH groups in mono-saccharides per number of superbase molecules ratios (nr. –OH eq./nr. SB: 0.25, 0.5, 0.625 and 1) were tested. Considering this approach, mixtures of monosaccharide : superbase with different viscosities were achieved for CO_2 capture studies. The other saccharide-based structures were alginic acid (two OH groups and one carboxylic acid group per monomer), β-cyclodextrin (three OH groups per unit and twenty-one per molecule) and D-mannitol (six OH groups per molecule). For these last saccharide scaffolds, the saccharide : superbase ratios (nr. –OH and COOH eq./nr. SB) were 1, 0.5 and 0.5 respectively. In the case of alginic acid, the carboxylic group was also considered to be deprotonated by the superbase, along with the alcohol groups, in order to determine the ratio under discussion.

In this context it is fundamental to determine the percentage of CO_2 uptake respective to the capture system (superbase alone and superbase + saccharide) as well as the number of alcohol groups of the saccharide converted to carbonates.

The superbase TMG can by itself react with carbon dioxide, forming carbamates according to the work of Pereira et al.[18] Considering this, in an initial stage of our studies, we measured the selectivity of the carbonate vs. carbamate in a mixture of D-mannose : TMG (ratio 1), using pressures of CO_2 up to 4 MPa, leading to 18 wt% of CO_2 uptake. The reaction was repeated, leading to 22.8 wt% of CO_2 uptake (Table 1) corresponding to 2.32 –OH groups of D-mannose (from 5 possible to be functionalized) being converted into carbonates (determined by ^{1}H-NMR with aid of HMBC). 1.58 equivalents of TMG (from 5 possible) were converted into carbamates, as determined by weighing the mass of CO_2 uptake and considering the fraction converted into carbonates. This result is supported by the work of Ozturk et al.[19] who performed a kinetic study of the reaction between CO_2, TMG and 1-hexanol, with the formation of a carbamate intermediate product (reaction with TMG), stabilized by the alcohol.

The authors proposed two alternative products: $TMGCO_2^- + TMGH^+$ + hexanol and the other configuration $HexCO_3^- + TMGH^+$ + hexanol. According to the authors, the second path is favoured and the carbonate product is preferred when compared with carbamate. In this context, we checked the reactivity of TMG towards CO_2, leading to 29.5% of CO_2 uptake (77.5% yield). It is important to note
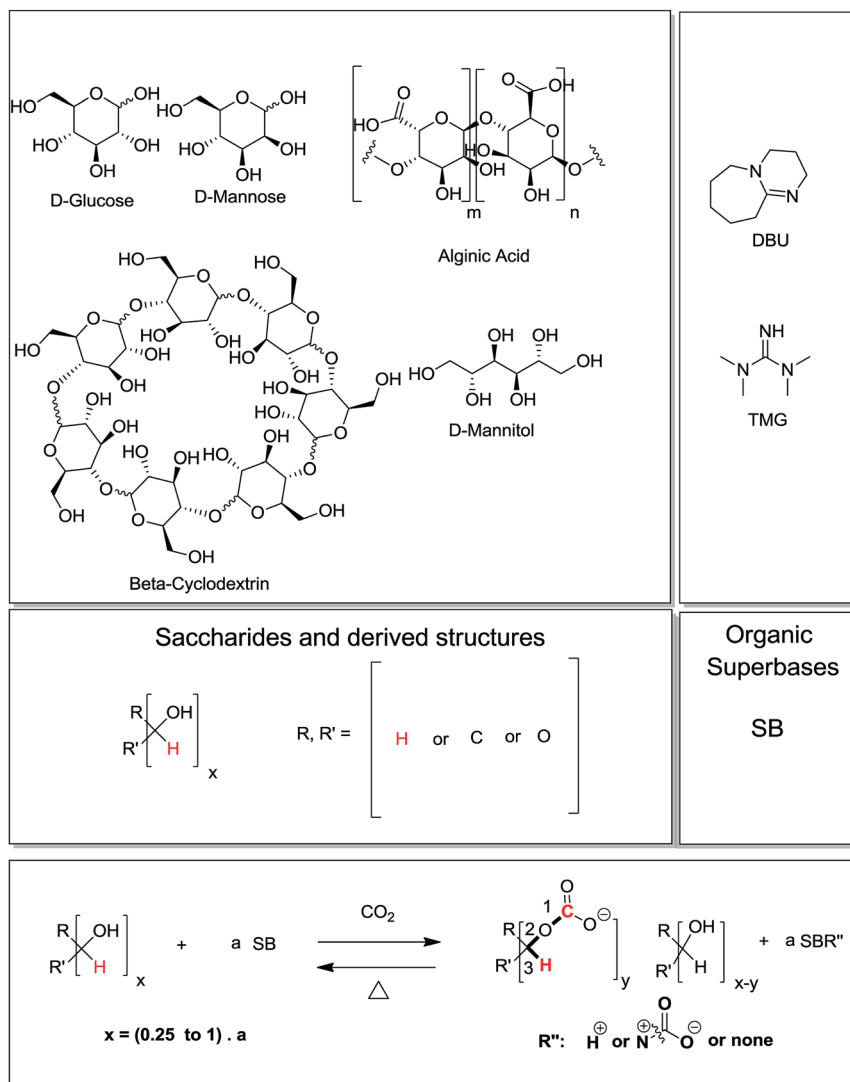
Fig. 1 Saccharides and derived compounds used in combination with an organic superbase to capture CO_2 leading to organic carbonates and also a carbamate when TMG is employed as organic superbase. CO_2 is released after heating. According to the change of functionalization from alcohol to carbonate, modification of the chemical shift in ^{1}H-NMR of the protons at a distance of three bonds from carbon and carbonate are detected as well as correlation by HMBC NMR spectroscopic techniques.

that the identity of the product was obtained by ^{1}H-NMR (by displacement of the $(N(CH_3)_2)_2C{=}N\underline{H}$ peak from 5.35 ppm in TMG to 5.93 ppm in the product $(N(CH_3)_2)_2C{=}N^+\underline{H}CO_2^-$), TOCSY (see ESI†; spectra of the product reveal a correlation $((C\underline{H}_3)_2N)_2C{=}N\underline{H}CO_2$ indication that the peak with a chemical shift of 5.93 ppm belongs to TMGCO$_2$), and ^{13}C-NMR spectra (the presence of an irregular peak at 165.8 ppm which can indicate the presence of two different quaternary

ART ■ C5FD00044K

Table 1 Tetramethylguanidine (TMG) based systems in the capture of CO_2 and the effect of the presence of D-mannose

System	wt% CO_2	[OH to CO_3^-][b] (=NH of TMG to NCO_2^-)[c]	FTIR NCO_2^- bands (cm^{-1})	^{1}H-NMR H bond peak [TMG–C$\underline{H}_3$ peak] (δ, area)	^{1}H-NMR– CO_3^- peaks (δ, area)	^{13}C-NMR TMG quat. carbon [TMG–$\underline{C}H_3$ peak]
TMG	—	[—] (—)	—	5.35, 0.94 [2.62, 12]	—	166.20 [39.04]
TMG w/CO_2	29.5^a	[—] (0.775 : 1^a)	3282 3107 1667	5.93, 1.09 [2.64, 12]	—	165.82 [39.04]
Man : TMG 1 : 1 eq.	—	[—] (—)	—	5.16, 9.38 [2.62, 60]	—	166.23 [39.07]
Man : TMG w/CO_2 1 : 1 eq.	22.8^a	[2.32 : 5^d] (1.58 : 5^a)	3129 1685	6.06, 10.75 [2.70, 60]	(5.25, 0.15) (4.92, 0.05) (4.84, 0.25) (4.48, 0.05) (4.36, 0.05) (4.29, 0.18) (4.20, 0.01) (4.12, 0.02) (3.94, 0.18) (3.86, 0.08) (3.79, 0.2) (3.51, 1.36)	164.71 [39.14]

^{a} Determined by weighed mass. ^{b} Number of OH groups from D-mannose converted to carbonates. ^{c} Number of =NH groups converted to carbamates. ^{d} Determined by ^{1}H-NMR and HMBC. NMR spectra obtained in d_6-DMSO.

carbons: $((CH_3)_2N)_2\underline{C}$=NH$\underline{C}O_2$, one from TMG and the other from the carbamate functionality). Moreover the presence of carbamate functionality is confirmed by the presence of characteristic bands at 3107, 3282 and 1667 cm^{-1} detected in the FTIR spectra (bands at a higher frequency give indication of a N–H stretch while the band of lower frequency is related with C=O stretch, both from carbamate functionality[5,20]). Differently from the work of Pereira *et al.*,[18] in our experimental work TMG was dried prior to its use in CO_2 capture.

In the case of the systems based on TMG or mannose/TMG the weight percentages of CO_2 uptake are very high, nevertheless, in addition to the reactivity of the alcohol groups from D-mannose in the presence of CO_2, TMG also reacts, leading to the respective carbamate. In order to increase the average number of –OH groups of saccharides converted into carbonates and simplify the system, avoiding multiple products after reaction with CO_2, we decided to use DBU as the organic superbase instead of TMG. Initially, only dry DBU was tested in CO_2 capture. After reaction, a CO_2 uptake of 2.4% was obtained with 13% of DBU protonated (by ^{1}H-NMR – slight shift of quaternary (N)$\underline{C}$(C)(=N) carbon, 159.66 ppm compared with the initial DBU signal, 159.54 ppm). Moreover, any H/C correlation from a possible carbamate or even from bicarbonate was not detected by HMBC. The only hypothesis that explains this residual CO_2 uptake and low protonation of DBU is the formation of carbonate $[CO_3]^{2-}$ by the reaction of residual water present in DBU with CO_2. From this assay we conclude that DBU

ART ■ C5FD00044K

doesn't react directly with CO_2 to originate the respective carbamate and it seems a good candidate to replace TMG in the activation of the alcohol groups of the saccharides and further reaction with CO_2, leading to carbonates. In the sequence of this reaction the mixture D-mannose : DBU (ratio of 1 in equivalents) was used to capture CO_2. Such a mixture is very viscous precluding stirring during the reaction. As result the wt% of CO_2 uptake was approximately 0. In order to improve the efficiency of the system and attain maximum functionalization of the saccharide we tested different ratios D-mannose : DBU (0.25, 0.5, 0.625 – besides 1). Prior to reaction with CO_2, the mixture is liquid and afterwards the product is solid as shown in Fig. 2.

The possibility to have a solid instead of a viscous liquid facilitates the transport of captured CO_2. ^{1}H-NMR spectra were used to access the average number of alcohol groups of D-mannose converted into carbonates. The protons adjacent to a carbonate functionality (Fig. 1 – at a distance of three bonds from carbon of carbonate) have a different chemical shift when compared with equivalent protons when alcohol functionality is present. Considering this fact and comparing the ^{1}H-NMR spectra of the systems under discussion with the spectra of D-mannose : DBU prior to its reaction with CO_2 it is possible to high-light the differences (Fig. 3) and account for areas of protons with modified chemical shift with the aid of HMBC spectra (H/C correlation – Fig. 1 shows the carbon of carbonate and the protons at a distance of three bonds) estimate the average number of alcohol groups converted into carbonates.

Considering the results presented in Table 2, it is possible to conclude that decreasing the proportion of saccharide respective to DBU leads to a much more effective CO_2 capture (13.9 wt% of CO_2 uptake in the case of the ratio Man : DBU = 0.625 in equivalents). In any case it is not possible to establish a direct relationship between the ratio Man : DBU and the wt% of CO_2 uptake nor for a relationship between the Man : DBU ratio and the number of alcohol groups converted into carbonates or an exact concordance between the two methodologies of calculation of the number of alcohol groups converted into carbonates (Table 2 – by mass or ^{1}H-NMR). In order to explain these results it is important to consider that magnetic bar based stirring is not the ideal method to promote the reaction and also obtain reproducible results. Moreover traces of water in DBU and/or even in D-mannose may be present, and partial precipitation of the product of reaction from d_6-DMSO solution may occur during storage, delay and acqui-sition of the NMR spectra. Additionally, when weighing the reactor before and after reaction with CO_2 we detect differences in the first or second decimal place

Fig. 2 System D-mannose : DBU (0.625 : 1 eq.). From left to right: before and after reaction with CO_2.
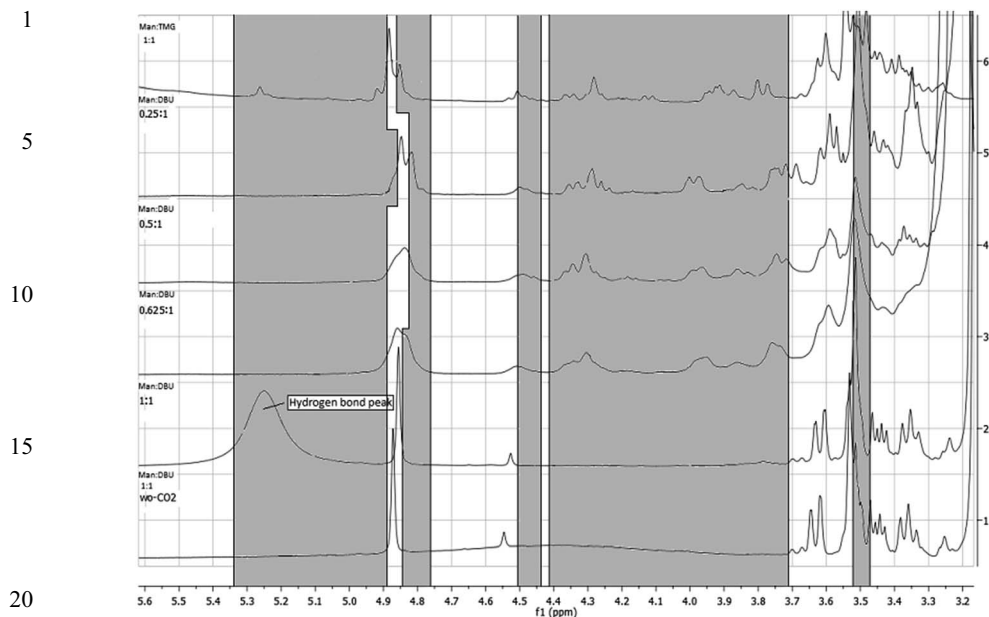
Fig. 3 ¹H-NMR spectra-systems based on mannose and an organic superbase (DBU or TMG). Highlighted in grey are the new peaks obtained after reaction with CO_2. From top to bottom: Man : TMG (1 : 1), Man : DBU (0.25 : 1), Man : DBU (0.5 : 1), Man : DBU (0.625 : 1), Man : DBU (1 : 1) and Man : DBU (1 : 1) prior to reaction with CO_2.

when the total mass of the reactor with the mixtures is around 1200 g. Nevertheless it is interesting to note by ¹H-NMR that the average number of alcohol groups converted into carbonates is ~3 out of 5 in all the systems studied except in the Man : DBU (ratio 1 in equivalents) system.

These results represent an improvement in the functionalization of D-mannose when compared with a similar system using TMG as the organic superbase (2.32 out of 5 – Table 1). Additionally, FTIR spectra confirm the presence of carbonates, as bands at 1585, ~1400 and 1271 cm⁻¹ appear in the studied systems, similar to in the work of Heldebrant *et al.*[21] While in DBU a C=N stretch band centred at 1610 cm⁻¹ is evident,[22] in our systems, DBU + D-mannose, the two bands at ~1650 cm⁻¹ and ~1610 cm⁻¹, are replaced by a single band at ~1650 cm⁻¹ after reaction with CO_2 (Table 2), which, according to Galezowski *et al.*[23] is indication that the DBU is protonated. Moreover, the value of the chemical shift of the quaternary carbon (C)(N)$\underline{C}$(=N) is also indicative of the degree of protonation of DBU with the highest value (161.07 ppm) corresponding to the system Man : DBU = 0.625. Factors such as the proportion of D-mannose and the percentage of incorporation of CO_2 increment the chemical shift of this carbon. The results obtained with D-mannose and DBU encouraged us to study D-glucose based systems as this saccharide is highly abundant. Again, saccharide : DBU ratios (in equivalents) of 1, 0.625, 0.5 and 0.25 were tested (Table 3 and Fig. 4). Different from the D-mannose case, a D-glucose based system in addition to the magnetic bar based stirring, was also tested magnetically coupled stirring in a much bigger reactor, as

ART ■ C5FD00044K

Table 2 Mannose series, effect of the mannose : DBU ratio on the performance of CO_2 capture

System	wt % CO_2 [NMR]	–OH to CO_3^{-a} mass [NMR]	FTIR CO_3^- [DBU] bands (cm^{-1})	^{1}H-NMR H adjacent to CO_3^- (δ, area)^b	^{13}C-NMR DBU quat. carbon peak^b	Man : SB eq. by ^{1}H-NMR
DBU	—	— [—]	— [1610]	—	159.54	—
DBU w/CO$_2$	2.4	— [—]	1372.18 1090.23 863.19 [1649.24] [1608.43]	—	159.66	—
Man : DBU 1 : 1 eq.	—	— [—]	— [1648.89] [1611.13]	—	159.78	1
Man : DBU w/ CO$_2$ 1 : 1 eq.	0	0 [0.21]	1585.77 1398.57 1271.80 [1651] [1615.08]	(3.74–3.89, 0.26)	160.12 160.05	1.008
Man : DBU w/ CO$_2$ 0.625 : 1 eq.	13.9	4.37 [3.3]	1585.47 1386.10 1271.69 [1645.60]	(4.83, 0.40) (4.51, 0.19) (4.34, 0.46) (4.19, 0.08) (4.07, 0.05) (3.97, 0.35) (3.87, 0.24) (3.75, 0.69) (3.52, 2.71)	161.07	0.814
Man : DBU w/ CO$_2$ 0.5 : 1 eq.	6.6	2.56 [3.06]	1585.79 1399.22 1271.89 [1642.71]	(4.84, 0.45) (4.46, 0.06) (4.36, 0.23) (4.19, 0.15) (3.98, 0.29) (3.86, 0.29) (3.74, 0.64) (3.52, 1.17)	160.69	0.492
Man : DBU w/ CO$_2$ 0.25 : 1 eq.	7.9	5.75 [2.61]	1585.33 1399.66 1271.66 [1645.45]	(4.82, 0.29) (4.50, 0.01) (4.30, 0.25) (4.17, 0.03) (3.99, 0.19) (3.86, 0.09) (3.74, 0.66) (3.51, 2.01)	160.24	0.281

^{a} Number of OH groups of D-mannose converted into carbonates. ^{b} NMR spectra obtained in d$_6$-DMSO. All the reactions were promoted using a magnetic bar.

a clear influence of stirring on the outcome of reaction of carbonation was detected.[2,13]

   With this test, we could obtain the maximum thermodynamically permitted number of alcohol groups converted into carbonates for a glucose : DBU 1 : 1

equivalent ratio. In a previous report, we had indication that multi-anionic charged organic molecules, with the charges in close vicinity, obtained from functionalization with CO_2 are not very stable.[6]

In this context this test could be an indication of the limits of glucose based systems to accommodate density of charge. Comparing identical systems (Glu : DBU of 1 : 1 ratio) differing in the type of stirring, it was possible to obtain a much higher number of alcohol groups converted into carbonates with magnetically coupled rather than with magnetic bar based stirring (2.47/5 vs. 1.08/5 – Table 3) as expected. The magnetically coupled stirred system is a 250 mL reactor that for obvious reasons could not be weighed before and after reaction with CO_2. Considering this limitation, the value of 11.5 wt% of CO_2 uptake was estimated based on ^{1}H-NMR analysis. This was the maximum percentage obtained in this series highlighting the importance of the type of stirring.

Curiously, a clear trend for all the magnetic bar stirred systems was observed, with the lower Glu : DBU ratios resulting in a higher number of alcohol groups converted into carbonates (Table 3) with a maximum of 3.28 groups converted (estimated by ^{1}H-NMR) using the Glu : DBU ratio of 0.25 : 1 equivalents.

Two different arguments could explain the results: first, lower ratios of glucose in the system lead to lower viscosities, leading to more effective mixing between gaseous CO_2 and the liquid phase until an extended functionalization is attained; differently, from a thermodynamic point of view, following the Le Châtelier principle, the increment of the reagents will shift the equilibrium towards the formation of more product. In this case an excess of DBU respective to the number of equivalents of alcohol groups in glucose if decreasing the glucose : DBU ratio (eq.). Another relevant fact is that the values of wt% uptake determined by different methods (weighing and NMR) are very similar, indicating that the methodologies used are reliable.

The presence of carbonate based functionalities was confirmed by FTIR, with bands centred at ~1590, ~1400 and ~1270 cm^{-1} (similar to in the case of D-mannose). Moreover a shift of band from ~1610 to ~1650 cm^{-1} was also detected in Glu : DBU systems after reaction with CO_2, indicating that DBU is protonated in the obtained products. It is also important to note that the degree of protonation of DBU, influenced by the extension of CO_2 uptake and ratio of D-glucose to DBU, is correlated with the chemical shift of the quaternary carbon (C)(N)$\underline{C}$=N of DBU, which is inversely correlated with the frequency of the band ~1650 cm^{-1} detected by FTIR ($R^2 = 0.91$). These results lead us to an empirical equation that relates the Glu : DBU ratio, the number of OH groups converted into carbonates and the number of alcohol groups that remained unchanged with a calculated factor that is well-correlated with the frequency of the band at ~1650 cm^{-1} in the FTIR spectra ($R^2 = 0.98$).

The empirical equation is:

$$\text{Factor} = (\text{ratio Glu : DBU in eq.})^{0.24} \times \text{nr. of} -CO_3 \text{ per glucose}^{0.7} \times \text{nr. of} -OH \text{ per glucose}^{0.81} \tag{1}$$

and the correlation equation that relates the FTIR frequency (cm^{-1}) with the determined factor in eqn (1):

$$\text{Frequency} = -4.9939 \times \text{factor} + 1661.9. \tag{2}$$

Table 3 Glucose based systems using DBU as the organic superbase in a CO_2 atmosphere. The effect of the ratio of glucose : DBU (in number of equivalents) and type of stirring[a]

System	wt% CO$_2$	OH to CO$_3^{-c}$ mass [NMR]	FTIR CO$_3^-$ [DBU] bands (cm^{-1})	^{1}H-NMR H adjacent to CO$_3^-$ peaks (δ, area)	^{13}C-NMR DBU quat. carbon peak	Glu : SB eq. by ^{1}H-NMR
DBU	—	— [—]	— [1610]	—	159.54	—
DBU w/CO$_2$	2.4	— [—]	1372.18 1090.23 863.19 [1649.24] [1608.43]	—	159.66	—
Glu : DBU 1 : 1 eq.	—	— [—]	—	—	159.97	0.71
Glu : DBU w/CO$_2$ 1 : 1 eq.	2.3	0.48 [1.08]	1589.12 1394 1274.55 [1645.99]	(5.01, 0.01) (4.86, 0.08) (3.99, 0.14) (3.90, 0.11) (3.82, 0.1) (3.77, 0.11) (3.54, 0.1)	160.38	0.5
Glu : DBU w/CO$_2$ 1 : 1 eq. w/magnetic coupled stirred[b]	11.5[b]	— [2.47]	1585.97 1399.59 1271.89 [1642.34]	(5.04, 0.05) (4.87, 0.17) (4.30, 0.18) (3.96, 0.44) (3.86, 0.49) (3.55, 0.91)	161.31	0.75
Glu : DBU w/CO$_2$ 0.625 : 1 eq.	6.1	1.94 [1.73]	1588.79 1378 1274.63 [1644.51]	(4.99, 0.02) (4.87, 0.1) (4.29, 0.19) (3.99, 0.28) (3.82, 0.24) (3.74, 0.29) (3.55, 0.25)	160.67	0.372
Glu : DBU w/CO$_2$ 0.5 : 1 eq.	7.9	3.04 [2.85]	1588.84 1394 1274.59 [1645.17]	(5.03, 0.08) (4.86, 0.15) (4.29, 0.33) (3.99, 0.47) (3.86, 0.76) (3.75, 0.53) (3.55, 0.25)	160.81	0.375
Glu : DBU w/CO$_2$ 0.25 : 1 eq.	4.9	3.59 [3.28]	1588.14 1365.92 1274.04 [1649.46] [1611.60]	(4.97, 0.02) (4.85, 0.13) (4.27, 0.23) (4.00, 0.24) (3.91, 0.09) (3.85, 0.08) (3.77, 0.42) (3.55, 0.24)	160.02	0.191

[a] In all entries, except when stated "magnetically coupled system", stirring was promoted using a magnetic bar. [b] The value of wt% CO_2 incorporation was estimated based on the number of equivalents of alcohol groups of glucose converted into carbonates. [c] Number of alcohol groups of D-glucose converted to carbonates.
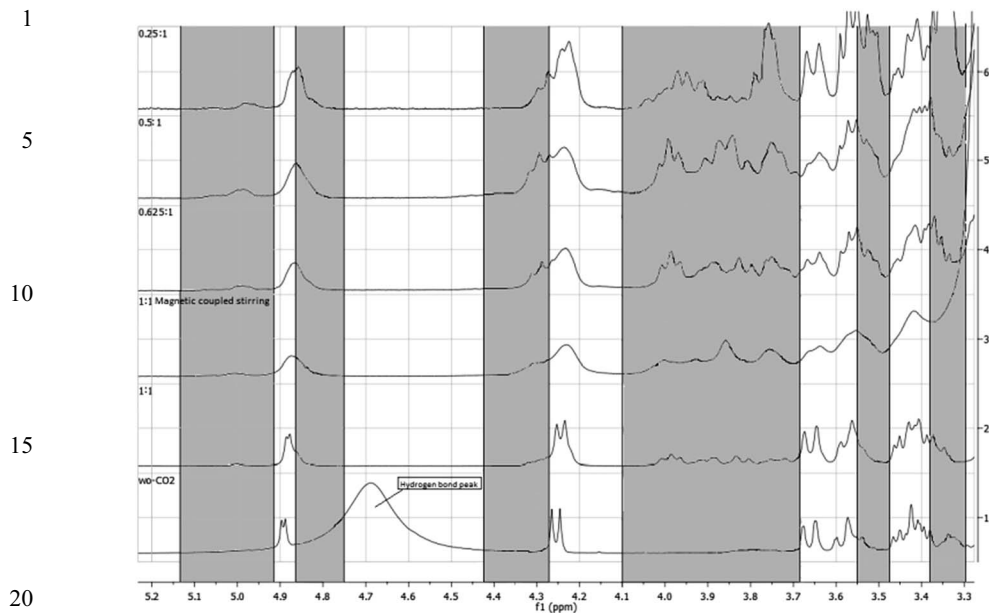
Fig. 4 ^{1}H-NMR spectra of the glucose : DBU systems. Highlighted are the new peaks obtained after reaction with CO_2. From top to bottom: Glu : DBU (0.25 : 1), Glu : DBU (0.5 : 1), Glu : DBU (0.625 : 1), Glu : DBU (1 : 1) with magnetically coupled stirrer, Glu : DBU (1 : 1) and Glu : DBU (1 : 1) prior to reaction with CO_2.

With both equations it is possible, by performing a FTIR spectra of the product of CO_2 capture and providing the Glu : DBU ratio (eq.), to access directly the average number of carbonate groups per molecule of functionalized glucose.

With D-glucose based systems, similarly to D-mannose, the estimation of the number of OH groups converted into carbonates was performed by highlighting the differences between Glu : DBU systems before and after reaction of CO_2 (Fig. 4) in ^{1}H-NMR spectra, with the aid of HMBC spectra (ESI† – long times of acquisition were required and low intensity correlations were detected in most cases, and in specific cases no correlation was detected). Other saccharides and related structures were tested for CO_2 capture such as β-cyclodextrin, alginic acid and mannitol with three, two and six alcohol groups per unit or molecule respectively. Again due to high viscosities it was necessary to use ratios of saccharide : DBU in equivalents lower than 1 in most cases (Table 4).

Relatively low values of wt% of CO_2 uptake were attained with these saccharides. The main reasons behind these results are the considerable excess of superbase used (in the case of β-cyclodextrin and mannitol), inefficient stirring at a relative early stage of reaction (all the reactions were promoted by the use of a magnetic bar) and the relatively low number of alcohol groups able to be functionalized (in the case of β-cyclodextrin and alginic acid). Again, determination by NMR of the number of alcohol groups converted into carbonates was based on the area of protons adjacent to carbonate functionalities that were unveiled with the aid of HMBC spectra. In this context, it is important to highlight the relative resemblance between the values determined by NMR and mass. In all the cases

ART ■ C5FD00044K

Table 4 Other saccharides combined with DBU to capture CO_2

System	wt% CO_2	OH to CO_3^{-a} mass [NMR]	FTIR CO_3^- [DBU] bands (cm^{-1})	^{1}H-NMR H adjacent to carbonate (δ, área)	^{13}C-NMR DBU quat. carbon peak
DBU	—	— [—]	— [1610]^d	—	159.54
DBU w/CO_2	2.4	— [—]	1372.18 1090.23 863.19 [1649.24] [1608.43]	—	159.66
β-CD : DBU w/CO_2 0.5 : 1 eq.	1.8	3.08 : 21 [3.93 : 21]	1586.87 1384.56 1270.36 [1652.19] [1612.66]	(4.72, 1.69) (4.01, 0.85) (3.57, 1.98)	160.15
Alginic acid : DBU w/CO_2 1 : 1 eq.	4.73	0.68 : 2 [—]^a	1586.62 1384.62 1270.18 [1651.65]	—^{a}	—^{a}
Mannitol : DBU w/ CO_2 0.5 : 1 eq.	4.73	2.16 : 6 [1.95 : 6]	1585.87 1385.77 1272.17 [1646.05]	(3.37, 2.21) (3.58, 1.04)	160.53

^{a} Number of OH groups of D-mannose converted into carbonates. ^{b} Solubility constraints didn't permit to obtain reliable NMR spectra. Magnetic bar stirring was used to promote reaction with CO_2 in all the cases.

Table 5 DSC thermal study of the saccharide based systems tested in this report after reaction with CO_2

Systems	T_d^e (°C)	T_g^e (°C)
(TMG)	56.52, 108.88^b	—
(Man : TMG) 1 : 1 (eq.)	103.15^b	—
(DBU)	118.01^b	—
(Man : DBU) 1 : 1 (eq.)	128.01^{b,d}	−44.39
(Man : DBU) 0.625 : 1 (eq.)	$T_d > 107.10^b$	−50.16
(Man : DBU) 0.5 : 1 (eq.)	122.1^b	—
(Man : DBU) 0.25 : 1 (eq.)	127.57^b	−66.68
(Glu : DBU) 1 : 1 (eq.)	102.56, 122.25, 147.37^b	−51.49
(Glu : DBU) 1 : 1 (eq.) magnetically coupled stirr	110.87, 145.48^b	−56.70
(Glu : DBU) 0.625 : 1 (eq.)	116.71, 146.26^b	—
(Glu : DBU) 0.5 : 1 (eq.)	119.21, 146.68^b	—
(Glu : DBU) 0.25 : 1 (eq.)	108.22^b, 134^c	−74.78
(β-CD : DBU) 0.5 : 1 (eq.)	127.78^b	−68.38
(Alginic acid : DBU) 1 : 1 (eq.)	125.08^b	−75.10
(Mannitol : DBU) 0.5 : 1 (eq.)	>112.70^a	−66.16

^{a} Onset. ^{b} Horizontal peak. ^{c} Curve point. ^{d} Exothermic peak. ^{e} T_d: decomposition temperature, T_g: glass transition temperature.

ART ■ C5FD00044K

tested, carbonate characteristic bands in the FTIR spectra (Table 4) were detected similarly as in D-mannose and D-glucose series. In the same spectra it is possible to verify that in the cases where the functionalization reaction is more extended (alginic acid and mannitol) a single band centred a ∼1650 cm^{-1} is obtained. In the case of β-cyclodextrin two bands arise at ∼1652 and 1613 cm^{-1} indication that DBU is partially protonated[23] and that the reaction was less extended when compared with other saccharides. The chemical shift of the quaternary carbon of DBU (C)(N)$\underline{C}$=N indicates that DBU is more protonated in the mannitol : DBU system with a ratio of 0.5 (eq.).

Additionally, a DSC thermal study of the products of reaction with CO_2 was performed (Table 5). The experiment consisted of lowering the temperature of the sample to −90 °C and increasing the temperature afterwards to 150 °C. T_g (glass transition temperature), mp (melting point) and T_d (decomposition temperature) measurements were performed, and finally a second cycle was performed to confirm CO_2 release by non-reproducibility of the second cycle respective to the first. In the case of the TMG based systems, two endothermic peaks were detected in the first cycle, one at 56.52 °C and the other at 108.88 °C. In the study by Pereira et al.,[18] two TGA losses were detected for the same system after CO_2 capture. According to the authors, the release at a lower temperature corresponds to carbamate, and the other is from bicarbonate. We agree with this interpretation however, considering also the T_d result of the DBU system (118.01 °C), that corresponds to CO_2 release from $[CO_3]^{2-}$, we hypothesise that instead of bicarbonate the reason behind the second peak in the TMG system is CO_2 release from carbonate.

Considering the mannose : DBU series, it is possible to verify that when the number of alcohol groups converted into carbonates is higher (Table 2 – by NMR) the value of T_d decreases (Table 5), indicating that a higher density of charge in a small molecule like D-mannose leads to higher destabilization of the product and consequently a lower temperature is required for CO_2 release.

It is also important to note that at this point that it is premature to discard the influence of dilution of the functionalized saccharide respective to DBU in increasing the value of T_d.

Considering T_g analysis, it is possible to observe that for all the cases that were detected, the value of T_g increases with the increment of the Man : DBU (eq.) ratio, indicating that a possible extended hydrogen bond network may lead to an increased value of T_g. Regarding the D-glucose series, a similar approach can be performed, and differently from the D-mannose series, it is possible to verify in the great majority of ratios a peak at >145 °C that should correspond to the melt/decomposition of glucose[24] after release of CO_2 from carbonate functionalized saccharide. In order to explain the values obtained at lower temperatures along the series we have to consider both the density of charge and the dilution of the functionalized saccharide, with the latest leading to an increased value of T_d, and the former leading to a lower value of decomposition temperature, for the ratios, 1 : 1 (magnetically coupled), 0.625 : 1 and 0.5 : 1. The trend is clear because there's only one value of T_d associated to CO_2 release from carbonates. Differently for the ratios 1 : 1 and 0.25 : 1 two peaks associated to CO_2 release from the different carbonates present in the mixture could be detected. An average of both peaks could lead to a value that is in agreement with the hypothesis of the influence of the effect of density of charge and dilution on the value of T_d.

Concerning the T_g values, and similar to the D-mannose series, an extended hydrogen bond network provided by higher Glu : DBU ratios leads to higher values of T_g. Other saccharides lead to similar values of T_d associated to CO_2 release.

Conclusions

Effective systems for CO_2 capture based on a cheap organic superbase (TMG or DBU) and highly abundant natural saccharides were designed and tested. The main objectives of this work were to obtain maximal percentages of CO_2 uptake and the number of alcohol groups of saccharides converted into carbonates. With TMG systems, very high percentages of CO_2 uptake were obtained, nevertheless when D-mannose is present, competition between carbonate and carbamate products was detected. In order to attain maximal conversion of alcohol groups into carbonates and to avoid competition with the superbase to react with CO_2, DBU was tested as an alternative organic superbase. Moreover in the case of D-mannose and D-glucose different ratios of saccharide : DBU were tested in order to find an optimal balance between the average number of alcohol groups functionalized into carbonates and the total wt% of CO_2 uptake. With D-mannose : DBU (ratio eq. = 0.625) an optimal wt% of CO_2 uptake of 13.9% was obtained corresponding to 3.3/5 alcohol groups being converted into carbonates. In the case of glucose : DBU (ratio eq. = 0.5) a maximum wt% of CO_2 uptake of 7.9%, corresponding to 3.04/5 alcohol groups converted into carbonates, was obtained with a magnetic bar based stirring method. In order to test the thermodynamic limit of the reaction and obtain maximal CO_2 uptake, a Glu : DBU system (ratio eq. = 1) was stirred in a magnetically coupled system. In that case, 2.47/5 alcohol groups were converted into carbonates, corresponding to 11.5 wt% of CO_2 uptake. Factors, such as the stirring efficiency in promoting solubilisation of CO_2 gas into the liquid phase, saccharide : organic superbase ratio and type of superbase were unveiled as fundamental in the outcome of the rreaction. Other saccharide based structures were also tested with interesting indications, especially mannitol, with six alcohol groups per molecule, where it's expected that the obtained results could improve significantly if magnetically coupled stirring is used instead of a magnetic bar. Thermal DSC analysis indicated that the stability of the obtained products are dependent on the dilution of the saccharide and the density of charge.

Acknowledgements

Notes and references

1 M. Mikkelsen, M. Jørgensen and F. C. Krebs, *Energy Environ. Sci.*, 2010, **3**, 43.

ART ■ C5FD00044K

2 D. J. Heldebrant, C. R. Yonker, P. G. Jessop and L. Phan, *Energy Environ. Sci.*, 2008, **1**, 487.

3 M. S. Shannon and J. E. Bara, *Sep. Sci. Technol.*, 2012, **47**, 178.

4 C. Wang, H. Luo, X. Luo, H. Li and S. Dai, *Green Chem.*, 2010, **12**, 2019.

5 E. D. Bates, R. D. Mayton, I. Ntai and J. H. Davies Jr, *J. Am. Chem. Soc.*, 2002, **124**, 926.

6 B. E. Gurkan, J. C. de la Fuente, E. M. Mindrup, L. E. Ficke, B. F. Goodrich, E. A. Price, W. F. Schneider and J. F. Brennecke, *J. Am. Chem. Soc.*, 2010, **132**, 2116.

7 P. G. Jessop, D. J. Heldebrant, X. Li, C. A. Eckert and C. L. Liotta, *Nature*, 2005, **436**, 1102.

8 T. Yamada, P. J. Lukac, M. George and R. G. Weiss, *Chem. Mater.*, 2007, **19**, 967.

9 G. V. S. M. Carrera, M. Nunes da Ponte and L. C. Branco, *Tetrahedron*, 2012, **68**, 7408.

10 T. Yamada, P. J. Lukac, T. Yu and R. G. Weiss, *Chem. Mater.*, 2007, **19**, 4761.

11 T. Yu, T. Yamada, G. C. Gaviola and R. G. Weiss, *Chem. Mater.*, 2008, **20**, 5337.

12 G. V. S. M. Carrera, N. Jordão, M. M. Santos, M. Nunes da Ponte and L. C. Branco, *RSC Adv.*, 2015, DOI: 10.1039/c5ra03474d.

13 G. V. S. M. Carrera, N. Jordão, L. C. Branco and M. Nunes da Ponte, *J. Supercrit. Fluids*, DOI: 10.1016/j.supflu.2015.02.015.

14 D. J. Heldebrant, C. R. Yonker, P. G. Jessop and L. Phan, *Chem.–Eur. J.*, 2009, **15**, 7619.

15 V. M. Blasucci, R. Hart, P. Pollet, C. L. Liotta and C. A. Eckert, *Fluid Phase Equilib.*, 2010, **294**, 1.

16 Q. Zhang, N. S. Oztekin, J. Barrault, K. de Oliveira Vigier and F. Jérôme, *ChemSusChem*, 2013, **6**, 593.

17 S. Abraham and R. G. Weiss, *Photochem. Photobiol. Sci.*, 2012, **11**, 1642.

18 F. S. Pereira, E. R. de Azevedo, E. F. da Silva, T. J. Bonagamba, D. L. S. Agostíni, A. Magalhães, A. E. Job and E. R. P. González, *Tetrahedron*, 2008, **64**, 10097.

19 M. C. Ozturk, O. Y. Orhan and E. Alper, *Int. J. Greenhouse Gas Control*, 2014, **26**, 76.

20 R. M. Silverstein and F. X. Webster, *Spectrometric Identification of Organic Compounds*, John Wiley & Sons, Inc, New York, 6th edn, 1997.

21 D. J. Heldebrant, P. K. Koech, M. T. C. Ang, C. Liang, J. E. Rainbolt, C. R. Yonker and P. G. Jessop, *Green Chem.*, 2010, **12**, 713.

22 Web page: http://sdbs.db.aist.go.jp/sdbs/cgi-bin/cre_index.cgi last check 23/04/2015.

23 W. Galezowski, A. Jarczewski, M. Stanczyk, B. Brzezinsky, F. Bartl and G. Zundel, *J. Chem. Soc., Faraday Trans.*, 1997, **93**, 2515.

24 http://www.chemicalbook.com last check 24/04/2015.

PAPER

Novel windows for "solar commodities": a device for CO_2 reduction using plasmonic catalyst activation

Alexander Navarrete,[a] Sergio Muñoz,[a] Luis M. Sanz-Moral,[a]
Juergen J. Brandner,[b] Peter Pfeifer,[b] Ángel Martín,[a] Roland Dittmeyer[b]
and María J. Cocero[a]

A novel plasmonic reactor concept is proposed and tested to work as a visible energy harvesting device while allowing reactions to transform CO_2 to be carried out. Particularly the reverse water gas shift (RWGS) reaction has been tested as a means to introduce renewable energy into the economy. The development of the new reactor concept involved the synthesis of a new composite capable of plasmonic activation with light; the development of an impregnation method to create a single catalyst-reactor entity; and finally, the assembly of a reaction system to test the reaction. The composite developed was based on a Cu/ZnO catalyst dispersed into transparent aerogels. This allows efficient light transmission and a high surface area for the catalyst. An effective yet simple impregnation method was developed that allowed introduction of the composites into glass microchannels. The activation of the reaction was made using LEDs that covered all the sides of the reactor allowing a high power delivery. The results of the reaction show a stable process capable of low temperature transformations.

Introduction

CO_2 as a renewable energy vector

One of the most industrially promising heterogeneous catalytic processes is carbon dioxide hydrogenation. In the process of catalytic hydrogenation, hydrogen obtained from carbon neutral energy sources (*e.g.* wind or solar) is reacted with CO_2 to obtain products such as fuels.[1] Thus, this process serves a double purpose: firstly, as chemical storage of the surplus energy generated by fluctuating renewable energies; and secondly, to reduce emissions of CO_2.

[a]*University of Valladolid, Department of Chemical Engineering and Environmental, Technology, High Pressure Processes Group, Paseo Prado de la Magdalena s/n, 47005 Valladolid, Spain*
[b]*Institute for Micro Process Engineering, Karlsruhe Institute for Technology, Eggenstein-Leopoldshafen, Germany*

The successful introduction of CO_2-use technologies requires plausible and profitable processes that use efficiently renewable energy. The most abundant and evenly distributed of such energies is the one provided by the Sun. If stored in the form of "solar commodities" such as methanol or olefins new opportunities for the use of CO_2 could be considered.[2] The production of methanol from CO_2 and hydrogen involves the following reactions:

$$CO_2 + H_2 \Leftrightarrow CO + H_2O; \Delta H^0 = +41.19 \text{ kJ mol}^{-1} \qquad (1)$$

$$CO + 2H_2 \Leftrightarrow CH_3OH; \Delta H^0 = -90.70 \text{ kJ mol}^{-1} \qquad (2)$$

$$CO_2 + 3H_2 \Leftrightarrow CH_3OH + H_2O; \Delta H^0 = -49.51 \text{ kJ mol}^{-1} \qquad (3)$$
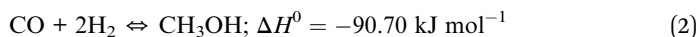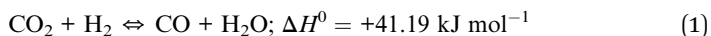
In order to capture that energy in chemical bonds there are several useful methods for reactions. From a chemical point of view, they can be grouped into photocatalytic, thermal and electrical routes. In electrical routes, the solar energy is first converted into electricity and then, the resultant electrical energy is used in the chemical transformation of CO_2;[3-7] the thermal routes concentrate solar radiation and convey that energy directly into the reactor.[8-10] Photocatalytic CO_2 conversion involves either water splitting connected to a CO_2 reduction reaction, or a process combining both in one "single pot".[11-13]

Selective use of visual light with plasmon catalysts

The surface plasmon resonance (SPR) phenomenon is commonly found in metallic (or carbon) nanostructures and allows the range of the solar spectrum used on a given photoinduced process to be increased.[14] This effect is the result of the response of the conduction electrons to the oscillations of the electric field of the light radiation. Increased energy absorption by the electrons is possible at selected wavelengths under the proper particle size and shape of the nano-particles for a given surrounding media (fluid or catalyst). This phenomenon produces a high light concentration up to the point that a reduction in the amount of semiconductor of three orders of magnitude for the same amount of light has been possible.[15] On the other hand, increased light capture with SPR for photothermal conversions is leading to breakthroughs in energy systems such as solar collectors.[16]

This work explores the reduction of CO_2 to CO as a first step in a solar-based process to produce methanol. Thus, it is based on the reverse water gas shift (RWGS) reaction as described by eqn (1). Recent approaches have used gold and semiconductor composites for plasmonic enhancement of the reduction.[17,18]

This process is commonly activated in industry using Cu/ZnO based cata-lysts.[19] Here, we have developed plasmonic catalytic composites in mesoporous silica structures (aerogels). For this, we have used the plasmon-tuneable Cu/ZnO catalyst reported by Tan *et al.* (2013).[20]

A plasmonic microreactor as a light harvesting device

The efficiency of the chemical reactions is not ruled only by the catalytic material but also by the reactor configuration and their mass and energy transport char-acteristics. On many occasions, promising catalytic materials have failed to reach

industrial success due to the disconnection between the catalytic structure and the reactor-level phenomena.[21,22]

Here we propose a novel concept for visual energy harvesting: a plasmonic microreactor device. It integrates a plasmon catalyst and reactor as one entity with a sole response to light (Fig. 1).

Microreactors allow efficient energy and mass transport while are easily scalable (numbering up). Thus, the combination of efficient microstructured devices and direct plasmonic absorption of solar energy by the catalyst would represent a major breakthrough in the CO_2-use field.

In this work, a plasmon-tuneable composite is integrated with a microchannel based reaction system under visual LED illumination for the RWGS reaction. This involved the synthesis of the new composite; the development of an impregnation method to create a catalyst-reactor entity; and finally, the assembly of a reaction system to test the reaction.

Methods

Plasmo-catalytic composite synthesis

The chemicals used during this stage are detailed: zinc acetate dihydrate (>98%), oleylamine (70%), tetramethyl orthosilicate (98%), ammonia (28–30%) and triethyleneglycol (99%) were purchased from Sigma-Aldrich. Ethyleneglycol (99.5%) (Merck) and copper acetate monohydrate (99.9%) were purchased from Alfa Aesar. Methanol (99.8%) (Panreac). All chemicals were used without further purification.

Synthesis of the Cu/ZnO bimetallic catalyst

This bimetallic (Cu : ZnO, 1 : 2) catalyst was synthesised following the procedure proposed by Tan *et al.* (2013).[20]

Briefly, first ZnO nanorods were prepared. Zinc acetate (3 mmol) was added to 1.3 mmol of oleylamine in a two necked flask. The oleylamine has not of high purity (70%), requiring a step where the reactants were degassed at 80 °C for 45
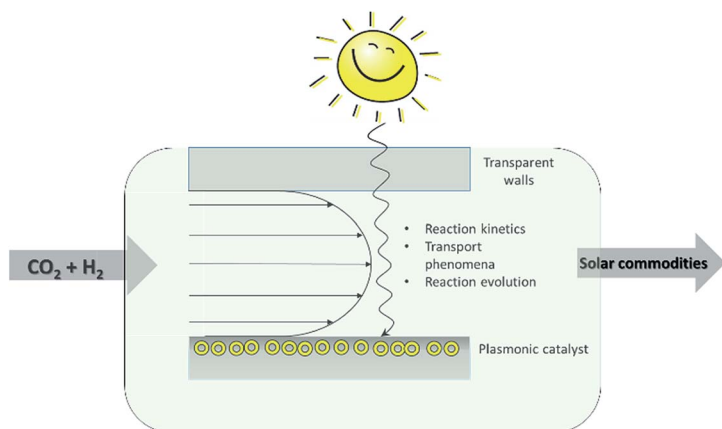
Fig. 1 Concept of the plasmonic microreactor device.

min under a vacuum atmosphere. Then, the temperature was increased to 220 °C under nitrogen purging. During the heating process, the solution turned white upon reaching 180 °C. After 15 min of heating, the mixture was cooled to atmospheric temperature, washed with ethanol and centrifuged in order to isolate the precipitate. It was washed with 6 ml of ethanol three times to ensure complete removal of the reactants or byproducts.

The ZnO nanorods prepared above were then redispersed in 20 ml of triethyleneglycol by sonication for two hours, followed by stirring under room conditions overnight. Ethyleneglycol (2 ml) was added to the ZnO dispersion, and the mixture was degassed at room temperature for 5 min before heating to 190 °C. Simultaneously, a second solution of copper acetate monohydrate was prepared by dissolving in ethyleneglycol. This mixture required sonication in order to dissolve the copper acetate in the liquid. This mixture was added to the ZnO mixture in a dropwise manner over 10 min. After this, 5 more min heating at 190 °C was allowed before the composite was washed with isopropanol, centrifuged for 15 minutes at 4500 rpm (centrifuge Kubota 5100, Japan) and isolated from the mixture.

Synthesis of the mesoporous silica composites

Light transmission to the catalytic structures is essential while enough surface area has to be provided in order to have enough metal loading to capture light. Transparent aerogels are mesoporous materials combining high surface areas and good light transmission.[23]

Aerogels were synthesised following the sol–gel route. The precursor for the silica hydrogel selected was tetramethyl orthosilicate (TMOS). The molar ratio of TMOS : CH_3OH : H_2O : NH_4 was 1 : 2.3 : 3.84 : 0.012.

Firstly, methanol was used to disperse the nanoparticles formed in the catalyst synthesis. Sonication (15 min) was applied to ensure a good dispersion of the nanoparticles in the liquid phase. Methanol with the particles and TMOS were mixed together. While this solution was stirred, a second solution of ammonium hydroxide and water was prepared and stirred. After a few minutes of stirring, both solutions were mixed, and the gelation process began.

In this moment, the gelation process of the silica hydrogel has started, but it is still liquid for a few minutes. This time lapse, before gelation, must be used to impregnate the solution inside the microchannels of the microreactors.

Integration of the composites and microreactor

In order to have a single integrated device it is necessary to integrate light transmission and composite activation in the same structure. Here, we have developed a method to integrate transparent aerogels in glass microchannels. The method used to impregnate the sol–gel that showed the best results was the suction of the liquid with a syringe, which was previously adapted to the microreactor on its top (Fig. 2). With this method, placing the microreactor in a vertical position, it was very easy to fill the microchannel placing the tip in the liquid. After a short time, the gelation process finished and the hydrogel formed had a good adherence inside the microchannels.

It is worth mentioning that one of the most important parameters during this step is the amount of ammonia, as it acts as a catalyst for the gelation process. It is

ART ◼ C5FD00109A
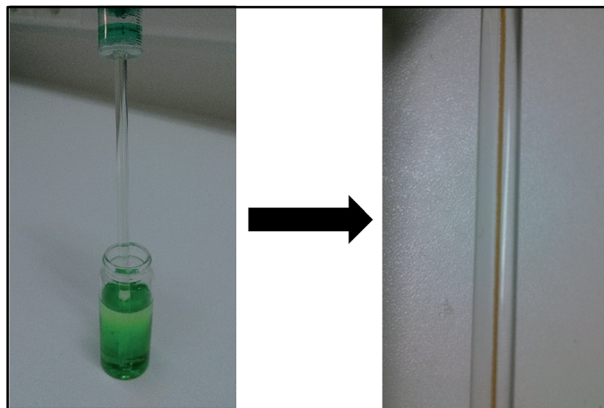
Fig. 2   Syringe filling of the microchannels.

necessary to use an amount of ammonia low enough that allows enough time to impregnate the hydrogel inside the microreactor, because it must be still a fluid. On the other hand, the amount of ammonia cannot be very low, because if the gelation process is too slow, the nanoparticles start to precipitate and they will not be inside the silica net. Finding an equilibrium between these two factors is the key to achieving good impregnation of the nanoparticles supported in the silica gels inside the microreactors.

In order to ensure good adherence of the aerogel to the walls of the micro-channels, it is necessary to perform a pretreatment to the glass microreactors (15.0 cm) to clean the walls of the microchannels. For this cleaning process, the most common option is to use a piranha solution, which reacts violently with most organic materials. The solution used was a mixture of sulfuric acid and hydrogen peroxide that can be prepared in different proportions; the most usual being 4 : 1 in concentrated sulfuric acid. For 15 to 30 minutes the material is submerged in the solution, then removed, washed with plenty of Milli-Q water and dried carefully.

The empty glass microreactors were put inside a glass pot, and the sulfuric acid was first added. Then, the hydrogen peroxide was added with extreme care because the reaction is very exothermic; the temperature is suddenly increased and some vapor can be formed. After 20 minutes, the slides were removed from the piranha solution, washed with Milli-Q water and dried carefully.

After the introduction of the nanoparticles in the sol–gel and its introduction into the microreactors, these were put in a vessel with methanol for aging. This vessel was carefully closed to avoid methanol evaporation, and it was heated to 50 °C in an oven. With this procedure the water contained in the silica net was replaced with methanol, resulting in alcogels.

After 24 hours of heating, the alcogels were dried using supercritical carbon dioxide. The microreactors were put in a high pressure vessel, and this vessel was filled completely with methanol. Carbon dioxide was introduced slowly in the vessel to allow a good diffusion into the methanol. The pressure was raised to 100 bar and the temperature to 40 °C, above the critical point of carbon dioxide. Three cycles of 45 minutes were performed, renewing the carbon dioxide between each

cycle to complete the drying process.[24] After this, silica aerogels were correctly obtained, keeping the adherence to the walls of the microchannels.

Proof-of-concept setup

Once the Cu/ZnO based plasmonic composites were integrated into the glass microchannels, a test of these devices was made. In order to test the reactor concept, a reaction system had been built that included visual LED illumination and control of the temperature the reaction while a precise control of the flow and pressure was provided. A scheme of the experimental plant is presented in Fig. 3.

Hydrogen and carbon dioxide were introduced in the system, and their flows were controlled with two different flow mass meter/controllers (EL-Flow F-200, Bronkhorst) with ranges from 0.02 to 1 ml min^{-1}.

Before the reaction was initiated, hydrogen and carbon dioxide were mixed in a 3 : 1 proportion, and sent to the vent while both flows were stabilized.

When the flows were correctly controlled, the mixture of the gases moved to the second part of the setup. In this part the gases were heated, together with the glass microreactor, in a gas chromatography oven (Agilent 7890). The microreactor consisted of a 0.5 mm ID glass capillary with an external diameter of 5 mm (Schott Duran, USA).

A second vent was used to take out the gases while the pressure was increased to 20 bar. Pressure was controlled by a pressure meter/controller (EL-Press series, Bronkhorst). When the pressure and flow were stable at 20 bar, the valve for extraction was closed, and the oven and LEDs were turned on.

Visual light stimulation was provided by 36 LEDs (superbright, inspired LED) surrounding the microreactor as shown in Fig. 4. In total, they provided the equivalent of a nominal power of 9780 W m^{-2} of white light.

The reaction began and the products of the reaction were measured in a Micro Gas Chromatograph (CP-4900, Varian) equipped with two columns: a poraplot 10 m and a 5A molsieve. Before the micro GC, the pressure of the gas stream was reduced to less than 5 bar.
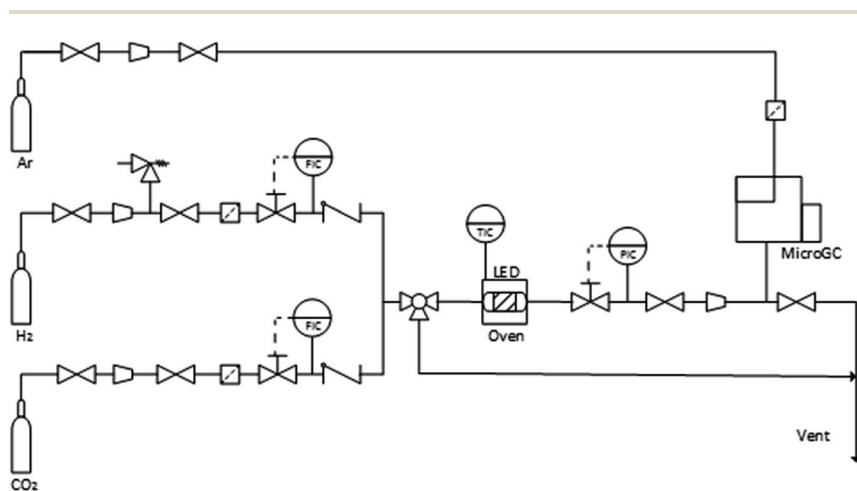
Fig. 3   Schematic flow diagram of the plant.

ART ■ C5FD00109A
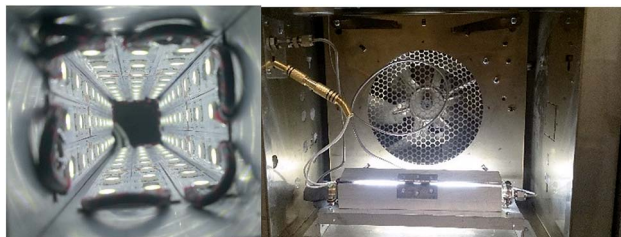
Fig. 4 LED light configuration. Left, detail of the inner LED distribution. Right, micro-reactor in the oven surrounded by the LEDs.

Composite characterization

Scans of the bimetallic catalysts to check absorbance of visual light were carried out using a UV-vis spectrometer (UV 2550, Shimadzu). XRD analysis was carried out using a Bruker Discover D8 diffractometer. The porosity measurements were carried out using a Surface Area and Porosity Analyzer (ASAP 2020, Micromeritics).

Results and discussion

Composite characterization

After the synthesis UV-vis scans were carried out in order to check the absorption of visual light from both the ZnO nanorods and the bimetallic Cu/ZnO catalyst (Fig. 5).

It can be seen that the bimetallic catalyst has a peak at 498 nm. This corresponds to absorption in the range close to the green colour.[25] The transparent aerogels change and acquire colour once the composite is formed (Fig. 6).

The XRD pattern shows the presence of ZnO and metallic copper in the silica amorphous structure. The ZnO planes 100 $(2\theta = 31.7°)$, 002 $(2\theta = 34.4°)$, 101 $(2\theta =$
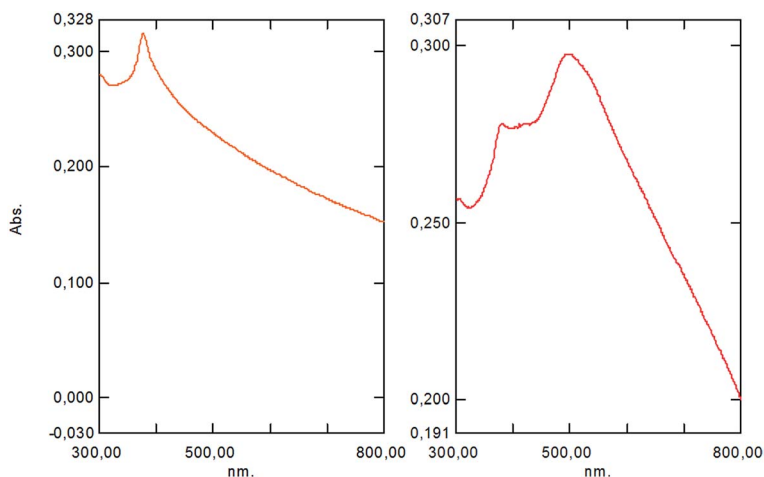
Fig. 5 Absorption spectra of ZnO (left) and Cu/ZnO (right).

Fig. 6   Silica aerogel before (left) and after (right) catalyst impregnation.

36.1°) and 110 ($2\theta = 56.4°$) can be identified in Fig. 7. Copper cannot be seen due to its lower proportion in the structure.

BET surface area and pore volume of the samples were calculated from N_2 isotherms. The adsorption–desorption curve shows a type IV isotherm curve typical for mesoporous silica aerogels[26] (Fig. 8). The BET surface area is 945.8 m^2 g^{-1} which indicates that the inclusion of the bimetallic catalyst does not have a significant influence on the textural properties of the aerogel. The BJH pore volume is equal to 2.29 cm^3 g^{-1} reinforcing that the structure is not affected.

Reaction test of the concept

The full power of the LEDs was applied and the evolution of the compounds were followed. In order to test the influence of the main variables of the process, changes in flow and temperature were made during the reaction (Fig. 9).

It could be observed that the reaction was stable at 50 °C at during more than 100 minutes. Then the temperature was increased at 70 °C and tested during the same time span. Finally, the flow was reduced to half of the initial conditions. No
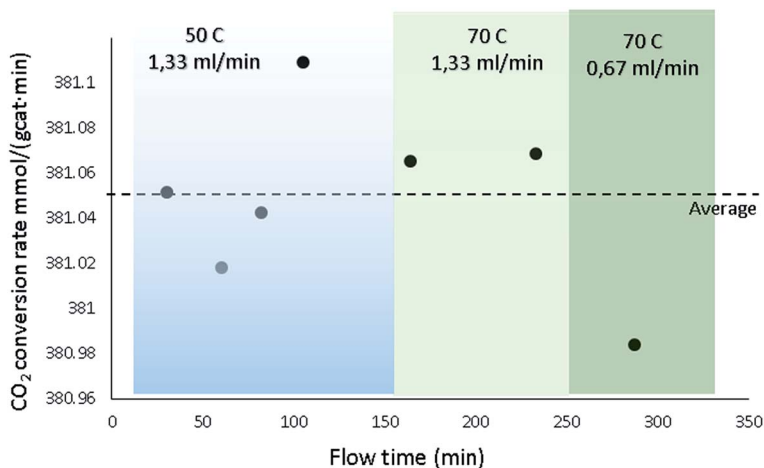
Fig. 7   XRD pattern of the plasmonic composite.

ART ■ C5FD00109A
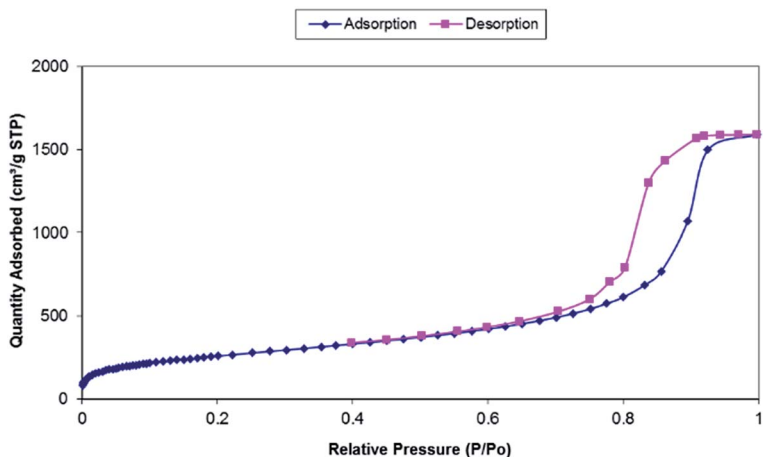
Fig. 8 Adsorption–desorption isotherms of the composites.

significant changes were observed during almost 300 minutes, which indicates the suitability of this system to test several catalyst loads under thermodynamic conditions.

It is important to note that the average conversion rate is similar to the one obtained in other works at temperatures around 200 °C.[17] Thus, the integrated plasmonic reactor concept proposed here opens new avenues to couple low temperature solar collectors and chemistry as a mean to introduce renewable energy in the economy, particularly for the conversion of CO_2.
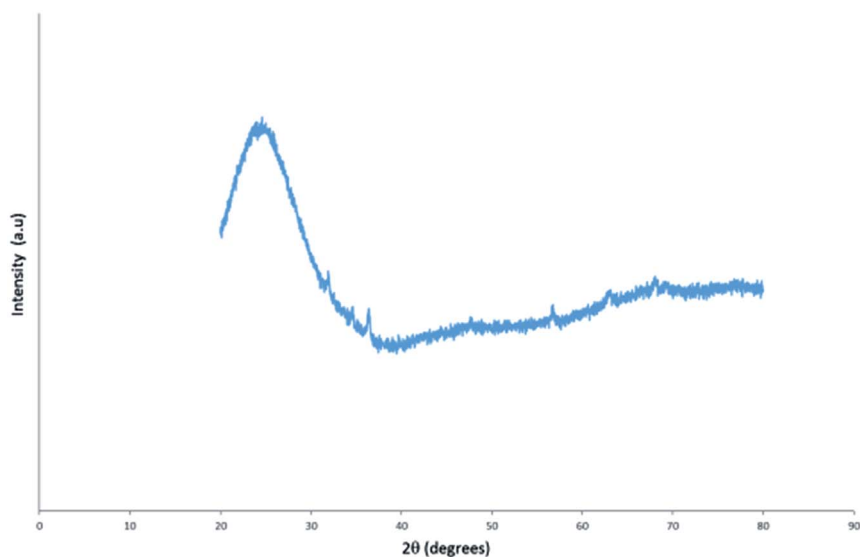
Fig. 9 Evolution of the reaction.

Conclusions

A novel plasmonic composite was developed that can absorb light from the visible spectrum. Its characterization evidenced a high surface area and proper integration with the metallic components of the catalyst.

It was possible to introduce this composite into glass microchannels in order to obtain a single entity that acts as both a light-harvesting device and as a reactor. This is possible due to the development of a simple yet effective impregnation method that allows the synthesis of the aerogels *in situ*.

The microreactor obtained was tested for RWGS in a system that allowed not only control of the reaction variables such as pressure, temperature and flow, but also, delivers visual light in an elegant way.

The CO_2 conversion rates were in accordance with other works testing plasmonic catalysts at higher temperatures. This can be due to the increased light energy delivery, the high surface area of the material and to the integrated and efficient way to deliver the radiant energy possible in this reactor. This is then a novel opportunity to gain understanding in the field of CO_2- use by applying solar energy.

Acknowledgements

References

1 G. Centi, E. A. Quadrelli and S. Perathoner, *Energy Environ. Sci.*, 2013, **6**, 1711–1731.

2 G. Centi and S. Perathoner, in *Green Carbon Dioxide: Advances in CO₂ Utilization*, ed. G. Centi and S. Perathoner, John Wiley & Sons, 2014.

3 K. Ogura, H. Yano and T. Tanaka, *Catal. Today*, 2004, **98**, 515–521.

4 R. Angamuthu, P. Byers, M. Lutz, A. L. Spek and E. Bouwman, *Science*, 2010, **327**, 313–315.

5 H. Li, P. H. Opgenorth, D. G. Wernick, S. Rogers, T.-Y. Wu, W. Higashide, P. Malati, Y.-X. Huo, K. M. Cho and J. C. Liao, *Science*, 2012, **335**, 1596.

6 B. A. Rosen, A. Salehi-Khojin, M. R. Thorson, W. Zhu, D. T. Whipple, P. J. A. Kenis and R. I. Masel, *Science*, 2011, **334**, 643–644.

7 E. E. Barton, D. M. Rampulla and A. B. Bocarsly, *J. Am. Chem. Soc.*, 2008, **130**, 6342–6344.

8 G. P. Smestad and A. Steinfeld, *Ind. Eng. Chem. Res.*, 2012, **51**, 11828–11840.

9 I. Ermanoski, J. E. Miller and M. D. Allendorf, *Phys. Chem. Chem. Phys.*, 2014, **16**, 8418–8427.

10 M. Forster, *J. CO₂ Util.*, 2014, **7**, 11–18.

11 A. Dhakshinamoorthy, S. Navalon, A. Corma and H. Garcia, *Energy Environ. Sci.*, 2012, **5**, 9217–9233.

12 P. D. Tran, L. H. Wong, J. Barber and J. S. C. Loo, *Energy Environ. Sci.*, 2012, **5**, 5902–5918.

13 Ş. Neaţu, J. Maciá-Agulló and H. Garcia, *Int. J. Mol. Sci.*, 2014, **15**, 5246.

14 S. Linic, P. Christopher and D. B. Ingram, *Nat. Mater.*, 2011, **10**, 911–921.

ART ■ C5FD00109A

15 C. Hägglund, S. P. Apell and B. Kasemo, *Nano Lett.*, 2010, **10**, 3135–3141.

16 M. A. Garcia, *J. Phys. D: Appl. Phys.*, 2011, **44**, 283001.

17 A. A. Upadhye, I. Ro, X. Zeng, H. J. Kim, I. Tejedor, M. A. Anderson, J. A. Dumesic and G. W. Huber, *Catal. Sci. Technol.*, 2015, **5**, 2590–2601.

18 C. Wang, O. Ranasingha, S. Natesakhawat, P. R. Ohodnicki, M. Andio, J. P. Lewis and C. Matranga, *Nanoscale*, 2013, **5**, 6968–6974.

19 M. Behrens, F. Studt, I. Kasatkin, S. Kühl, M. Hävecker, F. Abild-Pedersen, S. Zander, F. Girgsdies, P. Kurr, B.-L. Kniep, M. Tovar, R. W. Fischer, J. K. Nørskov and R. Schlögl, *Science*, 2012, **336**, 893–897.

20 Z. Y. Tan, D. W. Y. Yong, Z. Zhang, H. Y. Low, L. Chen and W. S. Chin, *J. Phys. Chem. C*, 2013, **117**, 10780–10787.

21 J. Gascon, J. R. van Ommen, J. A. Moulijn and F. Kapteijn, *Catal. Sci. Technol.*, 2015, **5**, 807–817.

22 B. Louis, G. Laugel, P. Pale and M. M. Pereira, *ChemCatChem*, 2011, **3**, 1263–1272.

23 G. M. Pajonk, *J. Non-Cryst. Solids*, 1998, **225**, 307–314.

24 L. M. Sanz-Moral, M. Rueda, R. Mato and Á. Martín, *J. Supercrit. Fluids*, 2014, **92**, 24–30.

25 NASA, What Wavelength Goes With a Color?, http://science-edu.larc.nasa.gov/EDDOCS/Wavelengths_for_Colors.html.

26 R. Al-Oweini and H. El-Rassy, *Appl. Surf. Sci.*, 2010, **257**, 276–281.

PAPER

Taming microwave plasma to beat thermodynamics in CO_2 dissociation

G. J. van Rooij,[*a] D. C. M. van den Bekerom,[a] N. den Harder,[a] T. Minea,[a] G. Berden,[b] W. A. Bongers,[a] R. Engeln,[c] M. F. Graswinckel,[a] E. Zoethout[a] and M. C. M. van de Sanden[ac]

The strong non-equilibrium conditions provided by the plasma phase offer the opportunity to beat traditional thermal process energy efficiencies *via* preferential excitation of molecular vibrations. Simple molecular physics considerations are presented to explain potential dissociation pathways in plasma and their effect on energy efficiency. A common microwave reactor approach is evaluated experimentally with Rayleigh scattering and Fourier transform infrared spectroscopy to assess gas temperatures (exceeding 10^4 K) and conversion degrees (up to 30%), respectively. The results are interpreted on a basis of estimates of the plasma dynamics obtained with electron energy distribution functions calculated with a Boltzmann solver. It indicates that the intrinsic electron energies are higher than is favorable for preferential vibrational excitation due to dissociative excitation, which causes thermodynamic equilibrium chemistry to dominate. The highest observed energy efficiencies of 45% indicate that non-equilibrium dynamics had been at play. A novel approach involving additives of low ionization potential to tailor the electron energies to the vibrational excitation regime is proposed.

1 Introduction

The emission of carbon dioxide into the atmosphere is widely regarded as a severe environmental issue due to concern over its effect on climate change. The consequent increasingly stronger limits on CO_2 exhausts are driving the transition to sustainable energy sources. The intermittent character of, particularly, solar photovoltaics and wind imposes the need for energy storage. At the same time, these sustainable energy sources produce electricity, whereas, globally, less

[a]*Dutch Institute for Fundamental Energy Research, P.O. box 6336, 5600 HH Eindhoven, The Netherlands. E-mail: g.j.vanrooij@differ.nl; Tel: +31 40 333 49 99*

[b]*Radboud University, Institute for Molecules and Materials, FELIX Laboratory, Toernooiveld 7c, 6525 ED Nijmegen, The Netherlands*

[c]*Department of Applied Physics, Plasma and Materials Processing Group, Eindhoven University of Technology, P.O. Box 513, 5600 MB Eindhoven, The Netherlands*

than 20% of the energy is consumed in that form. Converting temporary electrical energy surpluses into chemical fuels would, thus, be advantageous in view of energy density as well as to address CO_2 emissions in other areas of energy consumption (*e.g.* transportation). A promising approach for this conversion involves the non-equilibrium chemistry in the plasma phase. The present paper deals with the particular case of plasma chemical CO_2 reduction as the first step in the production of carbon-based fuels.

Electrical discharges are usually sustained by electric fields through which energy is, in the first instance, transferred to the free electrons. Subsequently, this energy is transferred by collisions to the (neutral) gas phase heavy particles (*e.g.* CO_2 molecules). Due to the large mass difference between collision partners, the elastic energy transfer is inefficient and hence there may be large differences between their temperatures. It is under such far from thermodynamic equilibrium conditions that it is possible to intensify traditional chemical processes and to achieve the highest energy efficiencies.[1]

If the energy of the electrons is high enough, the heavy gas particles may be excited into higher electronic states or even be ionized. Ionization is required for sustaining the plasma discharge. However, in the present context, the subsequent dissociative recombination should not become the dominant pathway to dissociation as it is energetically an inefficient way of initiating chemical reactions. After all, ionization of CO_2 requires $\sim$14 eV per molecule, whereas its "net" dissociation energy is $\sim$3 eV (considering the "net" reaction $CO_2 \rightarrow CO + \frac{1}{2}O_2$). This consideration implies a 20% maximum energy efficiency for dissociation *via* ionization.

On the other hand, low energy electron collisions can excite vibrational modes in the molecule. Such vibrationally excited molecules will further interact with each other, collisionally exchanging vibrational energy up along the energy scale until the dissociation limit is reached. In this scheme, the electrons, that were energetically "expensive" to create, are used many times to deliver energy specifically to the bonds that are to be broken up to the point where dissociation of the molecule is achieved. It is this qualitative mechanism that has been put forward to explain the up to 90% energy efficiencies that were demonstrated in the 70s and 80s.[2–7]

Having established that it is energetically attractive, we note that the plasma chemical approach for reduction of CO_2 is also inherently appropriate in the context of alleviating intermittency of sustainable energy sources. The main reason for this is the low "inertia" of a plasma reactor, *i.e.* the plasma can be turned off and on and the input power can be regulated quickly (sub-second time scale, no heating of *e.g.* catalytic surfaces is required) and thus can follow the availability of energy surpluses. Secondly, the reactor is compact and power (*e.g.* microwave) supplies are cheap (0.1 euro per W), thus the investment costs can be low enough to economically allow intermittent use. Both aspects are not self-evident for, *e.g.*, electrolysis installations.

Although the plasma chemical approach for CO_2 reduction has been proven to be promising in terms of energy efficiency, it is presently not clear how this holds under industrially relevant throughputs. Two aspects play a role here. Firstly, the highest (90%) energy efficiencies were achieved at only a moderate (20%) conversion efficiency. Conversely, the highest (90%) conversion efficiencies were

ART ■ C5FD00045A

achieved at a moderate (20%) energy efficiency.[1] Secondly, these experiments were performed at a strongly sub-atmospheric pressure. At elevated pressures, the efficiency remained very low level, typically <10%.

A microwave plasma approach for CO_2 dissociation has been recognized as the most favourable in terms of energy efficiency.[6,8] It is generally assumed that this is due to a low reduced electric field and hence preferential vibrational excitation. In recent years, a number of attempts have been undertaken with microwave discharges to reproduce these record values, experimentally as well as numerically.[8–12]

This paper also focuses on a microwave approach for CO_2 dissociation. Simple molecular physics considerations are discussed to illustrate the different CO_2 dissociation pathways. Conversion and energy efficiency are determined (from Fourier transform infrared spectroscopy, FT-IR, measurements) in scans of power, gas flow and reactor pressure. The level of non-equilibrium is assessed on the basis of gas temperatures that are determined from Rayleigh scattering density measurements combined with reactor pressure readings. These experimental results are interpreted in a comparison with estimated reaction rates on the basis of electron energy distribution calculations with a Boltzmann solver. Finally, a novel methodology to enhance the non-equilibrium is proposed.

2 Vibrational *versus* electronic excitation – elementary molecular physics

We discern three reaction pathways that may be relevant under common low temperature plasma conditions as expected in microwave CO_2 plasma. Each has its own intrinsic energy efficiency. These pathways are schematically drawn in Fig. 1 and the (in-)efficiency of each pathway is indicated by the amount of energy that is intrinsically converted to heat.

Firstly, dissociation may occur due to step-by-step vibrational excitation (see Fig. 1a). The reaction products may be formed without a significant amount of
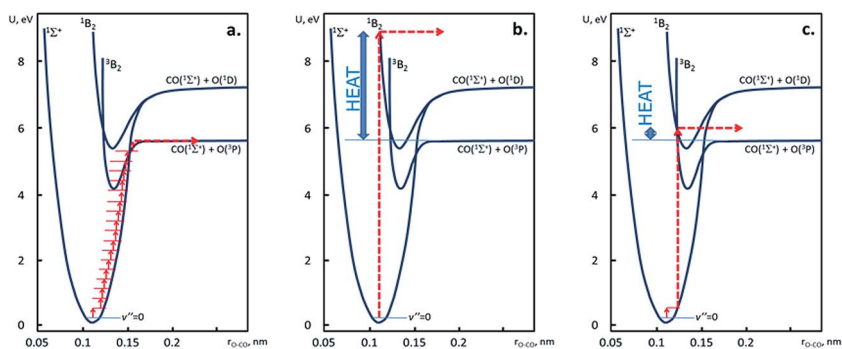
Fig. 1 Potential energy diagrams (as a function of one O−CO bond length) that illustrate the molecular physics behind three variants of CO_2 dissociation. Diagram (a) represents stepwise vibrational excitation that, after term crossing, causes ideally efficient dissociation. Contrary is the dissociative excitation in diagram (b), which involves a significant amount of heat to be released. A mix of these two cases is shown in diagram (c), vibrationally activated dissociative excitation, which is shown here as highly efficient as well.

kinetic energy and thus it is the dominant channel for CO_2 dissociation. As mentioned before, this mechanism was put forward to explain the high energy efficiencies achieved. Typical electron temperatures of ~1 eV ensure that a major portion of the discharge energy is transferred from the plasma electrons to the lower CO_2 vibrational levels. At the same time, conversion of vibrational energy into translational energy can be kept to a minimum by ensuring a low gas temperature. Instead, vibrational–vibrational exchange may lead to over-population of the higher vibrational levels. The non-adiabatic transition $^1\Sigma^+ \rightarrow$ $^3B_2$ opens the most effective dissociation pathway $CO_2(^1\Sigma^+) \rightarrow CO(^1\Sigma^+) + O(^3P)$.

Secondly, dissociation may be induced by dissociative excitation (Fig. 1b). It is evident that this pathway involves the highest dissociation barrier and will be the least efficient. Electronic excitation becomes increasingly effective if the plasma temperature rises above ~1 eV. This occurs for example when the input power exceeds the power loss to vibrational excitation (which leads to more electronic excitation upon an increase of the electron temperature).

Finally, vibrational stimulated electronic excitation (Fig. 1c) may occur as a mixture of the previous two. In the example sketched, a single vibrational excitation in the electronic ground state is sufficient to significantly decrease the excitation energy to the $^1B_2$ upper state. Again, the non-adiabatic term crossing presents a dissociation pathway with 90% energy efficiency.

The plasma temperature (or more precisely, the electron energy distribution function) will in the end determine the relative importance of these reaction pathways as it determines the balance between vibrational excitations and electronic excitations.

3 Experimental

3.1 Microwave flow reactor

A 1 kW (continuous wave) microwave source is used to produce 2.45 GHz microwaves that are transferred through WR340 waveguides to the flow reactor (Fig. 2). A 3-stub tuner is placed in the microwave circuit to match the load impedance and adjust the power transfer. A sliding short is positioned a quarter wavelength away from the center of the quartz tube. A quartz tube, which is placed perpendicularly through the broad wall of the waveguide, serves as flow reactor. A 27 mm inner diameter tube was used during the Rayleigh scattering measurements while during the FTIR measurements a 18 mm diameter tube was used.
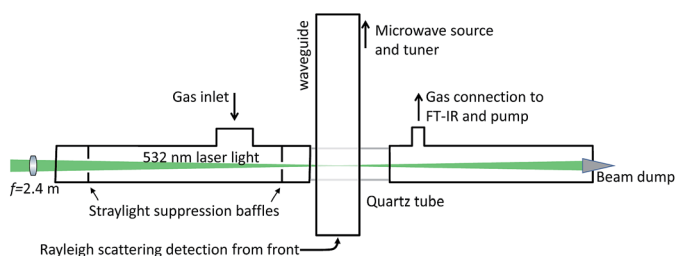
Fig. 2 Schematic of the microwave plasma source used for CO_2 dissociation. Indicated is the laser beam path that is used for the Rayleigh scattering experiment.

Gas flows of up to 15 slm of pure CO_2 were supplied. The operation pressure in the reactor was independently controlled in the range of 10–250 mbar by varying the effective pumping speed.

3.2 Rayleigh scattering

A Nd:YAG laser light was used for the Rayleigh scattering measurements. The laser delivered 0.5 J per pulse at 532 nm with a repetition frequency of 10 Hz. An anti-reflection coated UV fused silica window was used to couple the laser into the reactor. A 2.4 m lens was used to focus the laser beam at the detection volume in the center of the waveguide. Since the divergence of the laser beam was 0.45 mrad, this resulted in a 1.1 mm diameter beam at the focus. A 20 mm diameter hole in the 14 mm thick sliding short enabled the observation of laser scattering with minimal microwave leakage.

To suppress parasitic scattering of the laser light, *e.g.* from imperfections in the entrance window, baffles were installed in the vacuum components. A critical aperture of 6 mm diameter was installed 505 mm from the scattering volume, and a subcritical aperture with 12 mm diameter was placed at 100 mm distance. The beam dump was placed 2 meters after the scattering volume, and was installed in a vacuum.

The magnification of the collection optics resulted in an axial detection range of approximately 20 mm. A fiber packet was used to transport the scattered light from the collection optics to the spectrometer, a single-pass spectrometer in Littrow arrangement with a 0.3 m focal distance Littrow lens. The spectrometer was equipped with a third generation image intensifier of type EPM102G-04-22S and a Manta-G145B camera.

3.3 FT-IR effluent measurements

FT-IR spectra were taken with a Varian 670 FTIR spectrometer at a resolution of 0.09 cm^{-1}, so that individual ro-vibrational CO-peaks were resolved. A least square fit of the spectrum was used to obtain a species concentration c for different parameter settings using Beer–Lambert's law:

$$\ln\left(\frac{I}{I_0}\right) = -\varepsilon(p, \ T)cl. \tag{1}$$

The values for the molecule specific absorptivity ε were obtained from the HITEMP database,[13] where pressure and Doppler-broadening, as well as instrument-broadening are taken into account. The temperature was assumed to be constant at room temperature. Detailed fits showed this to be accurate within 15 K. At higher pressures and CO-concentrations, the most intense CO-peaks were saturated and thus disregarded in the fitting. The CO fraction f in the effluent was determined from the concentration and pressure, and subsequently converted into the conversion factor α using the relation:

$$f = \frac{\alpha}{(1 + \alpha/2)}. \tag{2}$$

For conversions lower than 2%, the fitting routine didn't converge and a 'best-fit' was estimated by inspection. Knowing the conversion efficiency, the energy efficiency can be calculated using:

$$\eta = \frac{q\alpha E_{d,\,CO_2}}{P_{in}}, \tag{3}$$

where q is the gas flow rate in molecules per second, E_{d,CO_2} is the effective dissociation energy per CO_2 molecule (2.9 eV) and P_{in} is the input power.

4 Experimental results

4.1 Discharge modes – spontaneous light emission

Depending on the operational conditions, particularly on the ratio between pressure and electric field, different modes of plasma operation are known to occur in microwave plasma discharges: diffuse, contracted, and a combination thereof.[1] The contracted plasma region forms at high electron densities. The high density prevents electromagnetic waves penetrating into the core of the plasma and, instead, the microwave power is absorbed in a skin layer at the boundary of the high density region. Generally, the plasma becomes also thermal in this mode, *i.e.* the neutral gas temperature approaches the plasma temperature. It is believed that a combined operation, in which the small volume of thermal plasma is surrounded by a large volume of non-equilibrium plasma, is best to achieve high energy efficiency conversion.

These different modes of operation and transitions in between occurred in the experiments that are discussed in this work as well. To illustrate the effect, images of the spontaneous light emission of the plasma inside the waveguide are shown in Fig. 3. The two cases differed mainly in reactor pressure and correspond to the extremes of the parameter space that was covered: 10 and 250 mbar (input power was 650 and 550 W, respectively; gas flow rate was 13 slm in both cases).
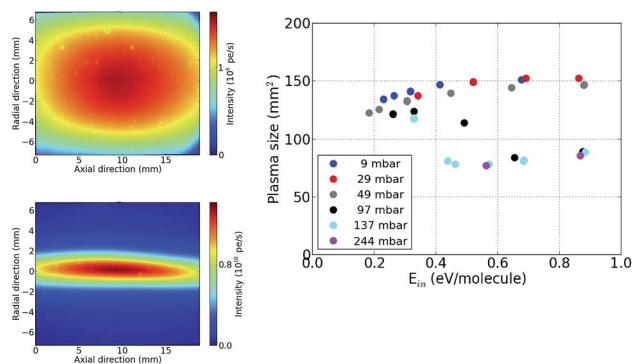
Fig. 3 Spontaneous light emission from the plasma inside the waveguide for (left top) 10 mbar (650 W, 13 slm) and (left bottom) 250 mbar (550 W, 13 slm), illustrating the two modes of operation: diffuse and contracted.[1] It is noted that vignetting at the sides of the images was not corrected for. The plot on the right shows the plasma cross sectional area determined from such emission images in dependence of pressure and specific energy. Plasma cross sectional areas of 120–150 mm² and 80 mm² correspond to diffuse and contracted operations, respectively.

ART ■ C5FD00045A

The emission images were used to estimate the (cross sectional) plasma size in order to qualify the mode of operation throughout the parameter space covered by the present experiments. The results are presented in dependence of the specific energy input in the plot in Fig. 3. In essence, full width half maxima values were used. The plot clearly resolves the diffuse mode with typical plasma cross sectional areas of 120–150 mm^2 and the contracted mode with a size of typically 80 mm^2. Reducing the specific energy input evidently causes back transition of the high pressure contracted mode to a high pressure diffuse mode.

4.2 Conversion degree and energy efficiency

The performance of microwave plasma dissociation of CO_2 was characterized firstly with respect to conversion degree (α). The conversion degrees were inferred from FT-IR measurements of the effluent. The results are plotted in Fig. 4 for scans of specific energy (input power, range 300–1000 W, divided by gas flow rate) and pressure (25–200 mbar) at gas flow rates of 5 and 15 slm. The following observations are made. (i) The pressure series that yield the highest conversions line up along a common linear dependence on the specific energy input. (ii) An optimum exists in operation pressure. This is most clearly seen for the 5 slm data, in which the 100 and 150 mbar series are at maximum conversion whereas the 37 and 200 mbar series show decreased performance. The 15 slm data step up in conversion as pressure goes up and reach a maximum for pressures of 150 and 200 mbar. The latter also implies that (iii) the optimum operation pressure shifts up with gas flow rate. Furthermore, returning to the previous discussion on the different modes of operation, (iv) it was observed that the highest conversion series all correspond to the plasma operating in the contracted mode. Finally, (iv) the high flow data peak at 0.8 eV per molecule energy input. We presently believe that this relates to a transition to the combined diffuse-contracted mode.

The same data is plotted in Fig. 5 in terms of energy efficiency for CO formation, this time with a logarithmic specific energy input axis. As to be expected, the trends are similar as before. Efficiencies range from 7% up to ~45%. In other words, the record high energy efficiencies of 90% are not reproduced in
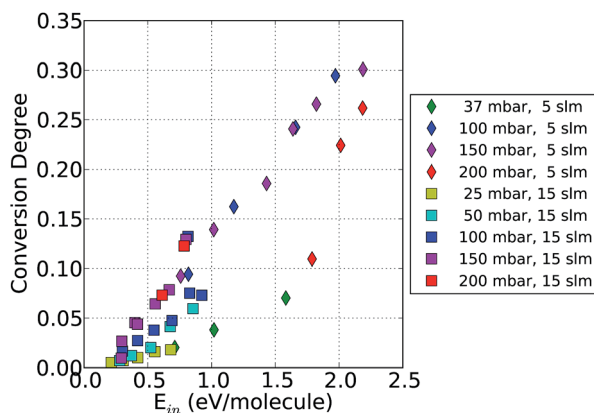
Fig. 4 Conversion degree measured in pure microwave CO_2 plasma as a function of the specific energy input, at 5 and 15 slm gas flow rate, in scans of the reactor pressure.

ART ■ C5FD00045A
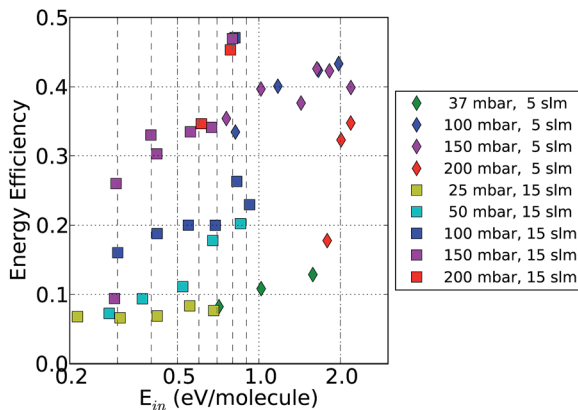
Fig. 5   Energy efficiency measured in pure microwave CO_2 plasma as a function of the specific energy input, at 5 and 15 slm gas flow rates, in scans of the reactor pressure. The underlying experimental data are identical to those of Fig. 4.

the present experiments, although similar conditions in terms of pressure and specific energy were covered.[2]

4.3   Gas temperature

A signature of reaching the desired non-equilibrium conditions is a low gas temperature that is maintained whilst vibrational temperatures (up to 8000 K [12,14]) and plasma temperatures (1–5 eV) are high. Usually, rotational distribution temperatures are determined by molecular spectroscopy as a measure for the gas temperature. This assumes equilibration between rotational and translational degrees of freedom, which is not always necessarily the case.[15] In this work, we rely on direct, *in situ* and spatially resolved, density measurements with laser Rayleigh scattering, from which temperatures are inferred using reactor pressure readings and the ideal gas law. Taking the parameter space covered by the conversion measurements as reference, we selected a high and low pressure condition (20 and 135 mbar) at a high flow rate (13 slm) to perform scans of the specific energy. The temperature results are presented in Fig. 6.

In the analysis, pure CO_2 was assumed as the scattering species. However, in the case of significant dissociation, considerable amounts of CO and O_2 would also have been present. This would disturb the temperature analysis as the total Rayleigh scattering caused by CO and $\frac{1}{2}O_2$ is a factor 1.5 less than the scattering from CO_2. So if locally all CO_2 was dissociated, the temperature would be over-estimated by the same factor of 1.5. A perhaps more realistic estimate of the maximum error is to assume at the highest specific energy input an energy effi-ciency of 50%, *i.e.* a maximum conversion degree of 15%. This would imply an overestimation of the neutral gas temperature of only 5%.

It is seen that gas temperatures are around 2000 K for the low pressure conditions but rise steeply to values that are usually assumed for the temperature of the plasma electrons for the high pressure conditions. Putting these observa-tions in the context of the earlier conversion measurements: the highest conversions are obtained as gas temperatures are also maximal.
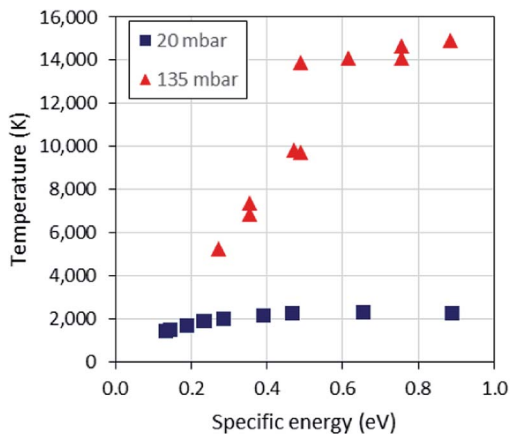
Fig. 6 Gas temperatures determined from neutral gas density measurements with Rayleigh scattering and reactor pressure readings in a scan of specific energy input. The gas flow was at 13 slm similar to the high flow conditions in Fig. 4 and 5, the pressure was tuned to 20 and 135 mbar, respectively.

The temperature data exhibit a sudden rise at a specific energy of about 0.5 eV. A closer inspection of the 137 mbar data series in the plot of the discharge cross sectional areas (Fig. 3) shows that this is exactly where the discharge undergoes a transition from diffuse to contracted. Apparently, contracted discharges have a central neutral gas temperature that is approximately constant at 1.4×10^4 K.

5 Electron energy distribution evaluation

The temperature of the electrons, or equivalently the mean energy, in a discharge is set by the requirement that on average an electron should be able to replace itself by an ionization event before it escapes to the wall or it recombines with a positively charged heavy particle in the volume. In other words: the production by ionization must be equal to the losses, or, the electron temperature is determined by the particle balance. For a discharge as studied here (simplified in the following by a uniform electron density n_e, electron temperature T_e, and gas density n_0 in a reactor of radius r), we write the particle balance as:

$$n_e n_0 k_{ion}(T_e) = n_e^2 k_{DR}(T_e) + \frac{n_e c_s(T_e)}{2r}. \tag{4}$$

The left hand side (LHS) of the equation is the production of ions (with $k_{ion}(T_e)$ the effective ionization rate per unit of volume). The first term on the RHS (right hand side) is volume recombination due to dissociative recombination, with the dissociative recombination rate $k_{DR} = 4.2 \times 10^{-13}(T_e/300\ \text{K})^{-0.75}\ \text{m}^3\ \text{s}^{-1}$.[16] The second term indicates wall recombination due to Bohm flux to the wall, *i.e.* ions reach sound speed c_s at the sheath in front of the wall. Note that plasma flow is disregarded as typical flow velocities of 100–500 m s^{-1} are negligible compared to the sound speed.

The electron density is determined by the requirement that the number of collisions between electrons and heavy particles is sufficient to transfer the power injected into the discharge, P_{in}, to the heavy particles. In other words, the electron density is determined by the power balance, which is written as:

$$\frac{P_{\text{in}}}{V} = n_e n_0 \sum_i (k_i U_i) \tag{5}$$

(with V the reactor volume and k_i and U_i the rate and energy loss of an energy transfer process). In the ideal case, vibrational excitation would dominate and would be the only term on the RHS.

In case of Maxwellian velocity distributions, these equations are straightforward to solve. However, the free electrons in microwave discharges are recognized to be more likely Druyvesteyn distributed.[1] This means that the high energy tail is decreased, which drives the mean electron energy up to still supply sufficient ionization. In such cases, a Boltzmann solver can be used to model the electron energy distribution function (EEDF), in which case effective rates of the relevant processes are calculated on a basis of the cross sections. The publicly available Bolsig$^+$ solver,[17] was used, which has been described by Hagelaar and Pitchford.[18]

The results of solving the balanced equations assuming Maxwellian distributions and EEDF calculations with Bolsig$^+$ are compared in Fig. 7. In the case of a Maxwellian distribution, the mean electron energy is taken as $\frac{3}{2} k_B T_e$. It is seen that the mean electron energy is indeed increased due to the non-Maxwellian nature of the discharge. Moreover, with increasing input power, the mean electron energy increases, thus opening direct electron excitation channels in addition to the preferred vibrational excitation.

At this point it is of interest to note that the mean electron energies calculated here are different from values that are calculated or estimated in other work, e.g.
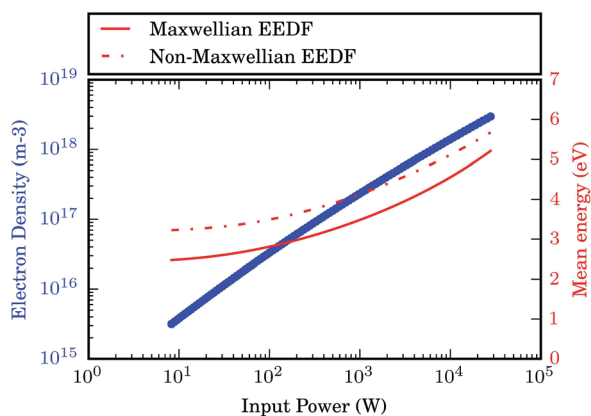
Fig. 7 Electron density (left axis) and mean energy (right axis) calculated as a function of input power for a CO_2 microwave discharge. Compared are solutions of the balanced equations assuming a Maxwellian EEDF and solutions which involved detailed Bolsig$^+$ calculations of the EEDF. The non-Maxwellian nature leads to increased mean electron energies. Dissociative recombination becomes more important as density increases, which causes the increase in mean electron energy with input power. Assumed was a neutral gas density of 10^{23} m^{-3}, which is similar to measured values.

by Kozák *et al.*[8] or Silva *et al.*[12] Usually, microwave discharges in CO_2 are assumed to operate at electron temperatures of 1–2 eV, *i.e.* mean energies of 1.5–3.5 eV. At modest power inputs of 10 W there is quantitative agreement with these literature values, but with increasing power, the mean electron energy increases significantly. One may be suspicious about the simplified wall losses in the particle balance that are used here (eqn (4)). After all, the electron density will in reality be lower near the walls compared to the center, especially in the contracted mode of operation, thus Bohm fluxes calculated on the basis that central densities overestimate the losses significantly. In fact, a radial ambipolar diffusion model (as used by *e.g.* Vijvers *et al.* for thermal arcs[19]) would have been more appropriate. This was not implemented since it is not significant compared to dissociative recombination. The main characteristic of dissociative recombination is its dependence on the square of the electron density (eqn 4). As a result, it causes the mean electron energy to increase with electron density, which is seen in Fig. 7. Already around an input power of 100 W, the electron energy is seen to increase, indicating that dissociative recombination is at play in the particle balance.

Knowing the EEDF enables calculation of the effective rates on the basis of the cross sections. These rates can be normalized to yield electron energy loss fractions giving more insight into the loss processes of the electrons. In Fig. 8 these loss fractions are shown for various processes. A major insight is obtained from this plot: the Bolsig$^+$ evaluations predict that at reactor relevant values of input power, the vibrational excitation is no longer dominant in the power balance. This is indirect, *via* increasing of the mean energy due to dissociative recombination.

Important in the present context is that dissociative recombination not only shortens the ion lifetime and therewith increases the electron energy, but also converts ionization energy into additional heating of the neutral gas. Since the vibration–translation exchange increases with gas temperature,[20] the extra gas heating might be sufficient to quench the vibrational excitation.
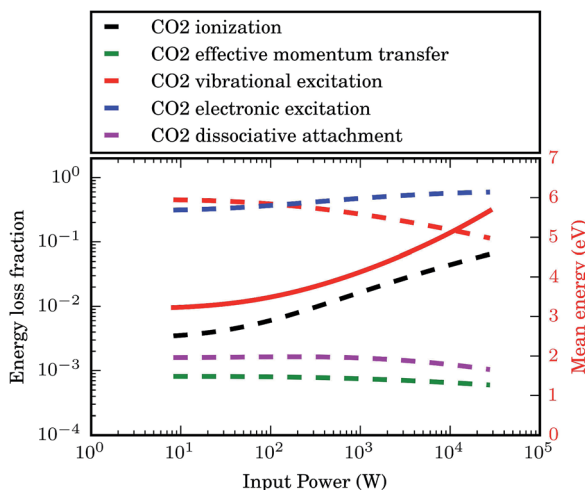
Fig. 8 Energy loss fractions for the various processes at play in a CO_2 microwave discharge. It shows that vibrational excitation is not the dominant energy loss channel for the electrons in conditions as investigated in the present work.

6 Discussion

Having explored CO_2 dissociation in microwave plasma both experimentally in terms of dissociation degree, energy efficiency, and neutral gas temperature, as well as numerically in terms of EEDF and energy loss fractions for the main reaction processes at play in the plasma, we summarize the main findings as follows:

• the energy efficiency for CO formation never exceeded the thermodynamic maximum of ∼45%;

• the conversion degree for CO formation never approached the thermodynamic maximum of ∼55%;

• the best performance was observed at pressures of around 150 mbar and also when the plasma operated in the contracted mode (in which gas temperatures in the center are too high to expect strong non-equilibrium conditions in view of vibration-to-translation relaxation);

• the electron energy estimates indicate that vibrational excitation is not dominant in the present conditions.

In other words, it is questionable whether vibrational excitation has been at play in the present experiments. Here, we will put these findings in the context of thermal equilibrium dissociation efficiencies, hypothesize on the mechanism of dissociation at play and how this relates to the observed scalings of dissociation degree and energy efficiency with input power.

As reference, thermodynamic equilibrium conversion data were calculated with the CEA package,[21] which are plotted in Fig. 9. Also included in the plot are energy efficiencies calculated assuming instantaneous cooling.[22]

Let's first put the *in situ* temperature measurements (Fig. 6) in the context of the chemical equilibrium data. Starting with the low pressure series (20 mbar, in a diffuse discharge mode), which were rather constant at around 2000 K, these
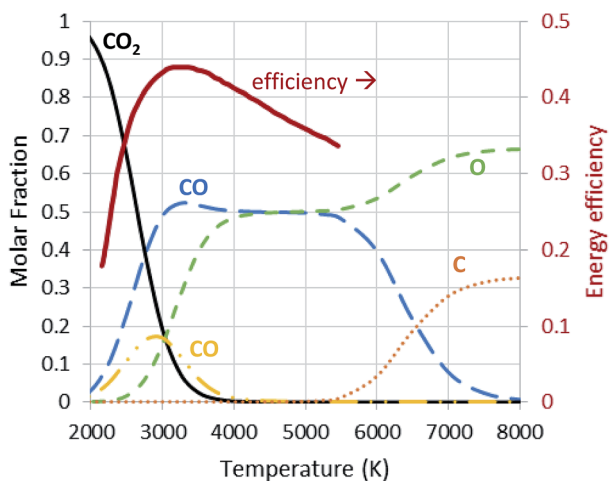
Fig. 9 Chemical equilibrium calculated molar fraction of the products of CO_2 dissociation at a fixed pressure of 100 mbar. Calculated energy efficiencies assuming instantaneous quenching after Polak *et al.* are plotted on the right axis.

would produce chemical equilibrium conversion degrees of about 5%. The measured data at a similar pressure (25 mbar, Fig. 4) increased with power from close to zero to up to ~2%. These measured conversion degrees thus make perfect sense if one realizes that the radial temperature must have peaked. As a result of the peaking, only the hotter centers would have contributed to dissociation. At increasing input power the radius of the dissociation zone would have increased thus producing more dissociation and hence the measured linear behavior.

Next is the high pressure series (135 mbar). The measured temperatures in the center of these contracted discharges started at 5000 K and increased to over 15 000 K. In terms of chemical equilibrium conversion, this corresponds to starting at a maximum conversion of 50% that subsequently drops down to 0% CO due to full dissociation. The measured conversions, however, go up from a few % to nearly 10%. The same temperature peaking argument holds again. However, this time the CO formation region moves out of the center as the temperature increases beyond the CO formation region. This extra hot center becomes even smaller as the discharge contracts. In this situation, the plasma acts as a central heat source that provides the outer regions with thermal heat and induces the dissociation. The amount of gas in the extra hot center is relatively small. Not only does geometry play a role here (the central cross section being smaller than the boundary area), but also the strong temperature peaking in the center in radially constant pressure implies rarefaction of the center.

An aspect that has not been considered in the present work is the quenching of the reaction products. In fact, no measures had been in place to optimize the quenching rate. Instead, the effluent had been flowing through a constant radius tube, only being cooled by the colder tube walls. Roughly estimating, this gives a quenching rate of only 10^6 K s^{-1} (assuming 1000 K cooling over 10 cm with a flow velocity of 100 m s^{-1}). As a consequence, back reactions might have deteriorated energy efficiencies in the effluent by a factor of more than 2 compared to inside the reactor.

These equilibrium features of the observed dissociation degrees are in line with the mean electron energy evaluations and the consequence that vibrational excitation is not the main electron energy loss process. However, both aspects are especially valid for the central regions of the reactor, *i.e.* the hotter plasma region and its direct hot neutral gas surroundings. So the non-equilibrium dynamics may still be at play further out, even closer to the reactor walls where the gas is colder and still an appreciable density of low energy electrons is available for vibrational excitation. Indeed, closer inspection of the energy efficiencies that are presented in Fig. 5 do show a sign thereof. Especially the outliers at about 0.8 eV specific energy, which were already indicated to correspond to the combined diffuse-contracted mode, point to partly non-equilibrium CO production. The achieved energy efficiency of just over 45% approaches the maximum of the calculated efficiency for instantaneous quenching (see Fig. 9), and it is thus improbable that this could have been achieved by thermal equilibrium chemistry alone in the present reactor geometry.

Having established that thermodynamic equilibrium chemistry dominates in the present work, the question arises how to move in operational space to strong non-equilibrium dominated conditions. One aspect that should help in this respect is lowering the pressure even further, to the 1 mbar range, *e.g.* by installing larger diameter flow tubes. This is based on the one hand on observing

lower neutral gas temperatures at lower pressure, and on the other hand on dissociative recombination strongly falling off with electron density. In the next Section, we propose an alternative, entirely novel, approach that relies on tailoring the EEDF by adding low ionization potential species to the reactor input.

7   Adding traces of low ionization potential alkali metals

Having established that the mean electron energy has been too high for preferential vibrational excitation leading to a strong non-equilibrium, the relevant question to ask is how to mitigate this effect induced by dissociative recombination. In other words, how to tame the CO_2 microwave discharge? We postulate that this can possibly be achieved by adding traces of low ionization potential species, *e.g.* alkali metals such as lithium, sodium or potassium. The effect of this action will be twofold. Firstly, the lower ionization potential will cause a lower plasma temperature *via* the particle balance. Secondly, the positive charge is no longer carried by molecular ions, so that volume recombination *via* dissociative recombination is no longer at play. Atomic ions can only recombine in the volume *via* three-body recombination, a process which has exceedingly small reaction rates. In the absence of dissociative recombination, the previously observed electron density dependence on the mean electron energy, as shown in Fig. 7, will vanish.

To estimate the effect of seeding sodium to the discharge, the addition of alkali impurities was modeled using Bolsig$^+$. Firstly, the calculated electron density and mean energy are presented as a function of input power in Fig. 10. It is seen that the mean electron energy is indeed significantly decreased, to 1 eV (*i.e.* in the case of a near Maxwellian distribution, this would mean 0.7 eV electron temperature) and its previous dependence on electron density (or input power) is no longer present.
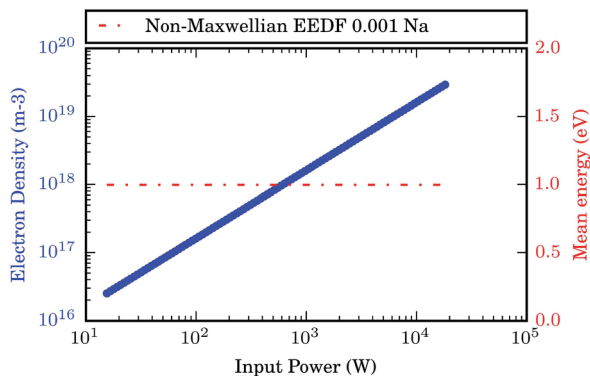
Fig. 10   The effect of sodium being added to a CO_2 microwave discharge on the mean electron energy as calculated with the Bolsig$^+$ solver. Assumed was 0.01% sodium added to a neutral gas density of 10^{23} m^{-3}. The mean electron energy is significantly decreased and lost any dependence on input power (compared to Fig. 7).

ART ■ C5FD00045A
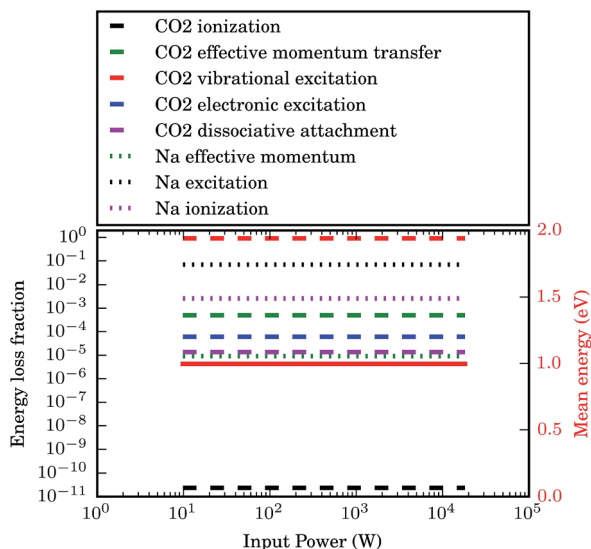
Fig. 11 The effect of 0.01% sodium added to a CO_2 microwave discharge on the relative energy loss fractions for the main processes at play. It shows that vibrational excitation has become the dominant energy loss channel for the electrons, which does not change within the conditions investigated in the present work.

As the mean electron energy has become independent of input power, so have the energy loss fractions, as can be seen in Fig. 11. More importantly, vibrational excitation has become the dominant energy loss channel for the electrons. In other words, these evaluations support the beneficial effect of adding low ionization species for reaching a strong non-equilibrium in a CO_2 microwave discharge.

An important result from analyzing the energy loss fractions is that adding sodium at amounts of 0.01% (which allows equal levels of ionization degree) does not add a significant amount of radiative losses to the power balance. This becomes important at levels of 0.1–1% and thus sets the limit on the amount of sodium that can be added. It is noted that this balance may be different for other alkali metals.

8 Conclusions

The present experiments and EEDF evaluations show that retaining a low electron temperature (mean energy) is required for realizing strongly non-equilibrium conditions that yield high energy efficiency CO_2 conversion. One possible route to follow is enhancing the volume of the non-equilibrium regions in the reactor compared to the high density chemical equilibrium plasma part. However, this will always mean compromising between high power input (*i.e.* reaching application relevant throughput) and achieving high efficiency. A successful development of the here proposed alkali additives would offer an alternative in which the plasma dynamics can be tailored to the non-equilibrium in the entire discharge volume. In effect, it would overcome the compromise, the trade-off between

conversion degree and energy efficiency. It would tame the microwave plasma to beat thermodynamics in CO_2 dissociation.

References

1 A. A. Fridman, *Plasma Chemistry*, Cambridge University Press, New York, 2008.

2 R. I. Azizov, A. K. Vakar, V. K. Zhivotov, M. F. Krotov, O. A. Zinov'ev, B. V. Potapkin, V. D. Rusanov, A. A. Rusanov and A. A. Fridman, *Sov. Phys. Dokl.*, 1983, **28**, 567.

3 I. A. Semiokhin, Y. P. Andreev and G. M. Panchenkov, *Russ. J. Phys. Chem.*, 1964, **38**, 1126.

4 A. N. Maltsev, E. N. Eremin and L. V. Ivanter, *Russ. J. Phys. Chem.*, 1967, **41**, 633.

5 Y. P. Andreev, I. A. Semiokhin, Y. M. Voronkov, V. A. Sirotkina and V. A. Kaigorodov, *Russ. J. Phys. Chem.*, 1971, **45**, 1587.

6 V. D. Rusanov, A. A. Fridman and G. V. Sholin, *Sov. Phys.-Usp.*, 1981, **24**, 447.

7 R. I. Asisov, A. A. Fridman, V. K. Givotov, E. G. Krasheninnikov, B. I. Petrushev, B. V. Potapkin, V. D. Rusanov, M. F. Krotov and I. V. Kurchatov, *5th Int. Symp. on Plasma Chemistry*, Scotland, Edinburgh, 1981, p. 774.

8 T. Kozák and A. Bogaerts, *Plasma Sources Sci. Technol.*, 2015, **24**, 015024.

9 L. F. Spencer and A. D. Gallimore, *Plasma Chem. Plasma Process.*, 2011, **31**, 79.

10 L. F. Spencer and A. D. Gallimore, *Plasma Sources Sci. Technol.*, 2013, **22**, 015019.

11 A. Goede, W. A. Bongers, M. F. Graswinckel, M. C. M. van de Sanden, M. Leins, J. Kopecki, A. Schulz and M. Walker, *3rd European Energy Conf.*, Hungary, Budapest, 2013.

12 T. Silva, N. Britun, T. Godfroid and R. Snyders, *Plasma Sources Sci. Technol.*, 2014, **23**, 025009.

13 L. S. Rothman, I. E. Gordon, R. J. Barber, H. Dothe, R. R. Gamache, A. Goldman, V. I. Perevalov, S. A. Tashkun and J. Tennyson, *J. Quant. Spectrosc. Radiat. Transfer*, 2010, **111**, 2139–2150.

14 A. K. Vakar, V. K. Zhivotov, F. F. Karimova, E. G. Krashenninikov, V. D. Rusanov and A. A. Fridman, *Sov. Tech. Phys. Lett.*, 1981, 7, 429.

15 N. den Harder, D. C. Schram, W. J. Goedheer, H. J. de Blank, M. C. M. van de Sanden and G. J. van Rooij, *Plasma Sources Sci. Technol.*, 2015, **24**, 025020.

16 A. A. Viggiano, A. Ehlerding, F. Hellberg, R. D. Thomas, V. Zhaunerchyk, W. D. Geppert, H. Montaigne, M. Larsson, M. Kaminska and F. Österdahl, *J. Chem. Phys.*, 2005, **122**, 226101.

17 http://www.bolsig.laplace.univ-tlse.fr/.

18 G. J. M. Hagelaar and L. C. Pitchford, *Plasma Sources Sci. Technol.*, 2005, **14**, 722.

19 W. A. J. Vijvers, D. C. Schram, A. E. Shumack, N. J. L. Cardozo, J. Rapp and G. J. van Rooij, *Plasma Sources Sci. Technol.*, 2010, **19**, 15.

20 E. Treanor, J. W. Rich and R. G. Rehm, *J. Chem. Phys.*, 1968, **48**, 1798–1807.

21 S. Gordon and B. J. McBride, NASA Reference Publication, 1996, vol. 1311.

22 A. A. Fridman, in *Plasma Chemistry*, Cambridge University Press, New York, 2008, p. 263, Fig. 5–4.